

UNIVERSIDADE DE LISBOA
INSTITUTO SUPERIOR TÉCNICO

**Development and application of a process-oriented model
for benthic marine systems**

Isabella Ascione

Supervisor

Doctor Ramiro Joaquim de Jesus Neves

**Thesis approved in public session to obtain the PhD Degree in
Environmental Engineering**

Jury final classification

Pass with Merit

Jury

Chairperson: Chairman of the IST Scientific Board

Members of the Committee:

Doctor João Carlos de Sousa Marques

Doctor João Pedro Salgueiro Gomes Ferreira

Doctor Ramiro Joaquim de Jesus Neves

Doctor Tiago Morais Delgado Domingos

2014

UNIVERSIDADE DE LISBOA
INSTITUTO SUPERIOR TÉCNICO

**Development and application of a process-oriented model
for benthic marine systems**

Isabella Ascione

Supervisor
Doctor Ramiro Neves

**Thesis approved in public session to obtain the PhD Degree in
Environmental Engineering**

Jury final classification
Pass with Merit

Jury

Chairperson: Chairman of the IST Scientific Board

Members of the Committee:

Doctor João Carlos de Sousa Marques, Professor Catedrático da Faculdade de Ciências e Tecnologia, da Universidade de Coimbra

Doctor João Pedro Salgueiro Gomes Ferreira, Professor Associado (com Agregação) da Faculdade de Ciências e Tecnologia, da Universidade Nova de Lisboa

Doctor Ramiro Joaquim de Jesus Neves, Professor Associado do Instituto Superior Técnico, da Universidade de Lisboa

Doctor Tiago Morais Delgado Domingos, Professor Auxiliar do Instituto Superior Técnico, da Universidade de Lisboa

Funding Institutions: Instituto Superior Técnico, Fundação para a Ciência e a Tecnologia

Abstract

This Ph.D. thesis presents the development, testing, and application of a benthic ecology model inside the MOHID water modeling system. The model enabled the simulation of the aquatic rooted plant *Zostera noltii*, filter feeders, deposit feeders, and microphytobenthos. The model was developed by following the MOHID object-oriented philosophy, which enables the integration of new model components and processes (collectively known as features). Schematic tests and sensitivity analysis were carried out to evaluate the performance of the model. The model was used to answer questions regarding the competition between macroalgae and *Zostera noltii* in Ria de Aveiro, Portugal. The results showed that *Zostera noltii* is mainly limited by space availability in the presence of macroalgae in Ria de Aveiro. The model was used to assess the role of filter feeders in the control of phytoplankton in a schematic case study. The model enabled the detection of feedback mechanisms between benthic and pelagic food webs, as a consequence of the filter feeders grazing on phytoplankton and particulate organic matter. Future developments may include calibration of uncertain parameters, real case studies, and development of more complex features.

Keywords: model, simulation, benthos, ecology, MOHID, Portugal, *Zostera noltii*, filter feeders, deposit feeders, seagrasses.

Resumo

Esta tese de doutoramento apresenta o desenvolvimento, teste e aplicação de um modelo de ecologia bentônica dentro do sistema de modelação MOHID. O modelo permitiu a simulação da planta aquática *Zostera noltii*, filtradores, detritívoros e microfitobentos. O modelo foi desenvolvido seguindo a filosofia orientada a objetos do MOHID, que permite a integração de novas componentes e processos. Testes esquemáticos e análise de sensibilidade foram realizados para avaliar o comportamento do modelo. O modelo foi usado para responder a perguntas sobre a competição entre macroalgas e *Zostera noltii* na Ria de Aveiro, Portugal. Os resultados mostraram que *Zostera noltii* é limitada principalmente pela disponibilidade de espaço na presença de macroalgas na Ria de Aveiro. O modelo foi utilizado para avaliar o papel de filtradores no controle do fitoplâncton num caso de estudo esquemático. O modelo permitiu a detecção de mecanismos de feedback entre teias alimentares bentônicas e pelágicas, como consequência do pastejo dos filtradores sobre o fitoplâncton e matéria orgânica particulada. Desenvolvimentos futuros podem incluir a calibração de parâmetros incertos, casos de estudos reais, e desenvolvimento de características mais complexas.

Palavras-chave: modelo, simulação, bentos, ecologia, MOHID, Portugal, *Zostera noltii*, filtradores, detritívoros, ervas marinhas.

Acknowledgments

I would like to thank Prof. Dr. Ramiro Neves, my thesis Supervisor, for accepting me in his group (MARETEC), and for his guidance and availability throughout these last four years during which I have been working with him.

The present study benefits of monitoring data collected in Ria de Aveiro by the University of Aveiro (Silva *et al.*, 2009). These data were of vital importance for this study because enabled to verify the model results against real observations. For this reason, I would like to thank Professor Doctor J.F. Da Silva of the Aveiro University for kindly providing such valuable information.

I would like to thank Pedro Chambel, who provided nutrients and freshwater inflows calculated by the SWAT model applied to the Vouga catchment.

I would like to thank Paulo Chambel, for the help in the discussion of the conceptual model for seagrasses, and for teaching me about how to implement nested models in MOHID. I would like to thank Marcos Mateus for the support in the beginning of this research and in the discussion of the conceptual model.

I would like to thank Angela Canas, for the help provided in the collection of information from previous projects carried out in the Mondego Estuary.

I would like to thank Luis Fernandes and Guillaume Riflet for the valuable support provided to the programming and understanding of the MOHID code.

I would like to thank Francisco Campuzano and Hilda de Pablo for the valuable help and for the great moments spent together.

I would like to thank Ana Rosa Trancoso, Madalena Santos, and David Brito for the kind help in the beginning of my work to understand how to use MOHID.

I would like to thank Rodrigo Fernandes and Claudia Neto for helping me to understand and use the Lagrangian module in MOHID.

I would like to thank Ricardo Deus and Simonny, for the great moments spent together.

Thanks to all the colleagues working at MARETEC for the inspiration and support provided.

I would like to thank my beloved husband Kaloyan N. Kenov, he was the one who was always there giving me continuous support, help, editing the text, and encouragement during the development of this research.

I would like to thank my mother, Maria Rosaria, my father Gennaro, my sisters Annamaria and Ilaria, my grandmother Carmela, and all my relatives, for being always supportive and for encouraging me in this journey.

The research has been financially supported by Instituto Superior Técnico (fellow number 7107, student number 72357/D), and Fundação para a Ciência e Tecnologia, through the following projects:

RECONNECT (System dynamic response to an ample artificial RE-establishment of the upstream CONNECTION between the two arms of the Mondego (PTDC/MAR/6427/2006).

DyEPlume – Dinâmica Estuarina e Propagação de Plumas na Costa Portuguesa – Impactos de Alterações Climáticas (PTDC/MAR/107939/2008).

Contents

Abstract	i
Resumo	iii
Acknowledgments	v
Overview	1
Chapter 1 – Introduction and objective	3
1.1. Introduction.....	3
1.2. Estuarine Ecosystem	3
1.2.1. Circulation.....	3
1.2.2. Ecology	4
1.2.3. Aquatic food webs.....	8
1.2.4. Biogeochemical cycles.....	10
1.2.5. Antropogenic pressures	11
1.3. The problem.....	12
1.4. State-of-the-art of benthic modelling	14
1.5. Conceptual approach.....	15
1.6. Coupling between physical and biological processes	19
1.7. Objectives	20
1.8. Hypotheses.....	21
Chapter 2 – Model formulation	25
2.1. Introduction.....	25
2.2. Assumptions.....	26
2.2.1. Driving factors	27

2.2.2.	Seagrass nutrient content.....	28
2.2.3.	Organisms' mobility.....	29
2.2.4.	The vertical dimension.....	29
2.3.	Units.....	30
2.4.	Conceptual model and equations.....	30
2.4.1.	Seagrasses.....	31
2.4.2.	Benthic feeders and microphytobenthos.....	48
2.5.	The MOHID water modelling system.....	71
2.5.1.	Hydrodynamics.....	71
2.5.2.	Water Quality.....	72
2.5.3.	Bottom shear stress.....	73
2.5.4.	Integration in MOHID.....	76
Chapter 3 – Model testing (part 1).....		79
3.1.	Introduction.....	79
3.2.	Function plots.....	79
3.3.	Preliminary model calibration.....	85
3.4.	Verification.....	90
3.5.	Testing.....	91
3.6.	Sensitivity analysis.....	98
Chapter 4 - Model testing (part 2).....		107
4.1.	Introduction.....	107
4.2.	Function plots.....	107
4.3.	Testing.....	111
4.4.	Sensitivity analysis.....	114
Chapter 5 – Case Study.....		119

5.1.	Introduction.....	119
5.2.	Study area	119
5.3.	Data.....	122
5.4.	Model set-up	123
5.4.1.	Initial conditions.....	124
5.4.2.	Boundary conditions	125
5.5.	Sensitivity analysis.....	127
5.6.	Model verification.....	128
5.7.	Results and discussion	129
5.7.1.	Sensitivity analysis results	129
5.7.2.	Model results	131
5.8.	Conclusion	142
Chapter 6 – Hypotheses Testing.....		143
6.1.	Introduction.....	143
6.2.	Q1: <i>When the growth of seagrasses limited by macroalgae?</i>	143
6.3.	Q2: <i>Can the model reproduce the control by filter feeders on phytoplankton biomass?</i>	157
Chapter 7 - Conclusion.....		163
7.1.	Conclusion	163
Bibliography.....		167
Appendix A		181
Appendix B		183
Appendix C		185
Appendix D		195

Overview

This introductory section provides an overview of the thesis structure and its content.

Chapter 1 – Introduction and objectives

In this chapter, an overview is given of the main characteristics of estuarine ecosystems, including the aspects of circulation, ecology, and anthropogenic pressures. A review of the state-of-the-art status and developments in the field of ecological modeling is provided here. The main objectives of the study, research questions, and hypotheses are described as well.

Chapter 2 – Model formulation

This chapter delineates the formulation of the model components. The main model assumptions, theoretical basis, and limitations are described. The link between the ecological model developed in this study and the MOHID modelling system is described as well.

Chapter 3 – Model testing (part 1)

Numerical tests on the seagrass model component are presented in this chapter. The analysis of the implemented functions is presented. A preliminary calibration of the model is carried out to find parameters specific for simulation of the seagrass *Zostera noltii*. A 0-D configuration is used to assess the model behavior. Model sensitivity analysis is performed and the results are discussed.

Chapter 4 - Model testing (part 2)

Numerical tests on the benthic ecology model component are presented in this chapter. The analysis of the implemented functions is presented. A 0-D configuration is used to assess the model behavior. Model sensitivity analysis is performed and the results are discussed.

Chapter 5 – Case study

This chapter deals with an application of the seagrass model to a real system: Ria de Aveiro. The model results are verified against real observations. A reference scenario for the model is defined to be used for the hypothesis verification.

Chapter 6 – Hypotheses verification

This chapter contains the verification of the hypothesis outlined in Chapter 1.

Chapter 7 - Conclusion

This concluding chapter provides concluding remarks about the work, main achievements, limitations and possible future developments.

Appendix A

Temperature limitation in seagrasses and in benthic organisms.

Appendix B

The ammonia preference factor in microphytobenthos.

Appendix C

Results of sensitivity analysis carried out on the seagrass model.

Appendix D

Results of sensitivity analysis carried out on the benthic ecology model.

Chapter 1 – Introduction and objective

1.1. Introduction

Mathematical models have been first applied by engineers and physicists as part of the scientific method to describe physical processes observed in nature. The use of mathematical models to describe ecosystem behavior dates back to the beginning of the 20th century. One of the earliest and most popular ecological models is the Lotka (1925) and Volterra (1926) model used to understand the predator-prey dynamics. Since then, there has been an increased interest to apply mathematical models to describe ecosystems (Odum, 1971). The first models to describe microbial loop of aquatic environments were proposed in the 1940s (Riley, 1946). The increase of the computational power contributed significantly to the growing complexity of ecological models used to describe water column biogeochemistry. The use of models increased in the last decades due to the growing concern about environmental pollution of water, air, and land. Models which are capable to simulate biological and physical processes are used as a complement to monitoring studies to assess water quality status and eutrophication of aquatic environments.

In this chapter, an overview is given of the main characteristics of estuarine ecosystems, including the aspects of circulation, ecology, and anthropogenic pressures. A review of the state-of-the-art and developments in the field of ecological modeling is provided here. The main objectives of the study, research questions, and hypotheses are described as well.

1.2. Estuarine Ecosystem

Estuaries have productive habitats with high ecological and economic importance. Most estuaries are characterized by proximity with large cities, and receive anthropogenic inputs coming from agriculture and urban wastes. Estuarine waters are used for aquaculture farming, fishing, recreation, and navigation.

1.2.1. Circulation

An estuary, according to the definition of Pritchard (1967), is “a semi-enclosed coastal body of water which has a free connection with the open sea and within which sea water is measurably diluted with fresh water derived from land drainage”. From this definition, it

follows that the water from rivers meets the salty water of open sea and oceans, creating a transitional area where the salinity of the ocean is decreased. The salty and deep water from the ocean enters the estuary as a deep layer, and the fresh, lighter water from the estuary flows out of the estuary closer to the surface. This pattern is usually observed in most estuaries with low tidal mixing and weak runoff. The freshwater flow is mixed with the underlying salty water by turbulence, reducing the differences between the two layers. The basic pattern of the estuarine circulation is often modified by several processes depending on geomorphology, intensity of freshwater inflows, and tidal mixing. The area where the salty water meets with the fresh waters moves up and down along the estuary with the intensity of the river flow. The changes in salinity lead to flocculation and sinking of fine particles carried in suspension. The suspended material is transported and redistributed over the area of the estuary, leading to the formation of mud flats. Some estuaries are dominated by the effect of tidal currents due to friction with the bottom. The tidal mixing produces turbulence that can break the stratification of the estuarine circulation.

The intensity of the freshwater runoff affects the primary production. In temperate areas, estuarine circulation is affected by seasonality of freshwater inflows. During winter, high freshwater inflows are usually caused by high freshwater runoff during rainy periods. In summer, low freshwater inflow determines increase of the residence time of water. The effect of the spring run-off at the head of an estuary usually leads to a strong stratification. Brandt *et al.* (1986) found that in the Chesapeake Bay a strong pycnocline was observed in correspondence with spring runoff. In an open ocean a strong stratification may cause a barrier to nutrients toward the surface. However, in estuarine systems, the effect of tides produces transfer of nutrients in the surface layer, enhancing primary production.

Some shallow estuaries can be mixed during the whole year by tidal action, primary production of tidally mixed areas tend to be higher than this of coastal waters (Mann and Lazier, 1996).

1.2.2. Ecology

A biocenosis (also called biotic community, or simply ecological community) is the set of organisms of all species coexisting in a defined space called biotope, which offers environmental conditions necessary for its survival. The biocenosis and the biotope together form the ecosystem. The biocenosis of estuarine ecosystems includes biological components

which are similar to other aquatic systems, such as sea, rivers, lakes, streams, and lagoons. These biological components can be divided into two main groups:

- Pelagos: organisms that live in the water column
- Benthos: organisms living on/inside the bottom sediment.

The Pelagos is divided into plankton and nekton. Plankton includes pelagic animals (zooplankton) and plants (phytoplankton) unable to move against the current. Some of them (oloplankton) spend their whole lives as pelagic organisms; others (meroplankton) spend part of their lives in the water column (e.g. juvenile stage) and partly on the sea floor. The plankton has two main adaptations: transparency (to escape grazers) and buoyancy (to avoid the sinking caused by the higher density of the protoplasmic material). The plankton is the most common form of life in the oceans and estuaries and it is the main source of energy and matter of the entire marine ecological system.

Nekton includes animals capable to swim and move against the currents and the waves, even if some of them are able to move counter current only during the adult stage. The nekton has developed adaptations for swimming such as long body and fins (or similar structures). Similarly to the plankton, the animals of the nekton try to avoid the sinking by adjustment of the gas and fat content in the body and with the replacement of heavy ions with lighter ions in body fluids. Some organisms' large skeletal structures replace the bone with cartilage (lighter) and swim continuously to avoid sinking.

Plankton and nekton interact in pelagic food webs: the phytoplankton lives in the photic zone, and uses solar energy for the synthesis of organic compounds from water and inorganic nutrients. Phytoplankton is food for microorganisms that form the zooplankton (first level consumers), which, in turn, constitute the main source of food for fish (second-level consumers). The nutrients are thus transferred from one trophic level to another or regenerated by decomposers, which include bacteria and fungi which can reduce complex organic compounds of dead plants and animals into simple inorganic compounds usable again by primary producers.

The term Benthos identifies plant and animal organisms that live on the bottom sediment. The benthic habitat, unlike the pelagic one that is three-dimensional, is essentially two-dimensional, similar to terrestrial systems. The benthos includes the same ecological categories which are also found in the water column: the producers (plants), consumers (animals) and decomposers (fungi and bacteria). The producers (phytobenthos) include algae

and cyanobacteria. An important category of plants found in shallow coastal waters is represented by seagrasses that make up the great prairies of *Posidonia*, *Zostera* and *Cymodocea*. Smaller groups include fungi and lichens. Consumers are animals (zoobenthos) and decomposers are bacteria and fungi, including autotrophic cyanobacteria (Cognetti *et al.*, 1999).

The benthic organisms are divided on the basis of their size into three categories:

- Macrobenthos (organisms which diameter is higher than 0.5 mm),
- Meiobenthos (organisms which diameter is between 0.5 and 0.062 mm).

From the point of view of the movement capability, the benthos is divided into three categories:

- Sessile (organisms that live fixed to the bottom for the entire duration of the adult life),
- Vagile (crawling organisms and organisms with jointed appendages), and
- Mobile (swimming organisms).

Water and substrate are the main elements that characterize the benthic environment and are often related to each other because water penetrates into the substrate, and the substrate may be dispersed in water. Regarding the position relative to the substrate (Figure 1) benthic fauna is divided into:

- Epifauna: organisms living on the substrate, and
- Infauna: organisms that live within the substrate.

Substrate is affecting the type of community that inhabits the sea bottom. Rocky bottoms are colonized by epifaunal communities including bivalves, encrusting sponges, macroalgae, and snails. These types of hard substrate are less common in estuarine environments, where there is a predominance of soft bottom due to sedimentation of large quantities of sediment. Soft bottoms are usually inhabited by infauna and epifauna, including worms, clams, and burrowing crabs.



Figure 1 - Distribution of benthic organisms relative to the substrate (hard bottom). After Cognetti *et al.* (1999).

On the basis of the strategies used to collect the food, benthic organisms are usually divided into two groups: filter feeders and deposit feeders. Benthic filter feeders collect the food by remaining anchored to the substrate, intercepting plankton and/or particulate organic matter in the water. The filter feeders catch food particles while they are still in suspension, while the deposit feeders collect them when they settle on the bottom. Benthic filter feeders have developed several strategies for feeding, such as filters, cilia and mucus, to trap food particles and transport them to the mouth. The Arthropoda, which lack cilia, use nets made of hair and bristles.

The benthos includes a large taxonomic group of deposit feeders. These organisms are able to ingest sediment and to extract the microorganisms and organic matter associated with debris or mineral particles, so they need to ingest large amounts of sediment to extract enough food. Since they tend to live on loose substrates, they are generally more mobile than filter feeders, show more adaptations for locomotion, and do not form the colonies that are characteristic of many filter feeding animals. Some organisms are capable to feed on both deposited and suspended material, thus a sharp division between deposit feeders and filter feeders is not always possible.

The benthic and pelagic systems are interconnected through several mechanisms such as the sedimentation of organic particles, trophic interactions, reproduction, and exchange of gases and dissolved substances. The organic material in the water column includes a dissolved

fraction (DOM, Dissolved Organic Matter) and a particulate fraction (POM, Organic Particulate Matter). Organic particles that are produced in the euphotic zone sink across the water column depending on weight, size, and density. The organic particles in water are affected by physical processes (water mixing and the stratification), chemical processes (oxidation and reduction of chemical compounds), and biological processes (predation). The organic particles that reach the bottom of the sea are food source for the benthic system and added to the in situ organic remains of benthic animals and plants.

The benthos is an important vehicle through which organic matter is processed and sent back to the pelagic food web. Deposit feeders are capable of processing large amounts of particulate organic matter and converting it into food for fishes (Levinton, 1989). Some benthic organisms, such as filter feeders can control the phytoplankton biomass (Jørgensen, 1990; Smaal *et al.*, 2013). Cloern (1982) showed this phenomenon in a study carried out in the San Francisco Bay. The latter is a shallow area that receives significant nutrient inputs, but in spite of nutrient enrichment, the phytoplankton biomass is unexpectedly low. The zooplankton grazing on phytoplankton is only partially responsible for the reduction in the net rate of growth of phytoplankton. It has been suggested that grazing by bivalves was the main factor that controlled the phytoplankton biomass in San Francisco Bay (Jørgensen, 1990).

Benthic organisms have developed strategies to ensure reproductive success. Several benthic invertebrates have pelagic larvae that serve to increase the chance for species survival and spreading. Some benthic worms develop specialized segments responsible for breeding (known as epitoke) and release them in the water.

1.2.3. Aquatic food webs

Aquatic food webs of estuarine ecosystems are similar to the food webs of other aquatic ecosystems. The aquatic organisms are usually grouped into two main categories: producers, consumers, and decomposers. Primary producers are producers that are capable to fixing carbon by photosynthesis (autotrophic organisms). The term primary producer includes different types of organisms, from single floating cells to multicellular organisms, which live attached to the substrate. In this group are included autotrophic organisms belonging to different phyla: prokaryotic bacteria (both eubacteria and archaea) and three categories of eukaryotes: green algae, brown algae and red algae. The vascular plants are represented by seagrasses such as *Zostera marina*, *Zostera noltii*, and *Posidonia oceanica*.

A difference with the terrestrial primary producers is that most primary producers of the oceans are microscopic organisms (phytoplankton). The large aquatic autotrophic organisms, such as seagrasses and macroalgae, are confined to the coastal zone and in relatively shallow water, where they can attach to the substrate but still be within the photic zone.

Consumers include heterotrophic organisms which feed on primary producers and on other consumers. Consumers which feed on primary producers are known as herbivores. Consumers which feed on other consumers are known as carnivores. Zooplankton is part of pelagic herbivores, while nekton includes herbivores and carnivores fishes. Producers and consumers can be ordered inside a food pyramid (Figure 2) in which each level is food for another level. Primary producers are the base of the pyramid because they do not eat other organisms. Primary consumers are those consumers which feed on primary producers. Secondary consumers are those which feed on primary consumers. At each passage from a lower to a higher trophic level, carbon is transferred from one level to the other. Not all of the ingested food is used, and it takes energy to break down the food and to convert it into new biomass, thus the efficiency of the transfer from lower levels to higher levels in the food web is always low, usually about 10%.

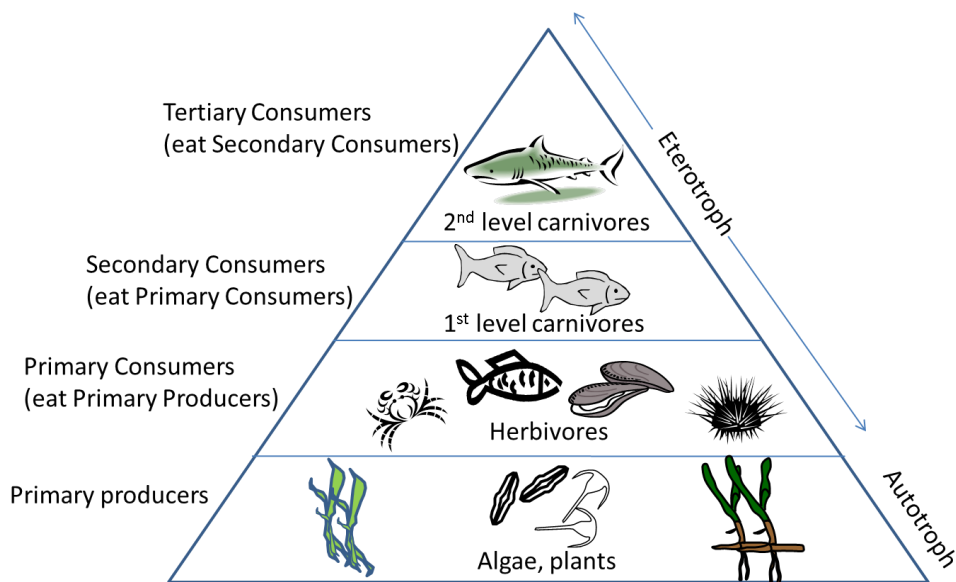


Figure 2 - Food pyramid in marine ecosystems.

1.2.4. Biogeochemical cycles

Chemical elements circulate inside the biosphere by following specific paths known as biogeochemical cycles. From among the more than 90 chemical elements available in nature, only 40 are used to sustain life, and only six are the most important components of the living molecules: carbon (C), oxygen (O), nitrogen (N), phosphorus (P), sulfur (S), and hydrogen (H). According to the principle that nothing is neither created nor destroyed, but everything is transformed, chemical elements, subject to the biogeochemical cycles, vary their chemical state due to oxidation-reduction reactions, catalyzed by living organisms. Physical processes move the elements on earth. Three different compartments in which the elements move can be identified: atmosphere, land, and water. The movement of an element on earth occurs in the atmosphere mostly in the form of gas. In water, the elements come as suspended or dissolved forms. When the element reaches the atmosphere it is moved by the atmospheric circulation relatively quickly. In the water, the elements are moved by the rivers into the sea and redistributed by the currents. When the element settles and is incorporated in ocean sediments, its cycle slows down. Part of the elements incorporated in the sediments will return to surface only in a cycle of millions of years due to tectonic, volcanic, and erosive forces.

Nutrients are “elements or compounds essential for animal and plant growth” (USGS, 2007). For autotrophic organisms, these nutrients include nitrogen, phosphorus, and potassium. In some phytoplankton species, such as diatoms, silica is an important nutrient used to build external shells. Nutrients are introduced in the water column by different sources, including land, atmosphere, and rivers (Figure 3). Sources of nutrients include anthropogenic activities, such as waste discharge and agricultural practices. Mineralization of organic matter is also a source of nutrients produced in situ by bacteriological and fungal activity. Along with light availability, nutrients represent a key factor for the life of aquatic primary producers. In the open sea, nitrogen is a limiting factor for primary production, while phosphorus is usually the limiting factor in freshwater ecosystems (Dodson, 2005).

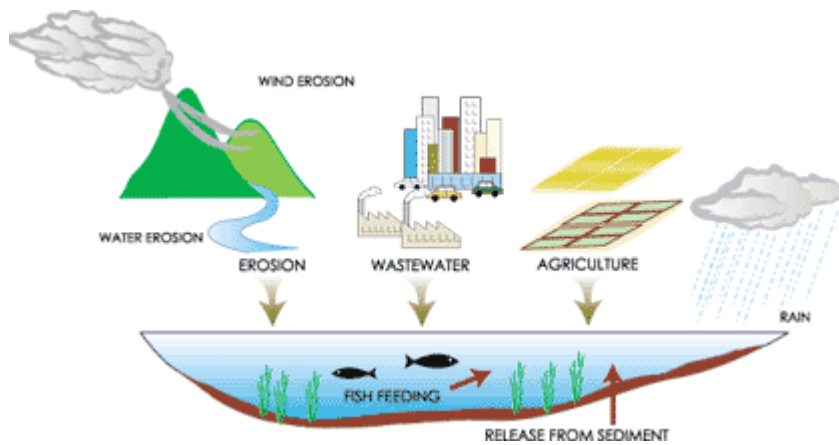


Figure 3 - Main sources of nutrients in aquatic environment (source: <http://www.unep.org>).

1.2.5. Antropogenic pressures

Many of the world's largest cities are in coastal zones and more than 75 per cent of people are expected to live within 100 km of a coast by 2025 (Bulleri and Chapman, 2010). The habitat of the coastal zone is affected by human intervention and modification, with consequences on the ecosystem. Dredging operations are usually carried out in estuaries and coastal areas to improve navigation. However, these operations may cause an increased tidal penetration and modification of the salinity gradients inside estuaries. The main effects of dredging and sand mining include water deepening, increase of sedimentation rates and turbidity. Consequences of water deepening include changes in the circulation and reduction of light availability on the bottom for benthic primary producers. Increase of sedimentation rates may cause burial of benthic communities, including seaweed and seagrass meadows.

Coastal structures such as breakwaters and sea walls are artificial structures to protect beaches by the erosion. The effect of the coastal structures is to reduce the intensity of the waves and therefore to reduce the erosion of the coast. For this purpose they are placed in shallow waters close or at a short distance from the coast. The building of coastal structures implies the modification of the physical environment, and often is anticipated by dredging operations. Coastal structures modify the circulation patterns and the morphology of the marine habitat, with consequences for the ecosystem (Bulleri and Chapman, 2010). Man-made structures tend to have vertical surfaces made of concrete materials opposed to the horizontal surfaces of natural aquatic habitats, which may include rocky and sandy bottoms, with heterogeneous shapes that provide refuge to organisms. These vertical surfaces can be suitable only to a few ranges of organisms, such as mussels and incrusting algae.

Significant issues related to damming have been identified in habitat modification and loss, alteration of water discharges, temperature, and water quality. Artificial reservoirs created upstream of a dam submerge large areas of land that was previously covered by vegetation. Dams affect fish migrations, because they are a barrier for fishes to reach spawning sites upstream. Sediments may be trapped inside the reservoir and never reach the areas downstream. On the other side, as the dam gets filled with sediments, it also loses the capability to store water.

Agricultural practices and urban activities are sources of sewage, fertilizers and contaminants into estuarine waters. Excess nutrients may enhance algal blooms, and production of particulate organic matter that is mineralized below the euphotic area. High respiration and mineralization rates imply high oxygen depletion in the water, which can pose a threat to the health of humans and estuarine wildlife.

1.3. The problem

Benthic organisms are important for the functioning of marine ecosystems. Benthic systems are similar to the terrestrial ones because of the more permanent physical structure, presence of hard surfaces, sedentary organisms, and a long-term chemical storage capacity (Duplisea, 1998). Zoobenthic communities mainly consist of sedentary organisms with no or little movement capabilities and usually live in a territory of a few square meters. This implies that long-living invertebrates experience environmental changes of the place where they live, witnessing both climatic and anthropogenic modifications. Sessile organisms may reshape the submerged landscape and influence the currents pattern. Benthos acts as an important vehicle through which the settled organic matter from the bottom is returned back into the pelagic food web. Deposit feeders are able to process large amounts of organic matter particles and to convert it into food for fish (Levinton, 1989). Filter feeders are consumers of organic matter produced in the pelagic system. High biomass filter feeders may control the phytoplankton growth and compete with zooplankton over phytoplankton (Jørgensen, 1990). Sediment reworking by benthic fauna facilitates the redistribution of organic particles, enhancing the microbial activity and the degradation of organic matter.

Mineralization of organic matter by bacteria in the sediments regenerates inorganic nutrients which are used by primary producers. Benthic primary producers use light to convert

inorganic nutrients into new biomass, to produce oxygen, and provide food for other organisms. Seagrasses have a significant ecological importance because they provide habitat for other species which use them as a site for breeding, feeding and sheltering. Along the coast, where physical conditions are favorable and the competition with other species (e.g. macroalgae) is not strong, seagrasses may proliferate (usually not more than 40 m depth because of light availability), providing a natural barrier to waves propagation.

In the last decades, a decline of seagrass meadows on a global scale has been observed (Burke, 2004). The present seagrass world coverage is 15% less than 10 years ago (Green and Short, 2008). Degradation of seagrass habitats negatively affects populations of species relevant for fishing. The importance of seagrass meadows as structural components of coastal ecosystems has resulted in research interest being focused on the biology and ecology of seagrasses and on methods for mapping, monitoring, modelling, and protection of seagrass habitats (Green and Short, 2008). Major causes of seagrass habitat decline were attributed to dredging operations, land reclamation, port construction, inlet opening, destructive fishing practices, and increasing water turbidity (Silva *et al.*, 2009; Cunha *et al.*, 2013). Consequences of climate changes were also identified as potential threat because of sea level rise and increase of storm frequency (Green and Short, 2008). Seagrasses are known to provide important ecosystem services (habitat for a wide range of species, storm buffering, and nutrient cycling, among others) and to offer a natural barrier against waves and erosion (Green and Short, 2008; Van der Heide *et al.*, 2011). The estimated economic value of seagrass meadows is 19,004\$ ha⁻¹ y⁻¹ (Constanza *et al.*, 1997). In Portugal, seagrass habitats experienced decline in the last 20 years (Cunha *et al.*, 2013), causing biodiversity loss, and contributed to the degradation of coastal fisheries and water quality. The main cause of seagrasses decline in Portugal was attributed to dredging, geomorphologic changes estuaries and lagoons. Eutrophication is one of the causes of seagrass meadows decline because increased nutrient availability may lead to proliferation of fast-growing algae, such as phytoplankton and macroalgae. The European Commission (EC) Urban Waste-Water Treatment Directive (91/271/EEC) classified the Ria de Aveiro, Portugal, as a “sensitive area” in terms of eutrophication. In Ria de Aveiro, the reduction of areas covered by seagrasses was followed by increase of the areas of uncovered sediment, supporting the growth of sparse macroalgae populations only (Silva *et al.*, 2009). Opportunistic and fast growing macroalgae can occupy the space above seagrass beds and reduce space and light availability for benthic plants.

Eutrophication is usually referred to as the increase of algae growth as a consequence of anthropogenic discharges. The control of the primary production in the system is usually achieved by reducing nutrient inputs in the system. However, there are mechanisms inside the ecosystem that can control phytoplankton biomass. Filter feeders process large volumes of water to retrieve food for their survival, growth, and reproduction. As a consequence of feeding over organic particles in the water, filter feeders may have important role in the control of phytoplankton biomass, such as in Chesapeake bay (Carmichael *et al.*, 2004; Newell *et al.*, 2010; Cerco *et al.*, 2013; Kellogg *et al.*, 2013). They also provide a mechanism for the removal of suspended particulate material from the water column, enhancing water clearing.

A few studies are available on the interaction between microphytobenthos, filter feeders, and phytoplankton at the sediment-water interface. MacIntyre *et al.* (2004) proposed a conceptual model for the role of microphytobenthos in the regulation of benthic-pelagic coupling. The study showed that water clearing could increase microphytobenthos productivity and biomass, enhancing the competition for nutrients between microphytobenthos and harmful pelagic algae. Furthermore, this competition between benthic and pelagic primary producers at the sediment-water interface could have feedback effects on benthic grazers. In a Mediterranean mussel culture area, it was found that mussel beds enhance the organic content of the sediment, and that microphytobenthos could affect the filter feeding efficiency (Barranguet, 1997). These feedback mechanisms between pelagic and benthic systems might have consequences on the ecosystem level.

1.4. State-of-the-art of benthic modelling

In the last few decades the interest of research centers, universities, government offices, local authorities, and environmental protection agencies, responsible for water quality issues, stimulated the development of computer models. The general trend of the last years is moving the modeling effort towards a more complex representation of ecosystems to accommodate for particular characteristics of study areas and to address specific water quality issues. These changes are accompanied by the increasing computational capacity, advances in knowledge about natural systems, limitations of experimental techniques, and the necessity of new tools to address multi-disciplinary problems (Mateus, 2006).

Recent developments in water quality modeling show the effort to understand complex dynamics of marine ecosystems. An example of such a complex model is ERSEM (European Regional System Ecological Model), which initially was developed as a rigid two-layer model (Baretta *et al.*, 1995), followed by a 3-D configuration (Moll, 2000; Moll and Radach, 2003). Seagrasses and macroalgae were added in ERSEM in Aveytua-Alcazar *et al.* (2008).

Models for benthic communities have been developed in the past (Ménésguen, 1991; Chardy and Dauvin, 1992; Baretta-Bekker and Baretta, 1997; Duplisea, 1998; Le Pape *et al.*, 1999). Ecosystem modelling, including benthic and pelagic processes has reached high complexity (Lumborg *et al.*, 2006; Sohma *et al.*, 2008; Nobre *et al.*, 2010). Presently, models of benthic food webs based on functional approach are largely used (Heath, 2012; Morris *et al.*, 2014). Recent research focused on benthos dynamics by using Dynamic Budget theory (Filgueira *et al.*, 2012; Filgueira *et al.*, 2014; Saraiva *et al.*, 2014). Some models include organisms age classes (Bendtsen and Hansen, 2013) and transport of benthic larvae (Savina and Ménésguen, 2008).

A number of models have been documented in literature to describe seagrass dynamics (Bocci *et al.*, 1997; Elkalay *et al.*, 2003; Simas and Ferreira, 2007; Zaldivar *et al.*, 2009). Effects of climate change have also been considered (Simas *et al.*, 2001; Macreadie *et al.*, 2013).

MOHID is a water modeling system which contains, among others, modules for water quality and macroalgae modeling (Trancoso *et al.*, 2005; Deus *et al.*, 2013). The ecology of the benthos is simplified and limited to mineralization processes, occurring at the sediment-water interface. With this research study, an effort was made to include a more comprehensive representation of the benthic system in MOHID, including seagrasses, benthic producers and consumers, based on developments found in literature.

1.5. Conceptual approach

This section describes the conceptual approach used in this research to represent marine organisms, together with its limitations and advantages. The choice of state variables to be considered in the ecosystem model is complicated by the diversity of species composition of natural communities. Every species shows a different response to the variability of environmental conditions. However, there are processes at the ecosystem level that are more stable and predictable when compared to processes occurring at population or

individual level (Odum, 1971). This aspect was attributed to the presence of groups of species that perform identical functions. Over time, the species may change, but this has a relatively small influence on the functional processes, which are regulated by abiotic factors and indicate that the ecosystem as a whole shows higher stability than the population (Pomeroy *et al.*, 1988). There is a widely used method for the construction of ecological models. It consists of the aggregation of groups with similar functions regardless of their taxonomy, and the parameterization is dependent only on their size (Platt, 1985). For aquatic ecosystems, probably the simplest form of aggregation is represented by the NPZD models:

N: Nutrients (nitrate, ammonium, silicate, phosphate)

P: Phytoplankton (diatoms, dinoflagellates, autotrophic bacterioplankton)

Z: Zooplankton (heterotrophic organisms such as copepods)

D: Detritus

These models aggregate the biological components into functional groups or classes: for example, different species of phytoplankton are aggregated in the same group and state variables are defined as nitrogen and carbon inside the group itself. These functional groups correspond to the main levels of the food web: producers (i.e. phytoplankton), consumers (i.e. zooplankton) and decomposers (bacteria). A key assumption is that organisms belonging to the same functional group have the same physiological processes and that population dynamics are described in terms of fluxes of carbon and nutrients between functional groups and between organic and inorganic pools (Figure 4). Functional groups can afterwards be divided into size classes to create a more complex food web. An overview of patterns of functional groups was provided by Totterdell (1993). Many NPZD models (Figure 4) derive from the work of Fasham (1990), who formulated a model to describe an oceanic mixed layer ecosystem, divided into 7 compartments (phytoplankton, zooplankton, nitrate, ammonium, detritus, dissolved organic nitrogen, and bacteria).

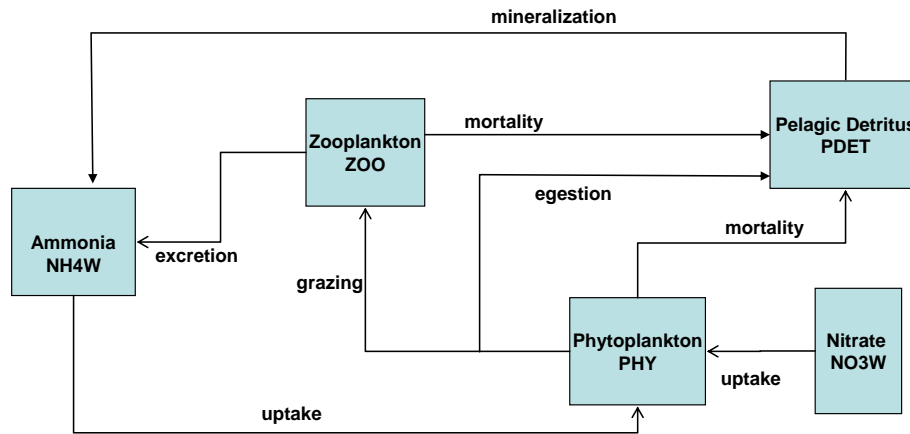


Figure 4 - Conceptual diagram of a NPZD model. The squares are used to represent functional groups (i.e. phytoplankton) and pools of inorganic matter (i.e. nitrate) and non-living organic matter (i.e. detritus). The arrows are fluxes of mass between compartments.

NPZD models have limitations in the representation of large organisms with longer life cycles compared to other organisms. For example, the increase in biomass may be due to the growth of individuals, but it can also be due to the increasing number of organisms belonging to the same size class. However, these models are suitable for the representation of aquatic organisms that are passively transported by currents and which size allows to be expressed as concentration.

The functional group approach gives a coarse representation of the complexity of the systems (Mann, 1988) with low predictive power (Cousins, 1985), but when used in conjunction with a good representation of physical factors, NPZD models can explain a substantial portion of the biology, especially if guided by high-resolution hydrodynamic processes (Hofman and Lascara, 1998).

The functional group approach (Figure 5) is usually applied to describe benthic organisms grouped according to their trophic role in the benthic food web: producers (i.e. benthic diatoms), consumers (i.e. deposit feeders) and decomposers (bacteria). Several authors used the approach of food webs for modeling of benthos (Pace *et al.*, 1984; Chardy and Dauvin, 1992; Duplisa, 1998; Le Pape *et al.*, 1999).

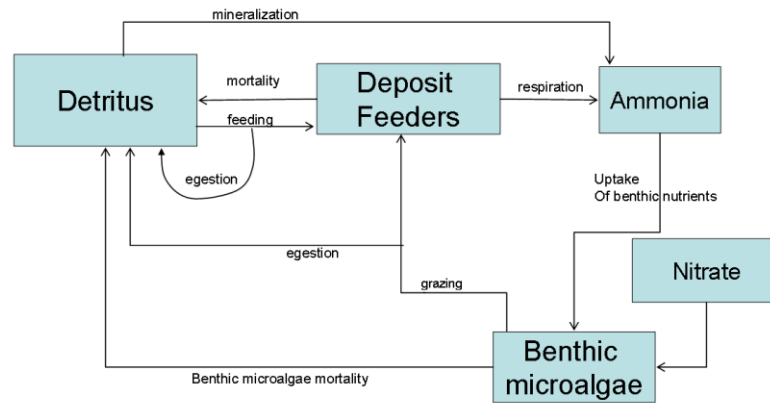


Figure 5 - Example of a conceptual diagram of a benthic food web model.

Water and substrate are the main conditioning factors for the benthic environment and are often related to each other because water penetrates downward the substrate and it can be dispersed again upward. Depth, temperature, oxygen availability, light, and salinity may affect the benthos as well. Where light reaches the bottom, benthic diatoms can proliferate.

The organic material in the water column includes a dissolved fraction (DOM, Dissolved Organic Matter) and a particulate fraction (POM, Particulate Organic Matter). The organic particles produced in the euphotic zone are transported along the water column depending on their weight, size, density difference with the surrounding medium, and are affected by physical (mixing and stratification of water masses), chemical (oxidation and reduction of chemical compounds), and biological (predation, mineralization, production of feces, etc.), processes. Organic particles deposited on the seafloor are a source of food for the benthic system and are added to in situ organic residues of dead plants and benthic animals.

The described functional is used in this study because the focus is the ecosystem and the community. However, there are also other approaches which focus on the individual and the population, such as the Dynamic Energy Budget (DEB) theory. The DEB approach is focused on the dynamics of physiological processes in the individual organism and describes the performance of an animal (growth, development, reproduction, respiration, etc.). A review of the DEB approach is given by Nisbet *et al.* (2010). DEB theory uses several state variables to characterize the state of an individual organism, thereby making the transition to population dynamics technically challenging (Nisbet *et al.*, 2010). Recently, the technical challenges are being overcome (e.g. bivalve populations (Saraiva *et al.*, 2014)), and the DEB approach is being used to simulate populations of specific organisms, and it is expected to produce

developments in the near future within the molecular, physiological and ecological domains (Sousa *et al.*, 2010).

1.6. Coupling between physical and biological processes

Models coupling physical and biological processes follow two main approaches: Lagrangian and Eulerian. The description of the two approaches and their differences is not the purposes of this research. However, in this section, a short description of the Eulerian approach is given, because this is the approach chosen in this study to describe the water properties. Additionally, this is the most commonly used approach in modeling when a point-to point comparison with observations is needed, and the model can use a suitable spatial resolution.

The most generic form of an Eulerian equation describes the evolution of a state variable P in the marine system as the sum of the variations due to transport processes and the variations due to biological processes:

$$\frac{DP}{Dt} = \left[\frac{\partial}{\partial t} + \vec{V} \cdot \nabla \right] P \quad \text{eq. 1}$$

where DP/Dt is the time rate of change inside a volume of fluid. \vec{V} is the flow velocity. $\partial/\partial t$ is the time rate of change of the fluid property at a given fixed point (local derivative). The fluid properties change due to local sources and sinks, and due to diffusion. Growth processes are considered as sources, while respiration and mortality are considered as sinks. $\vec{V} \cdot \nabla$ is the local time rate of change due to advective transport. The application of a model which describes both the physics and biology of the aquatic environment requires the solution of a set of equations, one equation for each state variable of the system, obtained by adding source and sink terms and diffusion to eq. 1:

$$\frac{DP}{Dt} = \frac{\partial P}{\partial t} + \vec{V} \cdot \nabla P = \vec{\nabla} \mu(\vec{\nabla} P) + Sources - Sinks$$

1.7. Objectives

The primary objective of this research is the design of a benthic module to simulate the dynamics of seagrasses, microphytobenthos, and benthic feeders. This module is integrated with the MOHID water modelling system, and uses the pelagic model Water Quality (IST, 2006). The integration with the MOHID modelling system is expected to provide a more comprehensive representation of marine ecosystem dynamics in coastal and estuarine waters. To achieve the objective, ecological mechanisms that control the structure and functioning of the ecosystem will be analysed to draw the conceptual diagram of the benthic ecosystem. Model equations will be formulated on the basis of the conceptual model. These equations will be checked for consistency and mass conservation. The model parameters will be assigned on the basis of literature sources, and sensitivity analysis will be carried out. Depending on data availability calibration and verification of the model will be carried out as well.

The model for seagrasses will be used to simulate the biomass of the seagrass *Zostera noltii*, one of the most common seagrass species in Ria de Aveiro and in Portuguese estuaries. The model will be used for simulating the seasonal pattern of deposit feeders and filter feeders in response to physical and biological factors, such as temperature variability, organic matter inputs and phytoplankton dynamics, as inputs from the MOHID water modelling system. In particular, the benthic ecology model will be used to test the feedback effect of filter feeders on phytoplankton at the water-sediment interface. These objectives are relevant for the assessment of the quality of marine coastal waters, because they are related with the control of eutrophication. These objectives are relevant for coastal habitat conservation as well, because seagrasses contribute to create habitat for feeding, breeding, and sheltering of protected species.

1.8. Hypotheses

In the introductory part of this chapter, the main aspects of the benthic-pelagic coupling in coastal water were outlined. In this research, the model will be used to address questions related to benthic ecosystems dynamics, such as the competition between seagrasses and macroalgae, and the control of primary production by benthic filter feeders. To be more specific, the hypotheses of the study will be grouped under two research questions (Q1 and Q2):

Q1: When the growth of seagrasses limited by macroalgae?

Q2: Can the model reproduce the control by filter feeders on phytoplankton biomass?

Regarding Q1, the hypothesis is that competition between primary producers may occur because of light, nutrients, and space. Modelling efforts have been recently addressed to understand the mechanisms of seagrass decline, to predict seagrass biomass, and to determine which factors lead to predominance of macroalgae over seagrass beds (Bocci *et al.*, 1997; Plus *et al.*, 2003; Aveytua-Alcazar *et al.*, 2008; Zaldivar *et al.*, 2009). In oligotrophic systems, with ample light availability, primary producers compete for nutrients (Passarge *et al.*, 2006). Seagrasses have roots which enable to sequester nutrients from the sediment and to survive to lack of nutrients in the water (Falls, 2008). In eutrophic systems with an ample nutrient supply, primary producers may compete for light. Fast growing macroalgae can occupy the space available to other primary producers, and shadow species that are confined to the bottom, such as rooted plants and benthic microalgae. For this reason, space availability is another factor of competition between primary producers. Nutrient inputs from anthropogenic activities may cause an increase of primary production and change the balance between primary producers in shallow-water estuarine systems. Following this, in relation to the research question, three hypotheses are formulated to assess the competition between *Zostera noltii* and macroalgae:

H1.1: The growth of *Zostera noltii* is limited by light availability in presence of macroalgae

H1.2: The growth of *Zostera noltii* is limited by nutrient availability in presence of macroalgae

H1.3: The growth of *Zostera noltii* is limited by space availability in presence of macroalgae

To verify the three hypotheses, the seagrass model developed in this research was tested in Ria de Aveiro, a shallow coastal lagoon of Portugal where *Zostera noltii* is a common species of the local seaweed. MOHID will be set up to simulate the spatial and temporal dynamics of *Zostera noltii* and macroalgae. A real case study application is described in Chapter 5. This solution will be used as a reference scenario. The model results are verified against real observations in the reference scenario.

In Chapter 6, a scenario will be built to simulate *Zostera noltii* and macroalgae in Ria de Aveiro. The results will be compared with the reference case study of Chapter 5. To assess the three hypotheses, the *Zostera noltii* growth limiting factors will be analysed to understand if the simulated species is limited by light, nutrients, and space availability in presence of macroalgae.

Regarding Q2, several researchers investigated the role of benthic bivalve filter feeders in the control of the primary production in the water column (Cloern, 1982), in the context of an increasing concern about the link between eutrophication and water quality. Water enrichment in nutrients may cause phytoplankton blooms and uncontrolled growth of other aquatic algae, such as macroalgae. Some undesirable effects of eutrophication are related to high concentrations of organic matter and toxic substances produced by some species of algae. Several natural factors can control the phytoplankton production, such as temperature, light, nutrient availability, residence time of water, and grazing by upper levels of the food web. Benthic bivalve filter feeders may have an important role in controlling the primary production in the water column. Officer *et al.* (1982) pointed benthic filter feeders as a natural eutrophication control in the San Francisco Bay, California. Le Pape *et al.* (1999) found that the grazing of phytoplankton by benthic filter feeders can reduce more than 50% of chlorophyll concentrations in the Bay of Brest. Based on these considerations, the following hypothesis is taken into account:

H2.1: Filter feeders in the model control phytoplankton by grazing

The model developed in this research will be used to assess the feedback of benthic bivalve filter feeders on phytoplankton concentrations in the water. To verify the hypothesis, feedbacks between benthic and pelagic systems will be identified by executing scenarios to detect the effect of presence/absence of components and processes described in the model, with a focus on the interactions between the filter feeders and producers. The feedback of filter feeders grazing on phytoplankton will be assessed by using a schematic case study described in Chapter 4.

Chapter 2 – Model formulation

This chapter delineates the formulation of the model developed in this research. The main assumptions of the model are listed, as well as its theoretical basis and limitations. The link between the ecological model and the MOHID modelling system is described as well.

2.1. Introduction

In this introduction the main assumptions of the model will be described, including its limitations. The diagram in Figure 6 describes the main components of the marine ecosystem.

The benthic ecosystem includes nutrients, microphytobenthos, filter feeders, deposit feeders, and seagrasses. Microphytobenthos represents benthic microalgae which live at the water-sediment interface and uptake nutrients from the water and from the sediment interface. Deposit feeders (such as *Alkmaria romijni*, *Melinna palmate*, *Tharyx* sp., *Corophium multisetosum*, common in Ria de Aveiro,(Nunes *et al.*, 2008)) are invertebrate organisms which feed on microphytobenthos and on bottom particulate organic matter. Filter feeders feed only on suspended organic matter. Seagrasses have roots that grow down into the sediment. Seagrass leaves uptake nutrients from water column and seagrass roots uptake nutrients from sediment. Inorganic nutrients produced by respiration are returned to the water and can be used by primary producers.

A detailed description of the main components of the benthic module is given in specific sections of this chapter. Conceptual diagrams, equations and parameters are provided as well.

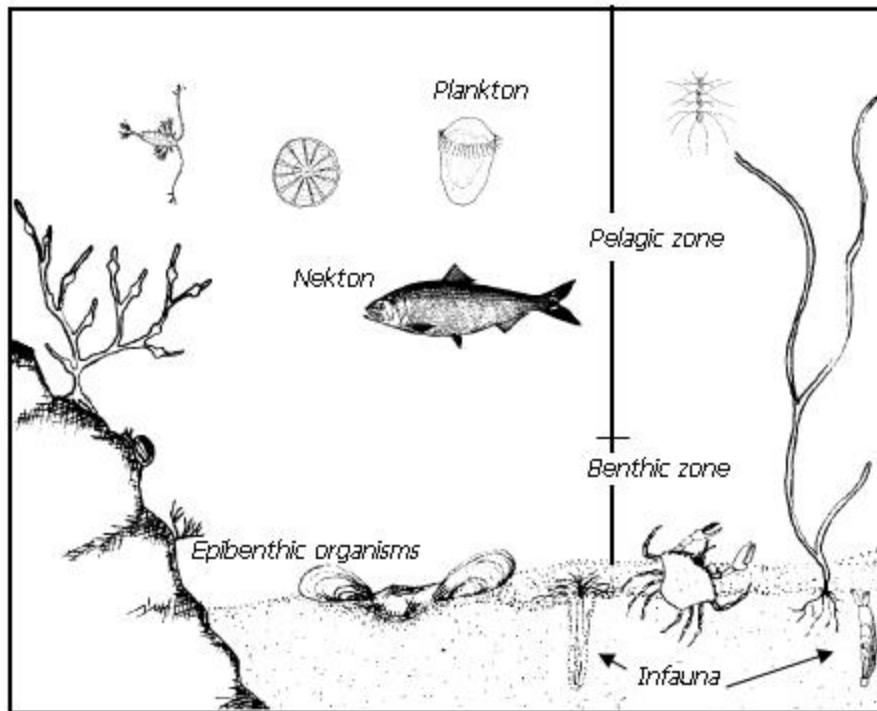


Figure 6 - Overview of the marine ecosystem. (Source: <http://www.glf.dfo-mpo.gc.ca/Gulf/By-The-Sea-Guide/The-Nearshore>)

2.2. Assumptions

A model is a simplified description of a real system and as such it does not contain all the properties of the real system, but only those ones which are necessary to describe the main processes. Models are generally based on several assumptions used as a baseline to define what the modeler considers relevant or not relevant for the description of the system. In this section, the main assumptions of the model used in this study, together with their limitations, are described.

The shallow water equations derived from the Navier-Stokes equations are physically based and demonstrated to be an appropriate tool for the description of the physics of the marine environment. On the contrary, the formulation of equations for the biological state variables is empirical and thus affected by many uncertainties due to the complexity and limits of knowledge about the marine ecosystem. Parameterizations used in biogeochemical modelling often neglect processes which may be important on small-scale. The limits due to approximations are more relevant in systems where the dynamics are dominated by local processes (Prandle *et al.*, 1993).

There is no model which offers a comprehensive description of all biological processes occurring in the marine system. In most cases, models are formulated to solve a specific problem, and the number of state variables is reduced to the necessary minimum to describe the system of interest. The modeller who wants to simulate biological properties of an ecosystem is facing uncertainties arising in the formulation of the conceptual diagram (Which/How many ecological components should be considered?), in the connections between components (How many links between ecosystem components should be considered?), in the parameterization of processes (Which processes should be expressed explicitly, which ones should be parameterized, which ones should be neglected?), and in the assignation of parameter values (Are there established values for biological parameters? Are biological parameters site specific?). In this section, the main assumptions used in this research are described, along with their basis and limitations.

2.2.1. Driving factors

This research was carried out under the assumption that tides, winds, and freshwater inflows the main forcing mechanisms for the water circulation. These forcing mechanisms are provided to the model as boundary conditions, estimated by wider models, or as measured time series. The ecological system is controlled mainly by water fluxes, temperature, incident light and nutrient discharges. Temperature controls the physiological processes of organisms. Many rates are modulated by temperature. This generic statement applies to physical, chemical, and physiological rates (Soetaert and Herman, 2001). Some biological rates may double or even triple with every 10° increase of temperature, but above some critical values, certain enzymes may denaturalize and organisms may die. There is thus a temperature tolerance interval where biological processes occur. Inside this interval, for temperatures lower than the optimal value, metabolic rates increase with temperature until the optimal temperature is reached at which the metabolic rates occur at their maximum value. For temperatures higher than the optimal value, a decline of metabolic rates is observed.

The fraction of light available for photosynthesis is known as Photosynthetic Active Radiation (PAR). In water, the decline of light with depth affects the distribution of organisms. “The response of photosynthesis to light is a well-known process, both from a biochemical and a physiological perspective. The typical response is a saturation curve, above a certain photosynthetic photon flux and a linear response at low light level. This reflects the

properties of the photosystem, which is light-limited at low light levels and limited by the functioning of the enzyme system at high light levels. Above a certain threshold, this may even lead to light inhibition, generating lower rates of photosynthesis than at the optimal light intensity. There are several mathematical formulations to describe this functional form, involving either one or two parameters. Some include light inhibition, other do not take this into account” (Soetaert and Herman, 2001; Soetaert, 2010). In this study, light inhibition was taken into account.

The model described in this research accounts for limitation due to nutrient availability for primary producers. “Nutrients are considered a key factor for pelagic and benthic primary producers. Nutrients from terrestrial systems wash into lakes and oceans, where additional primary production by phytoplankton and algae helps support large communities of zooplankton, fish, sea mammals, and birds [...]. Nitrogen and phosphorus are essential elements in living organisms, where they play central roles in the makeup of proteins, nucleic acids, and energetic compounds. These elements are not always readily available to organisms, so nutrient limitations can powerfully constrain biological strategies” (Malmstrom, 2012). To account for nutrient limitation, the model developed in this research includes the dependence of primary producers’ growth rates on nutrient availability. To do this, nutrient limiting factors are applied to the growth rates as multiplicative dimensionless factors.

2.2.2. Seagrass nutrient content

The Redfield ratio (Redfield, 1958) has been demonstrated to be stable in deep waters, although substantial deviations from the Redfield stoichiometry associated with the biological production have been reported (Sambrotto *et al.*, 1993). Nevertheless, the Redfield ratio is still used as a general average ratio which shows little variations in the long term and on the large scale basis (Körtzinger *et al.*, 2001). In seagrass models, the nutrient quota is considered variable because these organisms have specific mechanisms based on the variation of the nutrient content (Duarte, 1990). Accordingly, several authors found that carbon:nutrient (N and P) ratios in seagrasses are inversely related to changes in the nutrient content (Duarte, 1990), and that the rate of change in C:N and C:P ratios with increasing nitrogen or phosphorus content in plant tissues should shift from high to small as nutrient supply meets the plant’s demands. In this research, the seagrass nutrient quota is considered to be variable,

and the change in nutrient quota is used to assess the nutrient limitation, in conformity with Duarte (1990).

2.2.3. Organisms' mobility

In this research, one of the assumptions is that benthic flora and fauna have no horizontal movement on the sea bottom. Benthic organisms are not transported by currents, and their individual displacement capacity is small. This assumption is based on the consideration that, although some species of benthic fauna have movement capabilities, they are limited in the displacements and their movements are negligible if compared with the spatial scale of the movements occurring in the water column and with the model spatial resolution.

2.2.4. The vertical dimension

All benthic animals in this research were assumed to have no height, unless their height is comparable to the scale of the water depth. This assumption is based on the consideration that the size of most benthic organisms ranges between a fraction of millimeters and a few centimeters, which is negligible if compared with the spatial scale of most processes occurring in the water column. The consequence of this assumption is that the activity of benthic organisms is confined to the sea bottom and at the sediment-water interface.

On the contrary, plants and macroalgae were assumed to have a vertical dimension because they may have long leaves. As an example, seagrass leaves access nutrients and light at different depths. It is known that according to the type of species, the season and the stage of development of the plant, the leaves can reach several meters of length and the plants extend vertically in the water column. Therefore, in this research it was assumed that the seagrasses have a varying leaves height and that their activity is exerted until the top of the canopy height.

Seagrass roots were assumed to grow vertically down into the sediment. It is known that seagrass roots are found to be typically between the upper 2 and 40 cm of sediments (Fonseca and Thayer, 1990). The average depth occupied by the roots ranges between 1 and 14 cm below the surface of the sediment, depending on the species, as shown in Duarte *et al.*

(1998). However, in some species (i.e. genus *Zostera*), roots can grow both vertically and horizontally, with simple or branching shapes and fine hairs to facilitate nutrient absorption. In this research, it was assumed that seagrass roots grow only vertically down into the sediment. This is a model limitation, because horizontal growth is not explicitly represented. To parameterize the horizontal growth it was assumed that roots have a high biomass:length ratio. This hypothesis implies that the sediment column is accessed by roots even with low values of belowground biomass.

2.3. Units

In MOHID, all properties that are located on interfaces (water surface of bottom sediment) are expressed as mass per square meter in (kg/m^2). Properties of the water column are expressed as concentrations (g/m^3). The filter feeders, deposit feeders, microphytobenthos, and organic matter on the bottom sediment, are expressed as biomass in kg/m^2 . Seagrasses are expressed as biomass in $\text{kg DW}/\text{m}^2$. The choice of DW (dry weight) for seagrasses is due to the fact that most of the parameters found in literature are referred to dry weight of the plant's tissue. Moreover, existing models of seagrasses (Bocci *et al.*, 1997; Elkalay *et al.*, 2003) use dry weight to express seagrass biomass. Measurements of seagrass biomass available in literature are also expressed as dry weight (Silva *et al.*, 2009). The choice of dry weight to express seagrass biomass in the model simplifies the comparison of model results with existing data.

2.4. Conceptual model and equations

In this section, a description of the benthic model is provided. The benthic ecosystem includes seagrasses, microphytobenthos, filter feeders, and deposit feeders. Seagrasses are aquatic rooted plants which can uptake nutrients from the water and sediment. Microphytobenthos represents benthic microalgae which live on the surface of bottom sediment and uptake nutrients from the water-sediment interface. Deposit feeders are invertebrate organisms which feed particulate organic matter deposited on the bottom sediment. In the model, deposit feeders feed on microphytobenthos and detrital organic matter available on the surface of bottom sediment. Filter feeders feed only on organic matter that is suspended in the water-sediment interface. The overview of the benthic model is given in

Figure 7. In this chapter, the description of the model is provided in detail, starting from seagrasses, then benthic feeders and microphytobenthos.

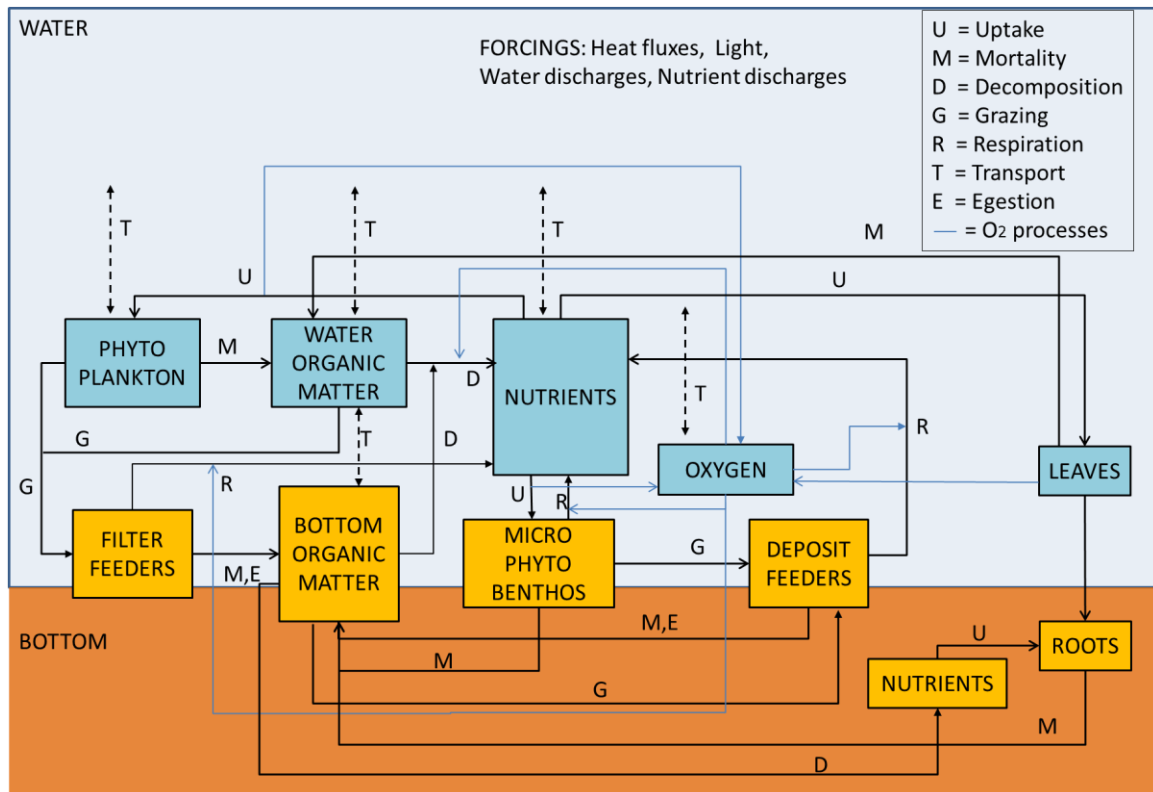


Figure 7 - Conceptual overview of the benthic model.

2.4.1. Seagrasses

A number of existing models included representation of seagrass dynamics, including formulations uptake of dissolved inorganic nitrogen, and processes related to the plant's nutrient content (Bocci *et al.*, 1997; Aveytua-Alcazar *et al.*, 2008; Zaldivar *et al.*, 2009). Dissolved inorganic phosphorus is a dominant component in total phosphorus pools in marine coastal waters and it was identified as a limiting nutrient to seagrass production (Touchette and Burkholder, 2000; Zhang and Huang, 2011). Seagrasses uptake phosphorus mainly through roots (McRoy and Barsdate, 1970). Seagrass models should include uptake of both nitrogen and phosphorus. In this study, a seagrass model was proposed which to include the main characteristics of all seagrasses. The model development followed existing approaches (Bocci *et al.*, 1997; Aveytua-Alcazar *et al.*, 2008; Zaldivar *et al.*, 2009) used for modelling of seagrasses by taking into account leaves, roots, variable nutrient content, and uptake of

nutrients through roots and leaves. Furthermore, the model includes phosphorus metabolism in the plant.

Conceptual diagram

The diagram in Figure 8 shows the conceptual model of seagrass developed in this research. The plants can uptake nutrients from water and from bottom sediments. The nutrients are represented in the model as nitrate ($\text{NO}_{3\text{w}}$) and ammonia ($\text{NH}_{4\text{w}}$) in the water, ammonia in the sediment ($\text{NH}_{4\text{s}}$), phosphate in the water ($\text{PO}_{4\text{w}}$), and phosphate in the sediment ($\text{PO}_{4\text{s}}$). Nutrient content inside plant is nitrogen (N) and phosphorus (P). Part of the carbon fixed by leaves (L) is transferred to roots (R). Mortality of leaves and roots generates detrital organic matter (OM) in the water and in the sediment, respectively. Mineralization of organic matter regenerates nutrients.

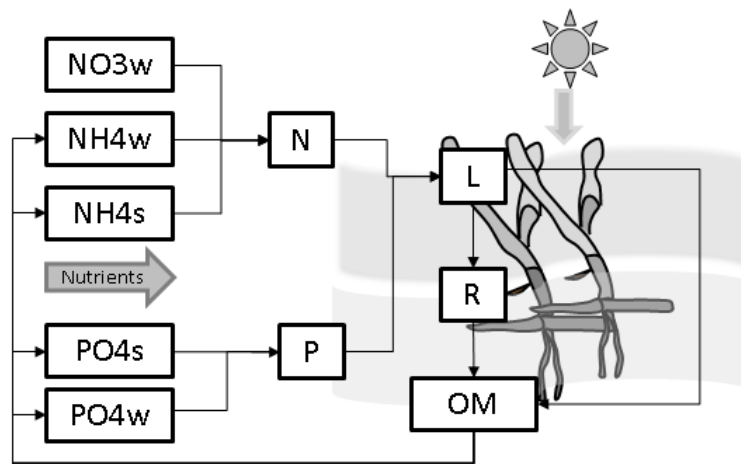


Figure 8 - Conceptual model of seagrass.

The seagrass model included the following state variables:

- Leaves biomass - L (kg DW/m^2);
- Roots biomass - R (kg DW/m^2);
- Plant's nitrogen content - N (g N/m^2);
- Plant's phosphorus content- P (g P/m^2);

- Ammonia in water - $NH4_w$ (g N/m³);
- Nitrate in water - $NO3_w$ (g N/m³);
- Ammonia in sediment - $NH4_s$ (g N/m³);
- Particulate organic nitrogen in water - PON_w (g N/m³);
- Particulate organic phosphorus in water - POP_w (g P/m³);
- Particulate organic nitrogen in sediment - PON_s (g N/m³);
- Particulate organic phosphorus in sediment - POP_s (g P/m³); and,
- Phosphate in sediment $PO4_s$ (g P/m³).

OM in Figure 8 is a generic designation to indicate state variables which represent detrital organic matter such as particulate organic nitrogen in water (PON_w), particulate organic phosphorus in the water (POP_w), particulate organic nitrogen in the sediment (PON_s), and particulate organic phosphorus in the sediment (POP_s).

Governing equations

A system of Ordinary Differential Equations (ODEs) was formulated. Leaves and roots dynamics were expressed as:

$$\frac{dL}{dt} = (1 - tr)G \cdot L - m_l \cdot L \quad \text{eq. 2}$$

$$\frac{dR}{dt} = tr \cdot G \cdot L - m_r \cdot R \quad \text{eq. 3}$$

where G is the gross growth rate (1/day) representing new material produced through photosynthesis, m_r is the roots' mortality rate (day⁻¹), and m_l is the leaves mortality rate (day⁻¹). Carbon transfer from leaves to roots was parameterized by using a translocation coefficient tr (dimensionless), based on Olesen and Sand-Jensen (1993). This coefficient is used in other seagrass models (Bocci *et al.*, 1997; Elkalay *et al.*, 2003; Zaldivar *et al.*, 2009).

Gross growth rate G (1/day) is formulated as:

$$G = g_{\max} \cdot F(T) \cdot F(I) \cdot F(L) \cdot F(N, P) \quad \text{eq. 4}$$

where g_{\max} is the maximum growth rate (1/day). $F(T)$ is the dimensionless temperature limiting factor (Appendix A). $F(I)$ is the dimensionless light limiting factor (eq. 5). $F(L)$ is the dimensionless space limiting factor (eq. 6). $F(N, P)$ is the dimensionless nutrient limiting factor, (eq. 7). Limiting factors can vary between 0 (total limitation) and 1 (no limitation), when the maximum growth rate is obtained.

Temperature limitation

The dependence of growth on temperature is expressed by a bell-shaped function for $F(T)$ described in Trancoso (2002), which values are 0 at the limits of the temperature tolerated by the plant, and 1 at optimal temperature. This formulation is also used by other authors (Bocci *et al.*, 1997; Elkalay *et al.*, 2003; Zaldivar *et al.*, 2009). Equations for the temperature limitation are given in Appendix A.

Light limitation

The light limiting factor $F(I)$, defines the relationship between ambient light levels and the primary producers' photosynthetic rate (Trancoso, 2002). In this model, seagrass growth dependence on light is described with a Michaelis-Menten kinetics according to experimental observations on growth (Dennison, 1979; Drew, 1979; Olesen and Sand-Jensen, 1993) and on photosynthesis dependence (Marsh *et al.*, 1986; Bulthuis, 1987). Half-saturation constant for growth (KL) has been estimated from data reported by Olesen and Sand-Jensen (1993) at a temperature of 21°C (Bocci *et al.*, 1997).

$$F(I) = \frac{I_c}{I_c + KL} \quad \text{eq. 5}$$

where I_c is the light available at the top of the seagrass canopy height calculated according to Steele (1962). KL in is the half-saturation constant for light, equal to about 500 kcal/m²/day (or 24 W/m²) (Bocci *et al.*, 1997).

Space limitation

The space limiting factor was proposed in other models for above- and below-ground biomass (Verhagen and Nienhuis, 1983; Bocci *et al.*, 1997; Elkalay *et al.*, 2003). In the seagrass model, a simple space limiting factor $F(L)$ (dimensionless), the equation from Bocci *et al.* (1997) based on the maximum leaves biomass only, was modified to include the dependence on the biomass of macroalgae:

$$F(L) = \left(\frac{L}{L+M} \right) \min \left[1, \max \left(0, 1 - \frac{L}{K_{\max}} \right) \right] \quad \text{eq. 6}$$

where K_{\max} (kg DW/m²) is the maximum biomass of seagrass leaves. M (kg DW/m²) is the biomass of macroalgae. If $M=0$, the space limiting factor depends only on the leaves biomass. If $M \neq 0$, the space available for seagrasses leaves depends also on the presence of other plants and macroalgae in the system. The maximum biomass of plants varies with the type of species and differentiates them in the model. Some values of K_{\max} were found in literature for some seagrass species. As an example, a modeling study developed for *Posidonia oceanica* (Elkalay *et al.*, 2003), used a maximum leaves biomass value of 0.750 kg DW/m². A modeling study developed for *Zostera marina* (Bocci *et al.*, 1997), used a maximum leaves biomass value of 0.5 kg DW/m².

Nutrient limitation

The nutrient limitation was expressed as:

$$f(N, P) = \min(f(P), f(N)) \quad \text{eq. 7}$$

where:

$$f(N) = \max \left(0, \min \left(1, \frac{1000 \frac{N}{L+R} - N \min}{N_{crit} - N \min} \right) \right) \quad \text{eq. 8}$$

$$f(P) = \max \left(0, \min \left(1, \frac{1000 \frac{P}{L+R} - P \min}{P_{crit} - P \min} \right) \right) \quad \text{eq. 9}$$

where N_{min} (g N/kg DW) and P_{min} (g P/kg DW) are the minimum nitrogen quota and the minimum phosphorus quota, respectively. N_{crit} (g N/kg DW) and P_{crit} (g P/kg DW) are the critical nitrogen quota and the critical phosphorus quota, respectively (Duarte, 1990; Bocci *et al.*, 1997). The multiplication by 1000 is done to convert P from kg P/m² to g P/m².

N and P increase with uptake of external nutrients, and decrease with the plant's growth. The dynamics of nitrogen and phosphorus content are described as:

$$\frac{dN}{dt} = \frac{U_N - G \cdot L \cdot r_N}{1000} \quad \text{eq. 10}$$

$$\frac{dP}{dt} = \frac{U_P - G \cdot L \cdot r_P}{1000} \quad \text{eq. 11}$$

The total uptake of nitrogen U_N (g N/m²/day), following the Michaelis-Menten kinetics (Bocci *et al.*, 1997; Elkalay *et al.*, 2003; Zaldivar *et al.*, 2009), is given as:

$$U_N = U_{NH_4}^w + U_{NO_3}^w + U_{NH_4}^s \quad \text{eq. 12}$$

The superscript w indicates uptake from water and s indicates uptake from sediment. $U_{NH_4}^w$ is the uptake of ammonia from water (g N/m²/day):

$$U_{NH4}^W = V_{\max}^{NH4w} \cdot \frac{NH4_w}{NH4_w + K_{NH4w}} \cdot fbn \cdot L \cdot 1000 \quad \text{eq. 13}$$

U_{NO3}^W is the uptake of nitrate from water (g N/m²/day):

$$U_{NO3}^W = V_{\max}^{NO3w} \cdot \frac{NO3_w}{NO3_w + K_{NO3w}} \cdot fbn \cdot L \cdot 1000 \quad \text{eq. 14}$$

U_{NH4}^S is the uptake of ammonia from sediment (g N/m²/day):

$$U_{NH4}^S = V_{\max}^{NH4s} \cdot \frac{NH4_s}{NH4_s + K_{NH4s}} \cdot fbn \cdot R \cdot 1000 \quad \text{eq. 15}$$

where V_{\max}^{NH4w} (kg N/kg DW/day), V_{\max}^{NO3w} (kg N/kg DW/day), and V_{\max}^{NH4s} (kg N/kg DW/day), are the maximum uptake rate of ammonia from water, the maximum uptake rate of nitrate from water, and the maximum uptake rate of ammonia from sediment, respectively.

The term fbn (eq. 16) describes the feedback of nitrogen content on the uptake of external nutrients (Bocci *et al.*, 1997):

$$fbn = \max \left(0, \min \left(1, \frac{N_{\max} - 1000 \frac{N}{L+R}}{N_{\max} - N_{\min}} \right) \right) \quad \text{eq. 16}$$

N_{\max} (g N/kg DW) is the maximum nitrogen quota (Bocci *et al.*, 1997). The uptake of phosphate U_P (g P/m²/day), is given as:

$$U_P = U_{PO4}^W + U_{PO4}^S \quad \text{eq. 17}$$

where:

$$U_{PO4}^W = V_{\max}^{PO4} \cdot \frac{PO4_w}{PO4_w + K_{PO4}} \cdot fbp \cdot L \cdot 1000 \quad \text{eq. 18}$$

$$U_{PO4}^S = V_{\max}^{PO4} \cdot \frac{PO4_s}{PO4_s + K_{PO4}} \cdot fbp \cdot R \cdot 1000 \quad \text{eq. 19}$$

where V_{\max}^{PO4} (kg P/kg DW/day) is the maximum uptake rate of phosphate. K_{NH4w} (g N/m³), K_{NO3w} (g N/m³), K_{NH4s} (g N/m³), and K_{PO4} (g P/m³), are the half-saturation concentrations for the uptake of ammonia from water, the half-saturation concentration for the uptake of nitrate from water, the half-saturation concentration for ammonia uptake from sediments, and the half-saturation concentration for phosphate uptake, respectively.

The feedback of phosphorus content on the phosphate uptake is described as:

$$fbp = \max \left(0, \min \left(1, \frac{P_{\max} - 1000 \frac{P}{L+R}}{P_{\max} - P_{\min}} \right) \right) \quad \text{eq. 20}$$

where P_{\max} (g P/kg DW) is the maximum phosphorus quota (Duarte, 1990). Mineralization of organic matter leads to recycling of nutrients (eq. 21 to eq. 24). For mass conservation, mortality of seagrasses is added to the organic matter pools:

$$\frac{dPON_s}{dt} = m_r \cdot R \cdot r_N \cdot \frac{1}{D_s} - \min_s PON_s \quad \text{eq. 21}$$

$$\frac{dPOPs}{dt} = m_r \cdot R \cdot r_p \cdot \frac{1}{D_s} - \min_s POPs \quad \text{eq. 22}$$

$$\frac{dPON_w}{dt} = m_l \cdot L \cdot r_N \cdot \frac{1}{D_w} - \min_w PON_w \quad \text{eq. 23}$$

$$\frac{dPOP_w}{dt} = m_l \cdot L \cdot r_p \cdot \frac{1}{D_w} - \min_w POP_w$$

eq. 24

where D_w (m) and D_s (m) is the thickness of the water layer and the thickness of the sediment layer, respectively. \min_s and \min_w is the mineralization rate in water and in sediment. For mass conservation, uptake of nutrients was subtracted from the equations for $NH4_w$, $NO3_w$, $NH4_s$, and $PO4_s$ (eq. 25 to eq. 29).

$$\frac{dNH4_w}{dt} = -U_{NH4}^W \frac{1}{D_w} + \min_w PON_w$$

eq. 25

$$\frac{dNH4_s}{dt} = -U_{NH4}^S \frac{1}{D_s} + \min_s PON_s$$

eq. 26

$$\frac{dNO3_w}{dt} = -U_{NO3}^W \frac{1}{D_w}$$

eq. 27

$$\frac{dPO4_s}{dt} = -\frac{U_{PO4}^S}{D_s} + \min_s POP_s$$

eq. 28

$$\frac{dPO4_w}{dt} = -\frac{U_{PO4}^W}{D_w} + \min_w POP_w$$

eq. 29

The growth of the plant generates oxygen production in the water. The mineralization of organic matter consumes oxygen from the water. The oxygen state variable in the water is updated as:

$$\frac{dO_2}{dt} = G \cdot L \cdot r_C \cdot \frac{1}{D_w} \cdot \frac{32}{12} - \min_w \cdot PON \cdot r_{NC} \cdot \frac{32}{12}$$

eq. 30

where O_2 is in mg O_2/l , (that is the same as g O_2/m^3). r_C is the ratio g C: kg DW in seagrasses (Duarte, 1990). 32 is the molecular weight of oxygen and 12 is the atomic weight

of carbon. r_{NC} is the ratio g N: g C in organic matter (Redfield, 1958). The process of mineralization in the water is calculated by the WaterQuality module in MOHID. For this reason it is not described in this section, and it can be found in the Water Quality manual (IST, 2006).

The mineralization process in the sediment is responsible for oxygen depletion, but it is also regulated by oxygen availability. Following the approach used in the MOHID benthos module¹, the oxygen limiting function is computed as:

$$f(O_2) = \frac{O_2}{O_2 + 0.5} \quad \text{eq. 31}$$

where O_2 is the oxygen concentration in mg O_2/l (or g O_2/m^3). Mineralization is computed as:

$$\min_s = \begin{cases} k_{\min s} \cdot f(O_2) & O_2 > O_{2\min} \\ 0.3 \cdot k_{\min s} \cdot f(O_2) & O_2 \leq O_{2\min} \end{cases} \quad \text{eq. 32}$$

where $k_{\min s}$ (1/day) is the reference mineralization rate for organic matter. If oxygen level reaches a minimum ($O_{2\min}$), anaerobic mineralization occurs at a rate that is 30% of the mineralization rate in aerobic conditions. This percentage was established by following the CAEDYM model (Hipsey *et al.*, 2003).

Plant's decay

The plant's decay rate is a function of plant's photoperiodicity. Several authors express the plant's decay as a function of respiration only, with the respiration rate increasing exponentially with temperature (Bocci *et al.*, 1997; Elkalay *et al.*, 2003; Zaldivar *et al.*, 2009). Some authors include exudation and natural mortality as constant rates (Aveytua-Alcazar *et al.*, 2008), or as a function of temperature and wind speed (Plus *et al.*, 2003). Seagrasses are

¹ (http://www.mohid.com/wiki/index.php?title=Module_Benthos)

vascular plants, and, similarly to terrestrial plants, are subject to leaves abscission before winter, when the duration of daylight shortens. In many temperate systems, fall is characterized by high absolute amounts of litter export because many seagrasses shed most of their leaves biomass in fall (Mateo *et al.*, 2006). Dead leaves are transported by the action of waves and currents. In this formulation, the plant's photoperiodicity and the mortality were expressed as:

$$m_t = m_{t0} e^{(q_f - q_t)} \quad \text{eq. 33}$$

where m_{t0} is the mortality rate, q_f is the daylight duration (9.5 hours) in fall, and q_t is the daylight duration (hours) at the simulation time t , calculated according to Forsythe *et al.* (1995). The same type of equation was used for roots decay rate, by replacing m_{t0} with m_{r0} , that is the roots mortality rate (1/day).

Canopy height

The canopy height is the average height of seagrass beds, and it depends on the length of the leaves and on the height of the water column. As an example, *Zostera noltii*, a largely diffuse species found in Portuguese estuaries, has ribbon-shaped, dark green leaves of 0.5-1.5 mm width and approximately 20 cm length (Phillips and Meñez, 1988). *Zostera noltii* canopy height can reach 10-20 cm (Paul *et al.*, 2011). *Zostera marina* is the dominant seagrass species in the northern Atlantic, but it is widely distributed in the northern Pacific as well (Short *et al.*, 2007). Its ribbon-shaped, dark green leaves generally grow 20-50 cm in length (although lengths up to 3 m have been observed) and vary in width between 2 and 10 mm (Fonseca and Cahalan, 1992). In this research it was assumed that the biomass of the leaves is proportional to the length of the leaves, thus the length of the leaves can be calculated from leaves biomass, by using an average ratio between leaves length and biomass. In this study, this ratio is indicated by the symbol r_{lb} ($\text{m}^3/\text{g DW}$). Some typical values of r_{lb} for *Zostera* species were drawn from data found in literature and summarized in Table 1.

Table 1 – Average ratio between leaves length and biomass for some seagrass species.

Specie	r_{lb} (m ³ /g DW)	Location	Reference
<i>Zostera marina</i>	0.008-0.02	California	Tennant (2006)
<i>Zostera capricorni</i>	0.0002-0.02	Australia	McKenzie (1994)
<i>Zostera caulescens</i>	0.008-0.123	Japan	Komatsu <i>et al.</i> (2003) Nakaoka <i>et al.</i> (2003)
<i>Zostera noltii</i>	0.002-0.005	France	Plus <i>et al.</i> (2001)

Light availability

When seagrass leaves are submerged, light availability decreases due to water deepening. During low tide, leaves proximity to the water surface increases, as well as light availability (Koch *et al.*, 2006). Leaves are bent by the flow during ebb tide as shown in Figure 9.

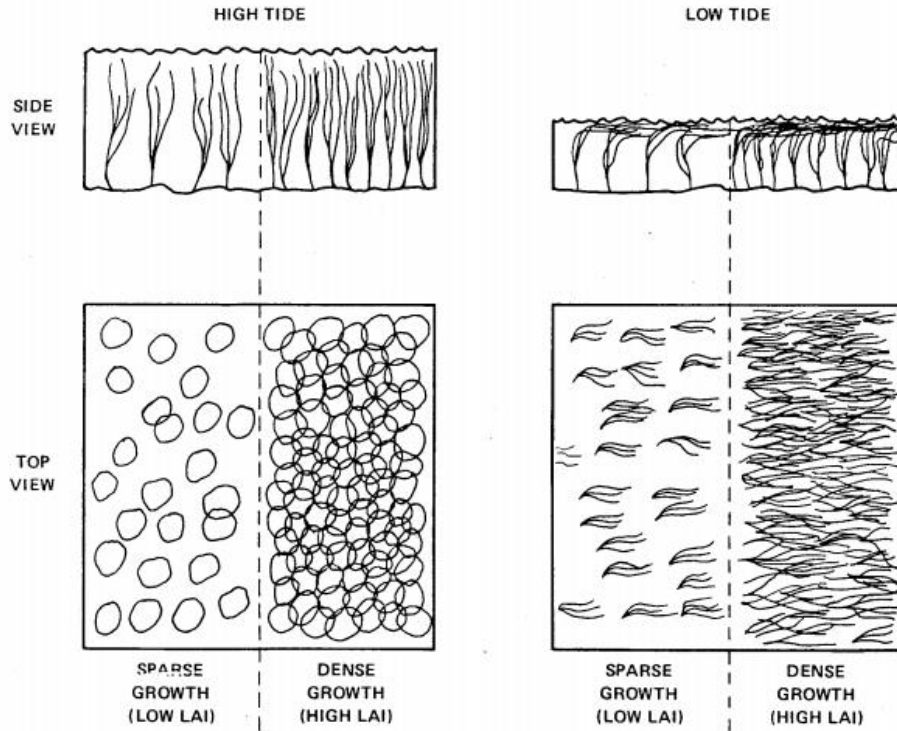


Figure 9 – Diagram of tidal influence on leaves canopy structure of *Zostera* plants. At high tide (left), the circles represent space occupied by plants with high density. At low tide (right), the lines represent leaves floating at the water surface. After Dennison (1979).

During ebb tide, the canopy height is shorter, and the leaves are floating on the water surface. In this situation, the leaves access the light available at the water surface. During flood tide, the plants are submerged, and light available at the top of canopy is lower because of light extinction with increasing depth. Following the conceptual diagram in Figure 9, the height of the canopy (h_c) can be calculated as the minimum between the length of the leaves (l_s), and the water depth (DZ):

$$h_c = \min(l_s, DZ) \quad \text{eq. 34}$$

l_s can be estimated from the average ratio between length and biomass of leaves (Table 1):

$$l_s = \min(1000 \times L \times r_{lb}, l_{max}) \quad \text{eq. 35}$$

where l_{max} (m) is the maximum leaves length. The light extinction along the depth is calculated by using the Steele's formulation. Considering that the water depth changes with tide, and that the length of the leaves changes with biomass, light availability at the top of the canopy changes dynamically with the height of the canopy and with the water depth:

$$I_c = \begin{cases} I_0 e^{-k(DZ-h_c)} & h_c < DZ \\ I_0 & h_c \geq DZ \end{cases} \quad \text{eq. 36}$$

where I_0 (W/m^2) is the light at the sea surface, and k ($1/\text{m}$) is the light extinction coefficient. An illustration of eq. 36 is provided in Figure 10.

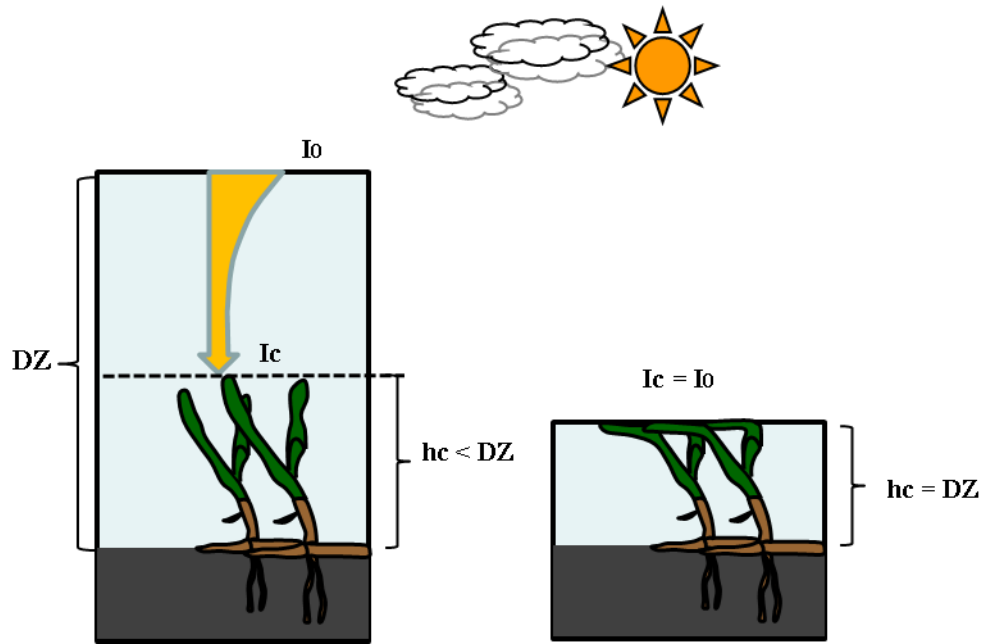


Figure 10 - Light extinction with increasing depth and light available at the top of seagrass canopy I_c (eq. 36), for high tide (left) and low tide (right). h_c is the height of the canopy, I_0 is the light available at the water surface, and DZ is the depth of the water column.

Parameters

The parameters of the seagrass model are listed in Table 2. Reference values are given for several species as well. The value of 0.06 for g_{max} (1/day) is for *Zostera marina* (Bocci *et al.*, 1997). The value of 1.24 for g_{max} (1/day) is referred to *Ruppia maritima* (Newell and Koch, 2004). The values of N_{min} (g N/kg DW), N_{crit} (g N/kg DW), N_{max} (g N/kg DW), K_{NH4w} (g N/ m^3), K_{NO3w} (g N/ m^3), K_{NH4s} (g N/ m^3), K_{max} (kg DW/ m^2) and V_{max}^{NH4s} (g N/kg DW/day) are referred to *Zostera marina* (Bocci *et al.*, 1997). The value of 1.98 for V_{max}^{NH4w} (g N/kg DW/day) is referred to *Amphibolis antarctica*. The value of 90.72 for V_{max}^{NH4w} (g N/kg DW/day) is referred to *Ruppia maritima*. The value of 31 for V_{max}^{PO4} (g P/kg DW/day) and 0.37 for K_{PO4} (g P/ m^3), are referred to *Zostera noltii*. Values in Table 2, reported from Duarte

(1990), are from a study on nutrient content of 27 seagrass species at 30 locations compiled from literature sources. The value of 0.0038 for m_{l0} (1/day) is referred to *Posidonia oceanica* (Elkalay *et al.*, 2003), and the value of 0.041 is referred to *Zostera marina* (Bocci *et al.*, 1997). The value of 0.0041 for m_{r0} (1/day) is referred to *Posidonia oceanica* (Elkalay *et al.*, 2003), and the value of 0.015 is referred to *Zostera marina* (Bocci *et al.*, 1997).

Table 2 - List of parameters used in the seagrass model. References to the sources of parameter values were given as well.

Symbol	Description	Unit	Value	Reference
g_{max}	Seagrass maximum growth rate	day ⁻¹	0.06 (<i>Zostera marina</i>) 1.24 (<i>Ruppia maritima</i>)	Bocci <i>et al.</i> (1997); Newell and Koch (2004)
K_{max}	Maximum leaves biomass	kg DW/m ²	0.5 (<i>Zostera marina</i>)	Bocci <i>et al.</i> (1997)
N_{min}	Minimum nitrogen quota	g N/kg DW	5 (<i>Zostera marina</i>)	Bocci <i>et al.</i> (1997)
N_{crit}	Critical nitrogen quota	g N/kg DW	15 (<i>Zostera marina</i>)	Bocci <i>et al.</i> (1997)
N_{max}	Maximum nitrogen quota	g N/kg DW	30 (<i>Zostera marina</i>)	Bocci <i>et al.</i> (1997)
P_{min}	Minimum phosphorus quota	g P/kg DW	0.44 (Several species)	Duarte (1990)
P_{crit}	Critical phosphorus quota	g P/kg DW	1.33 (Several species)	Duarte (1990)
P_{max}	Maximum internal phosphorus quota	g P/kg DW	2.67 (Several species)	Duarte (1990)
r_N	N: DW ratio in seagrasses	g N/kg DW	19 (Several species)	Duarte (1990)
r_P	P: DW ratio in seagrasses	g P/kg DW	2.3 (Several species)	Duarte (1990)
V_{max}^{NH4w}	Leaves maximum uptake of ammonia	g N/kg DW/day	1.98 (<i>Amphibolis Antarctica</i>) 90.72 (<i>Ruppia maritima</i>)	Touchette and Burkholder (2000)
K_{NH4w}	Leaves half-saturation constant for ammonia	g N/m ³	0.13 (<i>Zostera marina</i>)	Bocci <i>et al.</i> (1997)
V_{max}^{NO3w}	Leaves maximum uptake of nitrate	g N/kg DW/day	1.24 – 25	Touchette and Burkholder (2000)
K_{NO3w}	Leaves half-saturation constant for nitrate	g N/m ³	0.23 (<i>Zostera marina</i>)	Bocci <i>et al.</i> (1997)
V_{max}^{NH4s}	Roots maximum uptake rate of ammonia	g N/kg DW/day	0.48 (<i>Zostera marina</i>)	Bocci <i>et al.</i> (1997)
K_{NH4s}	Roots half-saturation constant for ammonia	g N/m ³	0.9 (<i>Zostera marina</i>)	Bocci <i>et al.</i> (1997)
V_{max}^{PO4}	Maximum uptake rate of phosphate	g P/kg DW/day	31 (<i>Zostera noltii</i>)	Touchette and Burkholder (2000)
K_{PO4}	Half-saturation constant for phosphate	g P/m ³	0.37	Touchette and Burkholder (2000)
m_{l0}	Leaves base decay rate	day ⁻¹	0.0038 (<i>Posidonia oceanica</i>) 0.041 (<i>Zostera marina</i>)	Elkalay <i>et al.</i> (2003) Bocci <i>et al.</i> (1997)
m_{r0}	Roots base decay rate	day ⁻¹	0.0041 (<i>Posidonia oceanica</i>) 0.015 (<i>Zostera marina</i>)	Elkalay <i>et al.</i> (2003) Bocci <i>et al.</i> (1997)
tr	Carbon translocation coefficient	-	0.25 (<i>Zostera marina</i>)	Olesen and Sand-Jensen (1993)

More details about seagrass uptake rates and half-saturation constants are provided in Table 3 which shows data compiled by Touchette and Burkholder (2000).

Table 3 - Uptake rates and half-saturation constant for several seagrass species. After Touchette and Burkholder (2000).

Nutrient uptake parameters reported in seagrass species based on the Michaelis–Menten model for uptake kinetics, including tissue (leaf, root), nutrient, V_{\max} (maximum uptake rate, $\mu\text{mol g}^{-1}$ dry weight h^{-1}), K_m (half-saturation constant, μM), and α (uptake affinity = V_{\max}/K_m)

Species	Nutrient	V_{\max}	K_m	α	Source
Leaf					
Temperate					
<i>Amphibolis antarctica</i>	NH_4^+	5.9–43.1	9.5–74.3	0.6–0.8	Pedersen et al. (1997)
<i>Phyllospadix torreyi</i>	NH_4^+	95.6–204.3	9.3–33.9	–	Terrados and Williams (1997)
<i>Phyllospadix torreyi</i>	NO_3^-	24.9–75.4	4.4–17.0	–	Terrados and Williams (1997)
<i>Ruppia maritima</i>	NH_4^+	243–270	9.0–17.7	5.5	Thursby and Harlin (1984)
<i>Zostera marina</i>	NH_4^+	20.5	9.2	2.2	Thursby and Harlin (1982)
<i>Zostera marina</i>	NO_3^-	–	23	–	Iizumi and Hattori (1982)
<i>Zostera noltii</i> (excised) ^a	PO_4^{3-}	7.0	10	0.7	Pérez-Lloréns and Niell (1995)
<i>Zostera noltii</i> ^a	PO_4^{3-}	43	12.1	1.1	Pérez-Lloréns and Niell (1995)
Tropical/subtropical					
<i>Thalassia hemprichii</i> ^a	PO_4^{3-}	2.2–3.2	7.7–15	0.12–0.19	Stapel et al. (1996)
<i>Thalassia hemprichii</i>	NH_4^+	32–37	21–60	0.52–0.85	Stapel et al. (1996)
<i>Thalassia testudinum</i>	NH_4^+	8.3–16.4	7.6–15	0.57–2.82	Lee and Dunton (1999)
<i>Thalassia testudinum</i>	NO_3^-	3.7–6.5	2.2–38.5	0.15–1.68	Lee and Dunton (1999)
Root					
Temperate					
<i>Amphibolis antarctica</i>	NH_4^+	1.1	4.7	0.2	Pedersen et al. (1997)
<i>Ruppia maritima</i>	NH_4^+	48–56	2.8–12.6	20.1	Thursby and Harlin (1984)
<i>Zostera marina</i>	NH_4^+	211	104	0.5	Thursby and Harlin (1982)
<i>Zostera marina</i>	NH_4^+	–	30	–	Iizumi and Hattori (1982)
Tropical/subtropical					
<i>Thalassia testudinum</i>	NH_4^+	7.9–73.3	34.4–765.5	0.03–0.30	Lee and Dunton (1999)

^a Note: minimum substrate level (S_{\min}) was also available for *Zostera noltii* (excised leaf, 2.5 μM ; leaf, 2.6 μM) and *Thalassia hemprichii* (leaf, 0.7–1.1 μM).

2.4.2. Benthic feeders and microphytobenthos

Benthic feeder

In this research, two categories of benthic feeders are taken into account: filter feeders and deposit feeders. The difference between filter feeders and deposit feeders are: 1) the type of kinetic equation used to express grazing; 2) the sources of food, and; 3) the parameter values. The cycle of organic matter at the sediment-water interface was represented by using a set of ODEs for the following benthic components: organic matter, nutrients, oxygen, benthic feeders, and microphytobenthos. The benthic model was structured in a way that several sources of food can be defined for a generic benthic feeder. The diagram in Figure 11 shows the conceptual model of a generic benthic feeder. Yellow boxes represent state variables of the benthic system, blue boxes represent state variables of the pelagic system, and arrows indicate mass flows. A generic benthic feeder (BENTHIC FEEDER) has access to several sources of food in the water: phytoplankton (PHYTO), benthic producers (MICROPHYTOBENTHOS), particulate organic matter in water (POM Water) and particulate organic matter on the bottom sediment (POM Bottom). Respiration processes consume oxygen and produce nutrients. Mortality and egestion are added to the existing pool of organic matter on the bottom sediment.

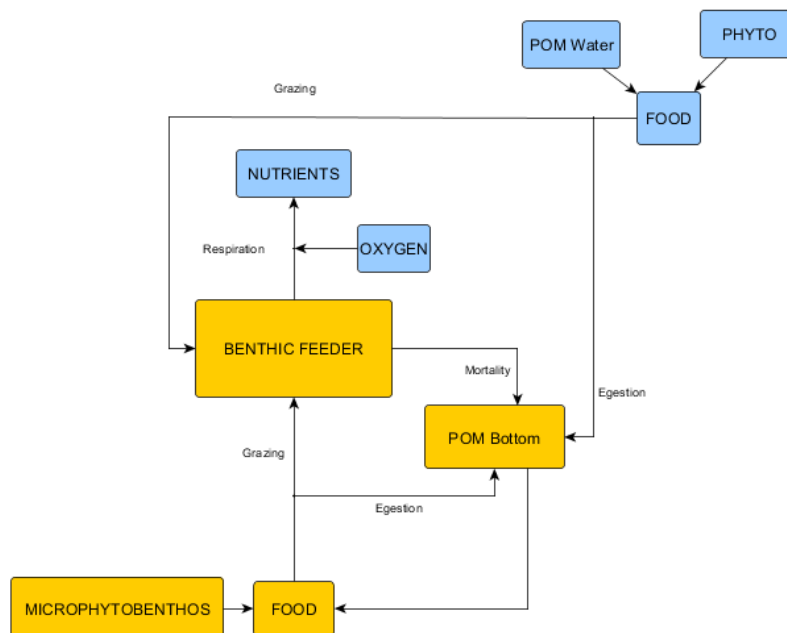


Figure 11 - Conceptual model of a generic benthic feeder.

Governing equations

The equation for a generic benthic feeder (BF), was formulated as (eq. 37):

$$\frac{dBF}{dt} = g_{BF}BF - r_{BF}BF - m_{BF}BF \quad \text{eq. 37}$$

where BF is the biomass of the benthic feeder (kg C/m^2), g_{BF} is the benthic feeder growth rate (1/day), r_{BF} is the benthic feeder respiration rate (1/day), and m_{BF} is the benthic feeder mortality rate (1/day). In the model, the benthic feeders were divided into two main groups: filter feeders (FF), and deposit feeders (DF).

Filter feeders are benthic invertebrates feeding on suspended particulate organic matter from the water at the sediment-water interface. Deposit feeders feed on microphytobenthos and on detrital organic matter which is deposited on the surface of the sediment. These two groups of benthic feeders are described in the next sections. The benthic ecology model includes the following state variables:

- Filter feeders - FF (kg C/m^2);
- Deposit feeders - DF (kg C/m^2);
- Microphytobenthos - MP (kg C/m^2);
- Ammonia in water - $NH4w$ (g N/m^3);
- Nitrate in water - $NO3w$ (g N/m^3);
- Phosphate in water - $PO4w$ (g P/m^3);
- Particulate organic carbon in water - $POCw$ (g C/m^3);
- Particulate organic nitrogen in water - $PONw$ (g N/m^3);
- Particulate organic phosphorus in water - $POPw$ (g P/m^3);
- Particulate organic carbon on the bottom sediment - $POCb$ (g C/m^2);
- Particulate organic nitrogen on the bottom sediment - $PONb$ (g N/m^2);
- Particulate organic phosphorus on the bottom sediment - $POPb$ (g P/m^2);
- Oxygen in water - O_2 ($\text{g O}_2/\text{m}^3$).

2.4.2.1. Filter feeders

Filter feeders are benthic invertebrates feeding on suspended particulate organic matter from the water at the sediment-water interface. In reality, some of them use tentacles; some others use filters to catch the food from the water. In the model, the name of filter feeders is used to indicate benthic feeders which use filtration mechanisms for feeding. Benthic feeders that use tentacles are not included in the model. The filter feeders growth rate is expressed as a function of filtration rate, temperature, oxygen concentration, and suspended sediment concentration at the sediment-water interface. The growth of the filter feeder was assumed to be proportional to the feeder's biomass and to food concentration in the water. The conceptual diagram of the filter feeder is shown in Figure 12. This diagram is obtained from the one in Figure 11, by including only the feeding on water organic particles (phytoplankton and POM Water). Yellow boxes in Figure 12 represent state variables of the benthic system, and blue boxes represent state variables of the pelagic system. Filter feeders mortality and egestion are added to the existing pool of detrital organic matter on the bottom sediment. Respiration of filter feeders implies oxygen consumption and ammonia production. Mineralization of organic matter in water and sediment, growth and decay of phytoplankton, and re-suspension of particulate organic matter, are taken into account as well, but not represented in the figure to keep the drawing clear.

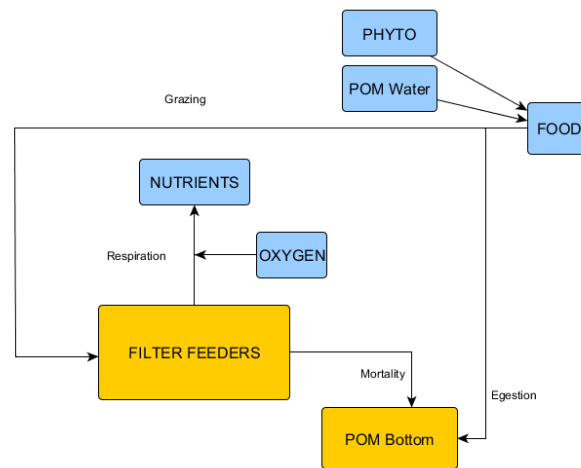


Figure 12 - Conceptual diagram of filter feeders in the model.

Detrital organic matter in the water column and phytoplankton were considered as food sources for filter feeders FF (kg C /m^2). Filter feeders growth, respiration and mortality, were formulated as:

$$\frac{dFF}{dt} = g_{FF}FF - r_{FF}FF - m_{FF}FF \quad \text{eq. 38}$$

where g_{FF} (1/day) is the filter feeder growth rate, r_{FF} (1/day) is the filter feeder respiration rate, and m_{FF} (1/day) is the filter feeder mortality rate. The filter feeders growth rate (eq. 39) was expressed as:

$$g_{FF} = I_{FF} \left(\alpha_{phy} \cdot \frac{Phy}{1000} + \alpha_{POM} \cdot \frac{POC_w}{1000} \right) \quad \text{eq. 39}$$

where Phy is the phytoplankton concentration at the sediment-water interface, expressed as $g\ C/m^3$ (or $mg\ C/l$). POC_w is the particulate organic carbon in water expressed as $g\ C/m^3$ (or $mg\ C/l$). α_{phy} (Table 4) is the filter feeders assimilation efficiency for grazing on phytoplankton. α_{POM} (Table 4) is the filter feeders assimilation efficiency for grazing on particulate organic matter in the water column. The clearance rate I_{FF} ($m^3/kg\ C/day$) (Meyers *et al.*, 2000) was expressed as a function of the maximum clearance rate I_{FFmax} ($m^3/kg\ C/day$) multiplied by the dimensionless temperature limiting factor $f(T)$ (appendix A), the suspended sediment limiting factor (eq. 41), the density limiting factor ($f(FF)$ in eq. 42), and the oxygen limiting factor $f(O_2)$, (eq. 43):

$$I_{FF} = I_{FFmax} \times f(T) \times f(SED) \times f(FF) \times f(O_2) \quad \text{eq. 40}$$

All limiting factors are dimensionless and bounded between 0 and 1. The dependence of the filtration rate on the concentration of total suspended sediments (eq. 41) was proposed by using a linear relationship given as:

$$f(SED) = \min \left\{ 0, \max \left[0, \left(1 - \frac{SED}{SED_{max}} \right) \right] \right\} \quad \text{eq. 41}$$

where SED (g/l) is the concentration of suspended sediments in water. SED_{max} (g/l) is the maximum concentration of suspended sediments tolerated by filter feeders. Density limiting factor $f(FF)$ was expressed as (eq. 42), following Le Pape *et al.* (1999):

$$f(FF) = 1 - \max \left[0, \min \left(1, \frac{FF - FF_{min}}{FF_{max} - FF_{min}} \right) \right] \quad \text{eq. 42}$$

where FF_{min} (kg C/m²) and FF_{max} (kg C/m²) are the minimum and maximum filter feeder's biomass values which are limiting the growth rate. Hypoxia may affect filtration rates and respiration processes. The dependence of the filtration rate on the oxygen concentration at the sediment-water interface was described by using the dimensionless oxygen limiting factor (eq. 43), $F(O_2)$, following the approach used in the MOHID Benthos model (http://www.mohid.com/wiki/index.php?title=Module_Benthos):

$$F(O_2) = \frac{O_2}{O_2 + K_{O_2}} \quad \text{eq. 43}$$

where O_2 is the oxygen concentration at the sediment-water interface in mg O₂/l. K_{O_2} is the concentration of oxygen (in mg O₂/l) under which the growth rate is reduced by 50%.

The grazing by filter feeders over phytoplankton is expressed as (eq. 44):

$$b_{phy} = I_{FF} \cdot FF \cdot \frac{A}{V} \quad \text{eq. 44}$$

b_{phy} (1/day) is a grazing rate by filter feeders, used in the differential equation of phytoplankton (see eq. 102). A is the area of the calculation cell (m²) and V is the volume of the calculation cell (m³). α_{phy} (dimensionless) is the assimilation efficiency for grazing of phytoplankton. The grazing by filter feeders on detrital organic matter in the water is expressed as:

$$POC_{w_to_FF} = -I_{FF} FF \frac{A}{V} POC_w \quad \text{eq. 45}$$

$POC_{w_to_FF}$ (g C/m³/day) is added to the differential equation of detrital organic carbon in the water (POC_w , g C/m³) (eq. 96).

$$PON_{w_to_FF} = POC_{w_to_FF} \cdot r_{NC} \quad \text{eq. 46}$$

$PON_{w_to_FF}$ (g N/m³/day) is added to the differential equation of particulate detrital organic nitrogen in the water (PON_w , g N/m³) (eq. 97).

$$POP_{w_to_FF} = POC_{w_to_FF} \cdot r_{PC} \quad \text{eq. 47}$$

$POP_{w_to_FF}$ (g P/m³/day) is added to the differential equation of particulate detrital organic phosphorus in the water (POP_w , in g P/m³) (eq. 98). The bottom sediment is represented as POC_b (particulate detrital organic carbon on the bottom sediment, in kg C/m²), PON_b (particulate detrital organic nitrogen on the bottom sediment, in kg N/m²) and POP_b (particulate detrital organic phosphorus on the bottom sediment, in kg P/m²). For the mass balance of particulate detrital organic matter on the bottom sediment, it is necessary to account for the mortality of filter feeders, and of the egested fractions of the growth term ($1-\alpha_{POM}$) and ($1-\alpha_{phy}$):

$$FF_to_POC_b = (1-\alpha_{POM}) \cdot I_{FF} \cdot \frac{POC_w}{1000} \cdot FF + (1-\alpha_{phy}) I_{FF} \cdot \frac{Phy}{1000} \cdot FF + m_{FF} FF \quad \text{eq. 48}$$

$FF_to_POC_b$ (kg C/m²/day) is added to the differential equation of detrital organic matter in the sediment (eq. 93). This flux of carbon can be converted into flux of nitrogen or flux of phosphorus by using fixed ratios between nitrogen, carbon, and phosphorus, in the detrital organic matter:

$$FF_to_PON_b = FF_to_POC_b \cdot r_{NC} \quad \text{eq. 49}$$

$$FF_to_POP_b = FF_to_POC_b \cdot r_{PC} \quad \text{eq. 50}$$

r_{NC} is the N:C ratio, and r_{PC} is the P:C ratio in detrital organic matter. $FF_to_PON_b$ (kg N/m²/day) is added to the differential equation of particulate detrital organic nitrogen in the sediment (eq. 94). $FF_to_POP_b$ (kg P/m²/day) is added to the differential equation of particulate organic phosphorus in the sediment (eq. 95).

The mortality rate, m_{FF} (1/day), was defined as a function of temperature and oxygen concentration (Meyers *et al.*, 2000) (eq. 51):

$$m_{FF} = m_{FF0} F_{FF}^{dec}(T) \cdot [1 - F(O_2)] \quad \text{eq. 51}$$

The oxygen limiting factor $F(O_2)$ tends to 0 with decreasing oxygen concentration. According to the above equation, the mortality rate increases with decreasing oxygen concentration, and with increasing temperature. The respiration rate, r_{FF} (1/day), was defined as a function of oxygen concentration and temperature (eq. 52):

$$r_{FF} = r_{FF0} F_{FF}^{dec}(T) F(O_2) \quad \text{eq. 52}$$

where r_{FF0} is the base respiration rate (1/day). The respiration rate decreases with decreasing oxygen concentration, because filter feeders are aerobic organisms, and they need oxygen for respiration process. $F_{FF}^{dec}(T)$ is the temperature decay factor, expressed as (eq. 53):

$$F_{FF}^{dec}(T) = T_{FF}^{fac(T-20)} \quad \text{eq. 53}$$

where T_{FF}^{fac} is the Arrhenius dimensionless coefficient for decay due to temperature (USCE, 2000). The respiration term is:

$$FF_to_NH4 = r_{FF} \cdot FF \cdot r_{NC} \cdot \frac{A}{V} \cdot 1000 \quad \text{eq. 54}$$

FF_to_NH4 (g N/m³/day) is added as negative flux to the differential equation of ammonia in the water $NH4_w$ (g N/m³) (eq. 90). The respiration term is converted into phosphate as follows:

$$FF_to_PO4 = r_{FF} \cdot FF \cdot r_{PC} \cdot \frac{A}{V} \cdot 1000$$

eq. 55

FF_to_PO4 (g P/m³/day) is added to the differential equation of the phosphate at the sediment-water interface $PO4_w$ (g P/m³) (eq. 91).

Oxygen consumption due to respiration is accounted for as follows:

$$O2_to_FF = -r_{FF} \cdot FF \cdot \frac{A}{V} \cdot \frac{32}{12} \cdot 1000$$

eq. 56

$O2_to_FF$ (g O₂/m³/day) is added as sink to the differential equation of the oxygen O_2 (g O₂/m³) at the sediment-water interface (eq. 92). 32/12 is the ratio between the molecular weight of oxygen, and the atomic weight of carbon.

Parameters

Parameters of the filter feeders model are given in Table 4. Reference values are provided as well.

Table 4 - Parameters of the filter feeders model.

Parameter	Description	Unit	Value	Reference
I_{fmax}	Filter feeder maximum filtration rate	$m^3/(\text{day}\cdot\text{kg C})$	0.216E3	(Meyers <i>et al.</i> , 2000)
α_{phy}	Filter feeder assimilation efficiency for phytoplankton	-	0.8	USCE (2000)
α_{POM}	Filter feeder assimilation efficiency for particulate organic matter	-	0.8	USCE (2000)
r_{FF0}	Filter feeder base respiration rate	1/day	0.013	USCE (2000)
m_{FF0}	Filter feeder base mortality rate	1/day	0.013	USCE (2000)
SED_{max}	Maximum sediment concentration tolerated by filter feeders	g/l	0.1	USCE (2000)
K_{O_2}	Oxygen concentration limitation constant	mg O_2 /l	0.5	www.mohid.com
T_{FF}^{fac}	Temperature respiration factor	-	1.08	USCE (2000)
r_{PC}	P:C ratio	g P:g C	0.024	IST (2006)
r_{NC}	N:C ratio	g N:g C	0.18	IST (2006)
FF_{min}	Minimum consumer biomass that limits filtration rate	kg C/m ²	0.005	Le Pape <i>et al.</i> (1999)
FF_{max}	Maximum consumer biomass that limits filtration rate	kg C/m ²	0.020	Le Pape <i>et al.</i> (1999)

2.4.2.2. Deposit feeders

Conceptual diagram

The conceptual diagram used for deposit feeders in the model is presented in Figure 13. Yellow boxes represent state variables of the benthic system, and blue boxes represent state variables of the pelagic system. Deposit feeders consume particulate organic matter and microphytobenthos in the sediment. Deposit feeders mortality and egestion are added to the existing pool of detrital organic matter in the sediment. Respiration of deposit feeders implies oxygen consumption and ammonia production. Mineralization of organic matter in water and sediment, growth and decay of microphytobenthos, and resuspension of particulate organic matter, were considered in the model as well, but not described in the figure to keep it clear.

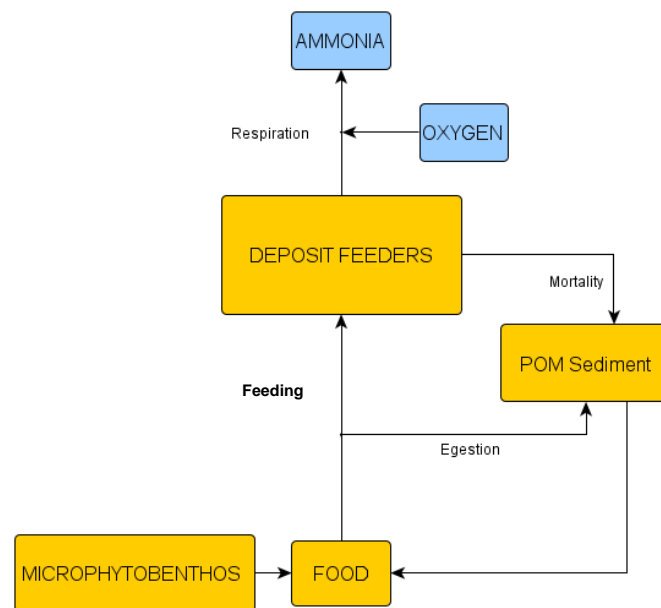


Figure 13 - Conceptual diagram of deposit feeders in the benthic model.

Governing equations

In the model, a deposit feeder can only feed on food available on the sea bottom (Figure 13), (microphytobenthos and particulate organic matter deposited at the interface sediment water). In deposit feeders, the growth rate is a function of the maximum ingestion rate, temperature, oxygen concentration, and deposit feeder biomass. The grazing in deposit

feeders was assumed to follow the Mikaelis-Menten kinetics (USCE, 2000). Deposit feeders source and sink terms (eq. 57) were described as:

$$\frac{dDF}{dt} = g_{DF}DF - r_{DF}DF - m_{DF}DF \quad \text{eq. 57}$$

For mass balance, the mortality term $m_{DF}DF$ was added to the existing pool of deposited particulate organic matter in the sediment. The respiration term $r_{DF}DF$ was added to the existing pool of dissolved ammonia at the sediment-water interface (eq. 90). Michaelis-Menten kinetics was used to express deposit feeders grazing on food (USCE, 2000) (eq. 58):

$$g_{DF} = I_{DF} \left(\alpha_{MP} \frac{MP}{MP + K_C} + \alpha_{POM_b} \frac{POC_b}{POC_b + K_C} \right) \quad \text{eq. 58}$$

MP is the microphytobenthos biomass (kg C/m^2). K_C is the half-saturation constant for food uptake (kg C/m^2). I_{DF} is the ingestion rate, limited by temperature, density of the feeder, and oxygen concentration modified from (USCE, 2000) (eq. 59):

$$I_{DF} = I_{DF_{\max}} \times f(T) \times f(O_2) \times f(DF) \quad \text{eq. 59}$$

Temperature limiting factor is described in Appendix A. The oxygen limiting factor is the same as in eq. 43 for filter feeders. For the mass balance, the grazing on microphytobenthos is subtracted to the differential equation of the microphytobenthos (eq. 70). The grazing on particulate organic matter is subtracted to the equation of the particulate organic matter (eq. 93). The density limiting factor is expressed as (following Le Pape *et al.* (1999)):

$$f(DF) = 1 - \max \left[0, \min \left(1, \frac{DF - DF_{\min}}{DF_{\max} - DF_{\min}} \right) \right] \quad \text{eq. 60}$$

where DF_{min} (kg C/m²) and DF_{max} (kg C/m²) are the minimum and maximum deposit feeder's biomass values which are limiting the growth rate. Similarly to filter feeders, the mortality rate, m_{DF} (1/day), was defined as a function of oxygen concentration and temperature, modified from (USCE, 2000) (eq. 61):

$$m_{DF} = m_{DF0} F_{DF}^{dec}(T) [1 - f(O_2)] \quad \text{eq. 61}$$

For the mass balance of particulate organic matter, it is necessary to account for the mortality of deposit feeders, and of the egested fractions ($1-\alpha_{POMb}$) and ($1-\alpha_{MP}$):

$$\begin{aligned} DF_to_POC_b = & -I_{DF} \alpha_{POM_b} \frac{POC_b}{POC_b + K_C} DF + \\ & + (1 - \alpha_{MP}) \frac{MP}{MP + K_C} DF + m_{DF} DF \end{aligned} \quad \text{eq. 62}$$

Considering the grazing on particulate organic matter, the difference between the grazing term and the fraction ($1-\alpha_{POMb}$) of the grazing term gives just the fraction $-\alpha_{POMb}$ to be added to the differential equation of the bottom particulate organic carbon (eq. 93). The egested fraction ($1-\alpha_{MP}$) of the grazing on microphytobenthos is added to the differential equation of bottom particulate organic matter as well:

$$DF_to_PON_b = DF_to_POC_b \cdot r_{NC} \quad \text{eq. 63}$$

$$DF_to_POP_b = DF_to_POC_b \cdot r_{PC} \quad \text{eq. 64}$$

$DF_to_PON_b$ (kg N/m²/day) is added to the differential equation of particulate organic nitrogen in the sediment (eq. 94). $DF_to_POP_b$ (kg P/m²/day) is added to the differential equation of particulate organic phosphorus in the sediment (eq. 95).

The respiration rate, r_{DF} (1/day), was defined as a function of oxygen concentration and temperature, modified from (USCE, 2000) (eq. 65).

$$r_{DF} = r_{DF0} F_{DF}^{dec}(T) f(O_2) \quad \text{eq. 65}$$

where r_{DF0} is the base respiration rate (1/day). Similarly to filter feeders, the respiration rate decreases with decreasing oxygen concentration, because deposit feeders are aerobic organisms, and they need oxygen for respiration process. $F_{DF}^{dec}(T)$ is the temperature decay factor, expressed as (USCE, 2000) (eq. 66):

$$F_{DF}^{dec}(T) = T_{DF}^{fac(T-20)} \quad \text{eq. 66}$$

where T_{DF}^{fac} is the Arrhenius dimensionless factor for temperature decay (USCE, 2000). The respiration term is considered as dissolved nutrients that are released in the water as ammonia and phosphate:

$$DF_to_NH4 = r_{DF} \cdot DF \cdot r_{NC} \frac{A}{V} \cdot 1000 \quad \text{eq. 67}$$

DF_to_NH4 (g N/m³/day) is added to the differential equation of the phosphate at the sediment-water interface $NH4_w$ (g N/m³) (eq. 90).

$$DF_to_PO4 = r_{DF} \cdot DF \cdot r_{PC} \frac{A}{V} \cdot 1000 \quad \text{eq. 68}$$

DF_to_PO4 (g P/m³/day) is added to the differential equation of the phosphate at the sediment-water interface $PO4_w$ (g P/m³) (eq. 91). Oxygen consumption due to respiration is accounted for as follows:

$$O2_to_DF = -r_{DF} \cdot DF \cdot \frac{A}{V} \cdot \frac{32}{12} \cdot 1000 \quad \text{eq. 69}$$

$O2_to_DF$ (g O₂/m³/day) is added as sink to the differential equation of the oxygen O₂ (g O₂/m³) at the sediment-water interface (eq. 92). 32/12 is the ratio between the molecular weight of oxygen and the atomic weight of carbon.

Parameters

Parameters of the deposit feeders model are given in Table 5. Reference values are given as well.

Table 5 - Parameters of the deposit feeders model.

Parameter	Description	Unit	Value	Reference
I_{DFmax}	Deposit feeder maximum ingestion rate	l/day	0.05	Le Pape <i>et al.</i> (1999)
r_{DF0}	Deposit feeder base respiration rate	1/day	0.0075	Le Pape <i>et al.</i> (1999)
α_{MP}	Deposit feeder assimilation efficiency for microphytobenthos	-	0.25	Le Pape <i>et al.</i> (1999)
α_{POMb}	Deposit feeder assimilation efficiency for particulate organic matter	-	0.25	Le Pape <i>et al.</i> (1999)
m_{DF0}	Deposit feeder base mortality rate	1/day	0.0018	Le Pape <i>et al.</i> (1999)
K_{O_2}	Oxygen concentration limitation constant	mg O ₂ /l	0.5	www.mohid.com
T_{fac}	Temperature respiration factor	-	1.08	USCE (2000)
DF_{min}	Minimum density that limits ingestion rate	kg C/m ²	0.002	Le Pape <i>et al.</i> (1999)
DF_{max}	Maximum density that limits ingestion rate	kg C/m ²	0.006	Le Pape <i>et al.</i> (1999)
K_C	Half-saturation constant for food uptake	kg C/m ²	0.001	Le Pape <i>et al.</i> (1999)
r_{PC}	P:C ratio	g P:g C	0.024	IST (2006)
r_{NC}	N:C ratio	g N:g C	0.18	IST (2006)

2.4.2.3. Microphytobentos

Conceptual diagram

A conceptual diagram of microphytobentos is given in Figure 14. Yellow boxes represent state variables of the benthic system, and blue boxes represent state variables of the pelagic system. Microphytobentos uptakes nutrients from the water at the sediment-water interface, and deposit feeders feed on microphytobentos. Oxygen is produced by photosynthesis and consumed by respiration. Dead microphytobentos is added to the existing pool of detrital organic matter on the bottom sediment.

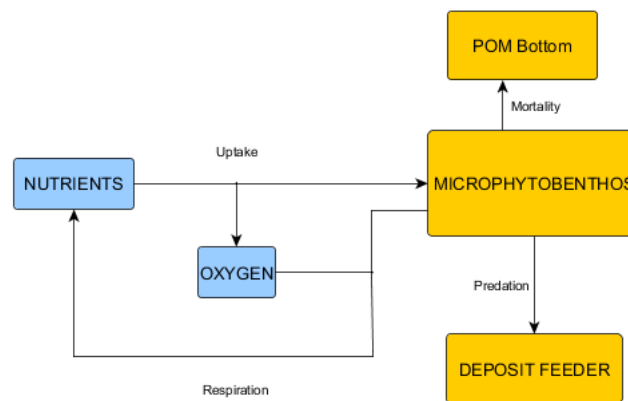


Figure 14 - Microphytobentos conceptual diagram.

Governing equations

The model for microphytobentos is used to represent benthic micro algae which are able to photosynthesize on the bottom sediment. These benthic micro algae are modeled by using the eq. 70:

$$\frac{dMP}{dt} = (1 - \phi)g_{MP}MP - m_{MP}MP - MF_{to_DF} \quad \text{eq. 70}$$

where MP is the microphytobentos in kg C/m^2 , g_{MP} is the microphytobentos growth rate (1/day), ϕ (-) is the fraction of the growth that goes to respiration (Blackford, 2002), m_{MP}

is the natural mortality rate of microphytobenthos (1/day), and MF_to_DF (kg C/m²/day) is the grazing rate by deposit feeders:

$$MF_to_DF = I_{DF} \frac{MP}{MP + K_C} DF \quad \text{eq. 71}$$

For the explanation of the grazing term by deposit feeders on microphytobenthos, please also refer to section 2.4.2.2. If no grazers of microphytobenthos are defined, the decay of microphytobenthos occurs only due to natural mortality, and $MF_to_DF = 0$. The microphytobenthos growth rate is expressed as (eq. 72):

$$g_{MP} = V_{max} f(I) f(T) f(MP) \min(f(N), f(P)) \quad \text{eq. 72}$$

where V_{max} is the maximum growth rate (1/day), $f(I)$ is the dimensionless light limiting factor, $f(T)$ is the dimensionless temperature limiting factor, $f(MP)$ is the dimensionless density limiting factor, $f(N)$ and $f(P)$ express the limitation due to nitrogen and phosphorus. The density limiting factor $f(MP)$ [-] is expressed in the same way as for benthic feeders (eq. 73):

$$f(MP) = 1. - \max \left[0., \min \left(1., \frac{MP - MP_{min}}{MP_{max} - MP_{min}} \right) \right] \quad \text{eq. 73}$$

where MP_{min} (kg C/m²) and MP_{max} (kg C/m²) are the minimum and maximum microphytobenthos biomass which are limiting the microphytobenthos growth rate.

The light limitation factor $f(I)$ (dimensionless), follows the Evans and Parslow (1985) model eq. 74:

$$f(I) = \frac{\alpha \cdot PAR_{bottom}}{\sqrt{V_{max}^2 + \alpha^2 PAR_{bottom}^2}} \quad \text{eq. 74}$$

α is the slope of the PI curve [$1/(\text{day}(\text{W}/\text{m}^2))$]. PAR_{bottom} is the Photosynthetic Active Radiation (W/m^2) which reaches the bottom sediment.

The dimensionless terms $f(N)$ and $f(P)$ are given as (eq. 75 and eq. 76) :

$$f(N) = \frac{NH4_w + NO3_w}{K_N + NH4_w + NO3_w} \quad \text{eq. 75}$$

$$f(P) = \frac{PO4_w}{K_P + PO4_w} \quad \text{eq. 76}$$

where $NH4_w$ (mg N/l) is the ammonia at the sediment water interface, $NO3_w$ (mg N/l) is the nitrate at the sediment water interface, and $PO4_w$ (mg P/l) is the phosphate at the sediment water interface. K_N (mg N/l) is the half-saturation constant for the uptake of nitrogen, and K_P (mg P/l) is the half-saturation constant for the uptake of phosphorus. The values of the saturation constants were given in Table 6. For mass conservation, ammonia is consumed by the microphytobenthos uptake and generated by microphytobenthos respiration (eq. 77):

$$MP_to_NH4 = \phi \cdot g_{MP} \cdot MP \cdot r_{NC} \frac{A}{V} \cdot 1000 - \Psi_{NH4} g_{MP} \cdot MP \cdot r_{NC} \frac{A}{V} \cdot 1000 \quad \text{eq. 77}$$

where Ψ_{NH4} is the dimensionless ammonia preference factor, calculated as described in Appendix B. r_{NC} is the N:C ratio.

Nitrate at the sediment-water interface is consumed by uptake (eq. 78):

$$MP_to_NO3 = -(1 - \Psi_{NH4}) g_{MP} MP \cdot r_{NC} \frac{A}{V} \cdot 1000 \quad \text{eq. 78}$$

MP_to_NO3 (g N/m³/day) is added to the equation of nitrate in water ($NO3_w$, gN/m³) (eq. 89).

Phosphate at the sediment water interface is consumed by uptake and generated by respiration (eq. 79):

$$MP_to_PO4 = \phi \cdot g_{MP} MP \cdot r_{PC} \frac{A}{V} \cdot 1000 - g_{MP} MP \cdot r_{PC} \frac{A}{V} \cdot 1000 \quad \text{eq. 79}$$

MP_to_PO4 (g P/m³/day) is added to the differential equation of phosphate in water ($PO4_w$, g P/m³) (eq. 91). Mortality is added to the existing pool of deposited organic matter on the bottom sediment (eq. 80):

$$MP_to_POC_b = +m_{MP} MP \quad \text{eq. 80}$$

$$MP_to_PON_b = MP_to_POC_b \cdot r_{NC} \quad \text{eq. 81}$$

$$MP_to_POP_b = MP_to_POC_b \cdot r_{PC} \quad \text{eq. 82}$$

$MP_to_POC_b$ (kg C/m²/day) is added to the equation of particulate organic carbon in the sediment (POC_b , kg C/m²) (eq. 93). $MP_to_PON_b$ (kg N/m²/day) is added to the equation of particulate organic carbon in the sediment (PON_b , kg N/m²) (eq. 94). $MP_to_POP_b$ (kg P/m²/day) is added to the equation of particulate organic phosphorus in the sediment (POP_b , kg P/m²) (eq. 95).

The mortality of the microphytobenthos is expressed as (eq. 83):

$$m_{MP} = m_{MPO} F_{MP}^{dec}(T) \quad \text{eq. 83}$$

where m_{MPO} is the base mortality rate (1/day) and the temperature decay function $F_{MP}^{dec}(T)$ is given as (eq. 84):

$$F_{MP}^{dec}(T) = F_{MP}^{fac(T-20)} \quad \text{eq. 84}$$

The oxygen is produced by growth, and it is consumed by respiration of microphytobenthos (eq. 85):

$$O2_to_MP = (1 - \phi) g_{MP} MP \frac{32 A}{12 V} \cdot 1000 \quad \text{eq. 85}$$

$O2_to_MP$ (g O₂/m³/day) is added to the differential equation of oxygen in water (eq. 92).

Parameters

Parameters of the microphytobenthos model are given in Table 6.

Table 6 - Parameters of the microphytobenthos model.

Parameter	Description	Unit	Value	Reference
V_{max}	Microphytobenthos maximum growth rate	1/day	2.	Blackford (2002)
m_{MP0}	Microphytobenthos mortality rate	1/day	0.02	IST (2006)
ϕ	Microphytobenthos respiration fraction	[-]	0.05	Blackford (2002)
α	Slope of PI curve	1/(day(W/m ²))	0.025	Evans and Parslow (1985)
K_N	Half-saturation constant for N uptake	mg N/l	0.014	IST (2006)
K_P	Half-saturation constant for P uptake	mg N/l	0.001	IST (2006)
MP_{min}	Minimum density that limits ingestion rate	kg C/m ²	0.001	Blackford (2002) Le Pape <i>et al.</i> (1999)
MP_{max}	Maximum density that limits ingestion rate	kg C/m ²	0.005	Blackford (2002) Le Pape <i>et al.</i> (1999)
T_{MP}^{fac}	Temperature respiration factor	-	1.08	USCE (2000)
Ψ	Ammonia preference factor	-	-	Appendix B
r_{PC}	P:C ratio	g P:g C	0.024	IST (2006)
r_{NC}	N:C ratio	g N:g C	0.18	IST (2006)

Summary of the equations for filter feeders, deposit feeders and microphytobenthos

In this section, a summary of the equations of the benthic feeders and microphytobenthos is provided.

$$\frac{dMP}{dt} = (1 - \phi)g_{MP}MP - m_{MP}MP - MF_to_DF$$

eq. 86

$$\frac{dFF}{dt} = g_{FF}FF - r_{FF}FF - m_{FF}FF$$

eq. 87

$$\frac{dDF}{dt} = g_{DF}DF - r_{DF}DF - m_{DF}DF$$

eq. 88

$$\frac{dNO3_w}{dt} = MP_to_NO3$$

eq. 89

$$\frac{dNH4_w}{dt} = MP_to_NH4 + DF_to_NH4 + FF_to_NH4$$

eq. 90

$$\frac{dPO4_w}{dt} = MP_to_PO4 + DF_to_PO4 + FF_to_PO4$$

eq. 91

$$\frac{dO_2}{dt} = O2_to_MP + O2_to_DF + O2_to_FF$$

eq. 92

$$\frac{dPOC_b}{dt} = MP_to_POC_b + DF_to_POC_b + FF_to_POC_b$$

eq. 93

$$\frac{dPON_b}{dt} = MP_to_PON_b + DF_to_PON_b + FF_to_PON_b$$

eq. 94

$$\frac{dPOP_b}{dt} = MP_to_POP_b + DF_to_POP_b + FF_to_POP_b$$

eq. 95

$$\frac{dPOC_w}{dt} = POC_w_to_FF$$

eq. 96

$$\frac{dPON_w}{dt} = PON_w_to_FF$$

eq. 97

$$\frac{dPOP_w}{dt} = POP_w_to_FF$$

eq. 98

It is important to say that the differential equations described above for nitrate, ammonia, phosphate, particulate organic matter in water, include only the processes described in the benthic ecology model. The modifications of these properties due to water column biogeochemistry (uptake of nutrients by phytoplankton, mortality and respiration of phytoplankton and zooplankton, mineralization of organic matter) were not included in this list, because they are already calculated by other modules in MOHID. For phytoplankton, which is not a state variable of the benthic ecology model, please refer to eq. 102.

2.5. The MOHID water modelling system

MOHID is a water modelling system developed at the Marine Technology Research Centre (MARETEC) at Instituto Superior Técnico (IST), Universidade de Lisboa, Portugal. MOHID was applied to estuaries, lagoons, reservoirs, and coastal areas, such as to the Sado Estuary (Cancino and Neves, 1998; Martins *et al.*, 2001), to the Aveiro lagoon in Portugal (Vaz *et al.*, 2007), to the Ria de Vigo in Spain (Taboada *et al.*, 1998), to the Western European Margin (Coelho *et al.*, 1999), and to the Tucuruí reservoir in Brazil (Deus *et al.*, 2013), among others. In this section, a partial description of the model is given, because a full description is out of the scope of the thesis. However, more details can be found in Miranda *et al.* (2000) and in Pina (2001).

2.5.1. Hydrodynamics

The Hydrodynamic Module is the core of the MOHID Water modelling system and it can be used for bi-dimensional (2-D) and three dimensional (3-D) applications. In this research, the model was applied with a 2-D configuration, and the corresponding equations are:

$$\frac{\partial \eta}{\partial t} + \left[\frac{\partial}{\partial x}(uD) + \frac{\partial}{\partial y}(vD) \right] = 0 \quad \text{eq. 99}$$

$$\frac{\partial}{\partial t}(uD) + \left[\frac{\partial}{\partial x}(u^2D) + \frac{\partial}{\partial y}(uvD) \right] - fvD = -g'D \frac{\partial \eta}{\partial x} + \tau^x + D \left[\frac{\partial}{\partial x} \left(Ah \frac{\partial u}{\partial x} \right) + \frac{\partial}{\partial y} \left(Ah \frac{\partial u}{\partial y} \right) \right] \quad \text{eq. 100}$$

$$\frac{\partial}{\partial t}(vD) + \left[\frac{\partial}{\partial x}(uvD) + \frac{\partial}{\partial y}(v^2D) \right] + fuD = -g'D \frac{\partial \eta}{\partial y} + \tau^y + D \left[\frac{\partial}{\partial x} \left(Ah \frac{\partial v}{\partial x} \right) + \frac{\partial}{\partial y} \left(Ah \frac{\partial v}{\partial y} \right) \right] \quad \text{eq. 101}$$

where u and v are the velocity components along the x and y directions; f is the Coriolis parameter and it is a function of latitude, Ah is the coefficient of horizontal viscosity, τ^x and τ^y are the wind stresses along the x and the y directions, respectively, D is the total depth of the upper layer calculated as $D=H+\eta$, where H is its undisturbed thickness, and η is the interfacial deflection (Kantha and Clayson, 2000).

In this research, the model was set up by using a 2-D depth integrated model. This means that the study area was assumed to have an intense vertical mixing, and that the water column is vertically homogeneous. Based on this assumption, a single water layer was defined for the study area, with a variable depth defined by the bottom topography. This choice is justified by the shallowness of the study areas considered in this work, and by the necessity to use a configuration with a relatively low-computational cost. However, it is important to highlight that shallow estuaries may have stratification, which influences water residence time as well as biological processes occurring in the water and at the water-sediment interface. A 3-D model would ensure a more detailed representation of the system, at an increased computational cost.

2.5.2. Water Quality

The water quality model calculates source and sink terms for biogeochemical properties, in each cell of the grid, and in each time instant. The source and sink terms of each property describe chemical and biological processes associated with the biogeochemical cycles of carbon, nitrogen and phosphorus. The Water Quality Module in MOHID includes more than 20 properties, including nutrients, organic matter phytoplankton, and zooplankton.

The processes involving phytoplankton and macroalgae are similar, since they are both photosynthetic organisms. The only difference is that macroalgae live fixed to a substrate, and the phytoplankton is transported in the water column. Seagrasses are different from phytoplankton and macroalgae because they uptake nutrients not only from water, but also from the sediment. When detached by erosion, seagrass leaves are transported by currents as detrital organic matter. This means that seagrasses are not capable of photosynthesis when detached, whereas macroalgae are capable of photosynthesis when detached.

The dynamics of phytoplankton and macroalgae are simulated in MOHID by considering growth, grazing, respiration, excretion, and natural mortality. The generic equation for phytoplankton is as follows:

$$\frac{dPhy}{dt} = (\mu_{phy} - r_{phy} - e_{phy} - m_{phy} - p_{phy} - b_{phy})Phy \quad \text{eq. 102}$$

where t is the time, and phytoplankton concentration (Phy) is expressed in $g\ C/m^3$ (or $mg\ C/l$). The terms in parenthesis represent the net growth rate, given by the sum of the following rates: the gross growth rate μ_{phy} (day^{-1}), the total respiration rate r_{phy} (day^{-1}), the excretion rate e_{phy} (day^{-1}), the natural mortality rate m_{phy} (day^{-1}), the grazing rate p_{phy} (day^{-1}) by zooplankton, and the grazing rate b_{phy} (day^{-1}) by filter feeders. The growth rate depends on water temperature, nutrients and light in the water column. The complete description of the terms in the parenthesis in eq. 102, along with model parameters, can be found in the MOHID Water Quality Manual (IST, 2006), Fernandes *et al.* (2006), and in Trancoso *et al.* (2005). The grazing rate b_{phy} (day^{-1}) by benthic feeders is described in eq. 44.

The light extinction coefficient k ($1/m$) in the water is calculated as:

$$k = k_w + k_p C_p + k_s C_s \quad \text{eq. 103}$$

where C indicates concentration, and indices w , p , and s refer to water, phytoplankton chlorophyll concentration, and cohesive sediment concentration, respectively. In MOHID there is an option to define the effect of other properties on the light extinction coefficient. For a given property with concentration C_{prop} and extinction coefficient k_{prop} , it is possible to account for its effect on the light extinction coefficient by adding the product $k_{prop} C_{prop}$ to the right side of eq. 103.

2.5.3. Bottom shear stress

In MOHID wave parameters are used by the sediment water interface module to compute bottom shear stress, which is used both in hydrodynamics and in sediment transport, controlling erosion and deposition processes. In MOHID, waves can erode seagrass bed when the critical shear stress is higher than a defined value (expressed in Pa) specified by the user. Eroded seagrass leaves are assumed to be particulate organic matter that can be transported passively by currents. When seagrass bed is eroded, its biomass is set to a minimum value. In general, it is estimated that seagrasses do not exist at flow velocities above 1.5 m per second

or at very exposed shores (Greve and Binzer, 2004). Currents and wave action prevent seagrass growth and distribution by causing suspension and transport of the sediment.

In this section some information is provided about how bottom shear stress is calculated in MOHID. This information can be used by model users to set a critical value for bottom shear stress for seagrass beds. In MOHID the bottom shear stress τ_b (Pa) can be calculated as a function of bottom velocity only, or as a function of waves. The general formula used in MOHID to calculate bottom shear stress is:

$$\tau_b = Ch \cdot u_b^2 \cdot \rho \text{ (due to currents)}$$

$$\tau_{bw} = Ch \cdot u_{bw}^2 \cdot \rho \text{ (due to waves)}$$

eq. 104

ρ (1000 kg/m³) is the water density, u_b (m/s) is the bottom fluid velocity, τ_b (Pa) is the bottom shear stress due to currents, τ_{bw} (Pa) is the bottom shear stress due to waves, u_{bw} (m/s) is the bottom orbital velocity, and Ch (-) is the Chezy number. According to the formulation based on bottom velocity only, the Chezy number is calculated as a function of water depth and rugosity:

$$Ch = \left[\frac{\textit{karman}}{\ln\left(\frac{r+h}{r}\right)} \right]^2$$

eq. 105

where *karman* (-) is the Von Karman constant (equal to 0.4), r (m) is the rugosity, and h (m) is the water depth. According to Greve and Binzer (2004), at a velocity of 1.5 m/s no seagrass bed is present. If the velocity $u_b=1.5$ m/s is considered as the critical bed shear stress for seagrass beds, for $h=1$ m, $r=0.0025$ m, $\tau_b=8.5$ Pa. Bottom shear stress at velocity $u_b=1.5$ m/s is depicted in Figure 15 for different depths.

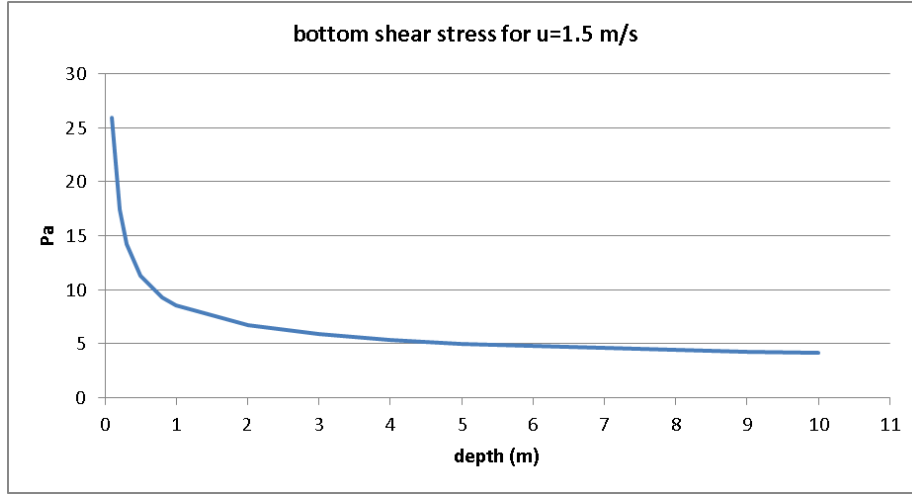


Figure 15 - Bottom shear stress at velocity $u_b=1.5$ m/s for different depths.

According to the formulation based on combined waves and currents, Ch is given as:

$$Ch = 0.25 \cdot F_w \quad \text{eq. 106}$$

F_w is a dimensionless factor calculated as:

$$F_w = e^{-5.977+5.213\left(\frac{Ab_w}{r}\right)^{c_1}} \quad c_1 = -0.194 \quad \text{eq. 107}$$

where r (m) is the bottom rugosity, $Ab_w = u_b / \Omega$; $\Omega = 2\pi / T$, and T (sec) is the wave period. The bottom orbital velocity u_{bw} (m/s) is given as:

$$u_{bw} = \frac{1}{2} \frac{\Omega \times h_w}{\sinh(N \times h)} \quad \text{eq. 108}$$

where h (m) is the water depth, h_w is the wave height (m), and $N = 2\pi / \lambda$. λ (m) is wave length $\lambda = c \times T$, and c is the wave celerity (m/s). For $h=1$ m, $T=10$ s, τ_b and u_{bw} vary with the wave height as shown in Table 7.

Table 7 - τ_{bw} and u_{bw} for different values of h_w ($h=1$ m, $T=10$ s)

h_w (m)	0.10	0.20	0.30	0.40	0.50	0.60	0.70	0.80	0.90	1.00	1.10	1.20	1.30	1.40
u_{bw} (m/s)	0.15	0.31	0.46	0.62	0.77	0.93	1.08	1.24	1.39	1.54	1.70	1.85	2.01	2.16
τ_{bw} (Pa)	0.13	0.39	0.77	1.24	1.81	2.47	3.21	4.04	4.96	5.95	7.02	8.17	9.39	10.69

2.5.4. Integration in MOHID

The model described in this chapter was integrated in the MOHID water modeling system by using a set of three modules:

- BenthicEcology module;
- SeagrassesWaterInteractions module; and,
- SeagrassesSedimInteractions module.

The BenthicEcology module is the module responsible for solving all the differential equations described in this chapter for seagrasses, benthic feeders, microphytobenthos, and particulate organic matter and nutrients at the sediment water interface. The other two modules are used only when seagrasses are computed, and they are responsible for the calculation of the seagrass uptake of nutrients from water column and sediment. The three modules were written in FORTRAN 95 and they were included in the MOHID code available at <http://mohid.codeplex.com/>. In MOHID there are interfaces which enable the transfer of information between modules. These interfaces are: Module Interface, Module InterfaceSedimentWater, and Module InterfaceWaterAir. In this research, Module Interface and Module InterfaceSedimentWater were modified to enable the transfer of information between BenthicEcology SeagrassWaterInteractions module and SeagrassSedimInteractions module (Figure 16).

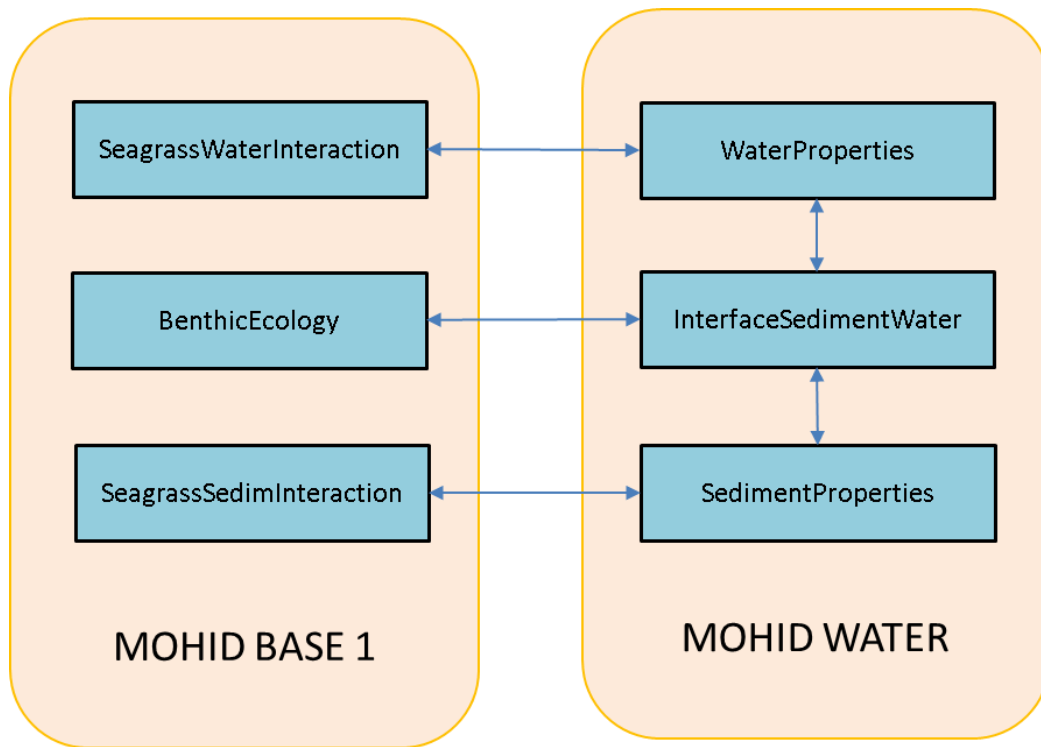


Figure 16 - Conceptual diagram of the links existing between the modules inside MOHID.

Chapter 3 – Model testing (part 1)

3.1. Introduction

In this chapter the main limiting functions of the seagrass model are described. A preliminary calibration of the model is carried out to estimate parameters specific for the seagrass *Zostera noltii*. Mass conservation tests are performed in a 0-D configuration of the model to verify the consistency of the numerical formulation with the estimated parameters. Sensitivity analysis is carried out to establish the influence of model parameters on the overall model results.

3.2. Function plots

In this section, the main limiting factors of the seagrasses are described.

Temperature limitation

Seagrass growth is dependent on temperature variations (Greve and Binzer, 2004). *Zostera* species can tolerate sea surface temperatures from about 5 °C, with an optimum growth and germination range starting from 10 - 15 °C (Yonge, 1949). According to recent studies, survival of *Zostera* is still possible at 37° C, while higher temperatures led to a sudden drop in photosynthetic capacity followed by mortality that occurs more rapidly with increasing temperatures (Massa *et al.*, 2009).

The formulation used to express dependence of growth on temperature in seagrasses is the same as the one used for other modules in MOHID to express the effect of temperature on the organisms' growth rates. The dependence of growth on temperature is expressed by establishing an optimal temperature for seagrass growth, and an optimal interval of tolerance. A bell-shaped function (appendix A), and described in Trancoso (2002), takes into account the range of temperature tolerated by seagrasses. The function varies between 0 and 1, with a maximum (equaling 1) in correspondence with the optimal temperature (Figure 17). This bell-shaped function is similar to already used formulations found in literature for seagrass species (Bocci *et al.*, 1997; Elkalay *et al.*, 2003; Zaldivar *et al.*, 2009).

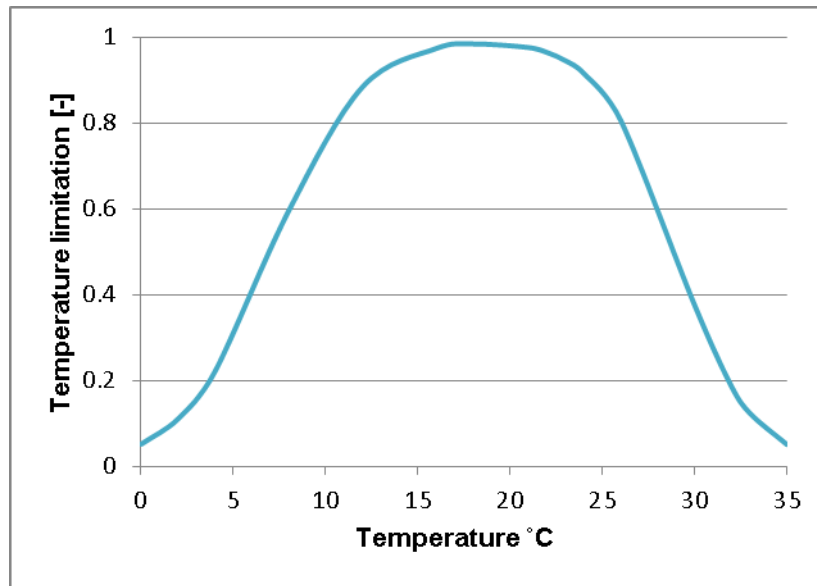


Figure 17 - Temperature limiting function calculated as in equation A.1, for $T_{\min}^{opt}=10^{\circ}\text{C}$; $T_{\max}^{opt}=30^{\circ}\text{C}$; $T_{\min}=5^{\circ}\text{C}$; $T_{\max}=37^{\circ}\text{C}$ (see appendix A).

Space limitation

Competition between different species of seagrasses and between macroalgae and seagrasses may also set limits to growth and distribution. Other plants and algae grow and become larger, and eventually cover the bottom and suppress the growth of other plants. “*Z. noltii* often colonises the intertidal zone or the shallow waters where other species cannot establish populations. In deeper waters where *Z. marina* or *C. nodosa* can establish, they apparently have a competitive advantage and *Z. noltii* beds will disappear” (Greve and Binzer, 2004).

The space limiting factor $f(L)$ used in this model was described in in Chapter 2 (eq. 6). The space limiting factor as a function of the leaves biomass is depicted in Figure 18 for $M=0$ kg DW/m², and for three different values of K_{max} . The parameter K_{max} depends on the study area and it is determined from data (Biber *et al.*, 2004). The formulation from Bocci *et al.* (1997) was extended to include the effect of macroalgae by adding the macroalgae biomass to K_{max} . This formulation can have limitations because the growth of seagrasses can be already limited at low values of macroalgae biomass. However, there is no information available in literature about the minimum macroalgae biomass at which seagrass starts to be affected by space limitation. A better formulation can be developed if data is available to test different formulations.

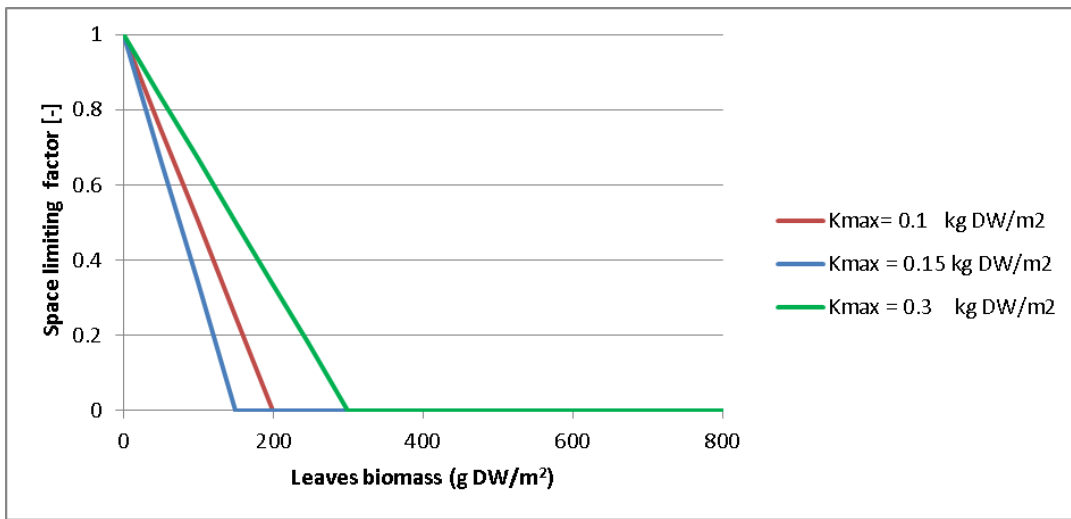


Figure 18 - Space limiting factor as a function of seagrass leaves, calculated from eq. 6, for $M=0$ kg DW/m², and for three different values of K_{max} .

When other plants or algae are present ($M > 0$ kg DW/m² in eq. 6), the space occupied by other plants and algae is limiting the growth of seagrasses leaves, as shown in Figure 19.

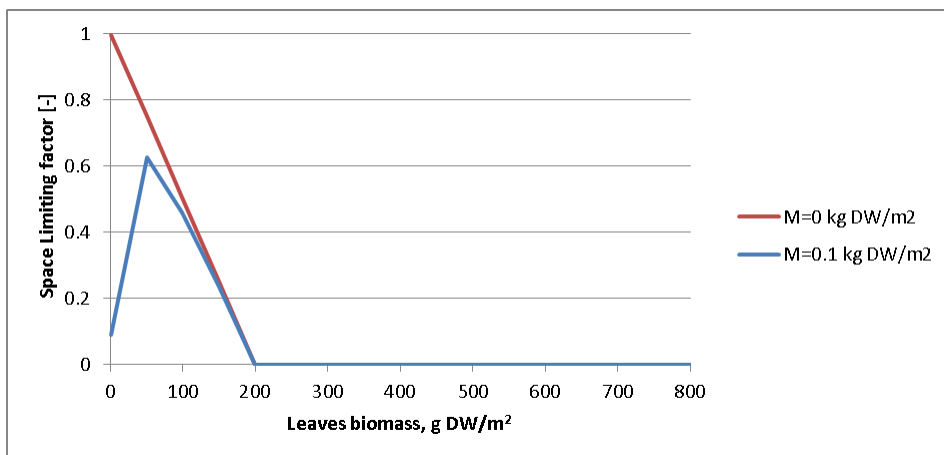


Figure 19 - Space limiting factor as a function of seagrass leaves, calculated as eq. 6, for two different values of M , and for $K_{max} = 0.2$ kg DW/m².

Nutrient limitation

The seagrass model accounts for the limiting effect of nutrient content on growth and uptake of nutrients, following the approach described in Bocci *et al.* (1997). The limiting factors $f(N)$ and fbn expressing the effect of nitrogen content on plant's growth and uptake were described in eq. 8 and in eq. 16 in Chapter 2, respectively. The function plots for these equations are given in Figure 20. The red line in Figure 20 shows that $f(N)$ increases (decreases) with the increasing (decreasing) of plant nitrogen content, which means that the growth is limited by low concentration of nitrogen in the plant. The blue line in Figure 20 shows that fbn decreases with increasing nitrogen content, which means that the plant uptakes nitrogen only if its reserve is not complete. This means that at low nitrogen quota in the plant, the plant is growing less and it will try to uptake more nitrogen from the environment. When the plant's nitrogen quota is high, the uptake of external nitrogen is reduced, suggesting that growth is limited by other factors.

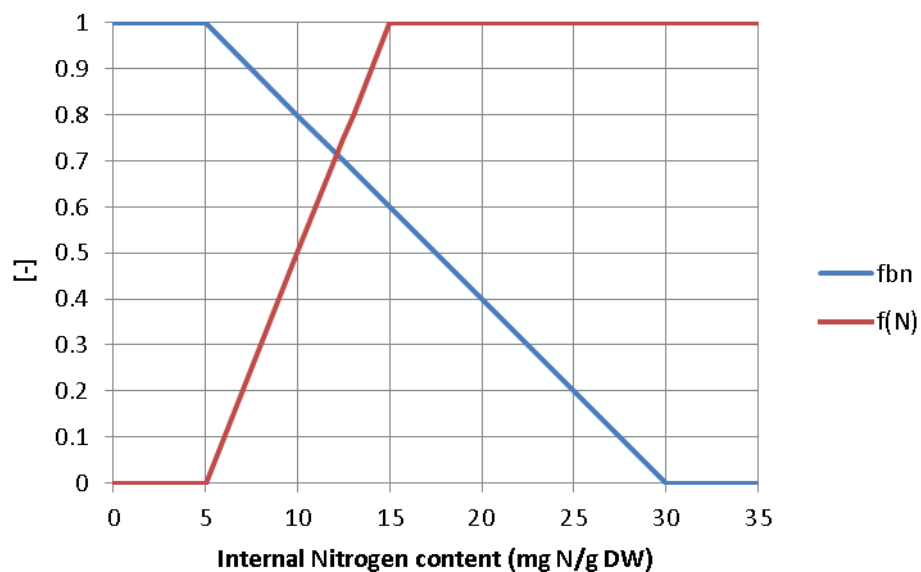


Figure 20 - Nitrogen limiting factors (eq. 8 and eq. 16).

The limiting factors $f(P)$ and fbp expressing the effect of phosphorus content on plant's growth and uptake are described in eq. 9 and in eq. 20 in Chapter 2, respectively. The function plots for these equations are given in Figure 21. The figure shows that $f(P)$ increases with increasing phosphorus content, which means that the growth is limited at low concentrations of phosphorus in the plant. Figure 21 also shows that fbp decreases with

increasing phosphorus content, which means that the uptake of phosphorus is limited at high phosphorus content in the plant. This means that at low phosphorus quota, the plant is growing less but it is uptaking more phosphorus from the environment. When the plant's phosphorus quota is high, the uptake of external phosphorus is reduced, and the phosphorus content is consumed to enable plant's growth.

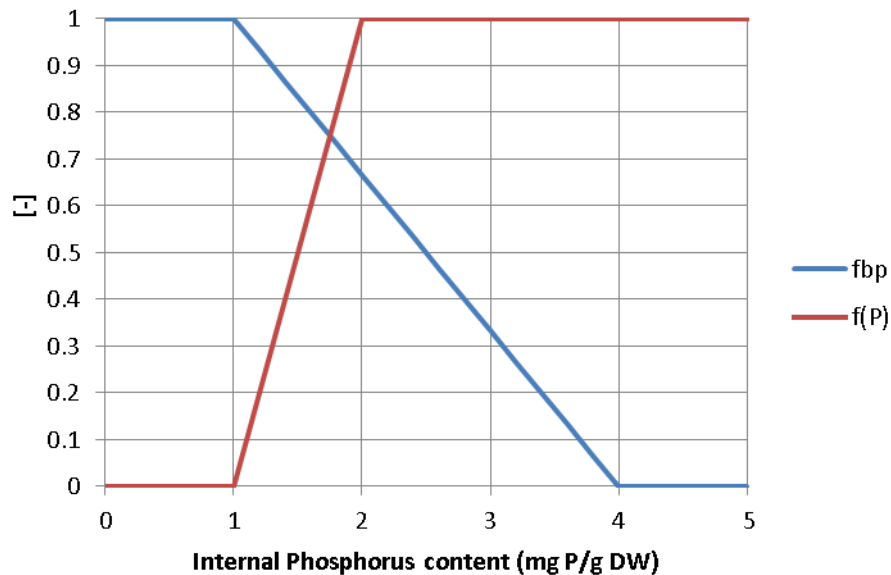


Figure 21 - Phosphorus limiting factors, (eq. 9 and eq. 20).

Light limitation

Seagrasses are limited by light availability as other primary producers of the aquatic environment. Light is a limited resource in the aquatic environment because it extinguishes exponentially with increasing depths. In this research, light limitation in seagrasses was expressed by using Michaelis-Menten saturation law, based on previous studies documented by Bocci *et al.* (1997). The light limiting factor (Figure 22) is calculated as a function of the light available at the top of the canopy I_c (W/m^2), (eq. 5).

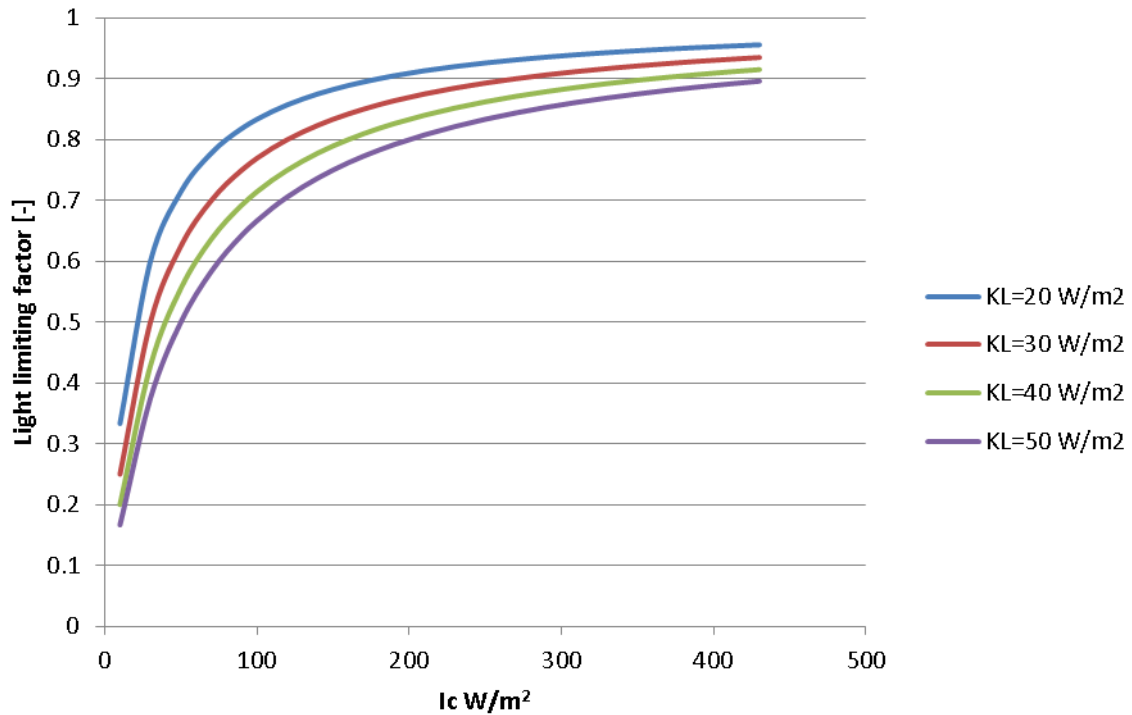


Figure 22 - Light limiting factor as a function of light available at top canopy (I_c), for different values of KL (eq. 5).

The light available at the top of the canopy is calculated by using the Steele's formula for light extinction with increasing depth, considering that the height of the canopy varies with tide and with the biomass of the plant (eq. 36). The example in Figure 23 shows the light available at top of canopy (I_c , W/m²) as a function of depth (Steele, 1962), for a canopy height $h_c = 1$ m. When the water depth is lower than the height of the canopy, the light available at the top of the canopy equals the light available at the surface of the water. When the water depth is higher than the height of the canopy, light available at the top of the canopy follows an exponential decay with increasing depth.

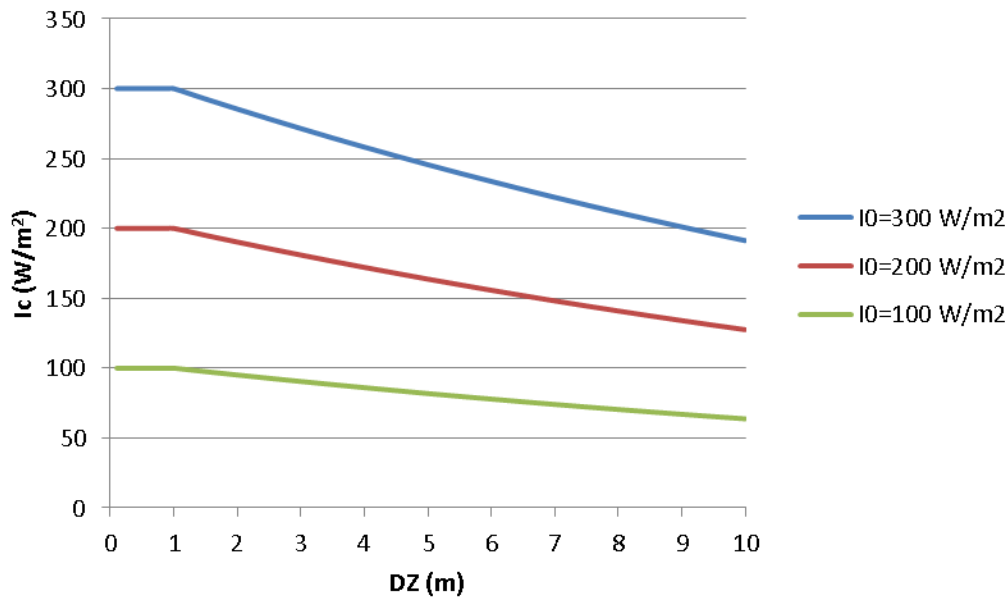


Figure 23 - Light available at the top of the canopy as a function of water depth for three different values of light available at the surface (I_0) (eq. 36), and considering $h_c=1$ m and $k=0.05$ 1/m.

3.3. Preliminary model calibration

In this section a preliminary model calibration of the seagrass model is carried out to estimate parameters specific for the seagrass *Zostera noltii*.

The seagrass model is generic because it contains characteristics common to several seagrass species. However, model parameters can vary from one species to another. Existing seagrass models use specific values for the species to be simulated (Bocci *et al.*, 1997; Elkalay *et al.*, 2003). As an example, a model developed for *Posidonia oceanica* (Elkalay *et al.*, 2003) uses a maximum leaves biomass value of 0.750 kg DW/m². A model for *Zostera marina* (Bocci *et al.*, 1997) uses a maximum leaves density of about 0.5 kg DW/m² (parameter K_{max}). In this research, the model was used to simulate the species *Zostera noltii*. Data found in literature show that maximum biomass of *Zostera noltii* in the Palmones Estuary, Spain, was about 0.26 kg DW/m² (Pérez-Lloréns and Niell, 1993). This suggests that the value of 0.5 kg DW/m² for the parameter K_{max} from Bocci *et al.* (1997) used for *Zostera*

marina is not adequate to describe *Zostera noltii* dynamics, although the two species belong to the same genus (*Zostera*).

No values were found in literature to express the maximum growth rate of *Zostera noltii*. Bocci *et al.* (1997) used a growth rate of 0.06 1/day for *Zostera marina*. However, this value of g_{max} may be inadequate to describe the growth rate of *Zostera noltii*. The lack of information about specific parameters for *Zostera noltii* led to the necessity to use a calibration tool which to compare real data and model results, to estimate a new set of parameter values that can be used for *Zostera noltii*.

Use of a calibration tool

When information to establish parameter values is insufficient, it may be necessary to calculate and deploy parameter values by using a calibration tool. Calibration is based on the optimization of an objective function that minimizes the difference between model results and real data. Model parameters are changed until a set of parameter values is found to minimize the difference between model results and field data (Ditmars, 1988).

In this research, a preliminary calibration of the model was carried out by using the MATLAB optimization toolbox. The calibration tool has the following inputs: a system of ODEs, a set of parameters, and a database. The system of ODEs is the system of equations already described for the seagrass model. The parameters were described in Table 8. The database consists of time series of measured *Zostera noltii* leaves and roots biomass by Pérez-Lloréns and Niell (1993). These time series are used to compare the simulated *Zostera noltii* biomass (leaves and roots) with data. The tool calculates the solution of the ODEs over a time interval, and calculates the difference between simulated and measured leaves and roots biomass over the same time interval. On the basis of this difference, the tool evaluates the error of the model with respect to data, and defines a new set of parameters that is expected to decrease the error between data and model. The new set is used for the next iteration, until a set of parameters is found to minimize the error of the model with respect to data. At the end of the iteration cycle, the new set of parameters is provided as output of the calibration.

Preliminary calibration results

The calibration produced a set of estimated parameters listed in Table 8. The overall results of the model calibration had a satisfactory agreement with data (Figure 24a). The calibration procedure changed the value of g_{max} from 0.06 to 0.23 day⁻¹. This value was in the range of previous studies, between 0.06 and 1.24 day⁻¹ (Bocci *et al.*, 1997; Hipsey *et al.*, 2003; Newell and Koch, 2004). A model which is using a parameter for maximum *Zostera noltii* leaves biomass (K_{max}) was not found in literature. The parameter was initialized to a value already used in a model for another *Zostera* species (in this case *Zostera marina*), and then the calibration tool changed it from 0.5 to 0.228 kg DW/m². This value was found to be more consistent with the maximum values found in literature for the same species: maximum values of *Zostera noltii* biomass in literature were found to be between 0.18 and 0.26 kg DW/m² (Pérez-Lloréns and Niell, 1993; Plus *et al.*, 2001). Leaves decay rate was changed from 0.0041 to 0.064 day⁻¹. This new value is in the same order of magnitude of the leaves decay rate of 0.041 used in a *Zostera marina* model (Bocci *et al.*, 1997). Roots decay rate was changed from 0.0038 to 0.035 day⁻¹. This new value is in the same order of magnitude of the roots decay rate of 0.015 day⁻¹ used in a *Zostera marina* model (Bocci *et al.*, 1997). The maximum uptake rates for nitrogen were changed to values very similar to the initial ones, and they remained in the range of the literature values reported in Touchette and Burkholder (2000). $V_{max}^{NH_4w}$ was changed from 2 to 1.7 g N/kg DW/day. $V_{max}^{NO_3w}$ was changed from 1.44 to 1.07 g N/kg DW/day. $V_{max}^{NH_4s}$ was changed from 0.48 to 0.14 g N/kg DW/day. $V_{max}^{PO_4}$ was changed from the initial value of 0.015 to 0.21 g P/kg DW/day, remaining in the range of data reported in Touchette and Burkholder (2000). Few studies on seagrasses phosphate uptake are available in literature (Romero *et al.*, 2006). These studies refer mostly to *Thalassia hemprichii*, for which the reported maximum phosphorus uptake rate from leaves ranges between 0.28 and 0.42 g P/kg DW/day, and shows that seagrasses have a phosphate affinity in the same order of magnitude as that for ammonium.

The translocation coefficient tr was slightly changed from 0.25 to 0.28. The internal nitrogen quota N_{crit} was changed from 15 to 16 g N/ kg DW. N_{max} was changed from 30 to 31 g N/kg DW. N_{min} remained unchanged after calibration. Parameters for the internal phosphorus quota P_{min} , P_{crit} , and P_{max} were changed from 0.44, 1.33, and 2.67 g P/kg DW to 0.14, 0.8, and 3.14 g P/kg DW, respectively. However, the value of 3.4 g P/kg DW for P_{max} provided by the automatic calibration was changed to 6 g P/kg DW in order to better adjust to data of phosphorus content reported in Pérez-Lloréns and Niell (1993). The half-

saturation constants for nutrient uptake were changed by the calibration procedure, but they remained in the same order of magnitude of the initial guess. The r_N ratio changed from 19 to 16.2 g N/kg DW, and the r_P ratio from 2.3 to 1.8 g P/kg DW.

Table 8 – Parameter values estimated by calibration

Symbol	Description	Unit	Estimated value
g_{max}	Seagrass maximum growth rate	day ⁻¹	0.23
K_{max}	Maximum leaves biomass	kg DW/m ²	0.228
N_{min}	Minimum internal nitrogen quota	g N/kg DW	5
N_{crit}	Critical internal nitrogen quota	g N/kg DW	16
N_{max}	Maximum internal nitrogen quota	g N/kg DW	31
P_{min}	Minimum internal phosphorus quota	g P/kg DW	0.14
P_{crit}	Critical internal phosphorus quota	g P/kg DW	0.8
P_{max}	Maximum internal phosphorus quota	g P/kg DW	3.14
r_N	N: DW ratio in seagrasses	g N/kg DW	16.2
r_P	P: DW ratio in seagrasses	g P/kg DW	1.8
$V_{max}^{NH_4w}$	Leaves maximum uptake of ammonia	g N/(kg DW·day)	1.7
K_{NH_4w}	Leaves half-saturation constant for ammonia	g N/m ³	0.13
$V_{max}^{NO_3w}$	Leaves maximum uptake of nitrate	g N/(kg DW·day)	1.07
K_{NO_3w}	Leaves half-saturation constant for nitrate	g N/m ³	0.12
$V_{max}^{NH_4s}$	Roots maximum uptake rate of ammonia	g N/(kg DW·day)	0.14
K_{NH_4s}	Roots half-saturation constant for ammonia	g N/m ³	0.8
$V_{max}^{PO_4}$	Maximum uptake rate of phosphate	g P/(kg DW·day)	0.21
K_{PO_4}	Half-saturation constant for phosphate	g P/m ³	0.017
m_{l0}	Leaves base decay rate	day ⁻¹	0.035
m_{r0}	Roots base decay rate	day ⁻¹	0.064
min_s	Mineralization rate in the sediment	day ⁻¹	0.06
min_w	Mineralization rate in the water	day ⁻¹	0.04
tr	Carbon translocation coefficient	-	0.28

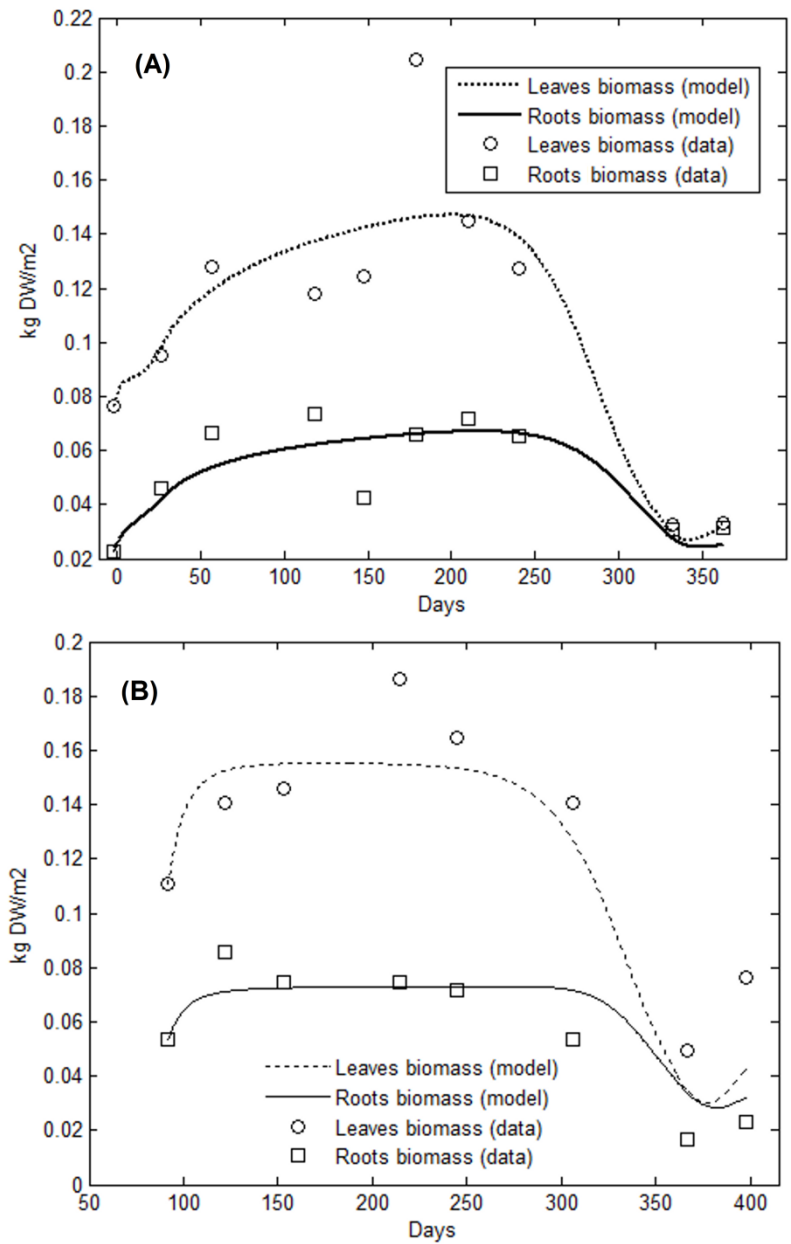


Figure 24 – Comparison of model results with data.

3.4. Verification

The new set of parameters established by calibration was used to verify the results of the model with observed data. Observed data used for verification consisted of time series of *Zostera noltii* leaves and roots biomass by Pérez-Lloréns and Niell (1993) and collected between April 1988 and December 1988, in the Palmones River estuary, Spain. The results of the verification are shown in Figure 24b. Simulated biomass of leaves and roots increased in response to light and nutrients in spring, reached a maximum in summer, and decreased in autumn. Simulated leaves biomass ranged between 0.03 and 0.16 kg DW/m², with an average of 0.12 kg DW/m². Simulated roots biomass ranged between 0.03 and 0.07 kg DW/m², with an average of 0.06 kg DW/m². Total plant's biomass ranged between 0.06 and 0.23 kg DW/m², with an average of 0.18 kg DW/m². These results are in agreement with previous studies: observed data reported for *Zostera noltii* in the Thau Lagoon, France (Plus *et al.*, 2001), showed that the biomass of the leaves along the year varied between 13.6 and 173.8 g DW/m². Leaves biomass of *Zostera noltii* in the Arcachon Bay, France, ranged between 81 and 101 g DW/m² (Plus *et al.*, 2001). A study concerning seasonal dynamics of *Zostera noltii* biomass in the Palmones River Estuary, Spain, (Pérez-Lloréns and Niell, 1993), revealed that plant's biomass ranged between 25 and 200 g DW/m², with the maximum in late summer. On the other hand, biomass of *Zostera noltii* in Ria Aveiro, Portugal, varied between 85 and 142 g DW/m², with an average value of 107 g DW/m² (Silva *et al.*, 2009).

3.5. Testing

In this section, mass conservation tests are performed in a 0-D configuration of the model to verify the consistency of the numerical formulation. A long term run is carried out to test the behavior of the model over time.

Multi-year run

The seagrass model was tested by using a 0-D configuration to execute simple tests to verify mass conservation in the system. The model was executed over a period of 10 years without advection-diffusion processes. For the model forcing, typical surface water temperature and surface radiation values for mid-latitude of the northern hemisphere were used (Figure 25 and Figure 26). The model parameters were assigned with values shown in Table 8. Initial conditions were used from Table 9. The variation of the state variables as a function of time was determined. The time step used was 10 sec.

Table 9 - Initial conditions used for seagrass model multi-years run.

State variable	Initial Value	Unit
<i>L</i>	0.11	kg DW/m ²
<i>R</i>	0.053	kg DW/m ²
<i>N</i>	0.0024	kg N/m ²
<i>P</i>	0.000164	kg P /m ²
<i>NH4_w</i>	1	g N/m ³
<i>NO3_w</i>	1	g N/m ³
<i>NH4_s</i>	1	g N/m ³
<i>PO4_s</i>	1	g P/m ³
<i>PON_s</i>	1	g N/m ³
<i>POP_s</i>	0.13	g P/m ³
<i>PON_w</i>	1	g N/m ³
<i>POP_w</i>	0.13	g P/m ³
<i>PO4_w</i>	0.1	g P/m ³

Simulated nitrogen and phosphorus percent are shown in Figure 27 and in Figure 28. Simulated ammonia, nitrate, and particulate organic nitrogen are shown in Figure 29. Simulated particulate organic nitrogen in sediment and particulate organic phosphorus in sediment are shown in Figure 30 and Figure 31. Simulated seagrass leaves and roots biomass is shown in Figure 32. Simulated C:N and C:P ratios were inversely related with nutrient content (Figure 33 and Figure 35), in conformity with previous studies (Duarte, 1990; Campbell *et al.*, 2012). The rate of change in C:N and C:P ratios with increasing nitrogen or phosphorus content in plant tissues should shift from high to small as nutrient supply meets the plant's demands (Duarte, 1990). The inverse relationship between C:N and C:P ratios and nutrient content was described by Duarte (1990) (Figure 34 and Figure 35).

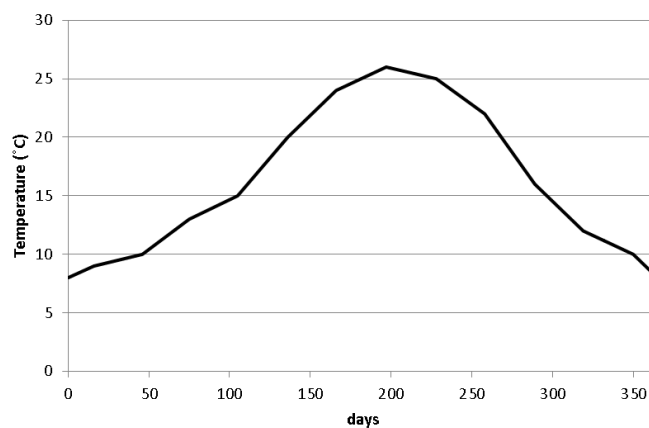


Figure 25 - Temperature used to force the model. For multi-year runs the same set of data was repeated.

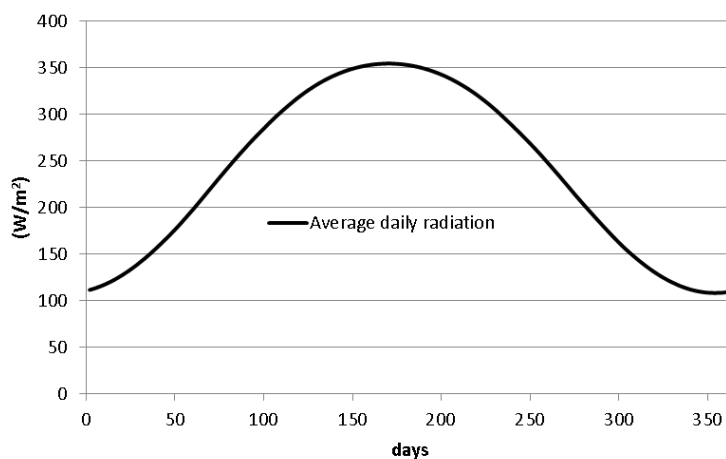


Figure 26 - Surface radiation used to force the seagrass model. For multi-year runs the same set of data was repeated.

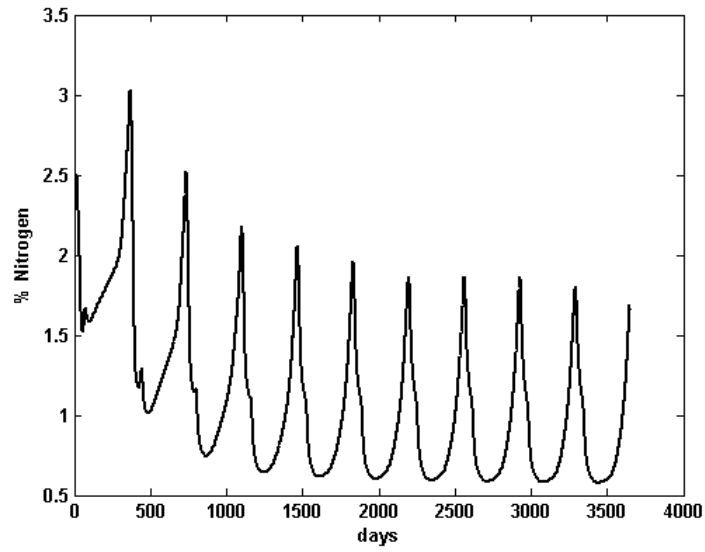


Figure 27 – Simulated nitrogen percent in the plant over a period of 10 years.

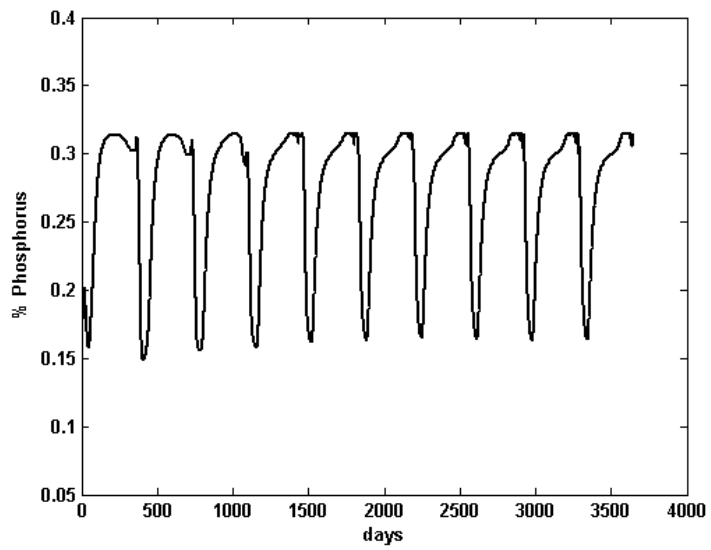


Figure 28 – Simulated phosphorus percent in the plant over a period of 10 years.

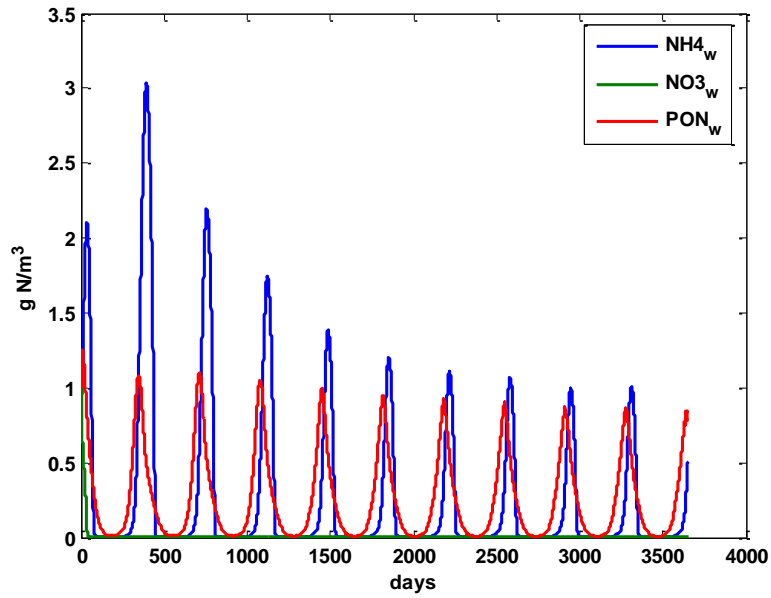


Figure 29 – Simulated ammonia (NH_4_w), nitrate (NO_3_w), and particulate organic nitrogen (PON_w) in water over a period of 10 years.

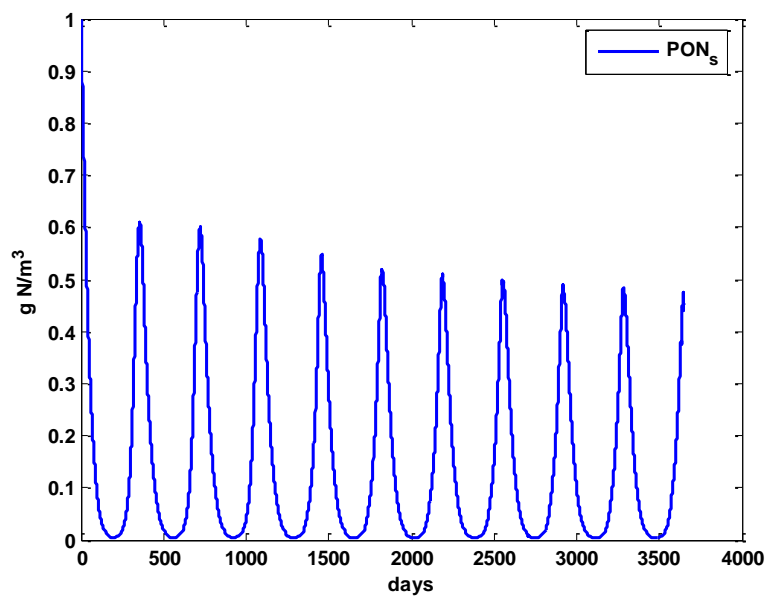


Figure 30 – Simulated particulate organic nitrogen (PON_s) in the sediment over a period of 10 years.

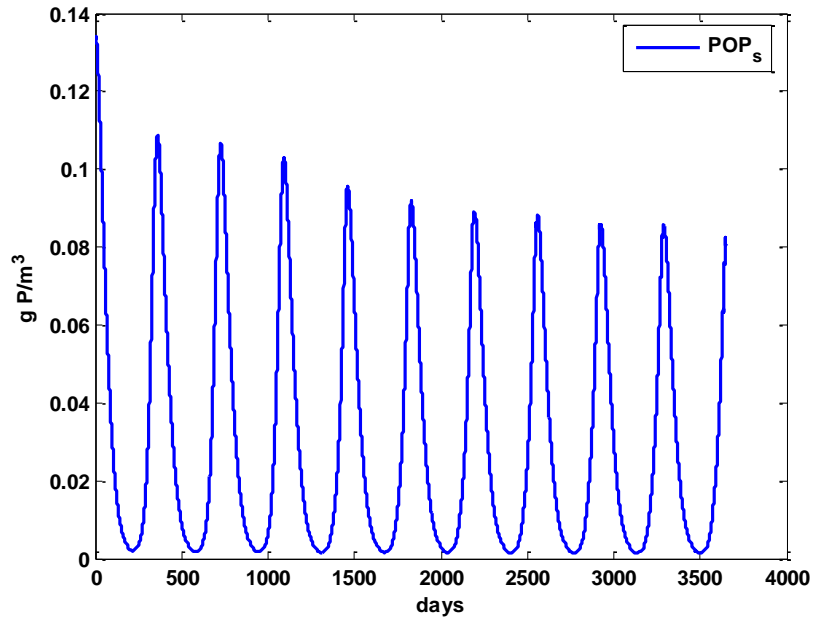


Figure 31 – Simulated particulate organic phosphorus (POP_s) in the sediment over a period of 10 years.

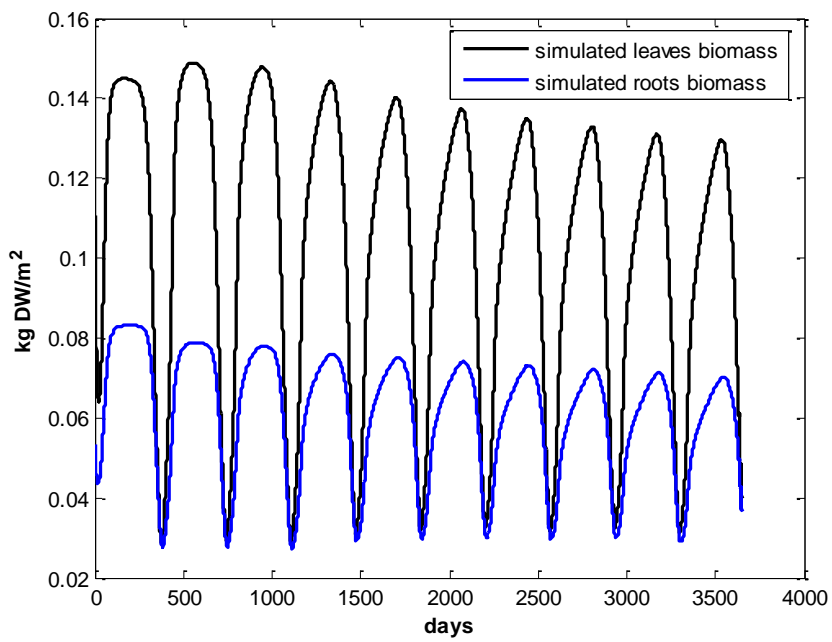


Figure 32 – Simulated seagrass leaves and roots biomass over a period of 10 years.

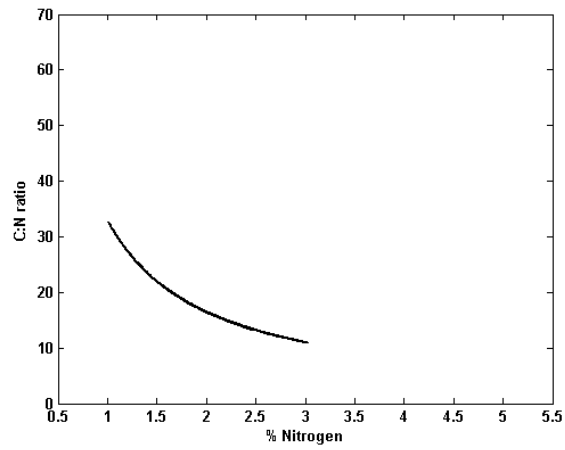


Figure 33 – Simulated C:N ratio versus nitrogen in the plant expressed as percent of dry weight. The model results were obtained with parameters from Table 8.

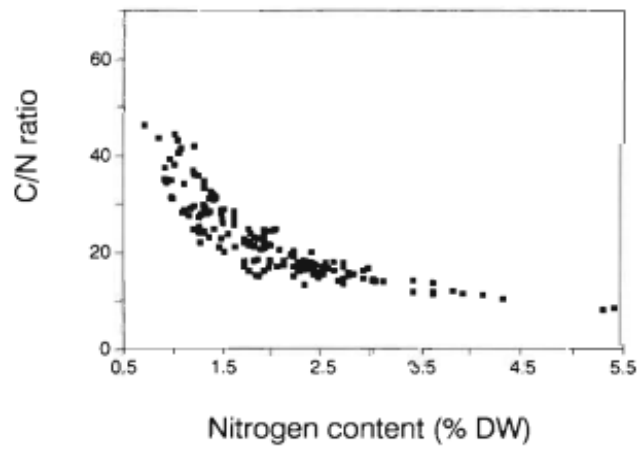


Figure 34 – Relationship between carbon:nitrogen (C:N) in seagrass and nitrogen content. After Duarte (1990).

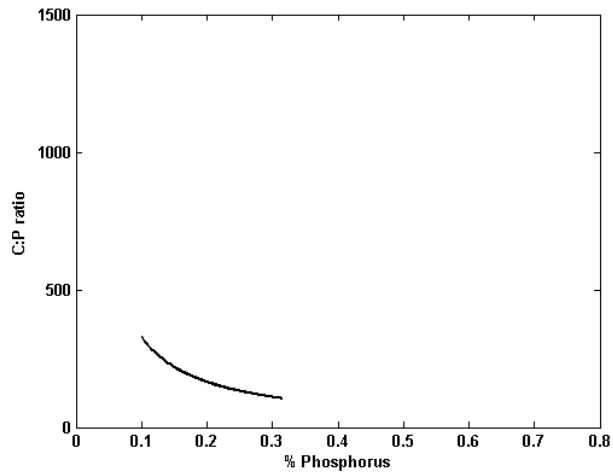


Figure 35 – Simulated C:P ratio versus phosphorus in the plant expressed as percent of dry weight. The model results were obtained with parameters from Table 8.

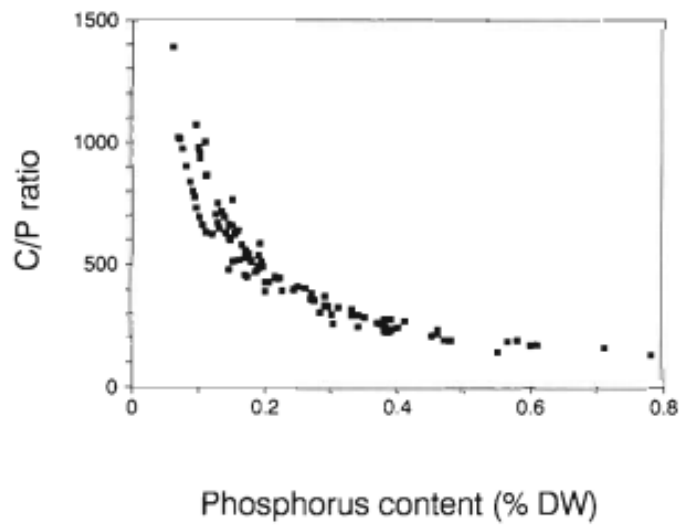


Figure 36 – Relationship between carbon:phosphorus (C:P) ratios of seagrass and phosphorus content. After Duarte (1990).

Mass conservation

This section describes the mass conservation in the simulated system. In this test, a closed system was considered, where total mass must be constant over time. As a consequence, no nutrient inputs/outputs were considered. Total mass (Figure 37) was expressed as total nitrogen and total phosphorus in the system. Total nitrogen at each time t was calculated by summing up the mass of the state variables L , R , $NO3_w$, $NH4_w$, N , PON_w , PON_s , and $NH4_s$, at time t , expressed as grams of nitrogen. Total phosphorus in the system at each time t was calculated by summing up the mass of the state variables L , R , POP_w , P , POP_s , $PO4_s$, and $PO4_w$, all expressed as grams of phosphorus. The results showed that total nitrogen and total phosphorus in the system were constant over time, and this demonstrated that the simulated system was conserving the mass.

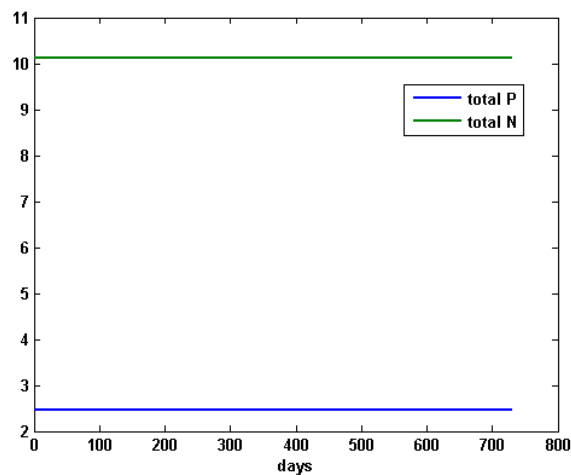


Figure 37 – Total mass in the simulated system expressed as total P and total N.

3.6. Sensitivity analysis

In this section, sensitivity analysis is carried out to establish the influence of model parameters on the overall model results. Sensitivity analysis is carried out by using two methodologies: Local Sensitivity analysis (LSA), and Global sensitivity analysis (GSA). The results of the two methodologies are compared.

Methodology

Model results strongly depend on initial conditions, forcing functions, equations, and parameters. The latter are not always known because of the lack of information and difficulty to measure them. The accuracy of biological models is often affected by the uncertainties in the measurement and estimation of model parameters (Marino *et al.*, 2008). Sensitivity analysis is a technique to evaluate the impact of parameter variations on simulated variables, and to assess uncertainty of model parameters. Several methodologies are available in literature for the calculation of the impact parameters on model outputs. These methodologies are divided into two main groups: Local Sensitivity Analysis (LSA) and Global Sensitivity Analysis (GSA). LSA evaluates parameter changes with respect to a baseline (nominal value), and the consequent variations of model outputs are quantified. LSA has low computational costs and they are useful when model parameters are known to be with low uncertainty. However, for quantitative analysis, these techniques were found to be inappropriate (Marino *et al.*, 2008). GSA is based on multiple model evaluations using Monte Carlo simulations. Monte Carlo simulation methods are commonly used to perform multiple model simulations by using randomly generated model inputs (Marino *et al.*, 2008). Recent studies demonstrated that LSA and GSA give very different results and that it is not advisable to draw conclusions about parameter sensitivity calculated by LSA (Marino *et al.*, 2008; Quillet *et al.*, 2013). The sensitivity analysis of the seagrass model was computed by using both methodologies. The results of LSA applied to the seagrass model can be found in Ascione Kenov *et al.* (2013). A brief comparison of the results of the two methodologies is presented at the end of this chapter. GSA techniques are implemented by using sampling and variance-based techniques (Saltelli, 2002; Saltelli *et al.*, 2004). Correlation coefficients are considered the most efficient and reliable ones among the sampling-based indices (Saltelli and Marivoet, 1990; Marino *et al.*, 2008).

In this section, GSA was carried out to quantify uncertainties of model parameters and to assess their effects on model results. The GSA aimed to identify model parameters with a high impact on the model results. Sampling-based sensitivity indices were calculated to assess the impact of parameters on model results. State variables of the model were considered as the response variables against which to test the effect of parameter changes. The methodology for sensitivity analysis (Figure 38) follows established GSA procedures (Marino *et al.*, 2008; Cazelles *et al.*, 2013).

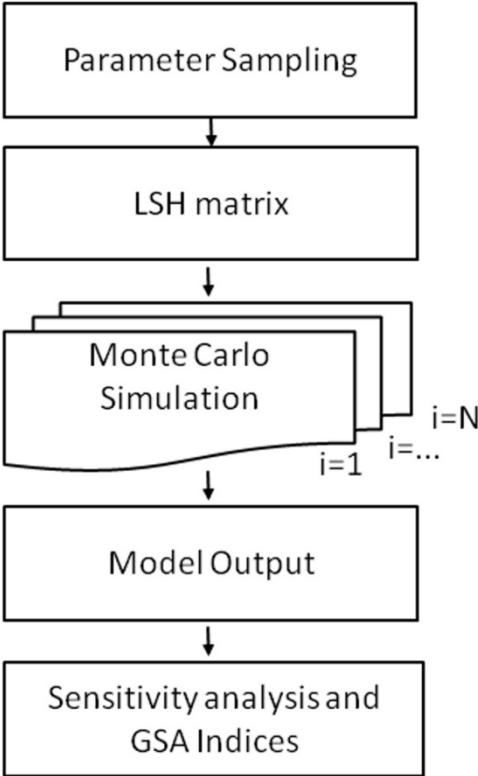


Figure 38 - Sensitivity analysis flow chart.

The GSA methodology was divided into 4 steps: (1) Sampling of parameters; (2) Monte Carlo simulation; (3) Calculation of global sensitivity indices; and, (4) Significance tests.

In step (1), the values of the parameters are established on the basis of random sampling from probability distribution functions (pdf). Every parameter is assumed to have a pdf (uniform or normal), which is divided into N intervals with an equal probability. N independent samples are extracted from each pdf (N equiprobable values of the same

parameter are drawn from the pdf). For the sampling of the pdf the Latin Hypercube Sampling (LSH) technique was used (McKay *et al.*, 2000; Marino *et al.*, 2008), which was found superior to random sampling, and explores the entire parameter space (Cazelles *et al.*, 2013). Parameter values were stored in a LSH matrix of $N \times n$ size (hereafter named as X), where n is the number of parameters and N is the sample size. In GSA techniques, parameters are assumed to have a uniform or normal distribution between a minimum and a maximum value. To define the interval of variation of model parameters, normal distributions were used with the mean equal to the values listed in Table 8, and the variance equal to $\pm 50\%$ of the mean.

In step (2), a set of $N = 1000$ simulations was carried out. At each simulation the solution of the model was calculated over a time interval of 360 days. The results of the runs were stored in a matrix of response variables (hereafter named as Y), containing time series of the model outputs for all of the state variables and N simulations.

In step (3), X and Y were used to calculate sampling-based GSA indices such as the Pearson correlation coefficient (PCC), the Spearman correlation coefficient (SCC), and the Partial ranked correlation coefficient (PRCC). When the correlation coefficient is greater than 0, this indicates a positive linear relationship. When the correlation coefficient is less than 0, this indicates a negative linear relationship. For the calculation of GSA indices, X and Y were considered as the independent variable and dependent variable, respectively. For each combination of state variable and parameter, the GSA indices were calculated. To calculate the SCC for a sample of size N , the elements of X and Y are converted into ranks. The ranking transformation consists of assigning scores to the elements of the X and Y . As an example, for each column of X , rank 1 is assigned to the smallest value, rank 2 is assigned to the second higher value, and so on until rank N is assigned to the highest value. The result is a matrix of scores (or ranks). PRCC is calculated by using rank-transformed data as well. The partial correlation between X and Y is given by the definition of n controlling variables $Z =$ (Bendtsen and Hansen, 2013), and by applying a rank transformation of X and Y . PRCC is the correlation between the residuals resulting from the linear regression of ranked X with Z , and of ranked Y with Z .

Finally, in step (4), significance tests were carried out to assess if relationships detected by the correlation coefficients were the result of a chance. In this research the model state variables are considered as dependent variables, and model parameters are independent variables. To assess significance of correlations, paired t-test hypothesis testing was carried out. Two hypotheses were proposed: the null hypothesis H_0 states that no correlation is

present between the state variable and the parameter. The alternative hypothesis H1 states that there is a correlation between the state variable and the parameter. The t-test was used to calculate the level of significance of the correlation, named as p-value. Three significance levels α (0.05, 0.01, 0.001) were established for the test. A p-value $< \alpha$ means that H0 can be rejected at the significance level α . For example for $\alpha=0.05$ and p-value $<\alpha$, there is 95% confidence that a linear relationship exists. As a consequence, H0 is rejected, and the alternative hypothesis H1 is accepted at the significance level α . If p-value $>\alpha$, it cannot be 95% confident that a relationship exists, so H1 (correlation exists) is rejected and H0 (no correlation exists) is accepted.

Global Sensitivity analysis results

Combination of GSA indices results and t-test results were given in Table 10. Three Global Sensitivity Indices (PCC, SCC, and PRCC) were given for each couple consisting of state variable and model parameter. Colors indicate significance level: from light grey to dark grey, three levels of significance are described: $0.01 < \text{p-value} < 0.05$; $0.001 < \text{p-value} < 0.01$; and, $\text{p-value} < 0.001$. Empty cells indicate that the correlation is not significant ($\text{p-value} > 0.05$). The sign indicates a positive (+) or a negative (-) correlation. The inter-comparison between GSA indices showed that PCC, SCC, and PRCC provided different correlations and significance levels for the same couple consisting of state variable and model parameter (Table 10). In overall, for the same couples of parameter-state variable, PRCC detected the highest number of correlations than the other two metrics (SCC and PCC). It can be concluded that PRCC is the most sensitive metric in the detection of correlations (negative or positive) between model parameters and model state variables. The higher sensitivity of PRCC with respect to SCC and PCC was in agreement with previous studies by Marino *et al.* (2008). Since PRCC was established to be the most sensitive metric, it was used in the analysis of results provided in Table 10. Following this choice, parameters were classified as follows:

- PRCC with p-value<0.001 (dark grey): high sensitivity
- PRCC with 0.001<p-value<0.01 (grey): medium sensitivity
- PRCC with 0.01<p-value<0.05 (light gray): low sensitivity
- PRCC with p-value > 0.05 (empty cells): no sensitivity

Results in Table 10 showed that K_{max} affected all state variables, thus it was the most sensitive parameter. This means that K_{max} is important in determining model uncertainty. The parameter K_{max} had positive correlation with state variables $PONs$, $POPs$, PON_w , POP_w , L , and R . This means that the maximum biomass of the plant has a feedback effect on organic matter in the system. K_{max} has negative correlation with nutrient concentration in water and sediment. This means that the higher the plant's biomass, the higher the nutrient consumption. This result is in conformity with the negative correlation existing between the maximum growth rate g_{max} and dissolved nutrients in the system. The parameters with no sensitivity were the half-saturation constants for nutrients uptake, namely K_{NH4w} , K_{NO3w} , and K_{PO4} , and parameters representing internal phosphorus content (P_{min} and P_{crit}). Among all the half-saturation constants, K_{NH4s} had the highest sensitivity with respect to ammonia in sediment (state variable $NH4s$). Parameters representing minimum and critical nitrogen quota (N_{min} , N_{crit}) had low to no sensitivity. The maximum nitrogen quota (N_{max}) affected state variables N , $NH4w$, $NO3w$, $POPs$, and POP_w . The maximum phosphorus quota (P_{max}) affected state variables P , $PO4w$, and $PO4s$. The parameter V_{max}^{NO3w} affected only the concentration of nitrate in the water ($NO3w$). Leaves and roots biomass (state variables L and R) were affected mostly by changes of parameters m_{l0} , m_{r0} , V_{max}^{NH4w} , tr , K_{max} , r_N , and g_{max} . The state variables that were less affected by changes of parameters were $NO3w$, $NH4s$, and $PONs$. Nitrogen content (N) was mostly affected by changes of parameters m_{l0} , m_{r0} , V_{max}^{NH4w} , K_{max} , r_N , and N_{max} . Phosphorus content (P) was mostly affected by changes of parameters m_{l0} , V_{max}^{PO4} , K_{max} , and P_{max} .

Comparison between LSA and GSA

The sensitivity analysis of the seagrass model was computed by using both LSA and GSA methodologies. The results of LSA applied to the seagrass model can be found in Appendix E. A brief comparison of the results of the two methodologies is provided in this section for the state variables which represent the seagrass, namely leaves biomass L , roots biomass R , nitrogen content N , and phosphorus content P . The GSA showed that leaves and roots biomass were affected mostly by changes of parameters m_{l0} , m_{r0} , $V_{\max}^{NH_4^w}$, tr , K_{max} , r_N , and g_{max} . On the other side, the LSA methodology revealed that roots were affected mainly by m_{r0} , tr , K_{max} , r_N and g_{max} . In overall, the LSA methodology did not detect the effect of the parameter $V_{\max}^{NH_4^w}$ on roots biomass results. This means that a variation of 10% of the parameter $V_{\max}^{NH_4^w}$ was not sufficient to determine the sensitivity of the parameter $V_{\max}^{NH_4^w}$. LSA results showed that $Nmin$ and $Ncrit$ have high impact on leaves biomass, whereas the GSA results revealed that these two parameters do not influence significantly the results of leaves biomass. The results of LSA methodology pointed out that nitrogen content (N) was affected mainly by parameters $Nmin$, $Nmax$, r_N and g_{max} , whereas the GSA results showed that nitrogen content was affected by parameters m_{l0} , m_{r0} , $V_{\max}^{NH_4^w}$, K_{max} , r_N , and $Nmax$. LSA results revealed that phosphorus content (P) was affected mainly by parameters $Pmin$, $Pmax$, $V_{\max}^{PO_4}$, K_{PO_4} , and m_{l0} , whereas the GSA results showed that phosphorus content was affected by parameters m_{l0} , $V_{\max}^{PO_4}$, K_{max} , r_P , and $Pmax$. These results confirmed that the LSA and GSA methodologies give different results. Following the findings of the most recent literature (Marino *et al.*, 2008; Quillet *et al.*, 2013), the results of GSA should be regarded as more reliable because they explore a wide spectrum of parameter values on a statistical basis. On the other side, LSA methods explore a very limited area of model response to parameter variation (Quillet *et al.*, 2013).

Table 10 – Global Sensitivity analysis results for the seagrass model.

		<i>L</i>	<i>R</i>	<i>N</i>	<i>P</i>	<i>NH4w</i>	<i>NO3w</i>	<i>NH4s</i>	<i>PO4s</i>	<i>PONs</i>	<i>POP_s</i>	<i>PON_w</i>	<i>POP_w</i>	<i>PO4_w</i>
<i>m_{l0}</i>	PCC	-	+	-	-	+			-			+	+	+
	SCC	-	+	-	-	+			-			+	+	+
	PRCC	-	+	-	-	+			-	+		+	+	+
<i>m_{r0}</i>	PCC	+	-	-	-	-		+	+	+	+		+	-
	SCC	+	-	-	-	-		+	+	+	+	+	+	-
	PRCC	+	-	-	-	-		+	+	+	+	+	+	-
<i>V^{NH4w}_{max}</i>	PCC	+	+	+	+	-			-				+	-
	SCC	+	+	+	+	-			-				+	-
	PRCC	+	+	+	+	-		+	-	+	+	+	+	-
<i>V^{NO3w}_{max}</i>	PCC			+			-							
	SCC						-							
	PRCC	+					-							
<i>V^{PO4}_{max}</i>	PCC	+	+		+	-			-		+		+	-
	SCC	+	+		+	-			-		+	+	+	-
	PRCC	+	+		+	-		-	-	+	+	+	+	-
<i>V^{NH4s}_{max}</i>	PCC			+				-			+			
	SCC			+				-			+			
	PRCC			+				-			+			
<i>tr</i>	PCC	-	+				+	-	-		+	-	-	+
	SCC	-	+					-	-	+	+	-	-	+
	PRCC	-	+	+				-	-	+	+	-	-	+
<i>g_{max}</i>	PCC	+	+		+	-	-		-	+	+	+	+	
	SCC	+	+		+	-	-		-	+	+	+	+	
	PRCC	+	+		+	-	-		-	+	+	+	+	-
<i>N_{min}</i>	PCC			+					+					
	SCC			+								-	-	
	PRCC			+								-		
<i>N_{crit}</i>	PCC					-	-							
	SCC						-					+		
	PRCC	+			+		-		-			+		-
<i>N_{max}</i>	PCC		-	+		-	-				+			
	SCC		-	+		-	-				+			
	PRCC			+		-	-	-		+	+	+	+	+
<i>K_{max}</i>	PCC	+	+	-	+	-	-	-	-		+	+	+	-
	SCC	+	+	-	+	-	-	-	-	+	+	+	+	-
	PRCC	+	+	-	+	-	-	-	-	+	+	+	+	-
<i>K_{NH4w}</i>	PCC													
	SCC													
	PRCC													
<i>K_{NO3w}</i>	PCC		-											
	SCC													
	PRCC													
<i>K_{PO4}</i>	PCC													
	SCC		+											
	PRCC													+
<i>K_{NH4s}</i>	PCC							+						
	SCC							+						
	PRCC							+						
<i>r_N</i>	PCC	-	-	-	-	+		+	+	+	-	+	-	+
	SCC	-	-	-	-	+		+	+	+		+		+
	PRCC	-	-	-	-	+		+	+	+		+	-	+
<i>r_P</i>	PCC	-	-		-	+	+		-		+		+	+
	SCC	-	-		-	+			-		+		+	+
	PRCC		-		-	+			-		+	-	+	+
<i>P_{min}</i>	PCC													
	SCC													
	PRCC													
<i>P_{crit}</i>	PCC													
	SCC													
	PRCC													
<i>P_{max}</i>	PCC				+				-					-
	SCC				+				-					-
	PRCC				+				-	+	+			-

Summary

This chapter described the main functions (section 3.2) used in the seagrass model presented in section 2.4.1. Model parameters were not available in literature for the species *Zostera noltii*, and this led to the necessity to use a calibration tool to estimate model parameters for this particular seagrass species (section 3.3). The calibration tool estimated a new set of model parameters that was found to minimize the difference between data and model results. This new set of parameters was used as reference to simulate *Zostera noltii* dynamics. The model simulated the evolution of plant's biomass, with minima in winter and maxima in late summer, in conformity with literature. Model equations were proven to be mathematically consistent and the integration method was demonstrated to be numerically correct, by performing mass conservation tests. Global Sensitivity Analysis was carried out to find parameters with the highest impact on model results. In overall, the maximum biomass of leaves was identified as an important parameter in determining model uncertainty. Plant's biomass was affected mostly by mortality rates, growth rates, and carbon translocation processes from leaves to roots. Half-saturation constants had no sensitivity on model results. The results of Global Sensitivity Analysis were compared with results of Local Sensitivity Analysis. The comparison revealed that the two methodologies can give different results.

The model presented in this work is generic and it can be applied to other seagrass species and to other study areas. For applications to different species it would be necessary to do a re-calibration of model parameters.

Chapter 4 - Model testing (part 2)

4.1. Introduction

In this chapter function plots of the benthic ecology model are described. Sensitivity analysis is performed to investigate the effect of parameters on model results. Mass conservation tests are performed in a 0-D configuration to verify the consistency of the numerical formulation.

4.2. Function plots

Sediment limiting factor

Filter feeders filtration rate is affected by the concentration of suspended solids. At high concentration of suspended solids, filtration rates are reduced as ingestion rates saturate. This is often the case under high inorganic solid loading, which can then lead to nutritional problems for bivalves (Meyers *et al.*, 2000; USCE, 2000). In the model, the dependence of filter feeders on the concentration of suspended solids is represented by a linear function of sediment concentrations (eq. 41 and Figure 39).

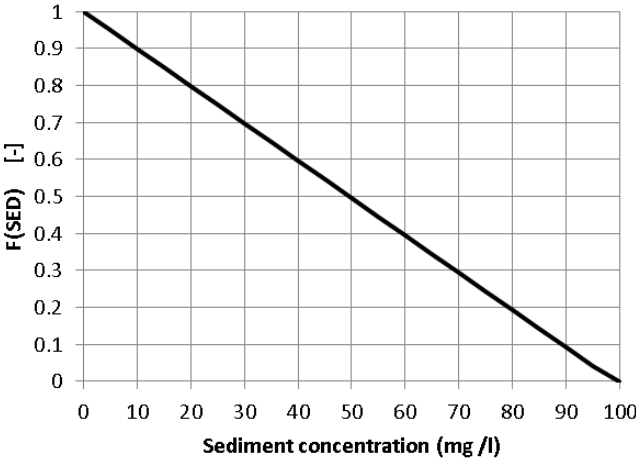


Figure 39 - Sediment limiting function as a function of sediment concentration (eq. 41). A value of $SED_{max}=100$ mg/l was considered in the chart.

Biomass limiting factor

The growth rate of benthic organisms has been observed to be regulated by the density of epibenthic populations (Fréchette and Lefavre, 1990). In the model, growth rate of benthic feeders (filter feeders and deposit feeders) and microphytobenthos was assumed to be dependent on the maximum biomass of the organisms (eq. 42, eq. 60, and eq. 73). The parameters used in this model for the representation of the biomass limiting factor were derived from Le Pape *et al.* (1999) and Blackford (2002). As an example, the biomass limiting factor for filter feeders (eq. 42) is described in Figure 40. The same type of chart is used to describe the dependence of deposit feeders and microphytobenthos on their biomass.

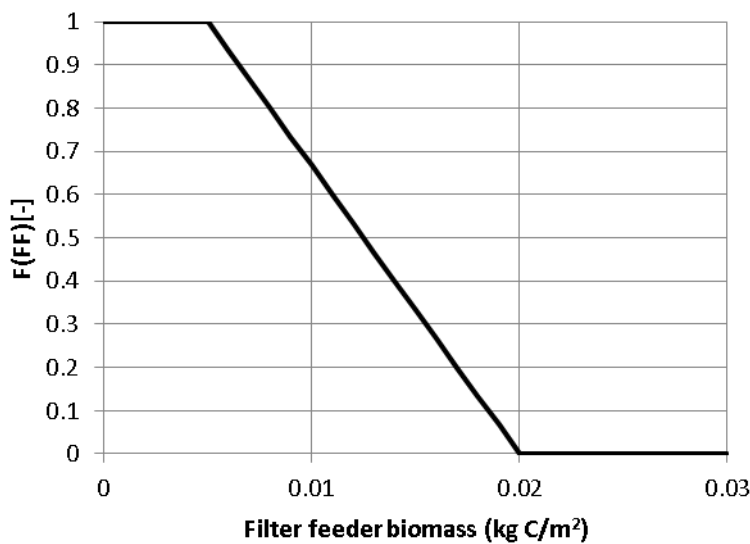


Figure 40 – Filter feeders biomass limiting factor (eq. 42).

Temperature dependence of benthic growth rates

The dependence of growth on temperature for benthic organisms is the same as the one used for other modules in MOHID to express the effect of temperature on the organisms' growth rates. The temperature limiting factor is expressed by a bell-shaped function for $F(T)$ described in Trancoso (2002), which values vary between 0 and 1, with a maximum (equaling 1) in correspondence with the optimal temperature and a minimum (equaling 0) in correspondence with minimum and maximum temperature values tolerated by the organisms

(Appendix A). The MOHID Water Quality model and the seagrass model use the same approach to describe the temperature limiting factor for plankton and seagrasses, respectively.

Oxygen limiting factor

In general, estuarine benthic invertebrates are not able to sustain themselves at oxygen concentration lower than 2.0-2.5 mg O₂/l (Pearson and Rosenberg, 1978; Meyers *et al.*, 2000). The model includes the dependence of benthic feeders on oxygen concentration (eq. 43). The oxygen limiting factor (Figure 41) tends to 1 with increasing oxygen concentration. This means that the growth rate will tend to the maximum growth rate with increasing oxygen concentration.

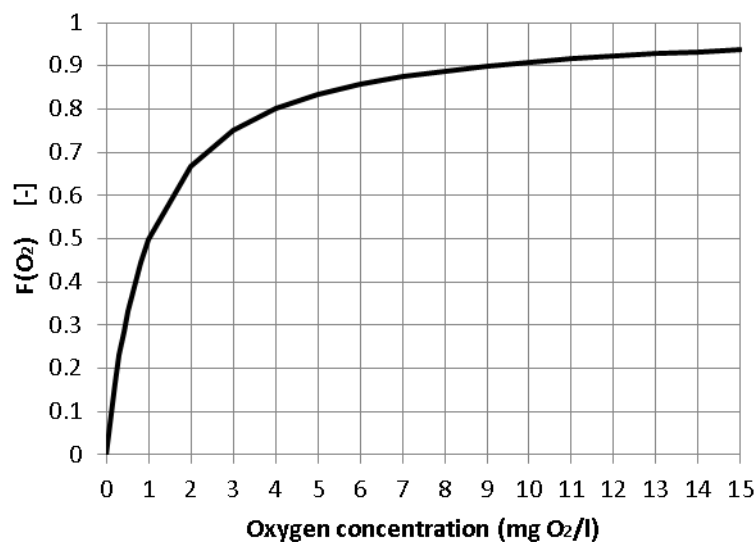


Figure 41 – Filter feeders and deposit feeders oxygen limiting factor (eq. 43).

Temperature dependence of benthic feeders mortality and respiration rates

Respiration by benthic macrofauna enhances the recycling of nutrients back to the water column and increases the sediment oxygen demand (USCE, 2000). In the model, both the respiration and the mortality rates have Arrhenius temperature dependencies (eq. 53), based on Meyers *et al.* (2000). The temperature dependence factor used in the model is depicted in Figure 42. This factor is used to represent the effect of temperature on respiration

and mortality processes for filter feeders and deposit feeders. In the case of microphytobenthos this approach is not used because microphytobenthos respiration is calculated as a fraction of the growth term, following the approach described in Blackford (2002).

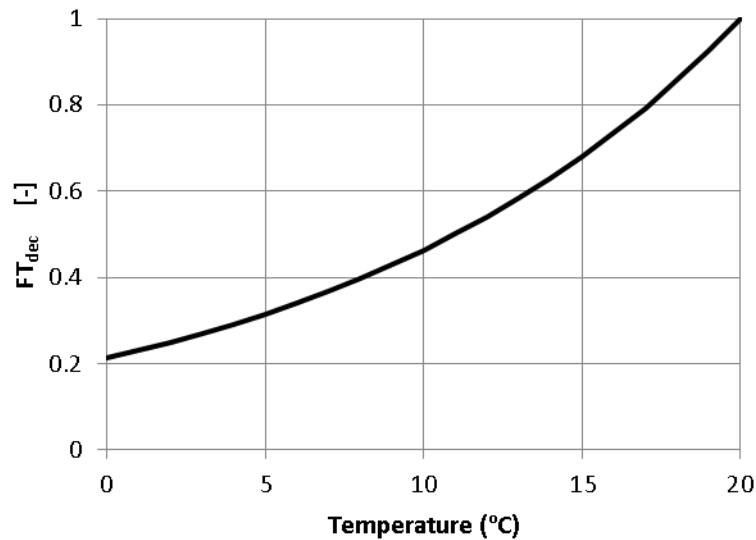


Figure 42 - Temperature dependence factor in benthic feeders respiration and mortality (eq. 53).

Microphytobenthos nutrient limiting factors

Nutrient limitation in microphytobenthos is described by using the Michaelis-Menten kinetics. This type of kinetic is frequently used in ecological models to describe uptake of nutrients by algae (phytoplankton, macroalgae, and microphytobenthos). In this research, the microphytobenthos uptake rate uses the Michaelis-Menten kinetics with the same parameterization used for phytoplankton in MOHID Water Quality model (IST, 2006) for nitrogen and phosphorus uptake (Figure 43 and Figure 44).

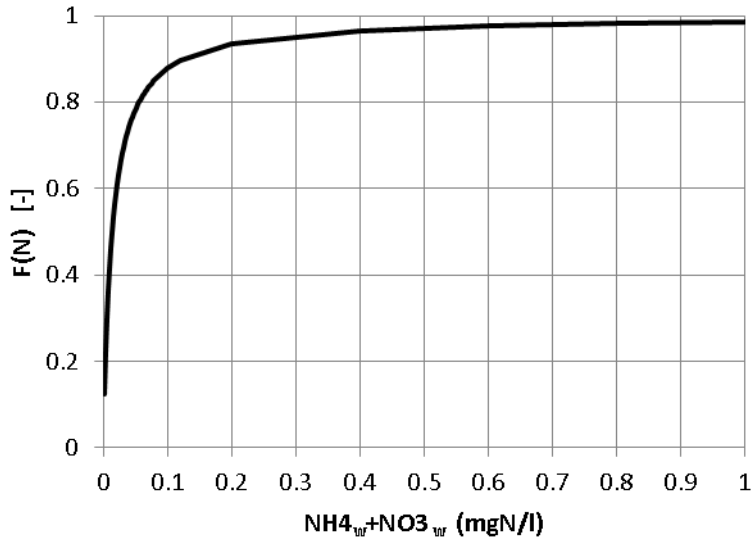


Figure 43 – Nitrogen limiting factor for microphytobenthos (eq. 75), for $K_N = 0.014$ mg N/l.

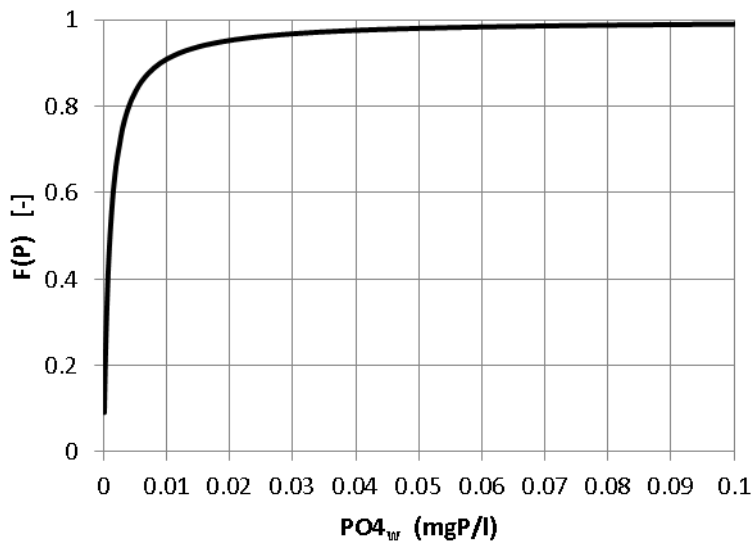


Figure 44 – Phosphorus limiting factor for microphytobenthos (eq. 76), for $K_P = 0.001$ mg P/l.

4.3. Testing

The benthic ecology model was tested by using a 0-D configuration to execute simple tests to verify the mass conservation in the system. The model was executed over a period of 5 years without advection-diffusion processes. No input/output of nutrients were considered. For the model forcing, typical temperature and surface radiation values for mid-latitude of the northern hemisphere were used (Figure 25 and Figure 26) (the same forcing used for seagrass

model testing). Initial conditions are presented in Table 11. The model parameters were assigned with values shown in Table 4, Table 5, and Table 6. The values of the state variables at time $t+dt$ were calculated by adding variables' sources and sinks to the values calculated at time t . In this way, the variation of the state variables as a function of time was determined. In this tests, the zooplankton is not present in the system.

Table 11 - Initial conditions used for benthic ecology model testing.

State variable	Value	Unit
MP	0.0001	kg C/m ²
DF	0.00001	kg C/m ²
FF	0.000001	kg C/m ²
NO _{3w}	0.002	g N/l
NH _{4w}	0.001	g N/l
PO _{4w}	0.001	g P/l
PHY	0.0001	g C/l
POC _w	0.001	g C/l
POC _b	0.01	kg C/m ²

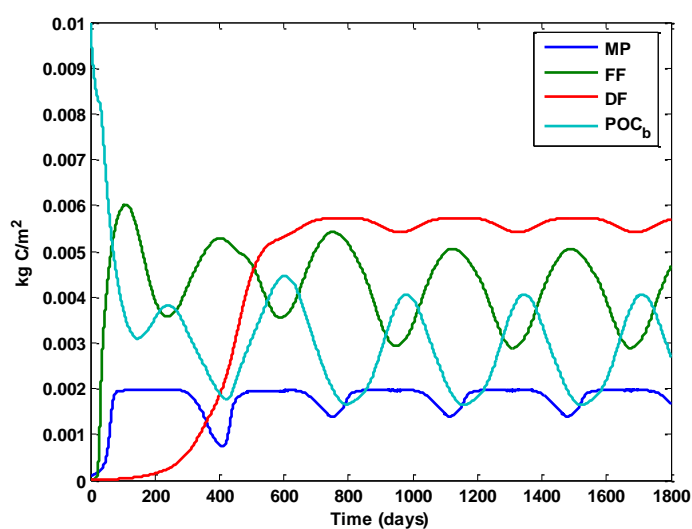


Figure 45 – Benthic model results for microphytobenthos (MP), filter feeders (FF), deposit feeders (DF), and particulate organic carbon on bottom sediment (POC_b), for a period of 5 years.

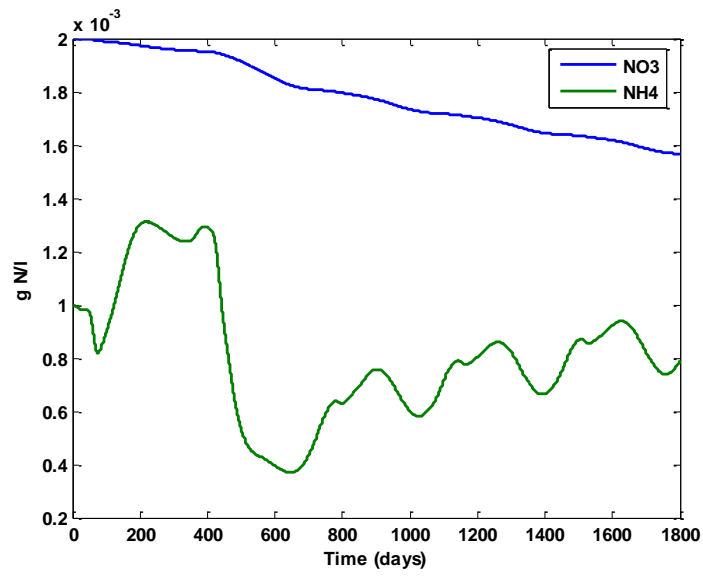


Figure 46 – Simulated concentrations of nitrate (NO₃) and ammonia (NH₄) in the water, for a period of 5 years.

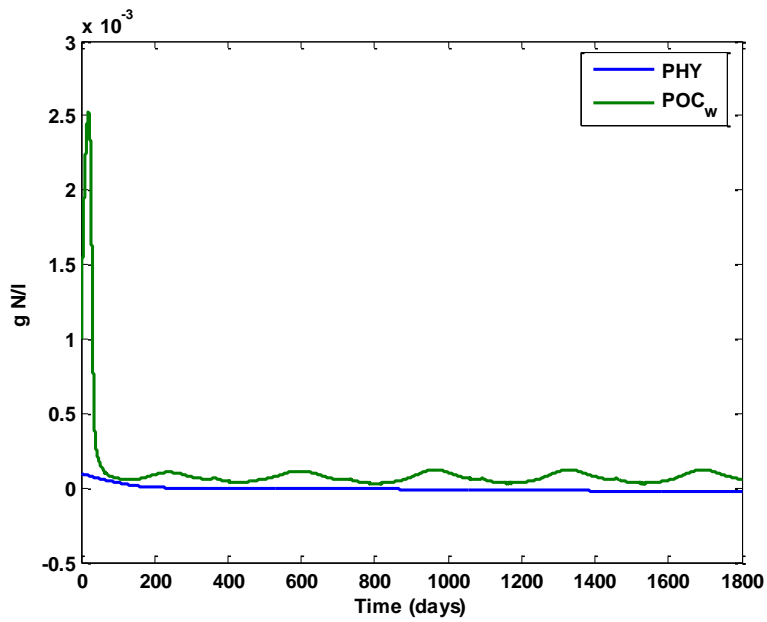


Figure 47 – Simulated concentrations of phytoplankton (PHY) and particulate organic carbon (POC_w) in the water for a period of 5 years.

Mass conservation

The system in consideration is a closed system, where no external inputs or outputs are taken into account; therefore the total mass must be constant over time. Total mass was expressed as total nitrogen and total phosphorus in the system. The results showed that total nitrogen and phosphorus in the system were constant over time, and that the mass was conserved.

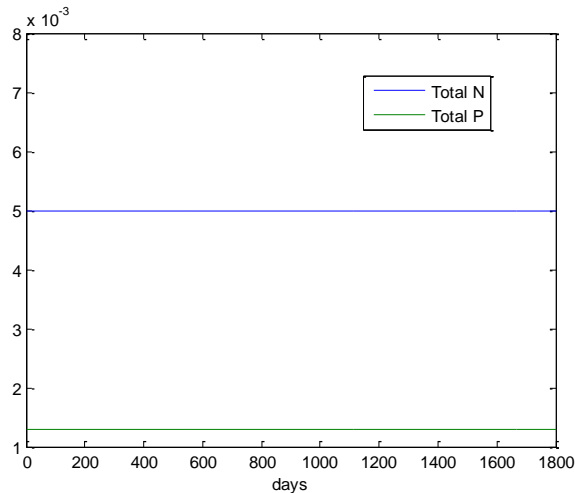


Figure 48 – Total mass in the system expressed as total N and total P.

4.4. Sensitivity analysis

Global Sensitivity Analysis was carried out to quantify uncertainties of model's parameters and to assess their effects on model results. The methodology for sensitivity analysis was the same as the one described for the Global Sensitivity Analysis of the seagrass model (see section 3.6). Sampling-based sensitivity indices were calculated to assess the impact of parameters on model results. State variables of the model were considered as the response variables against which to test the effect of parameter changes. Monte Carlo simulation methods were used to perform multiple model simulations by using randomly generated model inputs (Marino *et al.*, 2008).

The results of the combination of GSA indices and significance tests are reported in Table 12. Three Global Sensitivity Indices (PCC, SCC, and PRCC) are given in Table 12 for each couple consisting of state variable and model parameter. Colors indicate significance level: from light grey to dark grey, three levels of significance are described: $0.01 < p\text{-value} < 0.05$; $0.001 < p\text{-value} < 0.01$; and, $p\text{-value} < 0.001$. Empty cells indicate that the

correlation was not significant ($p\text{-value} > 0.05$). The sign indicates a positive (+) or a negative (-) correlation. State variables representing solutes are referred as concentrations at the water-sediment interface.

GSA results presented as box plots were included as well in Appendix D. Results show that phytoplankton was affected mostly by parameters V_{max} , m_{MPO} and r_{FF0} . Filter feeders were affected by m_{MPO} , r_{FF0} , and α_{FF} . Microphytobenthos was affected mostly by m_{MPO} , V_{max} and MP_{max} . Filter feeders showed a negative relationship with r_{FF0} , and a positive relationship with m_{MPO} (between 0.25 and 0.61). Deposit feeders were mostly affected by I_{DFmax} , α_{DF} , K_C , and r_{FF0} . Nutrients, particulate organic matter, and oxygen at the water-sediment interface, were also affected by V_{max} , m_{MPO} , and r_{FF0} . In overall, growth and respiration processes related to microphytobenthos and filter feeders are important in determining model uncertainty. Comparison between GSA indices showed that PCC, SCC, and PRCC, provide different correlations and significance levels for the same couple consisting of state variable and model parameter. PRCC absolute values were higher than the absolute values of PCC and SCC. This result is consistent with previous findings reported in Marino *et al.* (2008), comparing PCC, SCC, and PRCC.

Table 12 – Global Sensitivity analysis results for the benthic ecology model.

		MP	PHY	FF	DF	POCb	POCw	NO3w	NH4w	PO4w	O2w
m_{MPO}	PCC		+	+	+	+	+	-	-	-	+
	SCC	-	+	+	+	+	+	-	-	-	+
	PRCC	-	+	+	+	+	+	-	-	-	+
V_{max}	PCC					+		-	-	-	+
	SCC	+	-					-	-	-	+
	PRCC	+	-		+	+		-	-	-	+
ϕ	PCC										
	SCC										
	PRCC										
α	PCC										
	SCC						+				
	PRCC										
KN	PCC							-			
	SCC							-			
	PRCC							-			
KP	PCC										
	SCC										
	PRCC							+			
MPmin	PCC										
	SCC										
	PRCC					-					
MPmax	PCC	+									
	SCC	+									
	PRCC	+			+	+		-	-	-	+
r_{DF0}	PCC				-				+	+	-
	SCC				-				+	+	-
	PRCC				-			+	+	+	-
m_{DF0}	PCC										
	SCC										
	PRCC										
I_{DFmax}	PCC							-			
	SCC				+			-			
	PRCC				+						
K_C	PCC				-						
	SCC				-						
	PRCC	+			-				+	+	-
α_{DF}	PCC				+						
	SCC				+						
	PRCC				+						
T_{DF}^{fac}	PCC										
	SCC										
	PRCC										
DFmin	PCC										
	SCC										
	PRCC										
DFmax	PCC										
	SCC										
	PRCC										
r_{FF0}	PCC	-	+	-		+	-		+	+	-
	SCC		+	-		+	+		+	+	-
	PRCC		+	-	-	-	+	+	+	+	-
m_{FF0}	PCC	+									
	SCC	+									
	PRCC										
I_{FFmax}	PCC										
	SCC										
	PRCC						-				
α_{FF}	PCC			+		-					
	SCC			+	-		-				
	PRCC			+	-	-	-		+	+	-
T_{FF}^{fac}	PCC										
	SCC				+	+		-			
	PRCC										
FFmin	PCC										
	SCC						-				
	PRCC						-				
FFmax	PCC										
	SCC										
	PRCC										

Conclusion

The benthic ecology model described in Chapter 2 was tested to verify the consistency of the mathematical formulation. Sensitivity analysis was carried out to determine parameters to which the model is most sensitive on a statistical basis. The sensitivity analysis, based on Monte-Carlo simulations, calculated three Global Sensitivity Indices (Pearson, Spearman, and partial rank correlation coefficients), which enabled to classify parameters with different levels of impact on model results. The sensitivity analysis identified four main model parameters which affected model results: V_{max} , m_{MPO} , MP_{max} , and r_{FF0} . These parameters should be regarded as the main source of model uncertainty. The value of these parameters may be estimated through further model calibration, or they can be measured through laboratory experiments.

The benthic ecology model includes explicitly grazing on phytoplankton and particulate organic matter in the water by benthic bivalve filter feeders. The interaction between benthic grazers and phytoplankton can also affect water turbidity, which has an impact on benthic biota. Macrobenthos such as deposit and suspension feeders, play an important role in sediment-water interactions by processing organic matter from the water column and by releasing inorganic nutrients. Although the model is simplified and it does not contain all characteristics of the real system, it includes the main biogeochemical components needed to describe the coupling between aquatic and benthic food webs.

Chapter 5 – Case Study

This chapter deals with the application of the MOHID seagrass model to Ria de Aveiro, Portugal. The model results are verified against real observations. A reference scenario for the seagrass model is set-up and presented in this chapter and used for the hypotheses verification in Chapter 6.

5.1. Introduction

In Portugal, seagrass habitat experienced degradation in the last 20 years (Cunha *et al.*, 2013), causing biodiversity loss, and contributing to degradation of coastal fisheries and water quality. *Zostera noltii* coverage in Ria de Aveiro, Portugal, was about 8 km² in 1984, and it decreased down to 3 km² in 2004 (Silva *et al.*, 2009; Cunha *et al.*, 2013). This decline in Ria de Aveiro was attributed to a combination of factors such as dredging, deepening of channels, loss of fine sediments, siltation, nutrient washing, increasing tidal wave penetration, and increasing water currents (Silva *et al.*, 2009; Cunha *et al.*, 2013). In Ria de Aveiro, the reduction of areas covered by seagrasses was followed by an increase of the areas of uncovered sediment, supporting the growth of sparse macroalgae populations only (Silva *et al.*, 2009). Opportunistic and fast growing macroalgae can occupy the space above seagrasses beds and reduce space and light availability for benthic plants and microphytobenthos. Increase in nitrogen and phosphorus levels may affect the equilibrium between primary producers in the study area. Eutrophication is one of the causes of seagrass meadows decline because increased nutrient availability may lead to proliferation of light-absorbing algae, such as phytoplankton and macroalgae. In this chapter, the seagrass model is applied to Ria de Aveiro to study the distribution of *Zostera noltii* biomass over time and space. The model results are compared with real observations of *Zostera noltii* biomass in the study area. The application developed in this chapter will be used in Chapter 6 as a reference scenario to test the hypotheses described in Chapter 1 relative to the first research question (R1).

5.2. Study area

Ria de Aveiro (41°N, 9°W) is a shallow temperate marine coastal lagoon of Portugal, with a complex morphology, a wide intertidal area, and a productive ecosystem. The system

is characterized by five main canals (Caster, Antuã, Vouga, Boco, and Mira) divided into several channels which converge into a single outlet on the Portuguese Atlantic coast (Figure 49). The total submerged area of the estuary changes between 83 km² during spring tide and 66 km² during neap tide (Dias and Lopes, 2006). Average depth is 1 m (with respect to mean sea level), but maximum depths are artificially maintained by dredging varying between 1 and 4 m (Trancoso *et al.*, 2005). The inlet has a length of 1.3 km, a width of 0.35 km, and a depth of 20 m (Dias and Lopes, 2006). Previous studies from Vaz *et al.* (2009) indicated that the residence time of water in Ria de Aveiro varies according to the freshwater inflow regime, from a minimum of 4 days at extreme freshwater inflow (1000 m³/s) to more than 10 days at low freshwater inflow. During a tidal cycle, the tidal prism is between 20x (during minimum spring tide) and 76x (during maximum spring tide) higher than the total fluvial discharge (Dias *et al.*, 2000). Following this, it can be concluded that the circulation in the lagoon is driven mainly by tidal forcing. However, the combination of freshwater inflows and tides determines a salinity gradient along the lagoon varying between 0 in proximity of the Vouga river and 36 in the bar entrance (Vaz and Dias, 2008). The Ria de Aveiro has an important ecological role because it provides habitat to several protected species and site for feeding, sheltering, and breeding to many species valuable for fishing. Ria de Aveiro was classified as a Special Protection Area by the EU Bird directive (79/409/EEC). Nutrient inputs to the lagoon come mainly from surface runoff and from agriculture fields, while point sources are less than 10% of the total nutrient load (Ferreira *et al.*, 2003). However, the lagoon is considered a high productive system, with a moderate eutrophication level, being classified as a “sensitive area” in terms of eutrophication (91/271/EEC).

Historically, the luxuriant seagrass vegetation of Ria de Aveiro was used in agriculture for harvesting, but this activity declined after the 1960s because of economic and social reasons (Silva *et al.*, 2004). The dense seagrass coverage included *Potamogeton pectinatus*, *Ruppia cirrhosa*, *Zostera noltii*, and *Zostera marina*. *Zostera noltii* is a common plant in the Ria de Aveiro, with recognized ecological interest because it is the base of many food chains. Together with other algae and vascular plants, *Zostera noltii* is part of the seaweed of Ria de Aveiro (Figure 50). The plant has dark green leaves between 4 and 20 cm length by 0.5 to 2 mm width. The stems are simple or branched, usually up to 10 cm length (www.biorede.pt).

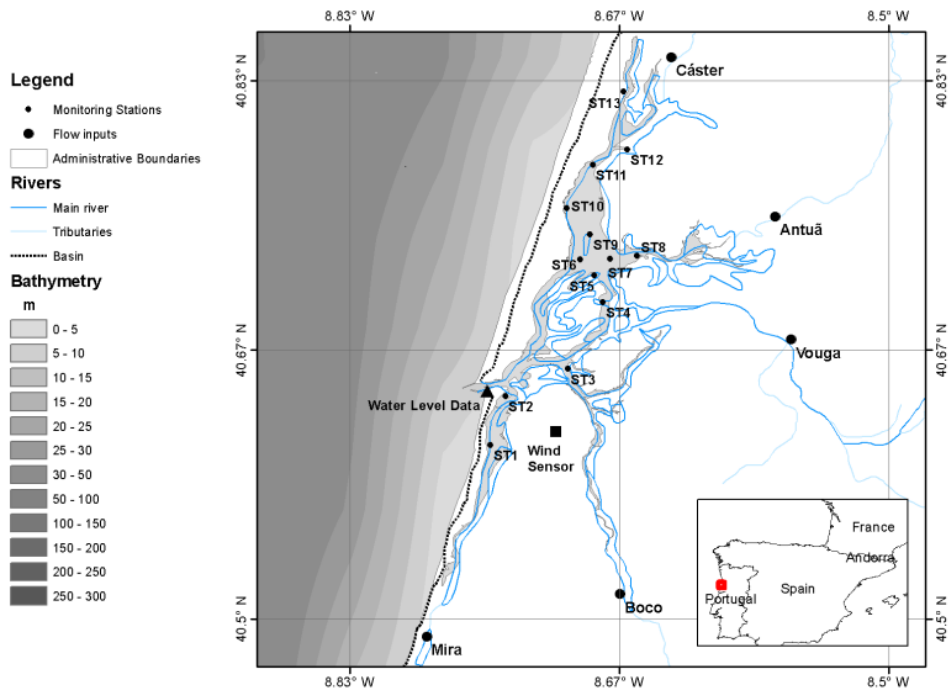


Figure 49 - Geographic location of Ria de Aveiro. Bathymetry of the coastal area, main rivers, flow inputs, wind sensor, and seagrass monitoring stations, are indicated as well.



Figure 50 – Salt marsh and marsh grass distribution in Ria de Aveiro (source: www.biorede.pt).

5.3. Data

Wind data used in this research to force the hydrodynamic model were retrieved from the database of the Portuguese National Information System of Water resources (SNIRH - <http://snirh.pt/>) for the period 01/01/2003-01/01/2005. Wind velocity and direction were measured by a Thies Clima/Young installed at a height of 2 m with respect to the ground level, at the Gafanha da Nazaré station (40.616 N, -8.706 E). Wind velocity was sampled every minute, and hourly mean values were stored. During rainy periods, the system stored every minute instantaneous values of wind velocity. Instantaneous values of wind direction were stored every hour. The geographic location of the sensor is displayed in Figure 49.

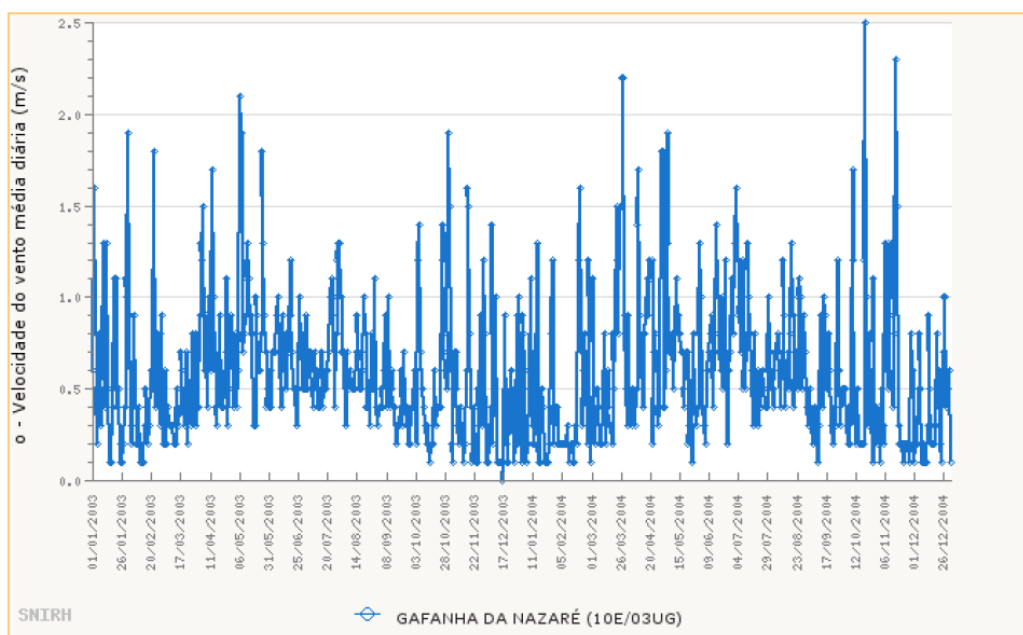


Figure 51 – Wind speed measured at Gafanha da Nazaré station (40.616 N, -8.706 E). Source: www.snirh.pt

Water level data used in this research to validate the hydrodynamic model were provided by the Portuguese Hydrographical Institute (IH), for Aveiro harbour (40.64 N, -8.74 E) (Figure 49). Water level data were calculated from harmonic analysis performed from one year of tide gauge observations (31/05/1999 to 31/05/2000) on a computer type IBM - PC compatible of the IH Oceanographic Division (<http://www.hidrografico.pt>).

The present research benefits from valuable monitoring data collected in Ria de Aveiro by the University of Aveiro (Silva *et al.*, 2009). These data were of vital importance because

they enabled to verify the model against real observations. *Zostera noltii* biomass data used to verify the model were collected in ten sampling points located in the intertidal areas of Ria de Aveiro with *Zostera noltii* beds, during the period October 2002 - December 2004. Biomass data were available at 10 out of 13 sampling stations displayed in Figure 49 (seagrass biomass data were not available at stations 7, 9, and 11). The complete description of sampling methods and laboratory analysis used to retrieve *Zostera noltii* biomass can be found in Silva *et al.* (2009).

5.4. Model set-up

A 2-D hydrodynamic-biogeochemical model of Ria de Aveiro was used. The grid of the 2-D model had 87 x 81 cells and a variable resolution between 0.2 and 1 km (Figure 52). The model was forced with average daily discharges (freshwater inflow and nutrient concentration) coming from the main canals of the Ria de Aveiro (Figure 56, Figure 57, and Figure 58). These discharges were calculated by the Soil and Water Assessment Tool (SWAT), applied to the Vouga catchment. SWAT is a spatially semi-distributed system, developed by the United States Department of Agriculture (USDA) Agricultural Research Service (ARS), to simulate the impact of management decision on the surface runoff, sediment transport and nutrients load in large basins, taking into account the land use, soil type and forest management practices.

At the open boundary, constant values were assumed for physical and biogeochemical properties. Wind data were retrieved from the SNIRH database (www.snirh.pt). The model simulated hydrodynamics and water biogeochemistry, and provided fields of velocity, temperature, salinity and biogeochemical properties as output over time. The model time span was two years (01/01/2003 - 01/01/2005), with a time step varying between 10 and 15 sec. The diffusion coefficients for water properties were calculated as a function of the Schmidt number and horizontal turbulent viscosity.

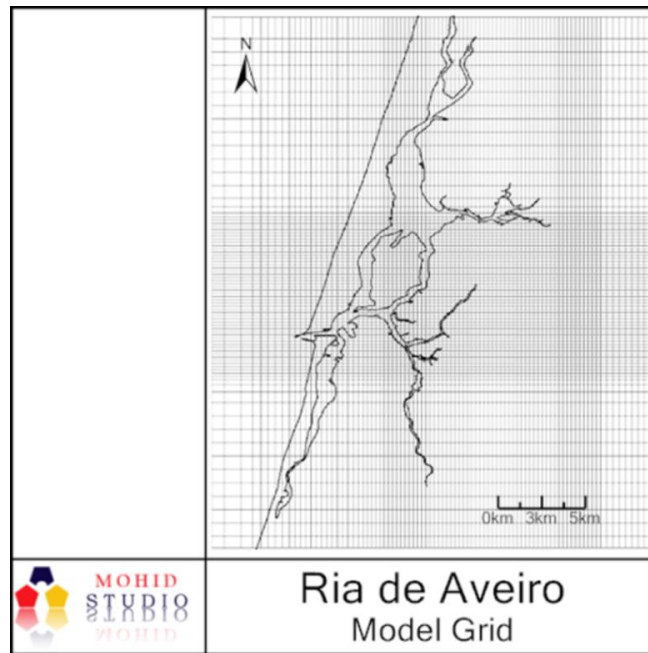


Figure 52 - Horizontal model grid.

5.4.1. Initial conditions

Initial conditions for seagrass biomass were defined on the basis of existing data of seagrass biomass in Ria de Aveiro (Silva *et al.*, 2009), described above. On the basis of these data, the Ria de Aveiro was divided into sub-areas, each of them having a different initial value for seagrass biomass. The initial conditions of seagrass leaves are shown in Figure 53. The initial conditions of seagrass roots are shown in Figure 54. The initial conditions used for the other properties in the model are reported at the end of this chapter.

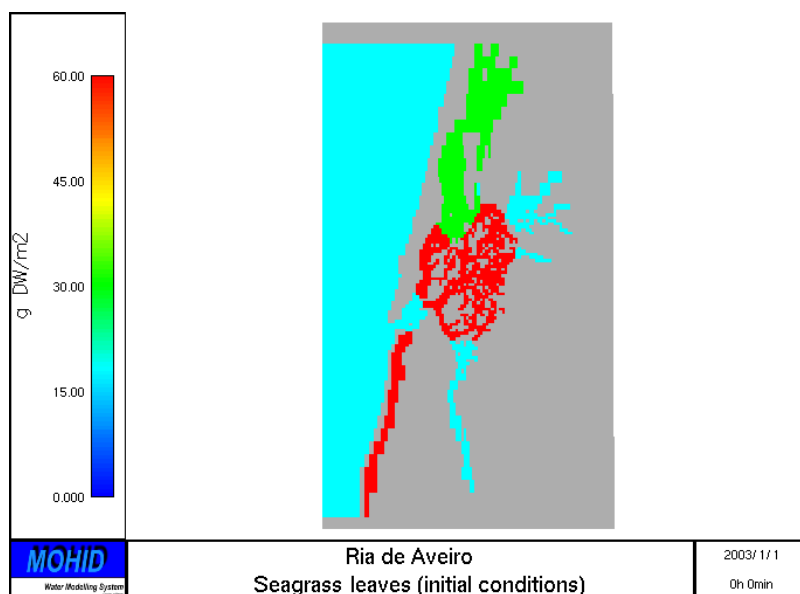


Figure 53 – Initial conditions for seagrass leaves.

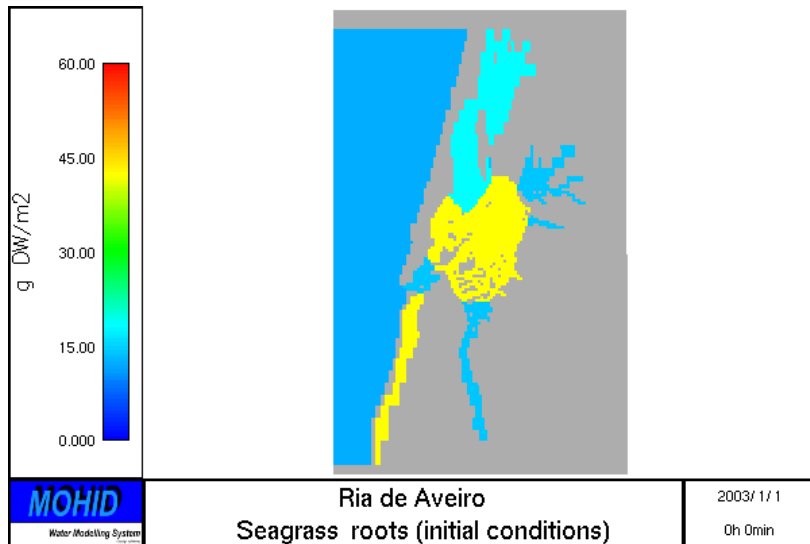


Figure 54 – Initial conditions for seagrass roots.

5.4.2. Boundary conditions

SWAT provided daily values of freshwater inflow and nutrient inputs for the MOHID application (Figure 55 to Figure 58).

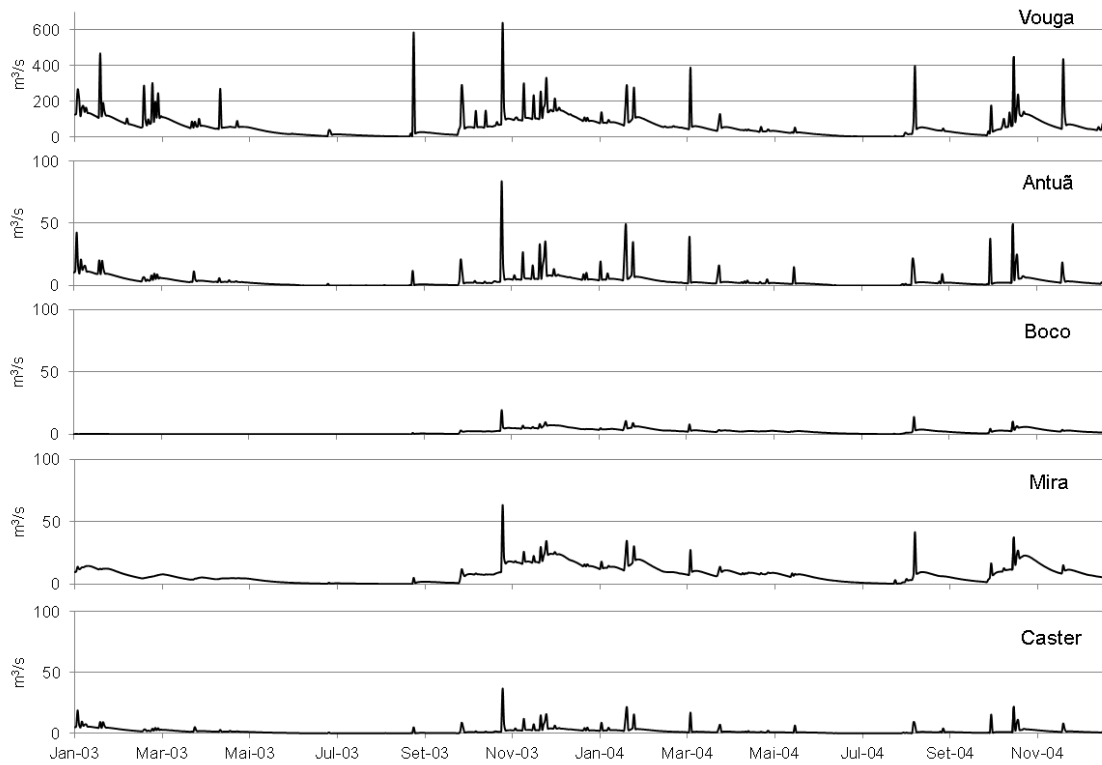


Figure 55 - Freshwater inflows at the main river canals, calculated by SWAT model applied to the Vouga catchment. Source of data: Eng. Pedro Chambel, MARETEC, IST.

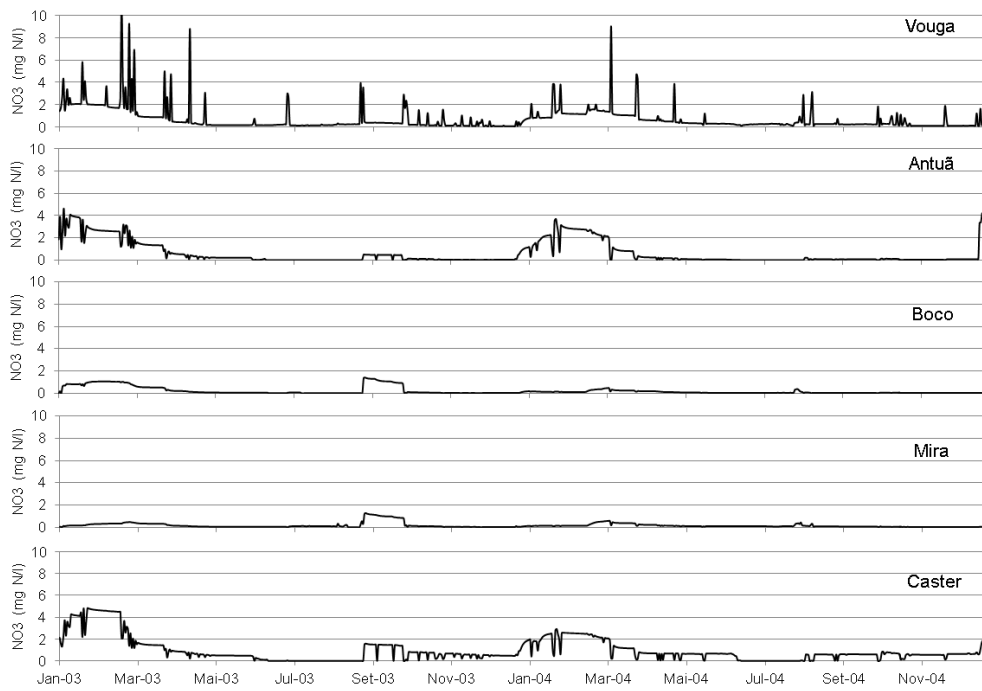


Figure 56 – Nitrate inflows at the main river canals, calculated by SWAT model applied to the Vouga catchment. Source of data: Eng. Pedro Chambel, MARETEC, IST.

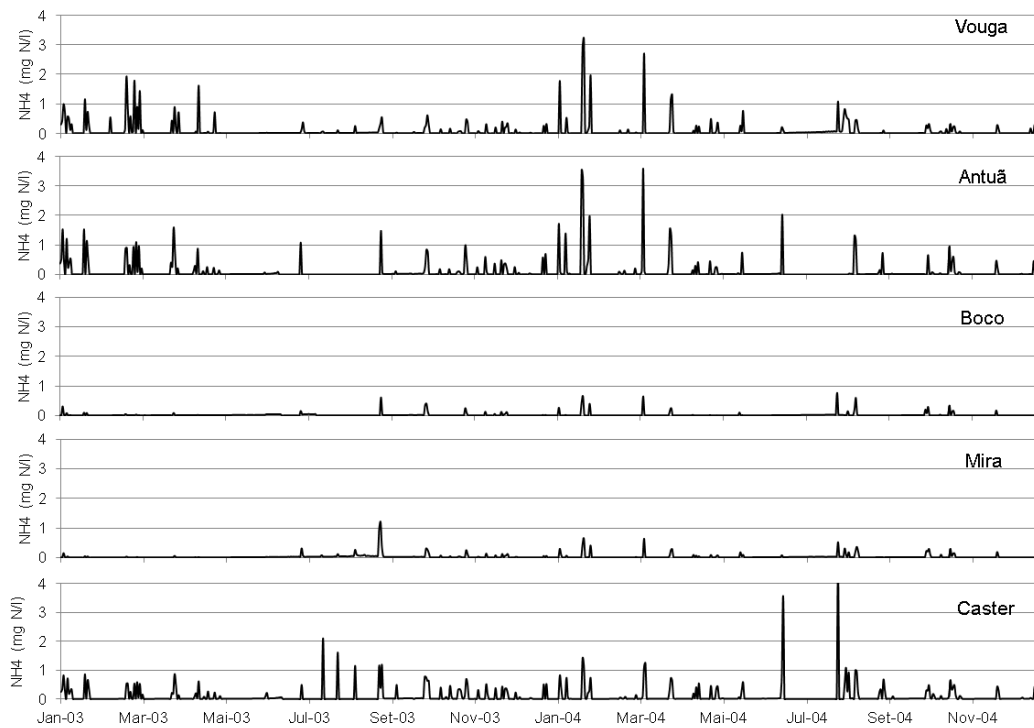


Figure 57 – Ammonia inflows at the main river canals, calculated by SWAT model applied to the Vouga catchment. Source of data: Eng. Pedro Chambel, MARETEC, IST.

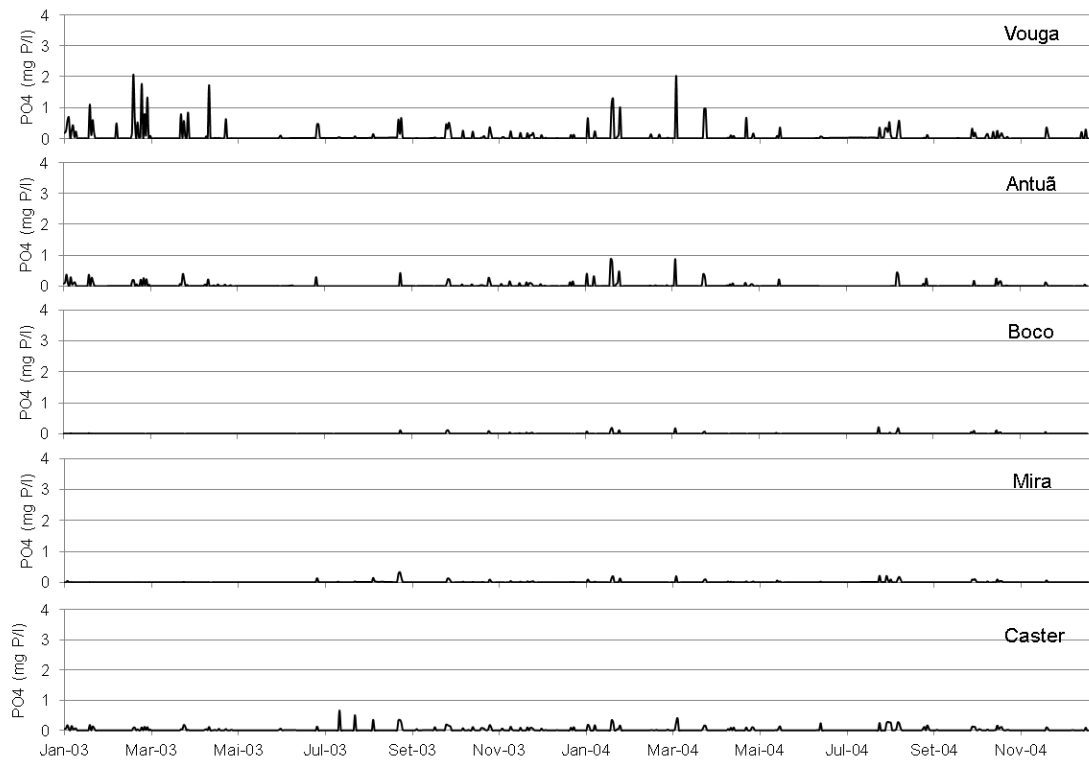


Figure 58 - Phosphate inflows at the main river canals, calculated by SWAT model applied to the Vouga catchment. Source of data: Eng. Pedro Chambel, MARETEC, IST.

5.5. Sensitivity analysis

The sensitivity analysis aimed to assess parameters with the highest impact on model's results. A Sensitivity Index (SI) was calculated, defined as:

$$SI_{ij} = \text{median} \frac{\Delta X_i / X_i}{|\Delta p_j / p_j|} \quad \text{eq. 109}$$

where X is the state variable, i is the index of the state variable, p is the parameter, and j is the index of the parameter. SI was computed for a $\pm 30\%$ parameters variation. When $SI < 0$ (or $SI > 0$), this means that the parameter variation produced a decrease (or an increase) of the state variable X (Ascione Kenov *et al.*, 2013). To address the impact of each parameter, the following criteria were used:

- If $SI < 0.025$, the parameter was classified with low impact
- If $0.025 < SI < 0.1$ the parameter was classified with medium impact;
- If $SI > 0.1$, the parameter is considered with high impact.

For each parameter variation, a model run was carried out for a 1 year duration. To account for the spatial distribution of the model results, time series were generated from model outputs at the stations from Figure 49. The average of the time series was taken into account as representative of the model results in the study area.

5.6. Model verification

The coherence between model and data in the reference scenario was analyzed in terms of correlation coefficient r , determination coefficient r^2 , and root mean square error $RMSE$. The correlation coefficient measures the strength and the direction of a linear relationship between two variables. The $RMSE$ is a measure frequently used to evaluate the differences between predictions and observations (Anderson and Woessner, 1992). The mathematical formula for computing r is:

$$r = \frac{n \sum_{i=1}^n x_i y_i - \sum_{i=1}^n x_i \sum_{i=1}^n y_i}{\sqrt{n \sum_{i=1}^n (x_i^2) - \sum_{i=1}^n (x_i)^2} \sqrt{n \sum_{i=1}^n (y_i^2) - \sum_{i=1}^n (y_i)^2}}, \quad -1 \leq r \leq 1$$

eq. 110

where x_i is the measured variable, y_i is the predicted variable, and n is the number of pairs of data. The $RMSE$ is a frequently used measure for the differences between predictions and observations (Anderson and Woessner, 1992). The $RMSE$ is given by:

$$RMSE = \sqrt{\frac{\sum_{i=1}^n (x_i - y_i)^2}{n}}$$

eq. 111

where x_i are the observations, y_i are the values predicted by the model, and n is the number of observations.

5.7. Results and discussion

5.7.1. Sensitivity analysis results

Results of sensitivity analysis are reported in Table 13. Light grey cells in table—refer to $|\text{SI}| < 0.025$; grey cells refer to $0.1 < |\text{SI}| < 0.025$; dark grey cells refer to $|\text{SI}| > 0.1$. The table includes the results obtained for 30% increase of the parameters. The sign +/- indicates positive/negative values of SI, respectively. Cells with no sign indicate $\text{SI} = 0$. The seagrass growth rate g_{max} and the leaves mortality rate ($mort_{r0}$) had the highest impact on seagrass state variables (leaves, roots, internal nitrogen and internal phosphorus). Ammonia and nitrate were affected mostly by changes in parameters N_{max} , $mort_{l0}$, P_{max} , and P_{crit} . Leaves mortality rate $mort_{l0}$ affected mostly seagrass state variables (leaves, roots, internal nitrogen and internal phosphorus) and the particulate organic matter in water, including particulate organic nitrogen (PON) and particulate organic phosphorus (POP). Roots mortality rate $mort_{r0}$ affected mostly seagrass roots and particulate organic matter in water. The seagrass maximum nitrogen content N_{max} affected inorganic nutrients (nitrate and ammonia) and seagrass nitrogen content. The other parameters had medium to low impact. It can be concluded that parameters with highest impact on model results are g_{max} , $mort_{l0}$, and P_{max} , because these parameters had high impact ($|\text{SI}| > 0.1$) on more than three state variables at the same time. This result is consistent with the sensitivity analysis of the seagrass model described Ascione Kenov *et al.* (2013), which classified g_{max} and $mort_{l0}$ and P_{max} as parameters with highest impact on model results.

Table 13 - Sensitivity analysis results

	NH4	NO3	NO2	DONr	DONnr	PONw	PO4	DOPr	DOPnr	POPw	PHY	O2	PONb	POPb	L	R	N	P
GMAX	+	-	+	+	-	+	-	+	-	+	-	+	+		+	+	+	+
MORTRO	+	+	+	-	-	-	-		-		-	+			+	-	+	-
NMAX	-	-	-	-	-	-	+		-	-	-	+			-	-	+	
NMIN	-	-	-	-	-	-	+		-	-	-	+			+	+	+	
MORTLO	+	+	+	+	+	+	+		+	+	+	-	+		-	-	-	-
NCRIT		+	+	-	+	-	+		+	-	+	-			-	-	+	
PMAX	-	-	-	-	-	-	-		-	-	-	+	-		+	+	-	+
PMIN	+	+	+		+	-	-		+		+	-			-	-	+	+
PCRIT	+	+	+		+				+		+	-			-	-	+	+
KTR															-	+	+	-
VMAXNH4W	-	-	-	-	-	-	+		-	-	-	+			+	+	+	+
VMAXNO3W	+	-	+	-	-	-	-		-	-	-	+			+	+	+	+
VMAXPO4W	+		-	-	-	-	-		-	-	-	+			+			+
VMAXPO4s																+		+
KNO3W	-	+		+	+	+	+		+	+	+	-			+	+	+	
KNH4W	+	+	+	+	+	+	-		+	+	+	-			-	-	-	
KNH4S	-	-	-		+	-					+	-			-	-	-	
KPO4W	-	-	-	+	+	+	+		+	+	+	-	+					+
KPO4S															+	+		+

5.7.2. Model results

The model results for water level were compared with data in the reference scenario (Figure 59). The results of the model gave a good agreement with data ($r = 0.99$, $RMSE = 0.12$ m).

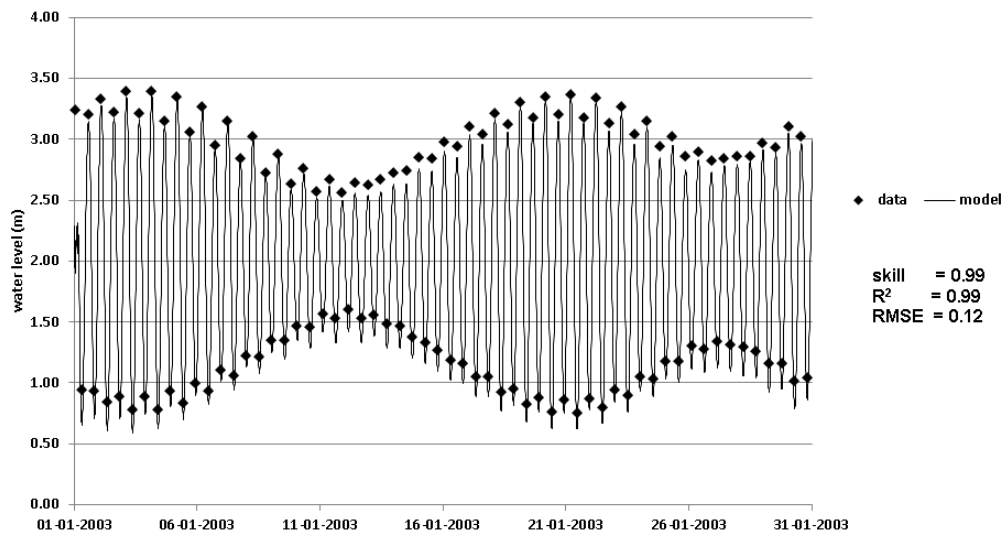


Figure 59 - Comparison between model results and water level of the Instituto Hidrográfico (see Figure 49).

Comparison between simulated and measured temperature data was provided in Figure 60. The results for temperature gave a good agreement with data in the stations (Table 14).

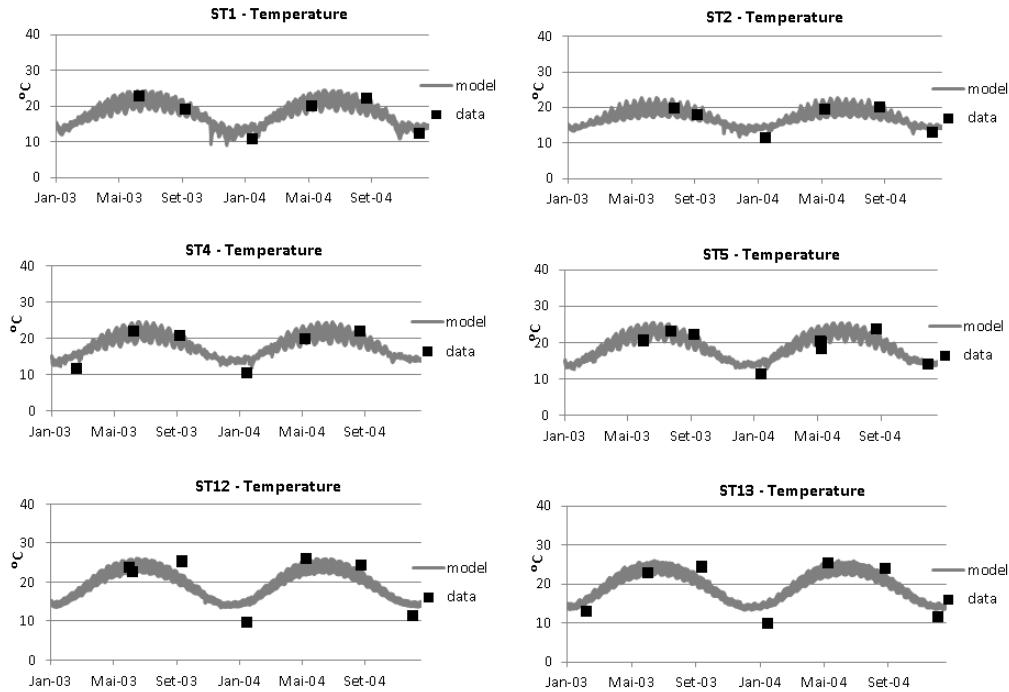


Figure 60 - Comparison between simulated and measured temperature in selected stations of Ria de Aveiro. For the location of the stations, please refer to Figure 49. Source of data: Universidade de Aveiro (Silva *et al.*, 2009).

Table 14 – Results of model verification for temperature. RMSE is the root mean square error, r is the correlation coefficient, and r^2 is the determination coefficient. For the location of the stations, please refer to Figure 49.

	ST1	ST2	ST3	ST4	ST5	ST6	ST8	ST10	ST11	ST12	ST13
RMSE	2.00	1.78	2.51	2.28	2.42	2.77	3.04	2.79	8.96	3.08	3.02
r	0.95	0.96	0.95	0.91	0.84	0.92	0.91	0.92	0.99	0.87	0.91
r^2	0.90	0.93	0.91	0.83	0.70	0.85	0.82	0.84	0.98	0.76	0.83

The results of the model gave a good agreement with data in stations ST6, ST8, ST12, and ST13 (Table 15), and lower agreement in the other stations. This result can be improved in the future by using a 3-D model to account for salinity stratification along the water column. Comparison between simulated and measured salinity was provided in Figure 61.

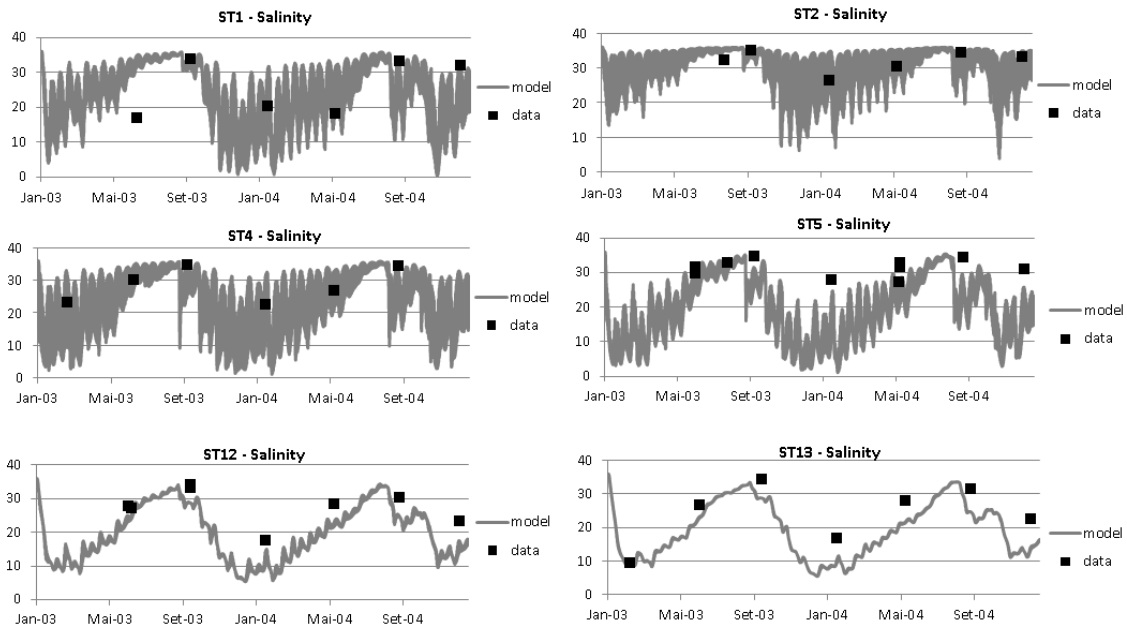


Figure 61 - Comparison between simulated and measured salinity in selected stations of Ria de Aveiro. For the location of the stations, please refer to Figure 49. Source of data: Universidade de Aveiro (Silva *et al.*, 2009).

Table 15 – Results of model verification for salinity. RMSE is the root mean square error, r is the correlation coefficient, and r^2 is the determination coefficient. For the location of the stations, please refer to Figure 49.

	ST1	ST2	ST3	ST4	ST5	ST6	ST8	ST10	ST11	ST12	ST13
RMSE	8.52	3.18	3.41	7.48	10.05	8.84	9.96	6.42	8.89	6.77	7.16
r	-0.04	0.26	0.68	0.66	0.46	0.85	0.79	0.71	0.98	0.86	0.89
r^2	0.00	0.07	0.46	0.44	0.21	0.72	0.63	0.50	0.95	0.74	0.80

Comparison between simulated and measured seagrass biomass was provided in Figure 62 and

Table 16. Seagrass biomass showed to be related to seasonal changes of temperature, with maxima in summer and minima in winter. The results of the seagrass model gave better agreement with data in stations ST2, ST4, and ST5, and ST12. *Zostera noltii* growth rate g_{max} was initially set to 0.23 1/day, but the results of the model showed better fit to data with $g_{max} = 0.12$ 1/day. The calibration results shown in

Figure 62 were obtained with the set of parameters given in Table 8 but with $g_{max} = 0.12$ 1/day.

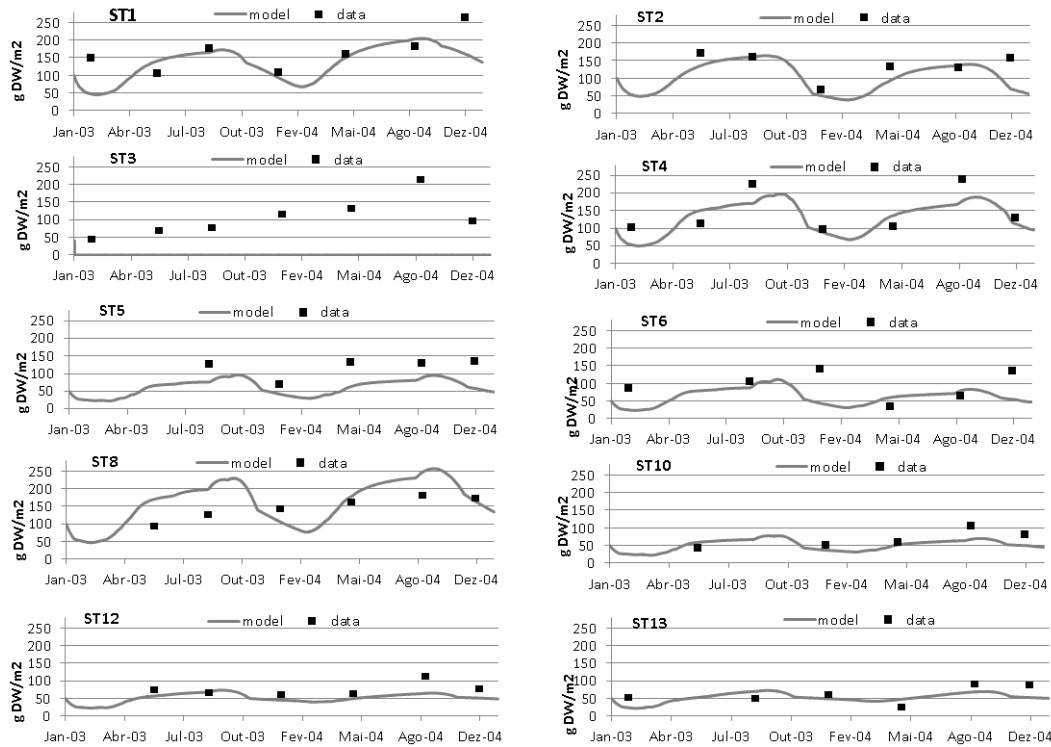


Figure 62 - Comparison between simulated and measured *Zostera noltii* biomass in the stations described in Figure 49. Source of data: Universidade de Aveiro (Silva *et al.*, 2009).

Table 16 - Results of seagrass model in the stations shown in Figure 49. RMSE is the root mean square error, r is the correlation coefficient, and r^2 is the determination coefficient. N.A. means Not Applicable.

	ST1	ST2	ST3	ST4	ST5	ST6	ST8	ST10	ST12	ST13
RMSE (kg DW)	0.06	0.04	N.A.	0.04	0.05	0.06	0.06	0.02	0.02	0.02
r	0.44	0.66	N.A.	0.77	0.65	-0.24	0.59	0.58	0.64	0.35
r^2	0.19	0.43	N.A.	0.60	0.42	0.06	0.35	0.34	0.40	0.12

Results of biomass in ST3 are not shown because the model simulated high shear stress in station 3, thus seagrasses were not simulated in ST3. The bottom shear stress in the model depends mostly on the bathymetry. This means that the bathymetry of the model should be improved in future applications of the model.

Zostera noltii only grows in muddy sediment, which can be related to water retention sediment during exposure (Silva *et al.*, 2009). The lower values of *Zostera noltii* biomass were simulated in the north of the lagoon (ST10, ST12 and ST13), in conformity with previous monitoring studies (Silva *et al.*, 2009).

Some examples of time series for the light limiting factor are displayed in Figure 63 for selected stations. During the year, the light limiting factor showed values close to 1 during the day (between 0.8 and 0.9) in all stations. This means that the growth of the plant was not limited by light availability. This result confirmed that *Zostera noltii* rarely shows adaptation to light since it primarily grows in shallow intertidal waters with sufficient light (Greve and Binzer, 2004), concluding that light is not a limiting factor for *Zostera noltii* in Ria de Aveiro.

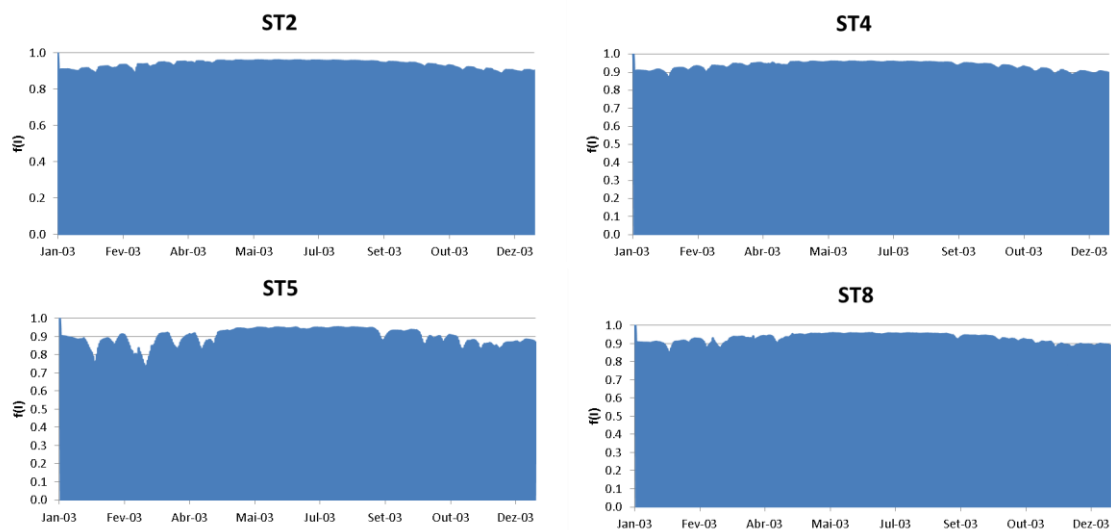


Figure 63 – Light limiting function (eq. 5) in selected stations.

The growth of the leaves was limited by maximum leaves biomass as shown in Figure 64. In ST2, the space limiting factor ranged between 0.5 and 0.9, with an average of 0.5. In ST4, the space limiting factor ranged between 0.4 and 0.8, with an average of 0.6. In ST5, the space limiting factor ranged between 0.7 and 0.9, with an average of 0.8. In ST8, the space limiting factor ranged between 0.2 and 0.9, with an average of 0.5. In overall, the space availability limited the growth of seagrasses in the late summer, when the biomass of the leaves reached its maximum. The space availability limited the growth of *Zostera noltii* in ST8 more than in the other three stations

displayed in Figure 64, because the biomass values in ST8 were higher than these for ST2, ST4, and ST5. The biomass of the plant in stations ST5, ST10, ST11, and ST12 was not significantly limited by space availability because the biomass of the plant was low.

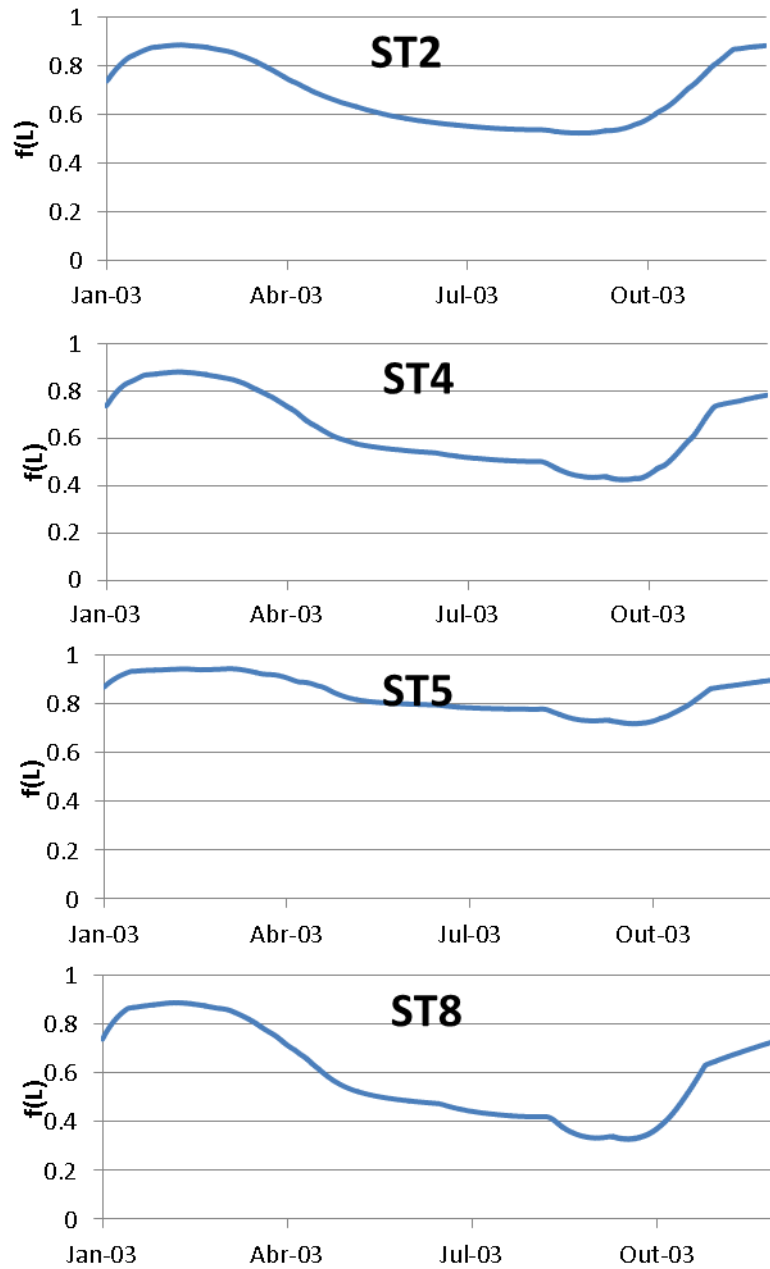


Figure 64 – Space limiting function (eq. 6) in selected stations.

The seagrass growth was limited by nutrients, as shown in Figure 65 for some selected stations. The results are referred to eq. 8 and eq. 16. The value of $f(N)$ in ST2 varied between a minimum of 0.06 and a maximum of 1, with an average of 0.6. The value of $f(N)$ in ST4 varied between a minimum of 0.6 and a maximum of 1, with an average of 0.8. The value of $f(N)$ in ST5 varied between a minimum of 0.8 and a maximum of 1, with an average of 0.9. The value of $f(N)$ in ST8 varied between a minimum of 0.94 and a maximum of 1, with an average of 0.98. The comparison between the stations shows that the plant's growth in ST5 and ST8 was less limited than this of ST2 and ST4, because the plant accumulated more nutrients in ST5 and ST8 than in ST2 and ST4. In overall, the results show that *Zostera noltii* was more limited by nutrients in summer than in winter. Similar results were obtained for $f(P)$ as well.

These results are related to the plant's internal nutrient quota. When the nitrogen quota (or phosphorus quota) decreases, the plant is depleted in nitrogen (or phosphorus) content with respect to carbon content, and the nutrient limiting factor $f(N)$ (or $f(P)$) decreases (higher limitation). This means that the lower the nitrogen (or phosphorus) quota, the higher the growth limitation due to nutrient depletion. The depletion of internal nutrients has the consequence to increase the internal ratio between carbon and nitrogen (or between carbon and phosphorus).

The results in Figure 65 show the uptake limitation due to nutrient content. The value of fbn in ST2 varied between a minimum of 0 and a maximum of 0.97, with an average of 0.64. The value of fbn in ST4 varied between a minimum of 0 and a maximum of 0.75, with an average of 0.47. The value of fbn in ST5 varied between a minimum of 0.0 and a maximum of 0.63, with an average of 0.36. The value of fbn in ST8 varied between a minimum of 0.0 and a maximum of 0.63, with an average of 0.40.

Results of fbn in Figure 65 show that when the plant's growth is limited by internal nutrient depletion, the uptake of nutrients increases. Following this, the nutrient uptake is limited more in the winter than in the summer. Since the depletion of nutrients has a positive feedback on the uptake of external nutrients, it can be concluded that the internal nutrient content regulates the uptake of external nutrients from the water.

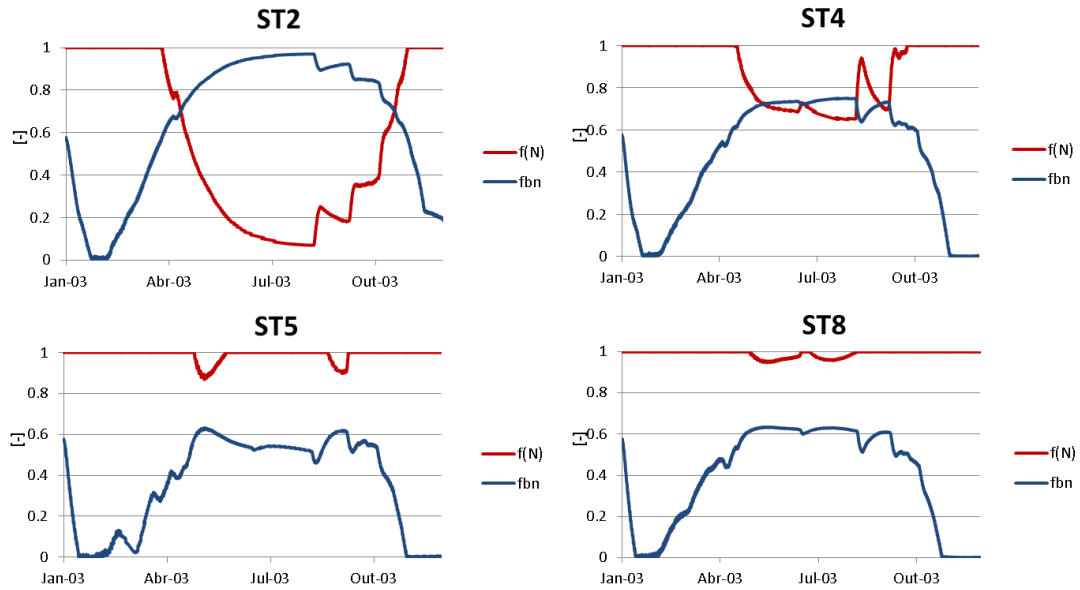


Figure 65 – Nitrogen limiting factors (eq. 8 and eq. 16) in selected stations.

Time series of nitrogen quota in the plant were provided in Figure 66. The internal nitrogen quota in the stations varied between a minimum of 5 g N/kg DW and a maximum of 30 g N/kg DW. Time series of phosphorus quota in the plant were provided in Figure 67. The phosphorus quota in the stations varied between a minimum of 0.14 g P/kg DW and a maximum of 3 g P/kg DW. In overall, nitrogen and phosphorus quota showed seasonality in all stations, with minima in spring/summer, and maxima in winter. This result is consistent with the seasonality of nutrient limitation described above.

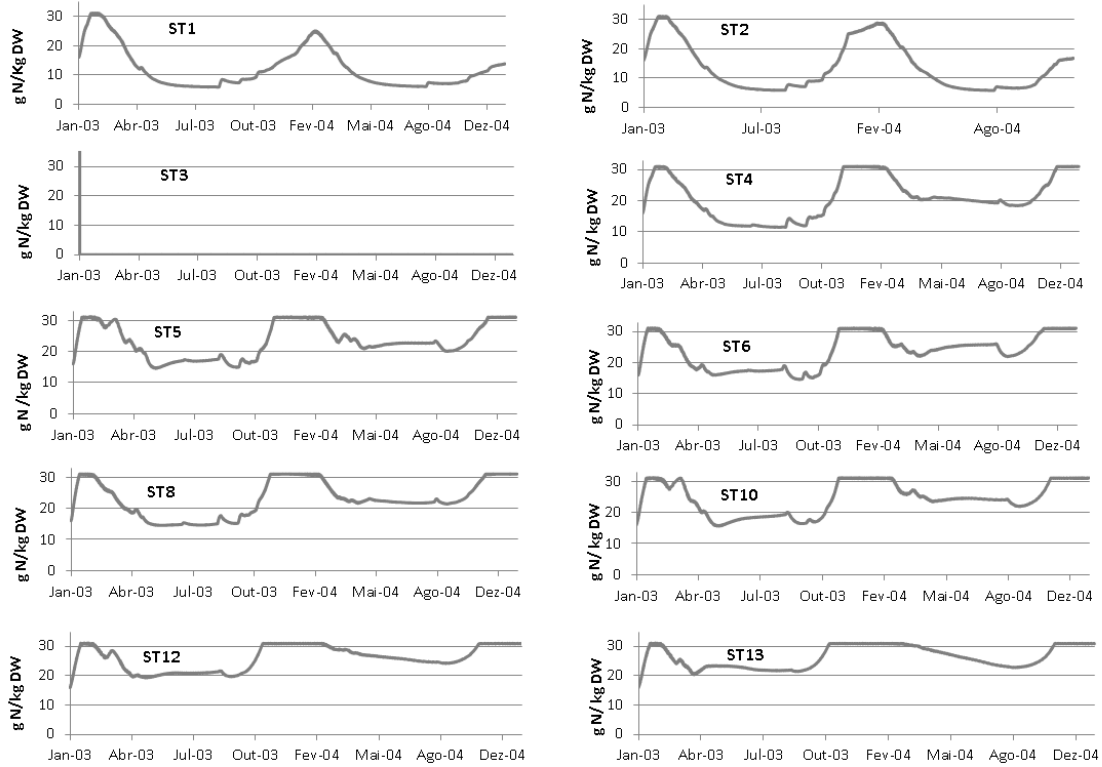


Figure 66 – Simulated *Zostera noltii* relative nitrogen content in the stations described in Figure 49.

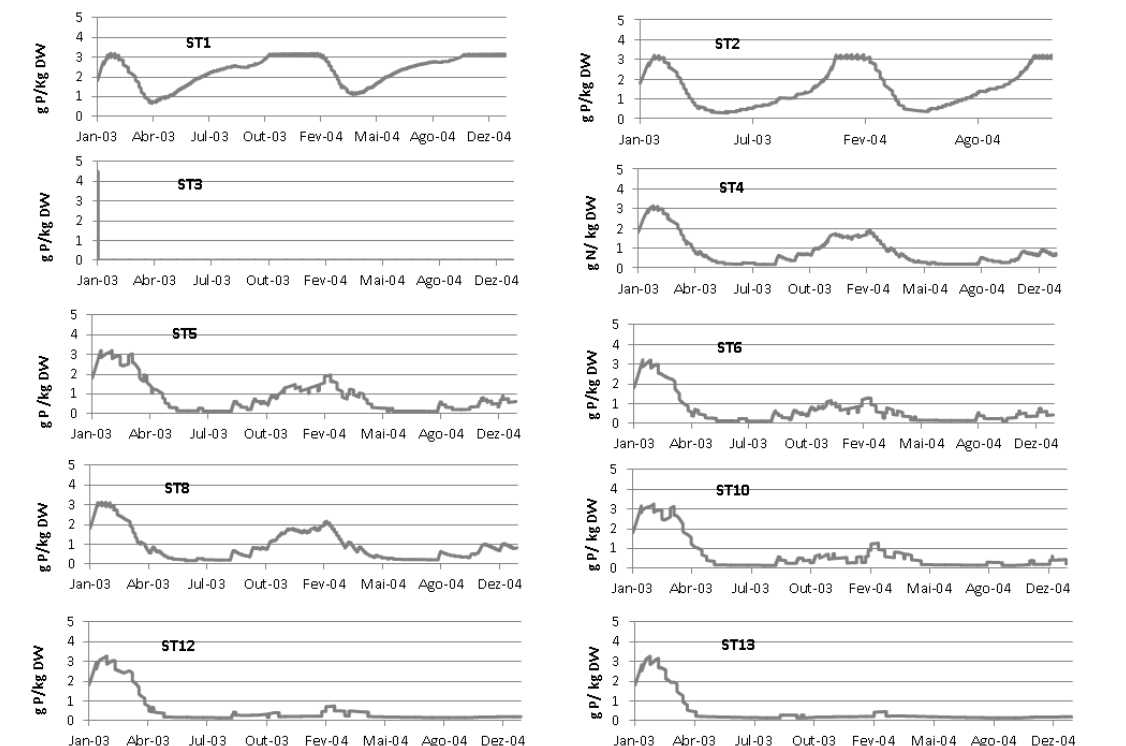


Figure 67 – Simulated *Zostera noltii* relative phosphorus content in the stations described in Figure 49.

Table 17 - Initial and boundary conditions used for water properties.

Property name	Initial condition value	Boundary condition value	Unit
salinity	36	36	psu
temperature	15	15	°C
ammonia	0.002	0	mg N/l
nitrate	0.1	0	mg N/l
nitrite	0.001	0	mg N/l
dissolved refractory organic nitrogen	0.001	0	mg N/l
dissolved non-refractory organic nitrogen	0.001	0	mg N/l
particulate organic nitrogen	0.001	0	mg N/l
inorganic phosphorus	0.02	0	mg P/l
dissolved refractory organic phosphorus	0.001	0	mg P/l
dissolved non-refractory organic phosphorus	0.001	0	mg P/l
particulate organic phosphorus	0.001	0	mg P/l
phytoplankton	0.001	0	mg C/l
zooplankton	0.001	0	mg N/l
cohesive sediment	10	0	mg/l
oxygen	8	8	mg/l

Table 18 - Initial conditions at the sediment-water interface.

Property name	Initial condition value	Unit
cohesive sediment	0	kg /m ²
particulate organic nitrogen	0	kg N/m ²
particulate organic phosphorus	0	kg P/m ²
ammonia	0	kg N/m ²
oxygen	0	kg O ₂ /m ²
inorganic phosphorus	0	kg/m ²

5.8. Conclusion

Zostera noltii is an intertidal species of Ria de Aveiro adapted to live under tidal regimes. In this research, a seagrass model was applied to simulate the spatial and temporal distribution of the seagrass *Zostera noltii* in Ria de Aveiro. The simulation was carried out over a period of 2 years (2003-2004). The model results showed good agreement with real observations of water level, salinity, temperature, and seagrass biomass. The formulation used in the model enabled the simulation of the response of the ecosystem to environmental changes, accounting for physical and biological factors simultaneously. The results showed that the growth of the plant is not limited by light availability, in conformity with literature studies, because the plant is living at low depth where light is enough to enable photosynthesis. The plant was limited by nutrient availability during summer, and less limited by nutrients during winter. Following this, the plant's internal nutrient quota increases during winter, and decreases during summer. This is reflected by the uptake of nutrients, which is higher in summer than in winter, needed to compensate for the depletion of internal nutrients.

Although the model is a simplified description of the reality, it contains the main characteristics of aquatic rooted plants and it could be used to simulate other seagrass species. Seagrasses are part of the benthic system and are different from pelagic producers, because they are not transported by advection-diffusion processes and their biology is connected to processes occurring in water and in sediment. Seagrasses stabilize the sediment, retain nutrients, and create habitat for many species. The importance of these plants as ecosystem engineers and sinks of carbon deserves investigation through the combination of monitoring and modeling studies. This research provided an example of how monitoring and modeling can be integrated to aid coastal habitat management.

Chapter 6 – Hypotheses Testing

This chapter is dedicated to the verification of the hypotheses described in Chapter 1.8.

6.1. Introduction

A methodology based on scenario comparison is used to verify the hypotheses related to the proposed research questions.

For the first research question (Q1 – When the growth of seagrasses limited by macroalgae?) a scenario is built to simulate *Zostera noltii* and macroalgae in Ria de Aveiro, and the results are compared with the case study of Chapter 5, used as a reference.

For the second research question (Q2 – Can the model reproduce the control by filter feeders on phytoplankton biomass?) a schematic case study is set up and three scenarios are used for the evaluation of the role of benthic filter feeders grazing on phytoplankton concentration.

6.2. Q1: *When the growth of seagrasses limited by macroalgae?*

In this section, the three hypotheses relative to the first research question (Q1) described in section 1.8 were verified. The case study described in Chapter 5 was used as a reference scenario against which to compare a second scenario in which both *Zostera noltii* and macroalgae are simulated in Ria de Aveiro.

For simplicity, the two scenarios were labelled as B1 and B2:

- B1: reference scenario (described in Chapter 5) with seagrasses only (*Zostera noltii*)
- B2: scenario with seagrasses (*Zostera noltii*) and macroalgae.

The two scenarios were used to assess the competition between macroalgae and seagrasses in terms of light, nutrients, and space.

Model setup

The model setup in B2 is the same as B1, described in Chapter 5. The only difference between the two scenarios was the presence of macroalgae in B2. This means that in the two scenarios, the same boundary conditions, the same freshwater inflows (Figure 55), and the same nutrient inputs (Figure 56, Figure 57, and Figure 58) were used. The macroalgae biomass in B2 was initialized with a value of 10 g C/m².

Results and discussion

In overall, the comparison of B1 with B2 shows that in the presence of macroalgae the biomass of *Zostera noltii* is lower than this in B1. The main evidence of this result is provided in Figure 68 and Figure 69. The reason for the decline of *Zostera noltii* in the presence of macroalgae is assessed in the next sections through hypotheses verification. Time series of seagrass limiting factors are analysed to understand which factors influence the growth of *Zostera noltii* when macroalgae are present.

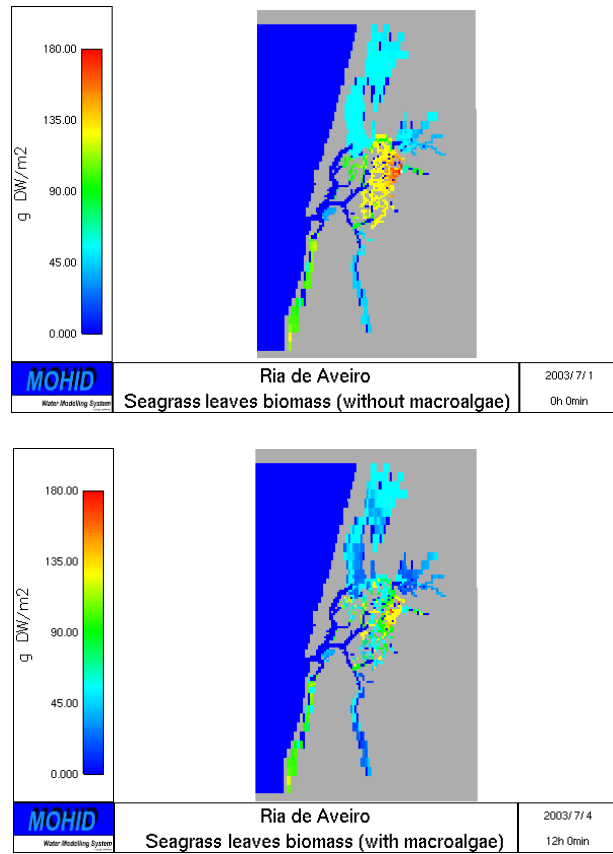


Figure 68 –Leaves biomass in B1 and B2 after 6 months simulation.

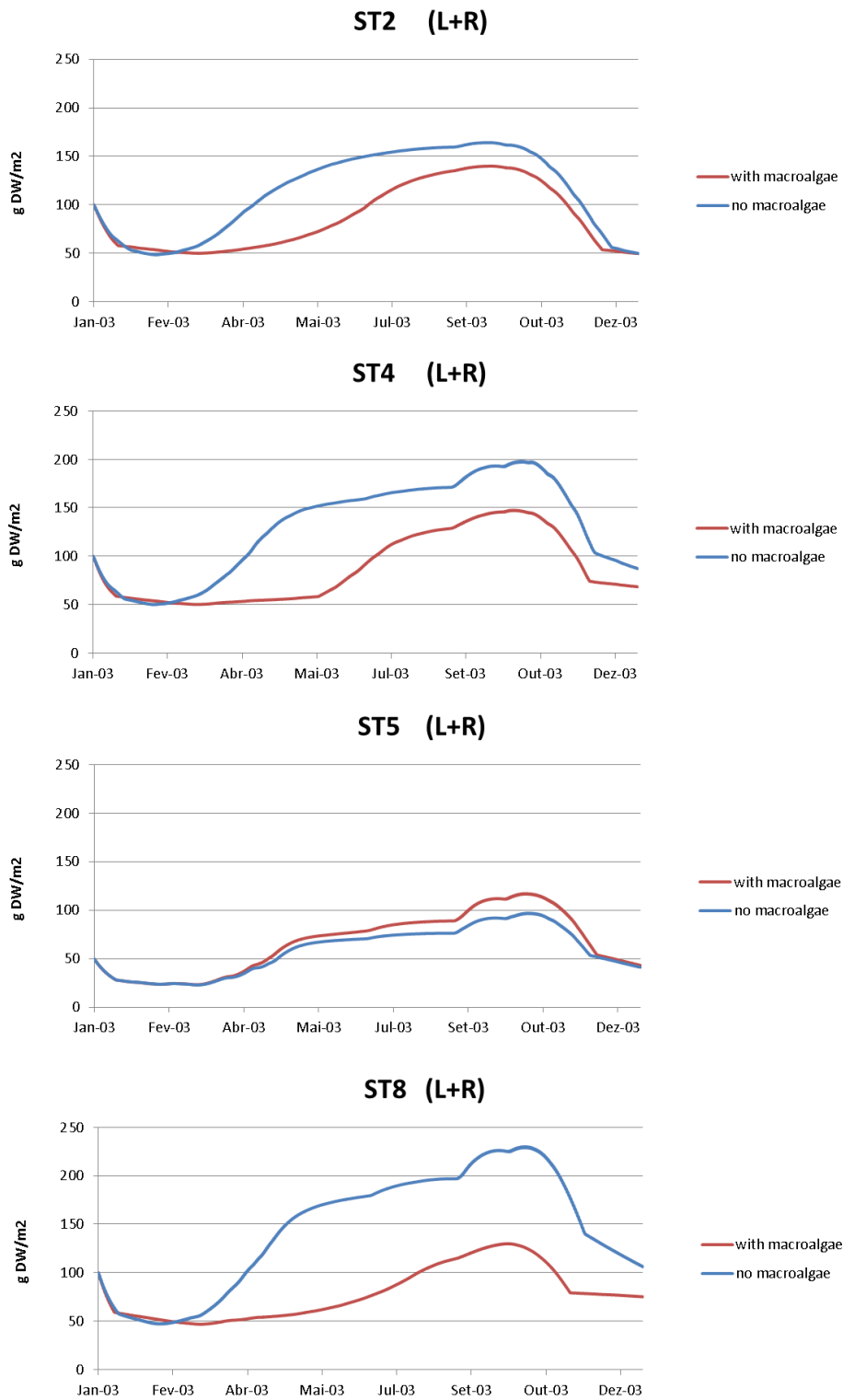


Figure 69 – Biomass of seagrasses in B1 (blue line) and in B2 (red line).

H1.1: The growth of Zostera noltii is limited by light availability in presence of macroalgae

To verify H1.1, the *Zostera noltii* light limiting factor in B1 was compared with the *Zostera noltii* light limiting factor in B2. Time series of the light limiting factor for selected stations were reported in Figure 70. In ST2, the *Zostera noltii* light limiting factor in B2 was 0.37% (average annual value) lower than this in B1. In ST5, the *Zostera noltii* light limiting factor in B2 was 0.3% (average annual value) lower than this in B1. In ST8, the *Zostera noltii* light limiting factor in B2 was 2.5% (average annual value) lower than this in B1. In overall, it can be concluded that *Zostera noltii* was not significantly limited by light in presence of macroalgae.

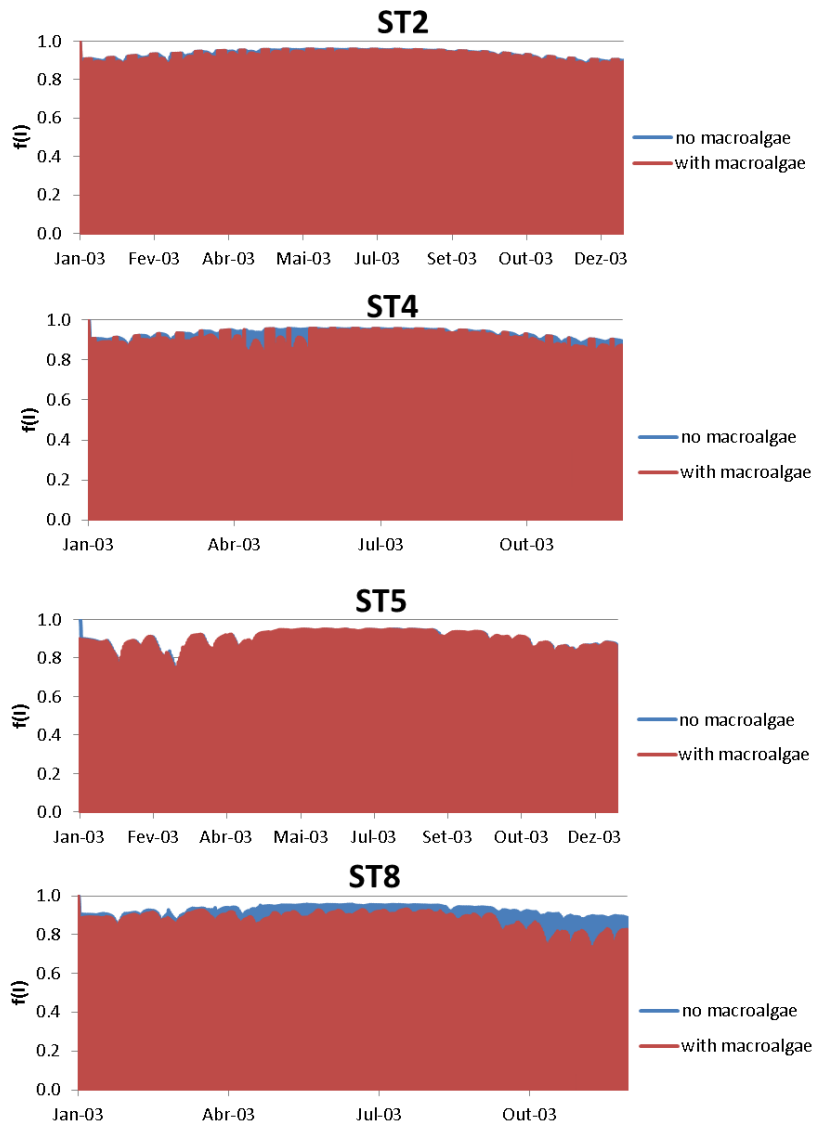


Figure 70 – Light limiting function (eq. 5) in B1 (blue line) and in B2 (red line).

*H1.2: The growth of *Zostera noltii* is limited by nutrient availability in presence of macroalgae*

Seagrasses should not be affected by lack of nutrients because they do not rely only on nutrients that are dissolved in the water, but plant's roots can absorb nutrients from sediment. Moreover, "nutrient requirements for seagrasses are lower than for other aquatic organisms such as macroalgae and phytoplankton. It is estimated that seagrasses require about 4 times less nitrogen and phosphorous per weight than phytoplankton cells." (Greve and Binzer, 2004). However, it has been demonstrated that nutrient limitation changes with the relative nutrient content of the plant (Duarte, 1990). The nutrient limitation in seagrasses can be analyzed in terms of C:N and C:P ratios: "plants that are strongly nitrogen (or phosphorus) limited should have tissues depleted in nitrogen (or phosphorus) relative to their carbon content, and should, therefore, show high C:N (or C:P) ratios. As nutrient availability increases to meet the plant's demands, their tissues should become progressively enriched in nitrogen and phosphorus relative to the carbon content, implying decreasing C:N and C:P ratios" (Duarte, 1990).

To verify H1.2, time series of *Zostera noltii* nutrient content were compared in B1 and B2. Examples of time series were provided for stations ST2, ST4, ST5, and ST8 (Figure 71, Figure 72, Figure 73, and Figure 74, respectively). The blue lines represent the scenario without macroalgae (B1), and the red lines represent the scenario with macroalgae (B2). The results show that nitrogen content N (kg/m^2) in B2 was lower than this in B1. The relative nutrient content (see Figure 71, Figure 72, Figure 73, and Figure 74) was higher in the presence of macroalgae because the biomass of the plant was lower in B2.

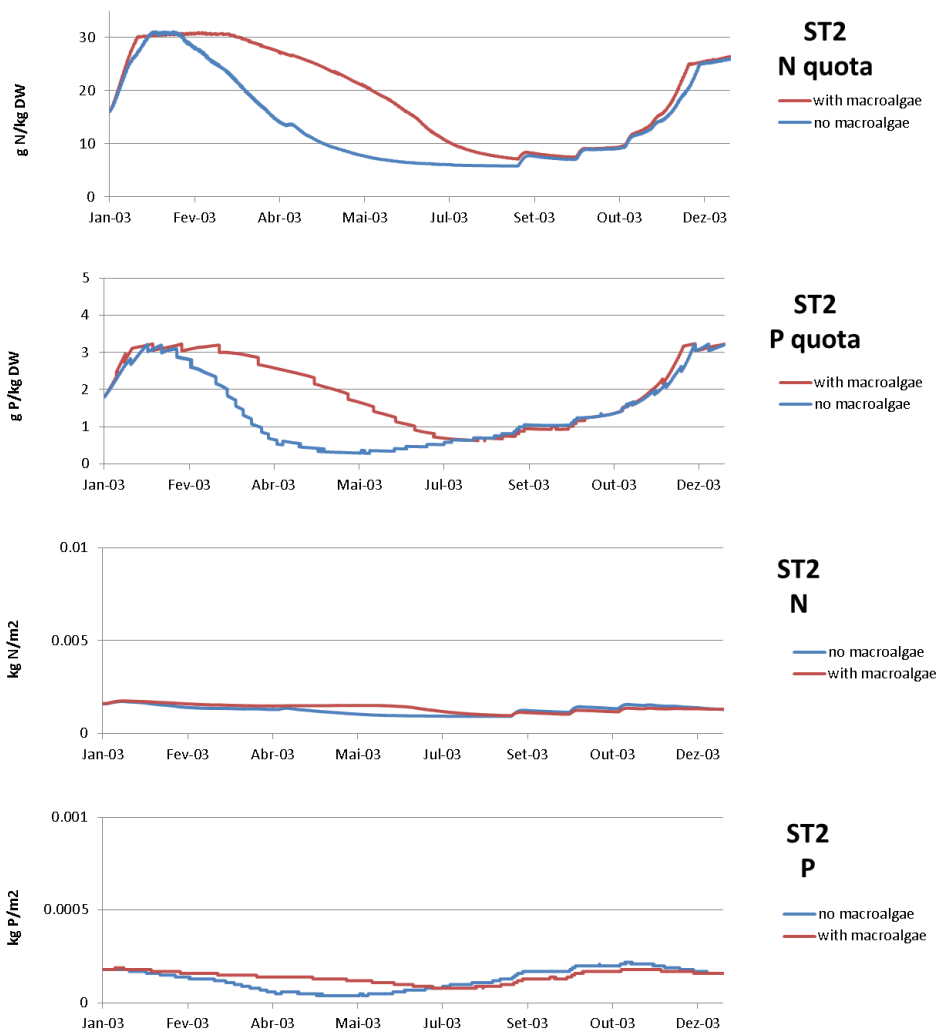


Figure 71 – Simulated *Zostera noltii* nutrient content in B1 (blue line) and in B2 (red line) in station ST2.

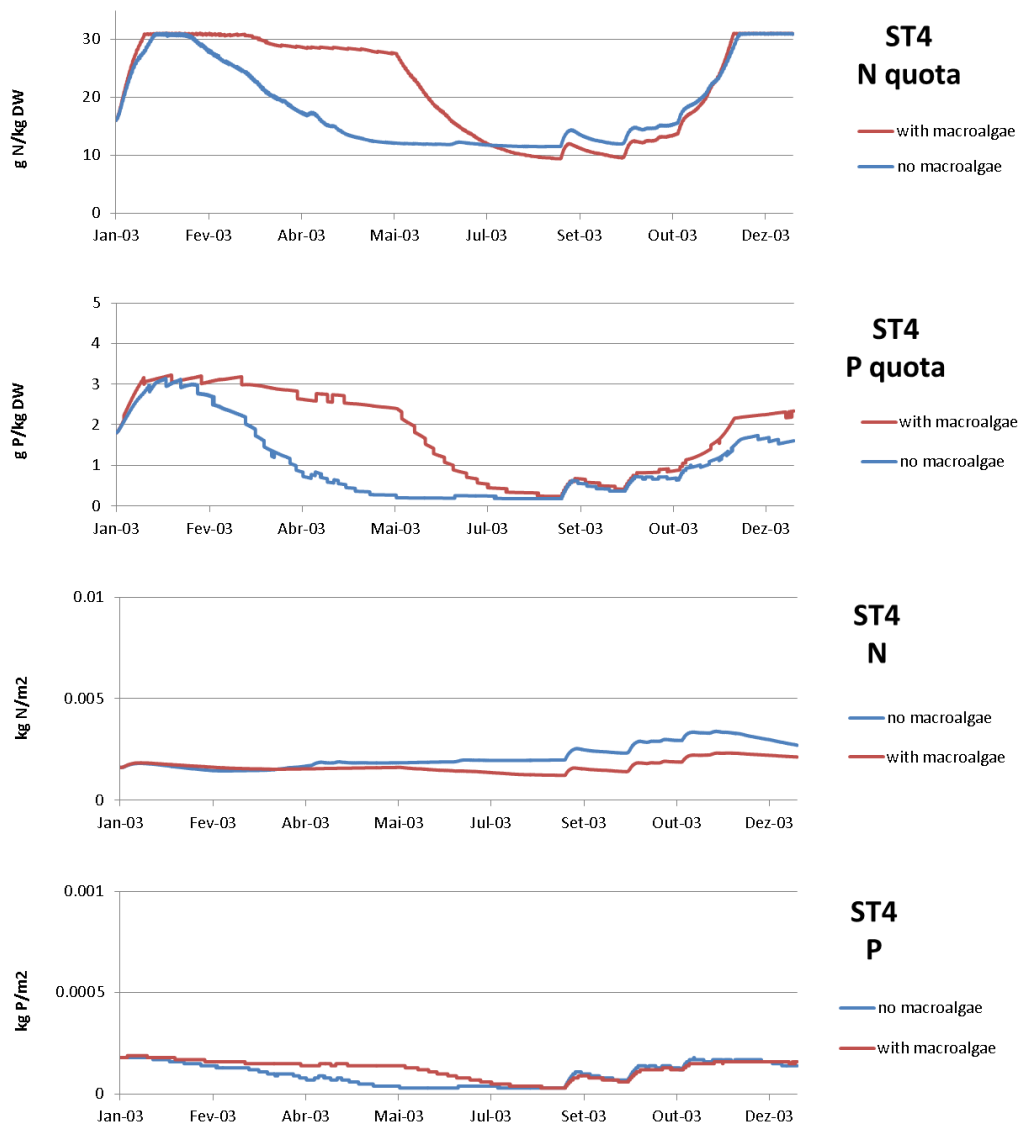


Figure 72 – Simulated *Zostera noltii* nutrient content in B1 (blue line) and in B2 (red line) in station ST4.

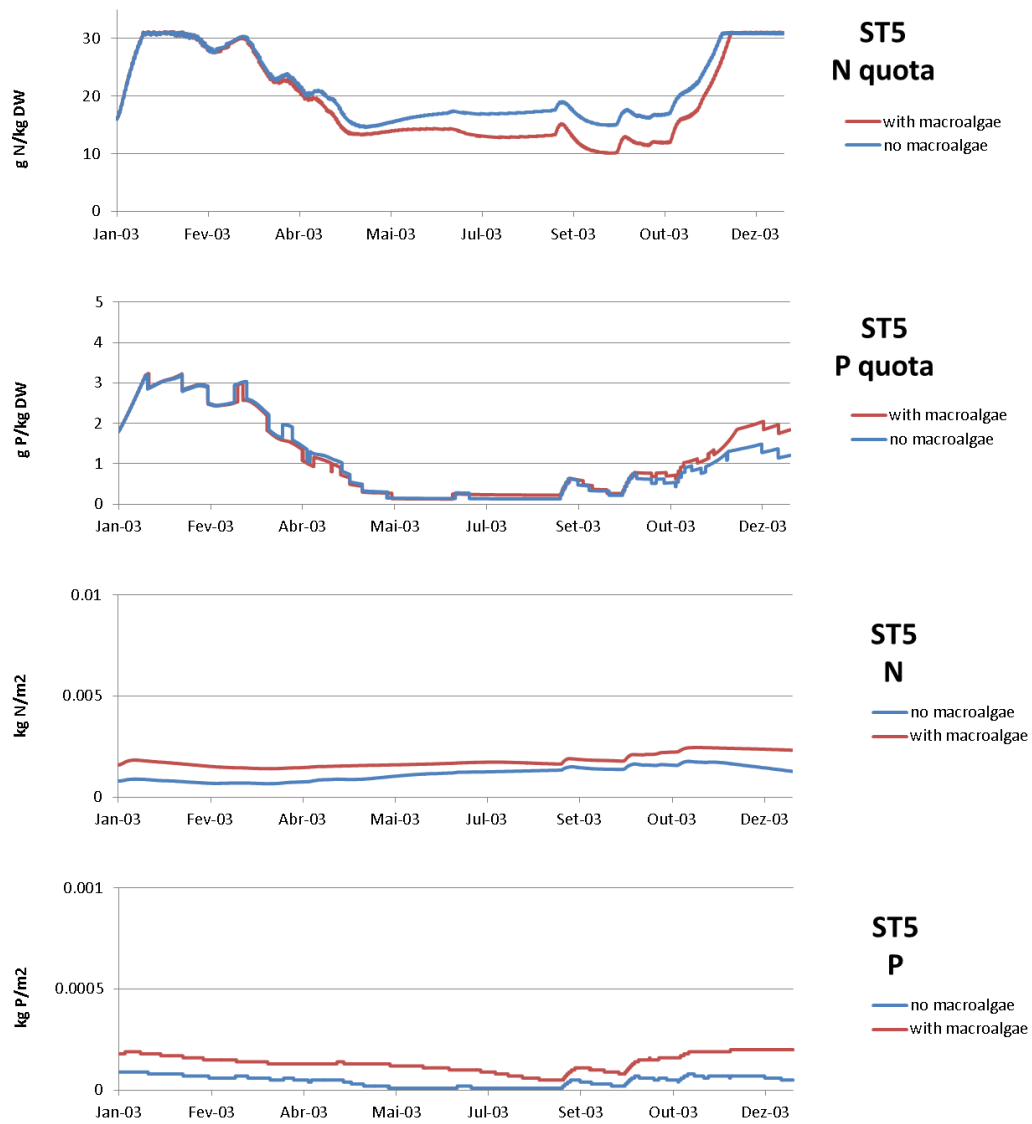


Figure 73 – Simulated *Zostera noltii* nutrient content in B1(blue line) and in B2 (red line) in station ST5.

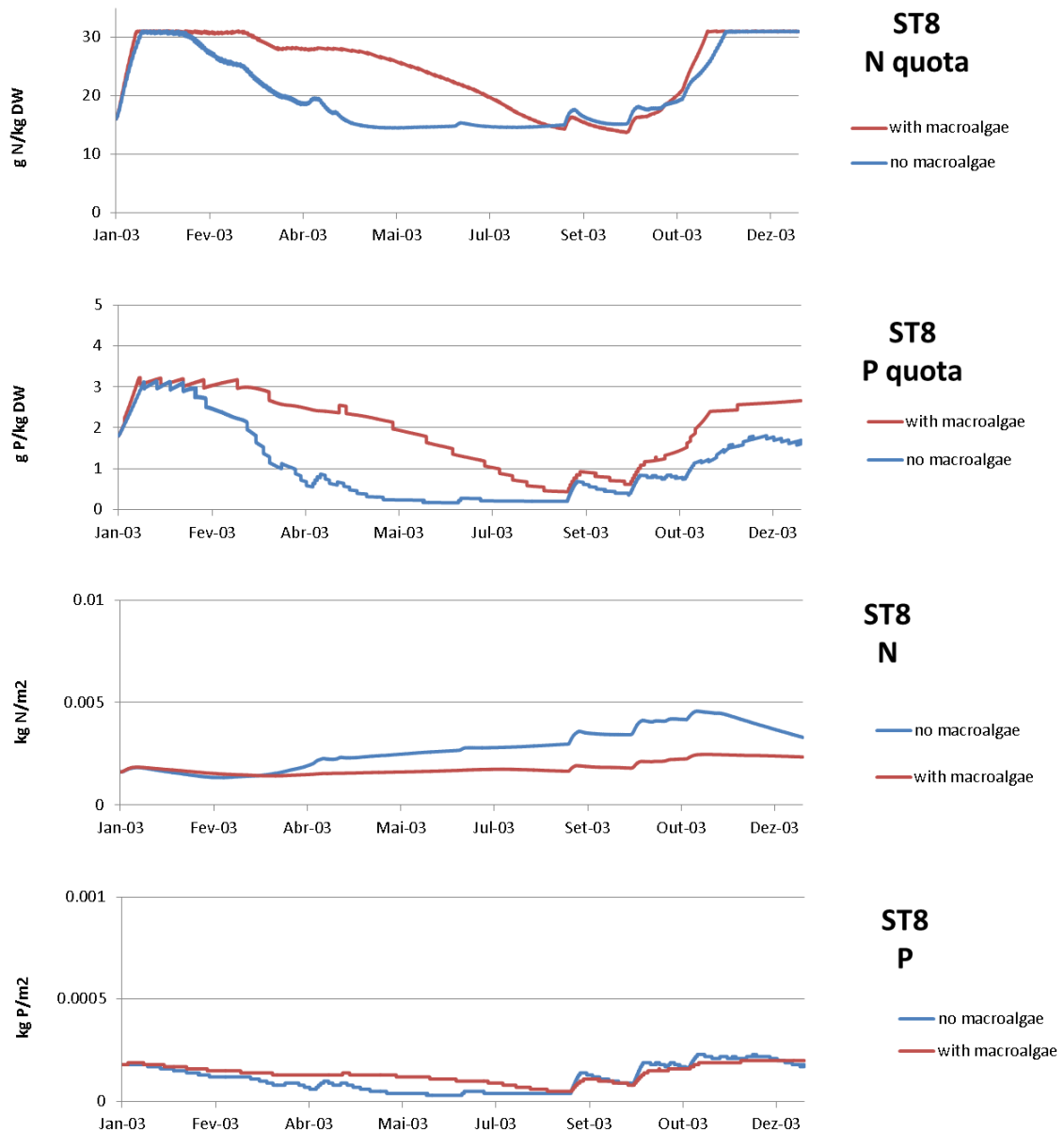


Figure 74 – Simulated *Zostera noltii* nutrient content in B1 (blue line) and in B2 (red line) in station ST8.

The rate of change in C:N and C:P ratios with increasing nitrogen or phosphorus content in plant tissues should shift from high to small as nutrient supply meets the plant's demands (Duarte, 1990). Following this, as the C:N (or C:P) ratio increases, the plant is more limited by the nutrients availability. As an example, the results for the C:N ratio simulated in ST2 are given in Figure 75. The results of the simulated C:N ratio show that the plant was limited by nutrients in summer and less limited by nutrients in

winter. The results obtained for the C:N ratio are reflected in the results of the nitrogen limiting factor $f(N)$ for ST2 (eq. 8), also presented in Figure 75. The value of $f(N)$ is higher in winter than in summer, showing that the plant's growth is limited by nutrients in the summer and less limited by nutrients in the winter. Similar results were obtained in the other stations as well.

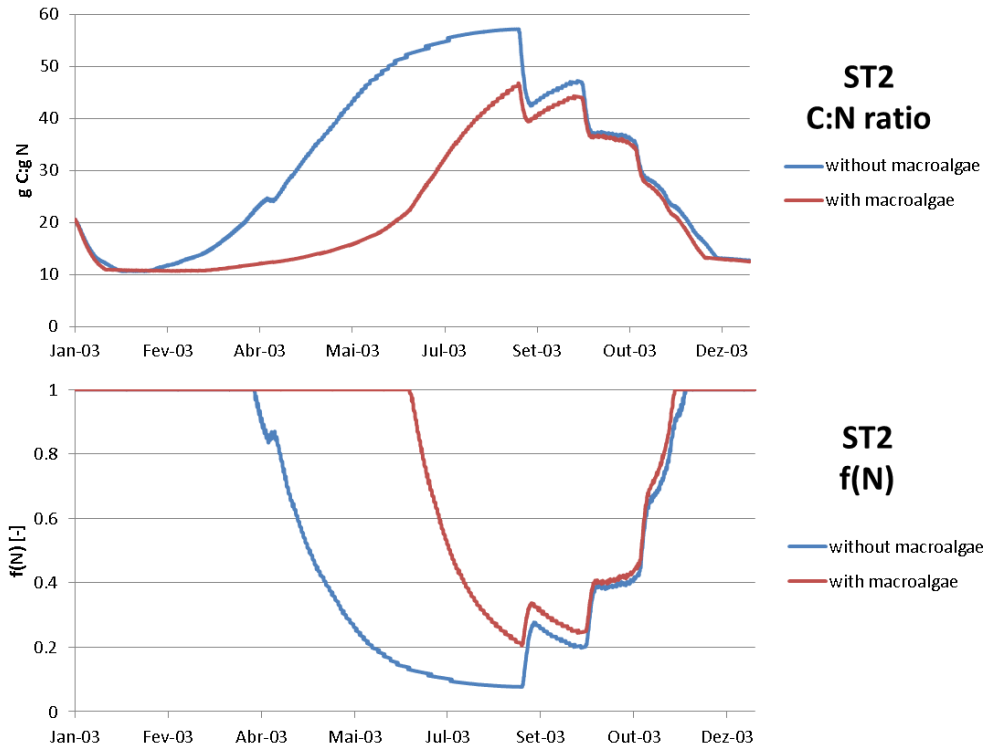


Figure 75 – Simulated *Zostera noltii* C:N ratio in B1 (blue line) and in B2 (red line) in station ST2.

In overall, the results of the model in B2 show higher concentrations of ammonia than this in B1. The explanation of this result is that the presence of macroalgae, additionally to seagrasses and phytoplankton, determines more respiration and mineralization of organic matter in the system. The overall increase of ammonia in the simulated system is consistent with previous applications of the MOHID macroalgae model in Ria de Aveiro (Trancoso *et al.*, 2005). Some examples of the increase of ammonia in the system are presented in Figure 76, Figure 77, and Figure 78 for ST4, ST5, and ST8, respectively. The results were similar in other stations as well.

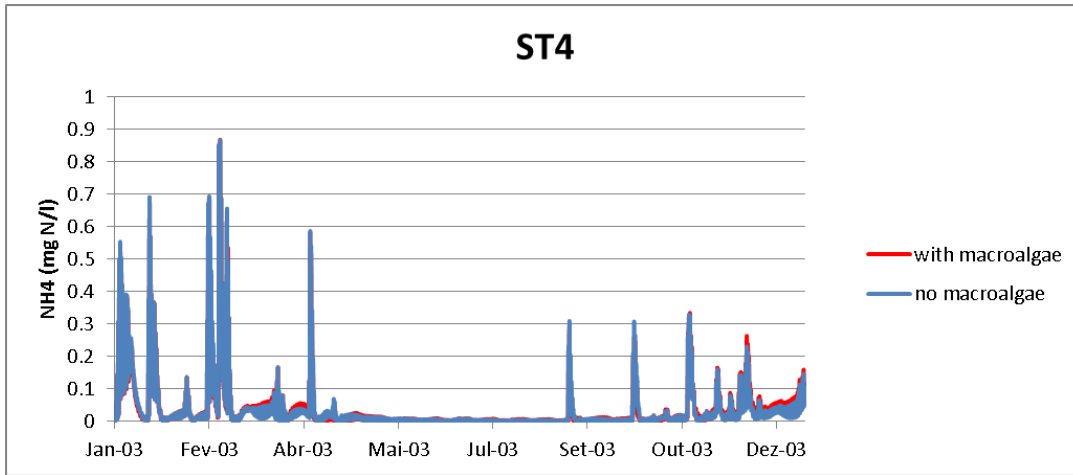


Figure 76 – Simulated ammonia concentration in the water in B1 (blue line) and in B2 (red line) in station ST4.

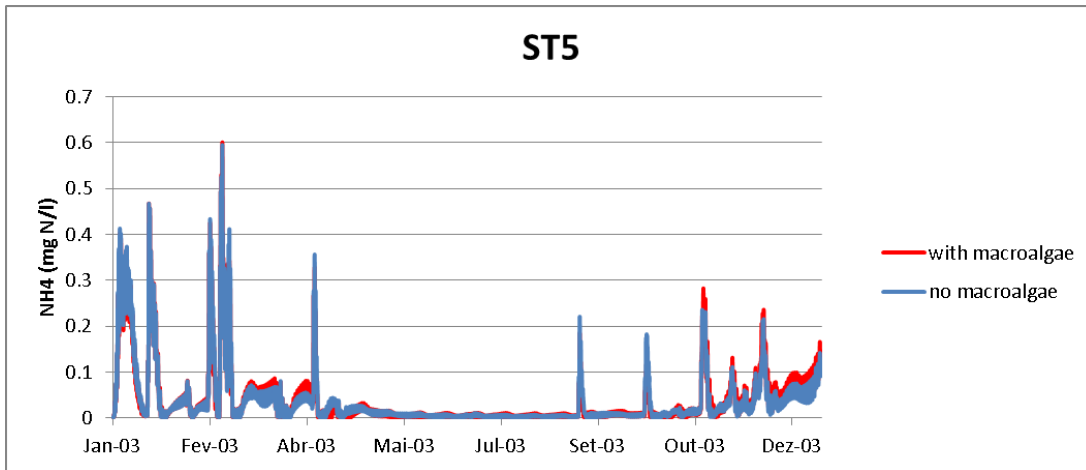


Figure 77 – Simulated ammonia concentration in the water in B1 (blue line) and in B2 (red line) in station ST5.

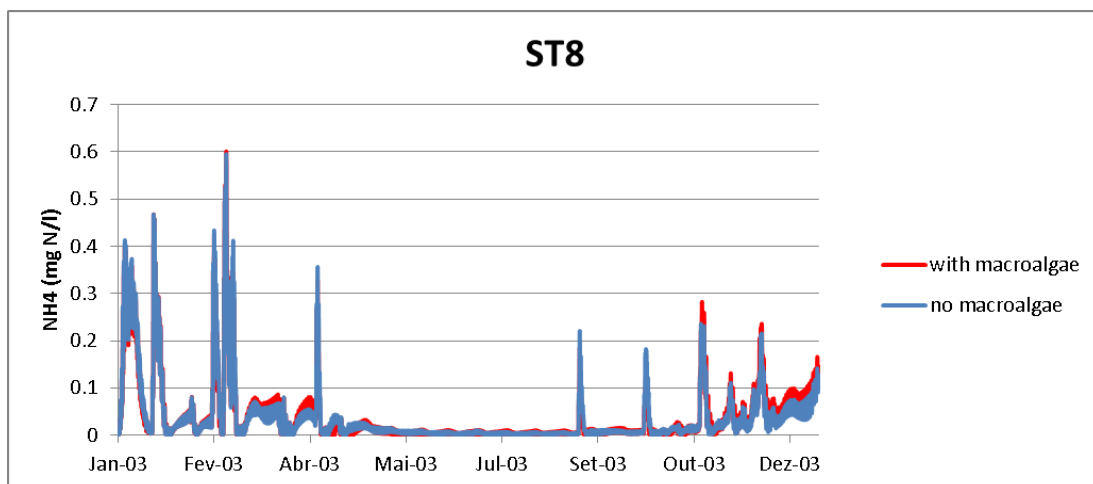


Figure 78 – Simulated ammonia concentration in the water in B1 (blue line) and B2 (red line) in station ST8.

Following these considerations, it can be concluded that there are two mechanisms contributing to the increase of the nitrogen quota in seagrasses in the presence of macroalgae: the first one is the reduction of the plant's biomass in terms of dry weight; and, the second one is the increase of external nutrients (ammonia) in the system in the presence of macroalgae. Subsequently, it is possible to conclude that the presence of macroalgae in the system is not limiting the nutrient availability for seagrasses.

*H1.3: The growth of *Zostera noltii* is limited by space availability in presence of macroalgae*

The third hypothesis is that seagrasses are limited by space availability in presence of macroalgae. To verify H1.3, the simulated *Zostera noltii* space limiting factor (eq. 6) was compared in B1 and B2. The results of the comparison are presented in Figure 79 for selected stations. The blue lines represent the scenario without macroalgae (B1), and the red lines represent the scenario with macroalgae (B2).

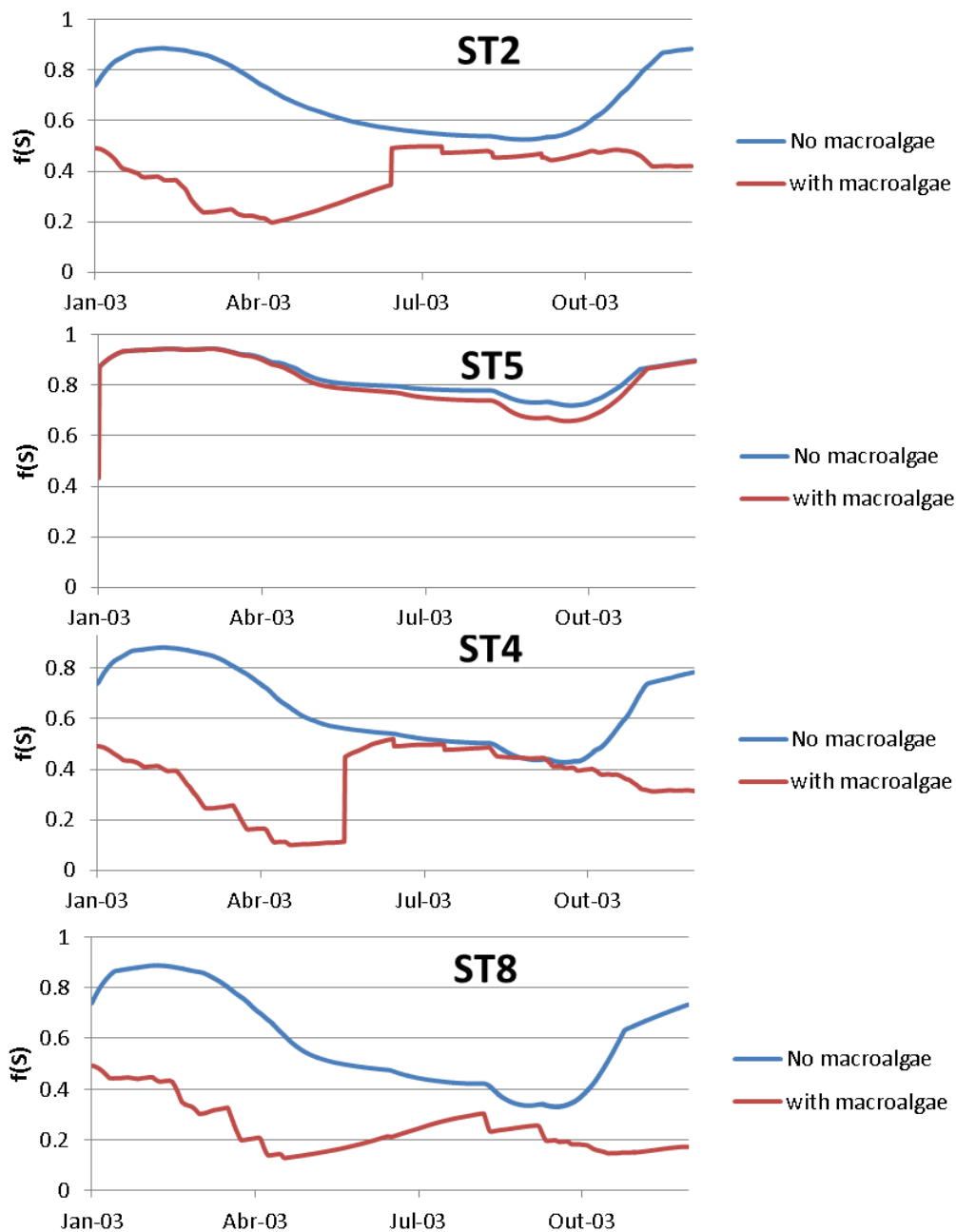


Figure 79 – Simulated *Zostera noltii* space limiting factor (eq. 6) in S1 (blue line) and in S2 (red line) in stations ST2, ST4, ST5, and ST8.

In overall, the space limiting factor in B2 was lower than this in B1. In ST2, the *Zostera noltii* space limiting factor in B2 was 54% (average annual value) lower than this of S1. In ST4, the *Zostera noltii* space limiting factor in B2 was 56% (average annual value) lower than this in B1. In ST5, the *Zostera noltii* space limiting factor in B2 was 11% (average annual value) lower than this in B1. In ST8, the *Zostera noltii* space limiting factor in B2 was 70% (average annual value) lower than this in B1. The biomass of the plant in B2 was lower than this of B1. It can be concluded that space is a

significant factor in the limitation of *Zostera noltii* growth when macroalgae are present. However, in some points of the domain, such as in ST5, the *Zostera noltii* biomass in B2 was higher than this in B1. In ST5, the macroalgae were present with very low biomass, thus they were not competing with plants for space. The same situation was found in ST1, where macroalgae biomass was lower than 10 g C/m². This result suggested that the presence of low macroalgae biomass is not limiting the space availability for seagrasses.

6.3.Q2: Can the model reproduce the control by filter feeders on phytoplankton biomass?

In this section, the hypothesis relative to the second research question (Q2) described in Chapter 1.8 was verified.

H2.1: Filter feeders in the model control phytoplankton biomass by grazing

To verify H2.1, a methodology based on scenario simulation was set. The overall settings used for the ecosystem simulation are described in this section. Three scenarios were built:

- 1) S1: Scenario without filter feeders grazing on phytoplankton and without microphytobenthos and deposit feeders;
- 2) S2: Scenario with filter feeders grazing on phytoplankton and without microphytobenthos and deposit feeders; and,
- 3) S3: Scenario with filter feeders grazing on phytoplankton and with microphytobenthos and deposit feeders.

In all scenarios the cycle of primary production and organic matter in the water was computed. For each scenario, the model was executed over a period of 360 days with reference parameter values from Table 4, Table 5, and Table 6. The time step used was 1 sec. The simulation domain was defined inside the model as a continuously stirred tank with dimension 15x15x15 m (Figure 80). The model spatial grid had 5 x 5

m horizontal resolution. The model is depth averaged and the transport of solutes and particulate properties due to advection and mixing were considered as well. An inlet was included at the N-E corner, containing input of water, nutrients, oxygen, and particulate organic matter. An outlet was included at the S-W corner, containing output of water, nutrients, oxygen, and particulate organic matter. The model was set to calculate the heat fluxes at the water-air interface, in order to simulate the shortwave solar radiation seasonal pattern at mid-latitudes, as described in the MOHID manual available online (www.mohid.com). The deposition of organic matter and inorganic sediments was assumed to occur at a constant sedimentation rate.

The model accounts for mineralization in the water and on the bottom sediments. The model was forced with nutrient input at the inlet (Figure 80), and with solar radiation calculated by the MOHID modules for surface heat exchange. Heat fluxes are computed at the water-air interface, in order to calculate the light extinction with depth. The water inflow was set to a constant value of $0.24 \text{ m}^3 \text{ day}^{-1}$ during the winter, and to a lower value of $0.12 \text{ m}^3 \text{ day}^{-1}$ during the summer, to reproduce a seasonal freshwater cycle at mid-latitudes. Nutrient concentrations at the inlet were assumed to be constant. More specifically, the discharged nitrate concentration was 0.02 mg N l^{-1} , the discharged ammonia concentration was $0.002 \text{ mg N l}^{-1}$, the discharged oxygen concentration was $8 \text{ mg O}_2 \text{ l}^{-1}$, the discharged cohesive sediment concentration was set to 10 mg l^{-1} , and the discharged phosphate concentration was set to $0.001 \text{ mg P l}^{-1}$.

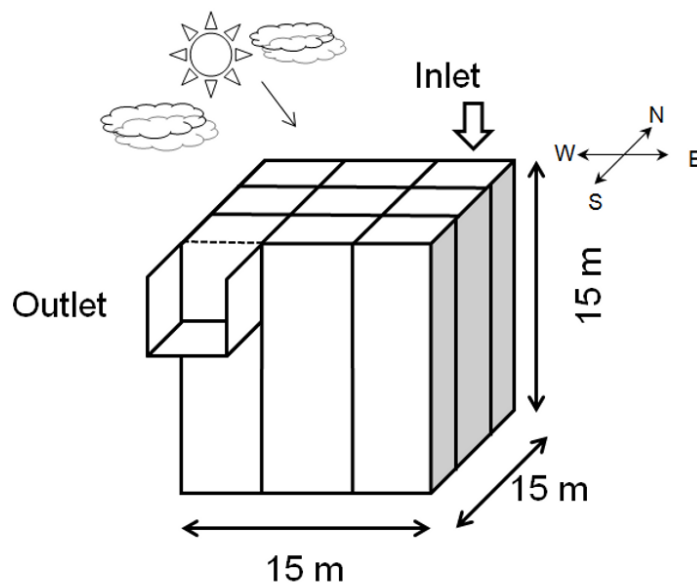


Figure 80 - Model domain. The domain has a constant depth of 15 m and the depth of the outlet is 5 m. An inlet is included in the N-E corner.

Three scenarios S1, S2, and S3 were carried out to detect feedbacks in the ecosystem. Figure 81 and Figure 82 provided the main evidence of these feedbacks. The widths of the lines in Figure 81 and Figure 82 represent the diurnal variations due to light and temperature cycle. The concentration of nitrate (Figure 81a) at the sediment-water interface in S2 and in S3 is higher than this in S1. This means that nitrate concentration at the water-sediment interface was higher when benthic filter feeders were included in the simulation. This suggested that the consumption of nitrate at the sediment-water interface was mainly due to phytoplankton activity, and that when phytoplankton decreases due to benthic grazing, the nitrate concentration increases in the water. The concentration of nitrate in S3 is lower than this in S2. This difference can be explained by consumption of nitrate at the sediment-water interface due to the inclusion of microphytobenthos in S3. The phytoplankton concentration (Figure 81b) in the water was reduced by benthic grazing, causing a lower consumption of nitrate and ammonia.

The results of S2 and S3 showed that benthic filter feeders had control on the phytoplankton biomass throughout the year. This comparison provided the evidence necessary to verify the hypothesis that filter feeders control phytoplankton concentrations in the water. The ammonia concentration (Figure 81c) was higher in S2 and S3 compared to S1 (positive feedbacks), because of the benthic feeders' respiration and mineralization of bio-deposits.

The filter feeders biomass in S1 is about 2.16 times lower (average annual value) than this in S2 and S3 because benthic grazing on phytoplankton is not simulated in S1. In S3, the competition between phytoplankton and microphytobenthos was added to the grazing effect by filter feeders, with enhanced negative feedback on phytoplankton biomass. As a consequence of the competition between microphytobenthos and phytoplankton, the introduction of microphytobenthos determined a reduction of phytoplankton biomass. This negative feedback on phytoplankton was reflected by the filter feeders (Figure 81d), which biomass in S3 was 5% lower (average annual value) than this in S2.

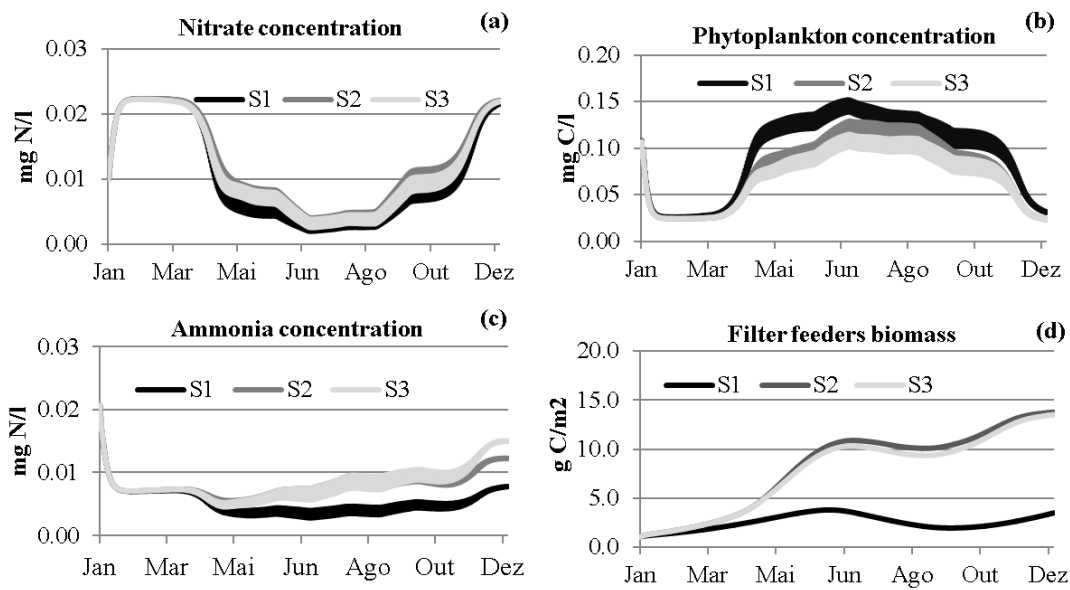


Figure 81 –Model results for the three scenarios S1, S2, and S3.

Deposit feeders and microphytobenthos were simulated in S3 only (Figure 82a and Figure 82b). The simulated deposit feeders biomass ranged between 1 and 3.5 g C m⁻², which is comparable to the range between 1 and 5 g C m⁻² reported in Le Pape *et al.* (1999). The microphytobenthos biomass (Figure 82b) varied during the year between 0.1 and 1.8 g C m⁻², with a maximum in summer and a minimum in winter, which is comparable with ranges between 0.5 and 2 g C m⁻² from Blackford (2002). In addition to the results about pelagic biogeochemistry, the feedback of phytoplankton grazing on the light extinction coefficient was observed in the model results (Figure 82c). The light extinction coefficient in S2 was 12% lower (average annual value) than this in S1. The light extinction coefficient in S3 was 17% lower (average annual value) than this in S1. The introduction of benthic grazing on phytoplankton determined a reduction of the light extinction coefficient in the S1-S2 scenario comparison. In overall, the concentration of oxygen at the sediment-water interface does not change significantly in the three scenarios. The concentration of oxygen in the water (Figure 82d) decreases slightly from S2 to S3, as a result of more respiration in the system due to the presence of benthic filter feeders and deposit feeders.

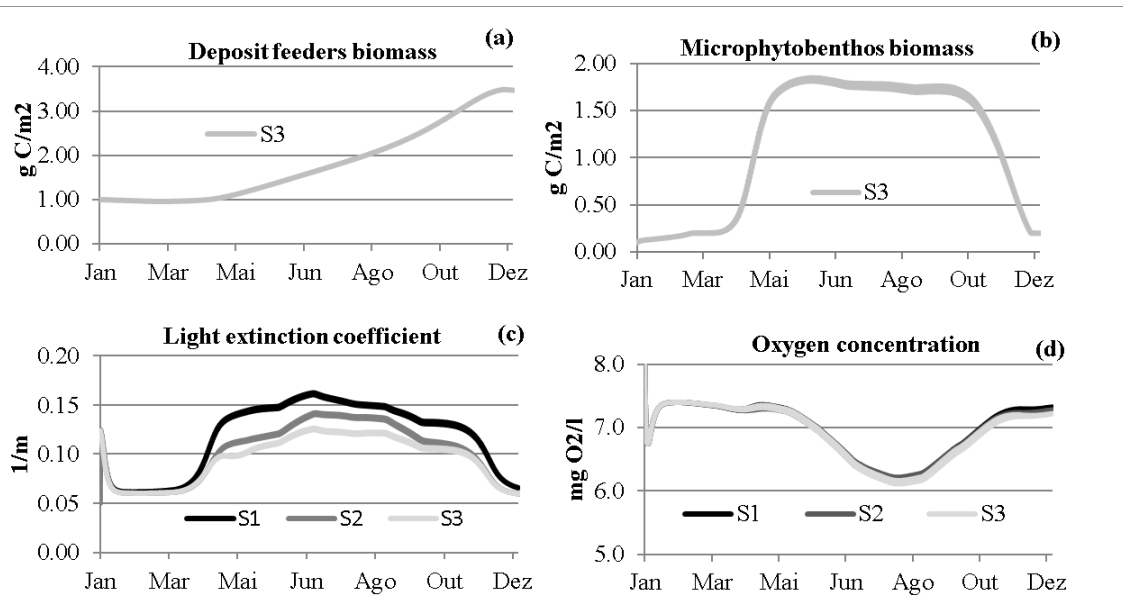


Figure 82 –Model results for the three scenarios S1, S2, and S3.

Simulated densities of filter feeders (Figure 81d) were comparable to literature values from Le Pape *et al.* (1999). However, results published in Le Pape *et al.* (1999), show a decline of the filter feeders biomass in fall, probably due to grazing by consumers in the upper levels of the food web. In the model, a compartment for carnivorous was not included, thus no decline of filter feeders during fall was observed. Simulated densities of filter feeders, ranging between 1 and 15 $g\ C\ m^{-2}$, are comparable to literature values between 1 and 8 $g\ C\ m^{-2}$ (Le Pape *et al.*, 1999), and between 5 and 20 $g\ C\ m^{-2}$ (Schöl *et al.*, 2002; Descy *et al.*, 2003).

In overall, the simulated phytoplankton and microphytobenthos biomasses were comparable between them. When integrated along the depth, the maximum biomass of phytoplankton was about 4 $g\ C\ m^{-2}$, and the maximum microphytobenthos biomass was about 1.8 $g\ C\ m^{-2}$. Results showed a qualitative agreement with literature reported ranges for filter feeders, deposit feeders, and microphytobenthos biomass. However, future developments of the model may include filter feeder decay due to grazing by upper trophic levels.

The presence of filter feeders in the system determined negative feedback on phytoplankton, and improvement of water transparency (by decreasing the light extinction coefficient). The model was capable to reproduce a mechanism for the

removal of suspended particulate material from the water column. The analysis of results also showed that the presence of organisms lead to more oxygen depletion from the water. Nutrients at the sediment-water interface are available to phytoplankton as well as to microalgae, identified in the model as microphytobenthos. The uptake of nutrients by microphytobenthos can be controlled by grazers. As an example, the decline of microphytobenthos in fall was due to grazing by deposit feeders. These results were consistent with previous studies from Blackford (2002) who simulated a benthic ecosystem of the Northern Adriatic Sea, including deposit feeders grazing on microphytobenthos. In this research, the presence of microphytobenthos triggered a competition for nutrients with pelagic primary producers at the sediment-water interface. This type of competition is important because it may have feedbacks on light extinction coefficients. The consequent feedback on light extinction was found to be a key factor in the control of harmful algal blooms (MacIntyre *et al.*, 2004).

This hypothesis was not investigated in this study. However, the model simulates the light extinction due to phytoplankton, thus it is ready to enable this type of analysis. The scenario with filter feeders does not include seagrasses and macroalgae. If they were included, it is expected to have an increase of nutrients due to the presence of more species (more respiration). These nutrients could be consumed by macroalgae and seagrasses. Since macroalgae have higher growth rate, they may outcompete seagrasses in areas where nutrient concentrations are higher.

Results showed a qualitative agreement with literature reported ranges of data for filter feeders, deposit feeders, and microphytobenthos biomass. However, future developments of the benthic ecology model may include filter feeders decay due to grazing by upper trophic levels. In this research, MOHID proved to be flexible in the incorporation of new properties of the ecosystem. Future developments may include experimental scenarios to calibrate uncertain parameters, real case studies, and validation of model results.

Chapter 7 - Conclusion

7.1. Conclusion

Estuarine and coastal waters are highly productive habitats, where the coupling between pelagic and benthic systems plays an important role on ecosystem dynamics. Producers, consumers, and decomposers in the ecosystem are affected by abiotic and biotic factors, including temperature, light availability, water turbidity, depth, nutrient inputs, water residence time, and grazing, among others (Fox *et al.*, 2010). There is still a lack of knowledge on the complex interactions between fauna, microflora, and sediment (Murphy *et al.*, 2008). Mathematical models, which integrate hydrodynamics, sediment transport and water quality processes, are useful tools to formulate hypotheses about ecosystem dynamics, and to simulate different scenarios. With this research, a modeling approach was set to investigate the relationships between benthic and pelagic components of the marine ecosystem, including seagrasses, benthic feeders, and microphytobenthos.

The seagrass model was applied to answer questions about the competition between macroalgae and seagrasses in Ria de Aveiro, Portugal. The results of the model show that *Zostera noltii* is not significantly limited by light in Ria de Aveiro, because of the shallowness of the lagoon. *Zostera noltii* is an intertidal species adapted to live under tidal regimes. The presence of macroalgae in the model does not affect significantly light availability for seagrasses. Two mechanisms contributed to nitrogen quota increase in seagrasses in presence of macroalgae: the first one is the reduction of the biomass of the plant in terms of dry weight and; the second one is the increase of external nutrients (ammonia) in the system in presence of macroalgae. In overall the main factor that is limiting the growth of seagrasses in presence of macroalgae in the model is the competition for space.

Seagrasses are part of the benthic system and are different from other primary producers in the water column, because they are not transported by advection-diffusion processes and their biology is connected to processes in water and sediment. Seagrasses stabilize the sediment, retain nutrients, and create habitat for many species. The importance of these plants as ecosystem engineers and sink of carbon deserves investigation through combination of monitoring and modeling studies. The formulation

used in the model enabled to simulate the response of the ecosystem to environmental changes, accounting for physical and biological factors at the same time. The seagrass model outputs can be easily analyzed in the form of time series and maps, enabling easy calibration (Trancoso *et al.*, 2005).

The space limiting function is a coarse representation of the process of competition for space between macroalgae and seagrasses. MOHID accounts for the effect of floating macroalgae on light extinction over the water column, and thus on the top of seagrass beds. The space limiting function was written under the hypothesis that macroalgae and seagrasses occupy the same physical space for rooting, and when this space is occupied by macroalgae, there is no space for seagrasses to establish roots. The conclusion of the study shows that seagrasses are limited by space and not by light availability in presence of macroalgae. This is not always true because light limitation due to floating macroalgae seem to be more important than space limitation (Marques J., pers.comm.). This means that the model formulation should be further investigated to improve the description of how space and light limit seagrasses in presence of macroalgae.

This study included the development and testing of a benthic ecology model including benthic filter feeders, deposit feeders, and microphytobenthos. Grazing by filter feeders on phytoplankton and particulate organic matter in the water were included in the model. The complexity of the links between the benthic and pelagic system were addressed by carrying out ecosystem simulations. Analysis of the scenarios enabled the detection and quantification of feedbacks between benthic and pelagic systems, with a focus on processes related to filter feeders and primary producers. Feedback mechanisms on light extinction in the water were observed in the model, as a consequence of filter feeders grazing on phytoplankton and particulate organic matter in the water.

The hypothesis of (MacIntyre *et al.*, 2004) was not investigated in this study. However, the model simulates the light extinction due to phytoplankton, thus it is ready to enable this type of analysis. The scenario with filter feeders does not include seagrasses and macroalgae. If they were included, it is expected to have an increase of nutrients due to the presence of more species (more respiration). These nutrients could be consumed by macroalgae and seagrasses. Since macroalgae have higher growth rate, they may outcompete seagrasses in areas where nutrient concentrations are higher.

The model is valuable for studying interactions between compartments inside the benthic system, and for investigating feedbacks between the benthic system and water column biogeochemistry. The coupling of the benthic model in MOHID may be used to support studies about management of eutrophication.

This model presented in this study represents advancement to the present development of MOHID water modelling system, which included only deposition and mineralization of organic matter.

The inclusion of the seagrass model in MOHID opened new possibilities to study interactions between primary producers (phytoplankton, macroalgae, and seagrasses) in response to natural and anthropogenic factors (nutrient inputs variations, temperature variations due to climate change, storms occurrence, among others). The flexibility of the model and its open source format enables to include new characteristics. For example, in the future the model may become more complex by adding a feedback effect by seagrasses over suspended sediment (seagrasses are capable to retain sediment), or over the bottom drag coefficient (seagrasses may alter the bed rugosity).

Recent developments in seagrass modelling are concerned with functional and structural plant modelling including apex and internode development for different plant species (Renton *et al.*, 2011). The calibration and validation of these models require a large amount of data for a period of at least two years, including total length of rhizome, the number of rhizome internodes, the total number of shoots and the length of the longest axis. On the other side, benthic food webs based on functional approach are still largely used (Heath, 2012; Morris *et al.*, 2014). Recent research focused on complex benthic food web models including age classes (Bendtsen and Hansen, 2013) and transport of benthic larvae (Savina and Ménesguen, 2008). The model proposed in this study does not include structural development and age classes, but it can be used to simulate and predict the average distribution of benthic organisms in the study area. With data availability, the model can be further developed and expanded to include structural development in different species. The present knowledge of the model shows that data availability is a threat to model development. Parameterization of processes was based mainly on data collected from literature sources. If the model was developed today, the first step should be a monitoring study to collect data for model parameterization, calibration, and validation. With data availability, it would be possible to think about a more complex model with age classes for benthic organisms and

structural plants development. The sensitivity analysis pointed out parameters with highest impact on model results. These parameters are the main source of model uncertainty, and should be further investigated for future model improvement.

Bibliography

- Anderson, M. P. and Woessner, W. W. (1992). Applied groundwater modeling: simulation of flow and advective transport. San Diego, CA, Academic Press. pp. 381.
- Ascione Kenov, I., Deus, R., Alves, C. N. and Neves, R. (2013). Modelling Seagrass Biomass and Relative Nutrient Content. Journal of Coastal Research.
- Aveytua-Alcazar, L., Camacho-Ibar, V. F., Souza, A. J., Allen, J. I. and Torres, R. (2008). Modelling *Zostera marina* and *Ulva* spp. in a coastal lagoon. Ecological Modelling **218**: 354-366.
- Baretta-Bekker, J. G. and Baretta, J. W. (1997). European Regional Seas Ecosystem Model (ERSEM) II. Journal of Sea Research **38**(3-4): 169-436.
- Baretta, J. W., Ebenhöh, W. and Ruardij, P. (1995). The European regional seas ecosystem model (ERSEM), a complex marine ecosystem model. Netherlands Journal of Sea Research **33**(3/4): 233-246.
- Barranguet, C. (1997). The Role of Microphytobenthic Primary Production in a Mediterranean Mussel Culture Area. Estuarine, Coastal and Shelf Science **44**(6): 753-765.
- Bendtsen, J. and Hansen, J. L. S. (2013). A model of life cycle, connectivity and population stability of benthic macro-invertebrates in the North Sea/Baltic Sea transition zone. Ecological Modelling **267**(0): 54-65.
- Biber, P. D., Harwell, M. A. and Cropper Jr, W. P. (2004). Modeling the dynamics of three functional groups of macroalgae in tropical seagrass habitats. Ecological Modelling **175**(1): 25-54.
- Blackford, J. C. (2002). The Influence of Microphytobenthos on the Northern Adriatic Ecosystem: Study. Estuarine, Coastal and Shelf Science **55**: 109-123.
- Bocci, M., Coffaro, G. and Bendoricchio, G. (1997). Modelling biomass and nutrient dynamics in eelgrass (*Zostera marina* L.): application to the lagoon of Venice (Italy) and Oresund (Denmark). Ecological Modelling **102**: 67-80.
- Brandt, A., Sarabun, C. C., Seliger, H. H. and Tyler, M. A. (1986). The Effects of the Broad Spectrum of Physical Activity on the Biological Processes in the Chesapeake Bay. In: Nihoul, J. C. J., (ed.) Elsevier Oceanography Series, Elsevier. **42**: 361-384.

- Bulleri, F. and Chapman, M. G. (2010). The introduction of coastal infrastructure as a driver of change in marine environments. *Journal of Applied Ecology* **47**: 26-35.
- Bulthuis, D. A. (1987). Effect of temperature on photosynthesis and growth of seagrass. *Aquatic Botany* **27**: 27-40.
- Burke, M. (2004). Seagrass under threat. *Environmental Science and Technology* **38**(2): 32A-32.
- Campbell, J. E., Yarbrow, L. A. and Fourqurean, J. W. (2012). Negative relationships between the nutrient and carbohydrate content of the seagrass *Thalassia testudinum*. *Aquatic Botany* **99**: 56-60.
- Cancino, L. and Neves, R. (1998). Hydrodynamic and sediment suspension modelling in estuarine systems. Part I: description of the numerical models. *Journal of Marine Systems* **22**: 105-116.
- Carmichael, R. H., Shriver, A. C. and Valiela, I. (2004). Changes in shell and soft tissue growth, tissue composition, and survival of quahogs, *Mercenaria mercenaria*, and softshell clams, *Mya arenaria*, in response to eutrophic-driven changes in food supply and habitat. *Journal of Experimental Marine Biology and Ecology* **313**(1): 75-104.
- Cazelles, K., Otten, W., Baveye, P. C. and Falconer, R. E. (2013). Soil fungal dynamics: Parameterisation and sensitivity analysis of modelled physiological processes, soil architecture and carbon distribution. *Ecological Modelling* **248**: 165-173.
- Cerco, C. F., Kim, S.-C. and Noel, M. R. (2013). Management modeling of suspended solids in the Chesapeake Bay, USA. *Estuarine, Coastal and Shelf Science* **116**(0): 87-98.
- Chardy, P. and Dauvin, J. C. (1992). Carbon flows in a subtidal fine sand community from the Western English-Channel - a simulation analysis. *Marine Ecology Progress Series* **81**: 147-161.
- Cloern, J. E. (1982). Does the benthos control phytoplankton biomass in South San Francisco Bay? *Marine Ecology Progress Series* **9**: 191-202.
- Coelho, H. S., Neves, R., Leitão, P. C., Martins, H. and Santos, A. (1999). The slope current along the Western European Margin: a numerical investigation. *Oceanography of the Iberian Continental Margin. Boletim del Instituto Espanol de Oceanografia* **15**: 61-72.
- Cognetti, G., Sarà, M. and Magazzù, G. (1999). *Biologia Marina*. Bologna, Calderini.

- Constanza, R., D'Arge, R., De Groot, R., Farber, S., Grasso, M., Hannon, B., Linburg, K., Naeem, S., O'Neill, R. V., Paruelo, J., Raskin, R. G., Sutton, P. and Van Den Belt, M. (1997). The value of the world's ecosystem services and natural capital. *Nature* **387**: 253-260.
- Cousins, S. H. (1985). The trophic continuum in marine ecosystems: structure and equations for a predictive model. In: Ulanovicz, R. E. and Platt, T., (eds.) *Ecosystem theory for biological oceanography*, Canadian Bulletin of Fisheries and Aquatic Sciences. **213**: 76-93.
- Cunha, A. H., Assis, J. F. and Serrão, E. A. (2013). Seagrasses in Portugal: A most endangered marine habitat. *Aquatic Botany* **104**: 193-203.
- Dennison, W. (1979) Light adaptations of plants: a model based on the seagrass *Zostera marina* L. **M.Sc. Thesis**, University of Alaska.
- Descy, J. P., Everbecq, E., Gosselain, V., Viroux, L. and Smithz, S. (2003). Modelling the impact of benthic filter-feeders on the composition and biomass of river plankton. *Freshwater Biology* **48**: 404-417.
- Deus, R., Brito, D., Ascione, K. I., Lima, M., Costa, V., Medeiros, A., Neves, R. and Alves, C. N. (2013). Three-dimensional model for analysis of spatial and temporal patterns of phytoplankton in Tucuruí reservoir, Pará, Brazil. *Ecological Modelling* **253**: 28-43.
- Dias, J. M. and Lopes, J. F. (2006). Implementation and assessment of hydrodynamic, salt, and heat transport models: the case of Ria de Aveiro Lagoon (Portugal). *Environmental Modelling and Software* **21**: 1-15.
- Dias, J. M., Lopes, J. F. and Dekeyser, I. (2000). Tidal propagation in Ria de Aveiro Lagoon, Portugal. *Physics and Chemistry of the Earth (B)* **25**(4): 369-374.
- Ditmars, J. D. (1988). Performance Evaluation of Surface Water Transport and Dispersion Models. *Journal of Hydraulic Engineering* **113**(EE8): 961-971.
- Dodson, S. I. (2005). *Introduction to Limnology*. McGraw Hill.
- Drew, E. A. (1979). Physiological aspects of primary production in seagrasses. *Aquatic Botany* **7**: 139-150.
- Duarte, C. M. (1990). Seagrass nutrient content. *Marine Ecology Progress Series* **67**: 201-207.

- Duarte, C. M., Merino, M., Agawin, S. R. N., Uri, J., Fortes, D. M., Gallegos, E. M. and Marbà, N. (1998). Root production and belowground seagrass biomass. *Marine Ecology Progress Series* **171**: 97-108.
- Duplisea, D. (1998). Feedbacks Between carbon mineralisation and community structure: a simulation-model analysis. *Ecological Modelling* **110**: 19-43.
- Elkalay, K., Frangoulis, C., Skliris, N., Goffart, A., Gobert, S., Lepoint, G. and Hecq, J. H. (2003). A model of the seasonal dynamics of biomass and production of the seagrass *Posidonia oceanica* in the Bay of Calvi (Northwestern Mediterranean). *Ecological Modelling* **167**: 1-18.
- Evans, G. T. and Parslow, J. S. (1985). A model of annual plankton cycles. *Biological Oceanography* **3**: 327-347.
- Falls, J. A. (2008) The Survival Benefit of Benthic Macroalgae *Gracilaria vermiculophylla* as an Alternative Nursery Habitat for Juvenile Blue Crabs. **M.Sc. Thesis**, College of William and Mary in Virginia, Virginia Institute of Marine Science.
- Fasham, J. C. (1990). A nitrogen-based model for plankton dynamics in the ocean mixed Layer. *Journal of marine research* **48**: 591-639.
- Fernandes, L., Saraiva, S., Leitão, P. C., Pina, P., Santos, A., Braunschweig, F. and Neves, R. (2006). Mabene Deliverable D4.3d-Code and description of the benthic biogeochemistry module-Managing benthic ecosystems in relation to physical forcing and environmental constraints. MaBenE-Managing Benthic Ecosystems in relation to physical forcing and environmental constraints. <http://www.nioo.knaw.nl/projects/mabene/>, Accessed Nov 2012.
- Ferreira, J. G., Simas, T., Nobre, A., Silva, M. C., Schifferegger, K. and Lencart-Silva, J. (2003). Identification of Sensitive Areas and Vulnerable Zones In Transitional and Coastal Portuguese Systems. INAG/IMAR.
- Filgueira, R., Grant, J., Bacher, C. and Carreau, M. (2012). A physical–biogeochemical coupling scheme for modeling marine coastal ecosystems. *Ecological Informatics* **7**(1): 71-80.
- Filgueira, R., Guyondet, T., Comeau, L. A. and Grant, J. (2014). A fully-spatial ecosystem-DEB model of oyster (*Crassostrea virginica*) carrying capacity in the Richibucto Estuary, Eastern Canada. *Journal of Marine Systems* **136**(0): 42-54.
- Fonseca, M. S. and Cahalan, J. A. (1992). A preliminary evaluation of wave attenuation by four species of seagrass. *Estuarine, Coastal and Shelf Science* **35**: 565-576.

- Fonseca, M. S. and Thayer, G. W. (1990). Root/shoot ratios. In: Phillips, R. C. and McRoy, C. P., (eds.) *Seagrass research methods. Monographs on oceanographic methodology* 9, Paris, UNESCO: 65-67.
- Forsythe, W. C., Rykiel Jr., E. J., Stahl, R. S., Wu, H. and Schoolfield, R. M. (1995). A model comparison for daylength as a function of latitude and day of year. *Ecological Modelling* **80**: 87-95.
- Fox, S. E., Olsen, Y. S. and Spivak, A. C. (2010). Effects of bottom-up and top-down controls and climate change on estuarine macrophyte communities and the ecosystem services they provide. In: Kemp, P. F., (ed.) *Eco-DAS VIII Symposium Proceedings*, Waco, TX, American Society of Limnology and Oceanography, Inc.: 129-145.
- Fréchette, M. and Lefaivre, D. (1990). Discriminating between food and space limitation in benthic suspension feeders using self-thinning relationships. *Marine Ecology Progress Series* **65**: 15-23.
- Green, E. P. and Short, F. T. (2008). *World Atlas of Seagrasses*. Berkeley, USA, University of California Press.
- Greve, T. and Binzer, T. (2004). Which factors regulate seagrass growth and distribution? In: Borum, J., Duarte, C. M., Krause-Jensen, D. and Greve, T. M., (eds.) *European seagrasses: an introduction to monitoring and management*: 19-23.
- Heath, M. R. (2012). Ecosystem limits to food web fluxes and fisheries yields in the North Sea simulated with an end-to-end food web model. *Progress in Oceanography* **102**(0): 42-66.
- Hipsey, M. R., Romero, J. R. R., Antenucci, J. P. and Hamilton, D. P. (2003). *Computational Aquatic Ecosystem Dynamic Model: CAEDYM v2 User Manual*. Center for Water Research, U. W. A.
- Hofman, E. E. and Lascara, C. M. (1998). Overview of Interdisciplinary Modeling for Marine Ecosystems. In: Brink, K. H. and Robinson, A. R., (eds.) *The Sea* volume, John Wiley Sons Inc. **10**: 507-540.
- IST (2006). *Water Quality Manual Version 1.0*. Instituto Superior Técnico, Technical University of Lisbon. Lisbon, Portugal. <http://maretec.mohid.com/PublicData/products/Manuals/>, Accessed Nov 2012.
- Jørgensen, C. B. (1990). *Bivalve filter feeding: Hydrodynamics, Bioenergetics, Physiology and Ecology*. Fredensborg, Denmark, Olsen & Olsen.

- Kantha, L. H. and Clayson, C. A. (2000). Numerical models of oceans and oceanic processes. International Geophysics Series, vol. 66, San Diego, CA, Academic Press. pp. 940.
- Kellogg, M. L., Cornwell, J. C., Owens, M. S. and Paynter, K. T. (2013). Denitrification and nutrient assimilation on a restored oyster reef. Marine Ecology Progress Series **480**: 1-19.
- Koch, E., Ackerman, J. D., Verduin, J. and Keulen, M. (2006). Fluid Dynamics in Seagrass Ecology from Molecules to Ecosystems. In: Larkum, A. W. D., Orth, R. J. and Duarte, C. M., (eds.) Seagrasses: Biology, Ecology and Conservation, The Netherlands, Springer: 193-225.
- Komatsu, T., Igarashi, C., Tatsukawa, K., Sultana, S., Matsuoka, Y. and Harada, S. (2003). Use of multi-beam sonar to map seagrass beds in Otsuchi Bay on the Sanriku Coast of Japan. Aquatic Living Resources **16**(3): 223-230.
- Körtzinger, A., Koeve, W., Kähler, P. and Mintrop, L. (2001). C:N ratios in the mixed layer during the productive season in the Northeast Atlantic Ocean. Deep Sea Research Part I **48**: 661-688.
- Le Pape, O., Jean, F. and Ménesguen, A. (1999). Pelagic and benthic trophic chain coupling in a semi-enclosed coastal system, the Bay of Brest (France): a modelling approach. Marine Ecology Progress Series **189**: 135-147.
- Levinton, J. S. (1989). Deposit feeding and Coastal Oceanography. In: Lopez, G., Taghon, G. and Levinton, J., (eds.) Ecology of Marine Deposit Feeders, New York, Springer-Verlag: 1-24.
- Lotka, A. J. (1925). Elements of physical biology. Baltimore, Williams and Wilkins Company.
- Lumborg, U., Andersen, T. J. and Pejrup, M. (2006). The effect of *Hydrobia ulvae* and microphytobenthos on cohesive sediment dynamics on an intertidal mudflat described by means of numerical modelling. Estuarine, Coastal and Shelf Science **68**(1-2): 208-220.
- MacIntyre, H. L., Lomas, M. W., Cornwell, J., Suggett, D. J., Gobler, C. J., Koch, E. W. and Kana, T. M. (2004). Mediation of benthic-pelagic coupling by microphytobenthos: an energy-and material-based model for initiation of blooms of *Aureococcus anophagefferens*. Harmful Algae **3**: 403-437.
- Macreadie, P. I., Baird, M. E., Trevathan-Tackett, S. M., Larkum, A. W. D. and Ralph, P. J. (2013). Quantifying and modelling the carbon sequestration capacity of seagrass meadows – A critical assessment. Marine Pollution Bulletin.

- Malmstrom, C. (2012). Ecologists Study the Interactions of Organisms and Their Environment. *Nature Education Knowledge* **3**(10): 88.
- Mann, K. H. (1988). Towards predictive models for coastal marine ecosystems. In: Pomeroy, L. R. and Alberts, J. J., (eds.) *Concepts of Ecosystem Ecology*, New York, Springer-Verlag: 291-316.
- Mann, K. H. and Lazier, J. R. N. (1996). *Dynamics of marine ecosystems*. London, Blackwell Science.
- Marino, S., Hogue, I. B., Ray, C. J. and Kirschner, D. E. (2008). A methodology for performing global uncertainty and sensitivity analysis in systems biology. *Journal of Theoretical Biology* **254**(1): 178-196.
- Marsh, J. A., Dennison, W. and Alberte, R. S. (1986). Effects of temperature on photosynthesis and respiration in eelgrass (*Zostera marina* L.). *Journal of Experimental Marine Biology and Ecology* **101**: 257-267.
- Martins, F., Leitão, P. C., Silva, A. and Neves, R. (2001). 3D modelling in the Sado estuary using a new generic vertical discretization approach. *Oceanologica Acta* **24**(Supplement 1): 551-562.
- Massa, S. I., Arnaud-Haond, S., Pearson, G. A. and Serrão, E. A. (2009). Temperature tolerance and survival of intertidal populations of the seagrass *Zostera noltii* (Hornemann) in Southern Europe (Ria Formosa, Portugal). *Hydrobiologia* **619**(1): 195-201.
- Mateo, M. A., Cebrián, J., Dunton, K. and Mutchler, T. (2006). Carbon flux in seagrass ecosystems. In: Larkum, A. W. D., Orth, R. J. and Duarte, C. M., (eds.) *Seagrasses: Biology, Ecology and Conservation*, The Netherlands, Springer: 159-192.
- Mateus, M. (2006) A process-oriented biogeochemical model for marine ecosystems: development, numerical study, and application. **Ph.D. Thesis**, Instituto Superior Técnico, Lisbon, Portugal.
- McKay, M. D., Beckman, R. J. and Conover, W. J. (2000). A Comparison of Three Methods for Selecting Values of Input Variables in the Analysis of Output from a Computer Code. *Technometrics* **42**(1): 55-61.
- McKenzie, L. J. (1994). Seasonal changes in biomass and shoot characteristics of a *Zostera capricorni* Aschers. Dominant meadow in Cairns Harbour, northern Queensland. *Australian Journal of Marine and Freshwater Research* **45**: 1337-1352.

- McRoy, C. P. and Barsdate, R. J. (1970). Phosphate absorption in eelgrass. *Limnology and Oceanography* **15**: 6-13.
- Ménesguen, A. (1991). "ELISE", an interactive software for modelling complex ecosystems. In: Arcilla, A. S., Pastor, M., Zienkiewicz, O. C. and Schrester, B. A., (eds.) *Computer modelling in Ocean Engineering*, Rotterdam, Balkema: 87-94.
- Meyers, M. B., Di Toro, D. M. and Lowe, S. A. (2000). Coupling Suspension Feeders to the Chesapeake Bay Eutrophication Model. *Water Quality and Ecosystem Modeling* **1**: 123-140.
- Miranda, R., Braunschweig, F., Leitão, P., Martins, F. and Santos, A. (2000). MOHID2000 - a coastal integrated object oriented model. *Hydraulic Engineering Software VIII*, WIT Press.
- Moll, A. (2000). Assessment of three-dimensional physical-biological ECOHAM1 simulations by quantified validation for the North Sea with ICES and ERSEM data. *ICES Journal of Marine Science* **57**(4): 1060-1068.
- Moll, A. and Radach, G. (2003). Review of three-dimensional ecological modelling related to the North Sea shelf system-Part 1: models and their results. *Progress in Oceanography* **57**(2): 175-217.
- Morris, D. J., Speirs, D. C., Cameron, A. I. and Heath, M. R. (2014). Global sensitivity analysis of an end-to-end marine ecosystem model of the North Sea: Factors affecting the biomass of fish and benthos. *Ecological Modelling* **273**(0): 251-263.
- Murphy, R. J., Tolhurst, T. and Chapman, M. A. (2008). Underwood Spatial variation of chlorophyll on estuarine mudflats determined by field-based remote sensing. *Marine Ecology Progress Series* **365**: 45-55.
- Nakaoka, M., Kouchi, N. and Aioi, K. (2003). Seasonal dynamics of *Zostera caulescens*: relative importance of flowering shoots to net production. *Aquatic Botany* **77**(4): 277-293.
- Newell, C. R., Short, F., Hoven, H., Healey, L., Panchang, V. and Cheng, G. (2010). The dispersal dynamics of juvenile plantigrade mussels (*Mytilus edulis* L.) from eelgrass (*Zostera marina*) meadows in Maine, U.S.A. *Journal of Experimental Marine Biology and Ecology* **394**(1-2): 45-52.
- Newell, R. I. E. and Koch, E. W. (2004). Modeling seagrass density and distribution in response to changes in turbidity stemming from bivalve filtration and seagrass sediment stabilization. *Estuaries* **27**(5): 793-806.

- Nisbet, R. M., McCauley, E. and Johnson, L. R. (2010). Dynamic energy budget theory and population ecology: lessons from *Daphnia*. *Philosophical Transactions of the Royal Society B: Biological Sciences* **365**(1557): 3541-3552.
- Nobre, A. M., Ferreira, J. G., Nunes, J. P., Yan, X., Bricker, S., Corner, R., Groom, S., Gu, H., Hawkins, A. J. S., Hutson, R., Lan, D., Lencart e Silva, J. D., Pascoe, P., Telfer, T., Zhang, X. and Zhu, M. (2010). Assessment of coastal management options by means of multilayered ecosystem models. *Estuarine, Coastal and Shelf Science* **87**(1): 43-62.
- Nunes, M., Coelho, J. P., Cardoso, P. G., Pereira, M. E., Duarte, A. C. and Pardal, M. A. (2008). The macrobenthic community along a mercury contamination in a temperate estuarine system (Ria de Aveiro, Portugal). *Science of The Total Environment* **405**(1-3): 186-194.
- Odum, H. T. (1971). *Environment, Power, and Society*. New York, NY, Wiley-Interscience.
- Officer, C. B., Smayda, T. J. and Mann, R. (1982). Benthic Filter Feeding: A Natural Eutrophication Control. *Marine Ecology Progress Series* **9**: 203-210.
- Olesen, B. and Sand-Jensen, K. (1993). Seasonal acclimatation of eelgrass *Zostera marina* growth to light. *Marine Ecology Progress Series* **94**: 91-99.
- Pace, M. L., Glasser, J. E. and Pomeroy, L. R. (1984). A simulation analysis of continental shelf foodwebs. *Marine Biology* **82**: 47-63.
- Passarge, J., Hol, S., Escher, M. and Huisman, J. (2006). Competition for nutrients and light: stable coexistence, alternative stable states, or competitive exclusion? *Ecological Monographs* **76**: 57-72.
- Paul, M., Lefebvre, A., Manca, E. and Amos, C. L. (2011). An acoustic method for the remote measurement of seagrass metrics. *Estuarine, Coastal and Shelf Science* **93**(1): 68-79.
- Pearson, T. and Rosenberg, R. (1978). Macrobenthic succession in relation to organic enrichment and pollution of the marine environment. *Oceanography and Marine Biology-An Annual Review* **16**: 229-311.
- Pérez-Lloréns, J. L. and Niell, F. X. (1993). Seasonal dynamics of biomass and nutrient content in the intertidal seagrass *Zostera noltii* Hornem from Palmones River estuary, Spain. *Aquatic Botany* **46**: 49-66.

- Phillips, R. C. and Meñez, E. G. (1988). Seagrasses. Smithsonian Contributions to the Marine Sciences **34**.
- Pina, P. (2001) An integrated approach to study the Tagus estuary water quality. **M.Sc. Thesis**, Instituto Superior Técnico, Lisbon, Portugal.
- Platt, T. (1985). The structure of marine ecosystems: its allometric basis. In: Ulanovicz, R. E. and Platt, T., (eds.) Ecosystem theory for biological oceanography, Canadian Bulletin of Fisheries and Aquatic Sciences. **213**: 55-64.
- Plus, M., Chapelle, A., Menesguen, A., Deslous-Paoli, J. M. and Auby, I. (2003). Modelling seasonal dynamics of biomasses and nitrogen contents in a seagrass meadow (*Zostera noltii* Hornem.): application to the Thau lagoon French Mediterranean coast Ecological Modelling **161**(3): 213-238.
- Plus, M., Deslous-Paoli, J. M., Auby, I. and Dagault, F. (2001). Factors influencing primary production of seagrass beds (*Zostera noltii* Hornem.) in the Thau lagoon (French Mediterranean coast). Journal of experimental marine biology and ecology **259**(1): 63-84.
- Pomeroy, L. R., Hargrove, E. C. and Alberts, J. J. (1988). The ecosystem perspective. In: Pomeroy, L. R. and Alberts, J. J., (eds.) Concepts of Ecosystem Ecology, Springer-Verlag: 1-17.
- Prandle, D., Jago, C. F., Jones, S. E., Purdie, D. A. and Tappin, A. (1993). The influence of horizontal circulation in the supply and distribution of tracers. Philosophical Transactions of the Royal Society of London **343**(1669): 405-422.
- Pritchard, D. W. (1967). What is an estuary: physical viewpoint. In: Lauff, G. H., (ed.) Estuaries, Washington D.C, American Association for the Advancement of Science: 52-63.
- Quillet, A., Frohling, S., Garneau, M., Talbot, J. and Peng, C. (2013). Assessing the role of parameter interactions in the sensitivity analysis of a model of peatland dynamics. Ecological Modelling **248**: 30-40.
- Redfield, A. C. (1958). The biological control of chemical factors in the environment. American Scientist **46**: 205-221.
- Renton, M., Airey, M., Cambridge, M. L. and Kendrick, G. A. (2011). Modelling seagrass growth and development to evaluate transplanting strategies for restoration. Ann Bot **108**(6): 1213-1223.
- Riley, G. A. (1946). Factors controlling phytoplankton populations on georges bank. Journal of Marine Research, **6**(1): 54-73.

- Romero, J., Lee, K. S., Pérez, M., Mateo, M. A. and Alcoverro, T. (2006). Nutrients Dynamics in Seagrass Ecosystems. In: Larkum, A. W. D., Orth, R. J. and Duarte, C. M., (eds.) *Seagrasses: Biology, Ecology and Conservation*, The Netherlands, Springer: 227-254.
- Saltelli, A. (2002). Making best use of model evaluations to compute sensitivity indices. *Computer Physics Communications* **145**(2): 280-297.
- Saltelli, A. and Marivoet, J. (1990). Nonparametric statistics in sensitivity analysis for model output-a comparison of selected techniques. *Reliability Engineering & System Safety* **28**(2): 229-253.
- Saltelli, A., Tarantola, S., Campolongo, F. and Ratto, M. (2004). *Sensitivity Analysis in Practice: A Guide to Assessing Scientific Models*. West Sussex, John Wiley & Sons Ltd.
- Sambrotto, R. N., Savidge, G., Robinson, C., Boyd, P., Takahash, T., Karl, D. M., Langdon, C., Chipman, D., Marra, J. and Codispoti, L. (1993). Elevated consumption of carbon relative to nitrogen in the surface ocean. *Nature* **363**: 248-250.
- Saraiva, S., van der Meer, J., Kooijman, S. A. L. M. and Ruardij, P. (2014). Bivalves: From individual to population modelling. *Journal of Sea Research*(0): In press.
- Savina, M. and Ménesguen, A. (2008). A deterministic population dynamics model to study the distribution of a benthic bivalve with planktonic larvae (*Paphia rhomboïdes*) in the English Channel (NW Europe). *Journal of Marine Systems* **70**(1–2): 63-76.
- Schöl, A., Kirchesch, V., Bergfeld, T., Schöll, F., Borchering, J. and Müller, D. (2002). Modelling the Chlorophyll a Content of the River Rhine –Interrelation between Riverine Algal Production and Population Biomass of Grazers, Rotifers and the Zebra Mussel, *Dreissena polymorpha*. *International Review of Hydrobiology* **87**: 295-317.
- Short, F. T., Carruthers, T. J. B., Dennison, W. C. and Waycott, M. (2007). Global seagrass distribution and diversity: a bioregional model. *Journal of Experimental Marine Biology and Ecology* **350**: 3-20.
- Silva, J. F., Duck, R. W. and Catarino, J. B. (2004). Seagrasses and sediment response to changing physical forcing in a coastal lagoon. *Hydrology and Earth System Sciences* **8**(151-159).

- Silva, J. F., Duck, R. W. and Catarino, J. B. (2009). Nutrient retention in the sediments and the submerged aquatic vegetation of the coastal lagoon of the Ria de Aveiro, Portugal. *Journal of Sea Research* **62**: 276-285.
- Simas, T., Nunes, J. P. and Ferreira, J. G. (2001). Effects of global climate change on coastal salt marshes. *Ecological Modelling* **139**: 1-15.
- Simas, T. C. and Ferreira, J. G. (2007). Nutrient enrichment and the role of salt marshes in the Tagus estuary (Portugal). *Estuarine, Coastal and Shelf Science* **75**(3): 393-407.
- Smaal, A. C., Schellekens, T., van Stralen, M. R. and Kromkamp, J. C. (2013). Decrease of the carrying capacity of the Oosterschelde estuary (SW Delta, NL) for bivalve filter feeders due to overgrazing? *Aquaculture* **404–405**(0): 28-34.
- Soetaert, K. (2010). *A Practical Guide to Ecological Modelling: Using R as a Simulation Platform*. Yerseke, Springer. pp. 372.
- Soetaert, K. and Herman, P. M. J. (2001). *Ecological Modelling Lecture Notes*. NIOO-CEME. The Netherlands.
- Sohma, A., Sekiguchi, Y., Kuwae, T. and Nakamura, Y. (2008). A benthic-pelagic coupled ecosystem model to estimate the hypoxic estuary including tidal flat-Model description and validation of seasonal/daily dynamics. *Ecological modelling* **215**: 10-39.
- Sousa, T., Domingos, T., Poggiale, J.-C. and Kooijman, S. A. L. M. (2010). Dynamic energy budget theory restores coherence in biology. *Philosophical Transactions of the Royal Society B: Biological Sciences* **365**(1557): 3413-3428.
- Steele, J. H. (1962). Environmental Control of Photosynthesis in the Sea. *Limnology and Oceanography* **7**: 137-150.
- Taboada, J. J., Prego, R., Ruiz-Villarreal, M., Montero, P., Gómez-Gesteira, M., Santos, A. P. and Pérez-Villar, V. (1998). Evaluation of the seasonal variations in the residual patterns in the Ria de Vigo (NW Spain) by means of a 3D baroclinic model. *Estuarine, Coastal and Shelf Science* **47**: 661-670.
- Tennant, G. (2006) Experimental effects of ammonium on eelgrass (*Zostera marina* L.) shoot density in Humboldt Bay, California. **M.Sc. Thesis**, Humboldt State University, California.
- Totterdell, I. J. (1993). An annotated bibliography of marine biological models. In: Evans, G. T. and Fasham, M. J. R., (eds.) *Towards a model of biogeochemical processes*, Berlin, Springer-Verlag: 317-339.

- Touchette, B. W. and Burkholder, J. M. (2000). Review of nitrogen and phosphorus metabolism in seagrasses. *Journal of Experimental Marine Biology and Ecology* **250**: 133-167.
- Trancoso, A. R. (2002) Modeling Macroalgae in Estuaries. **M.Sc. Thesis**, Instituto Superior Técnico, Lisbon, Portugal.
- Trancoso, A. R., Saraiva, S., Fernandes, L., Pina, P., Leitão, P. C. and Neves, R. (2005). Modelling macroalgae using a 3D hydrodynamic-ecological model in a shallow, temperate estuary. *Ecological Modelling* **187**: 232-246.
- USCE (2000). Development of a suspension feeding and deposit feeding benthos model for Chesapeake Bay. <http://www.chesapeakebay.net/content/publications>, Accessed Nov 2012.
- USGS (2007). Glossary. <http://water.usgs.gov/nawqa/glos.html>, Accessed Nov 2011.
- Van der Heide, T., van Nes, E. H., van Katwijk, M. M., Olf, H. and Smolders, A. J. P. (2011). Positive feedbacks in seagrass ecosystems-evidence from large-scale empirical data. *PLoS ONE* **6**(1): e16504.
- Vaz, N. and Dias, J. M. (2008). Hydrographic characterization of an estuarine tidal channel. *Journal of marine systems* **70**(1-2): 168-181.
- Vaz, N., Dias, J. M., Leitão, P. C. and Nolasco, R. (2007). Application of the MOHID-2D model to a mesotidal temperate coastal lagoon. *Computers & Geosciences* **33**: 1204-1209.
- Vaz, N., Dias, J. M. and Neves, R. (2009). Modelling Salinity and Residence Time Under Different Freshwater Inflow Scenarios: the Case of Ria de Aveiro. 11th International Conference on Environmental Science and Technology. Chania, Grécia.
- Verhagen, J. H. G. and Nienhuis, P. H. (1983). A simulation model of production, seasonal changes in biomass and distribution of eelgrass (*Zostera marina*) in lake Grevelingen. *Marine Ecology Progress Series* **10**: 187-195.
- Volterra, V. (1926). Variazioni e fluttuazioni del numero d'individui in specie animali conviventi. *Memorie della Reale Accademia Nazionale dei Lincei* **2**: 31-113.
- Yonge, C. M. (1949). *The Sea Shore*. The New Naturalist Series, London, William Collins Sons & Co. Ltd.

Zaldivar, J. M., Bacelar, F. S., Dueri, S., Marinov, D., Viaroli, P. and Hernández-García, E. (2009). Modeling approach to regime shifts of primary production in shallow coastal ecosystems. *Ecological Modelling* **220**(21): 3100-3110.

Zhang, J. and Huang, X. (2011). Spatial Variation in Sediment-Water Exchange of Phosphorus in Florida Bay: AMP As a Model Organic Compound. *Environmental Science & Technology* **45**(16): 6831-6837.

Appendix A

Temperature limitation in Seagrasses and in benthic organisms was expressed by a bell-shaped function varying between 0 and 1, with a maximum in correspondence of the optimal temperature. According to Trancoso (2002), the temperature dependence $F(T)$ can be expressed as (eqs. A.1-A.5):

$$F(T) = K_A(T) \cdot K_B(T) \quad (\text{A.1})$$

$$K_A(T) = \frac{K_1 e^{\gamma_1(T-T_{\min})}}{1 + K_1 [e^{\gamma_1(T-T_{\min})} - 1]} \quad (\text{A.2})$$

$$K_B(T) = \frac{K_4 e^{\gamma_2(T_{\max}-T)}}{1 + K_4 [e^{\gamma_2(T_{\max}-T)} - 1]} \quad (\text{A.3})$$

$$\gamma_1 = \frac{1}{(T_{\min}^{opt} - T_{\min})} \ln \left(\frac{K_2(1 - K_1)}{K_1(1 - K_2)} \right) \quad (\text{A.4})$$

$$\gamma_2 = \frac{1}{(T_{\max} - T_{\max}^{opt})} \ln \left(\frac{K_3(1 - K_4)}{K_4(1 - K_3)} \right) \quad (\text{A.5})$$

where:

T_{\min}^{opt} is the minimum temperature for the optimal growth interval (13 °C)

T_{\max}^{opt} is the maximum temperature for the optimal growth interval (28 °C)

T_{\min} is the minimum tolerable temperature (6 °C)

T_{\max} is the maximum tolerable temperature (37 °C)

K_1, K_2, K_3, K_4 are dimensionless constants to control temperature response.

Appendix B

The ammonia preference factor Ψ_{NH4} is calculated in the same way as for phytoplankton in the MOHID Water Quality module (IST, 2006):

$$x_1 = NH4_w \cdot NO3_w$$

$$x_2 = (K_N + NH4_w) \times (K_N + NO3_w)$$

$$x_3 = K_N \times NH4_w$$

$$x_4 = (NH4_w + NO3_w) \times (K_N + NO3_w)$$

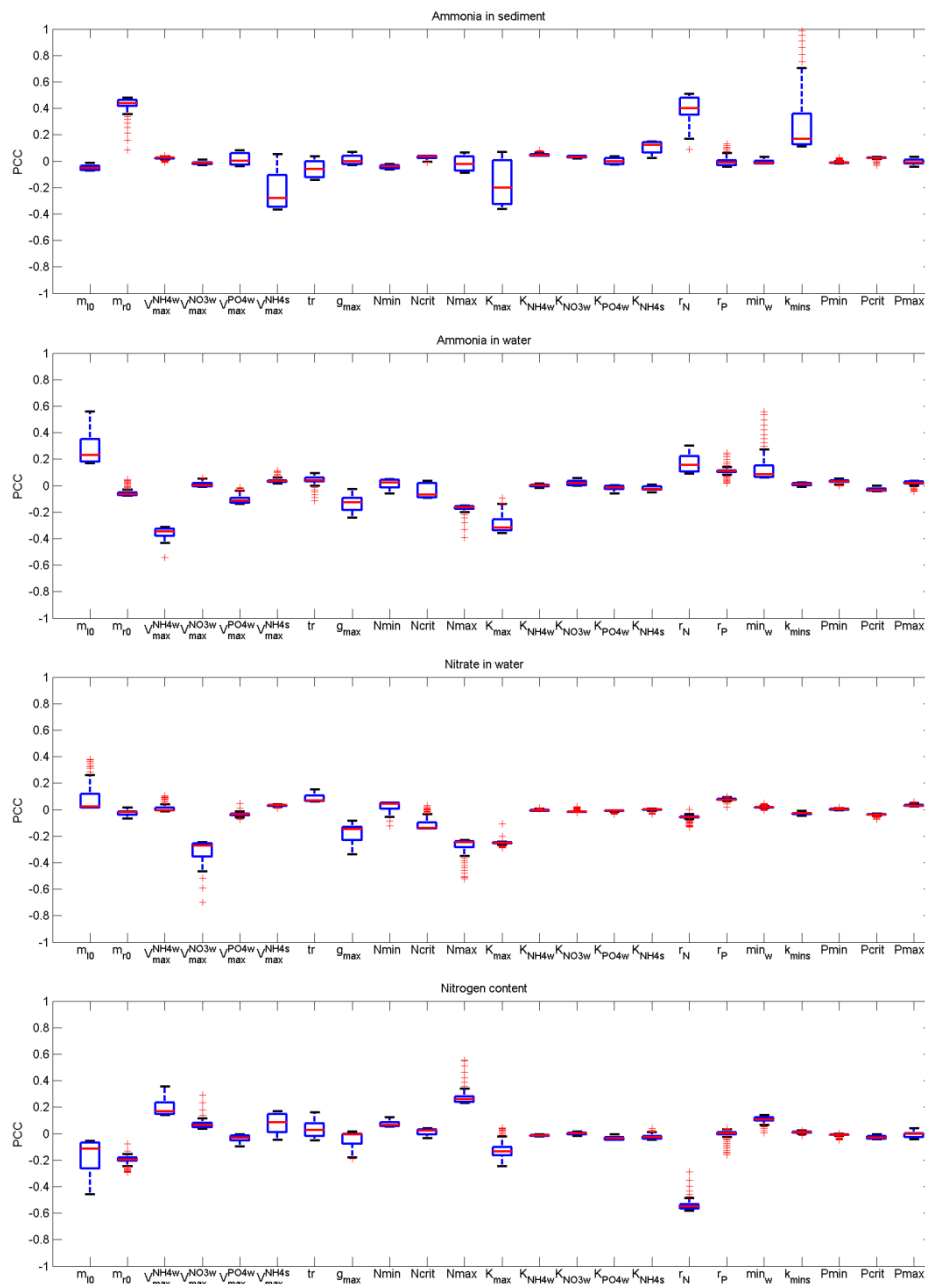
$$\Psi_{NH4} \begin{cases} 0 & \text{for } x_1 = 0 \text{ and for } x_3 = 0 \\ x_1 / x_2 + x_3 / x_4 \end{cases}$$

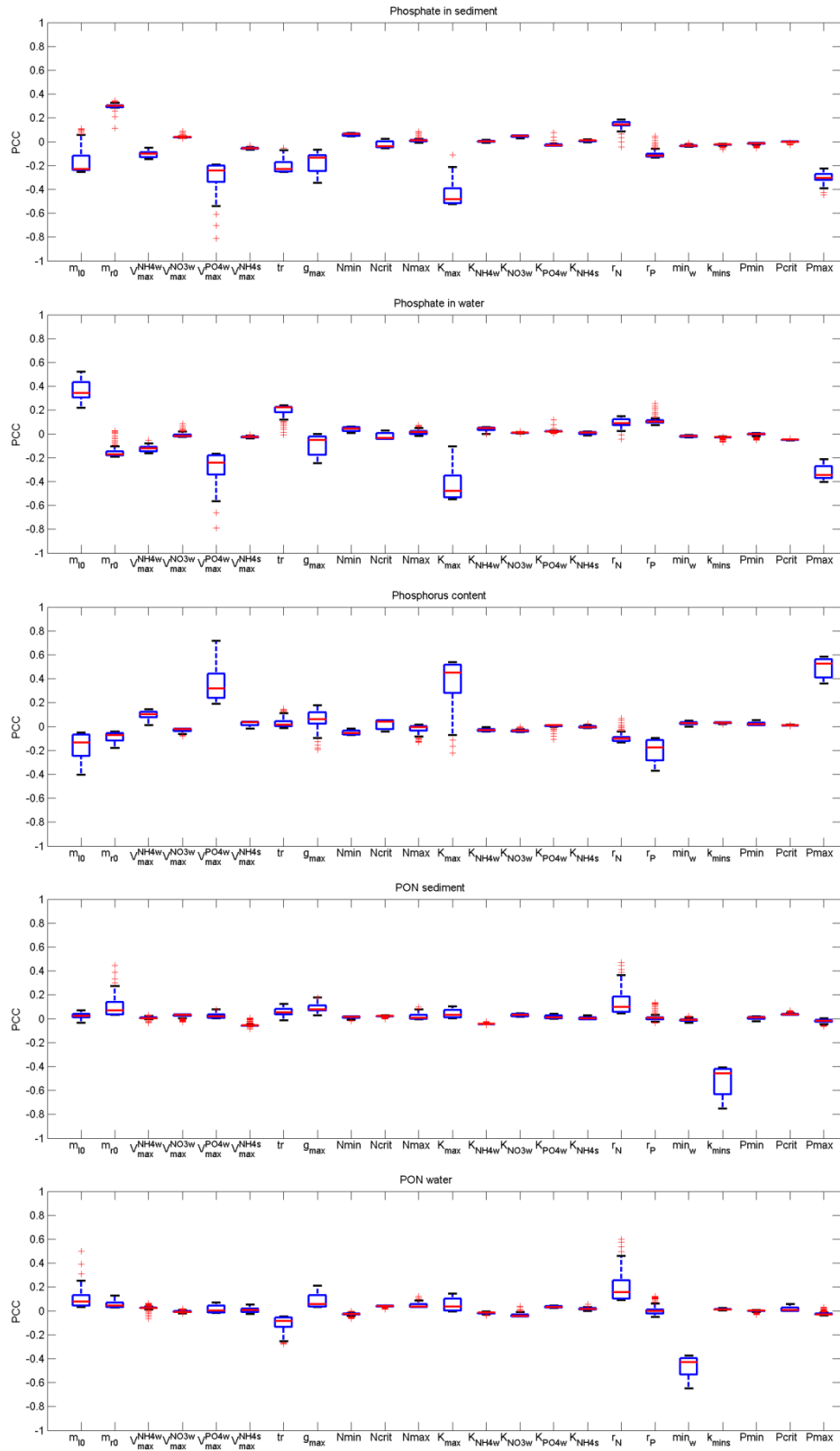
$NH4_w$ is the ammonia concentration in the water in g N/l (in the cell closest to the bottom, where the vertical layer $k=1$) $NO3_w$ (g N/l) is the nitrate concentration at the sediment-water interface (in the cell closest to the bottom, where the vertical layer $k=1$). K_N is the half-saturation constant for the nitrogen uptake by microphytobenthos, described in Table 6.

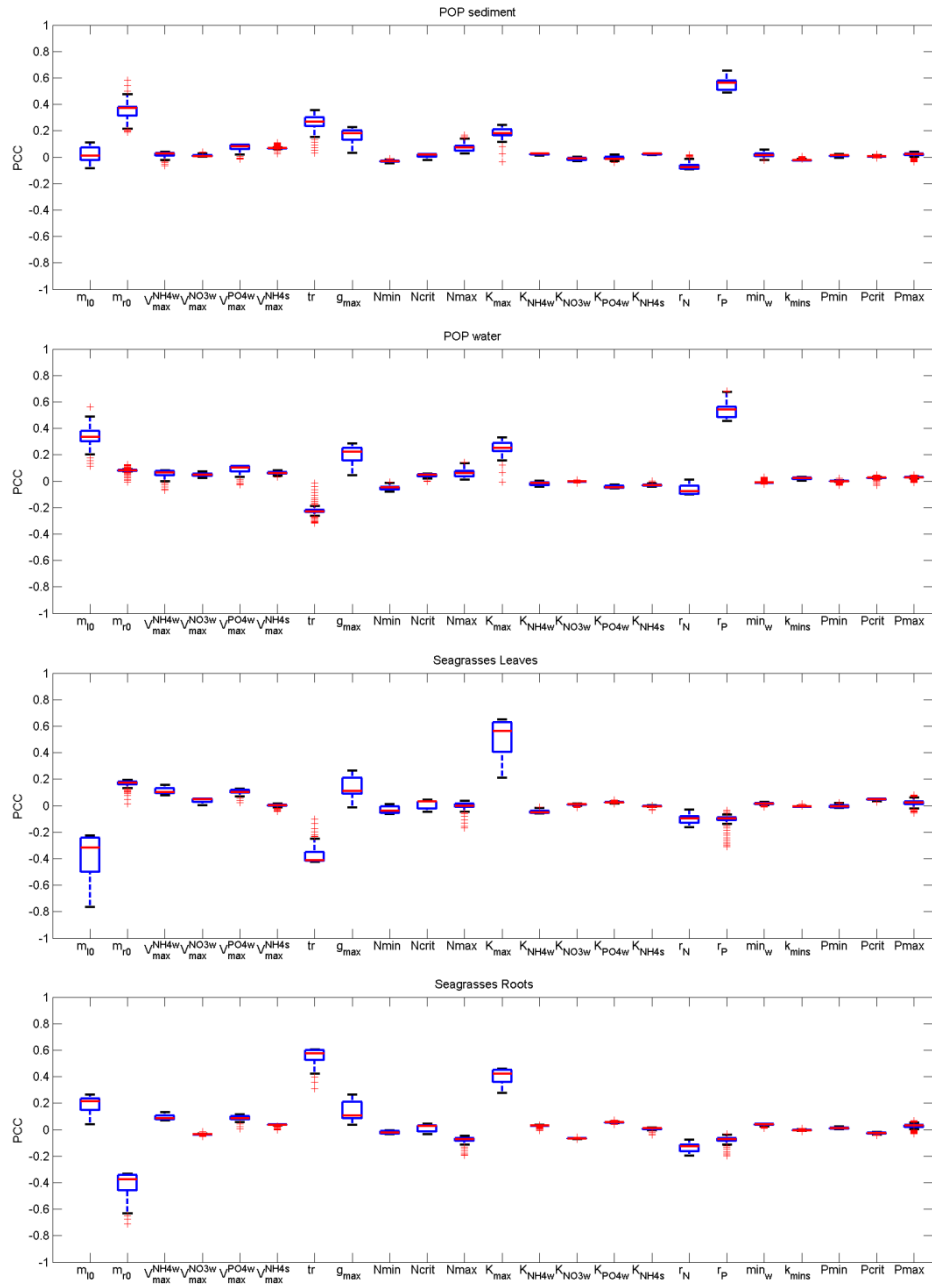
Appendix C

Results of sensitivity analysis carried out on the seagrass model. On each box, the central mark is the median, the edges of the box are the 25th and the 75th percentiles, the whiskers extend to the most extreme data points not considered outliers, and outliers are plotted individually.

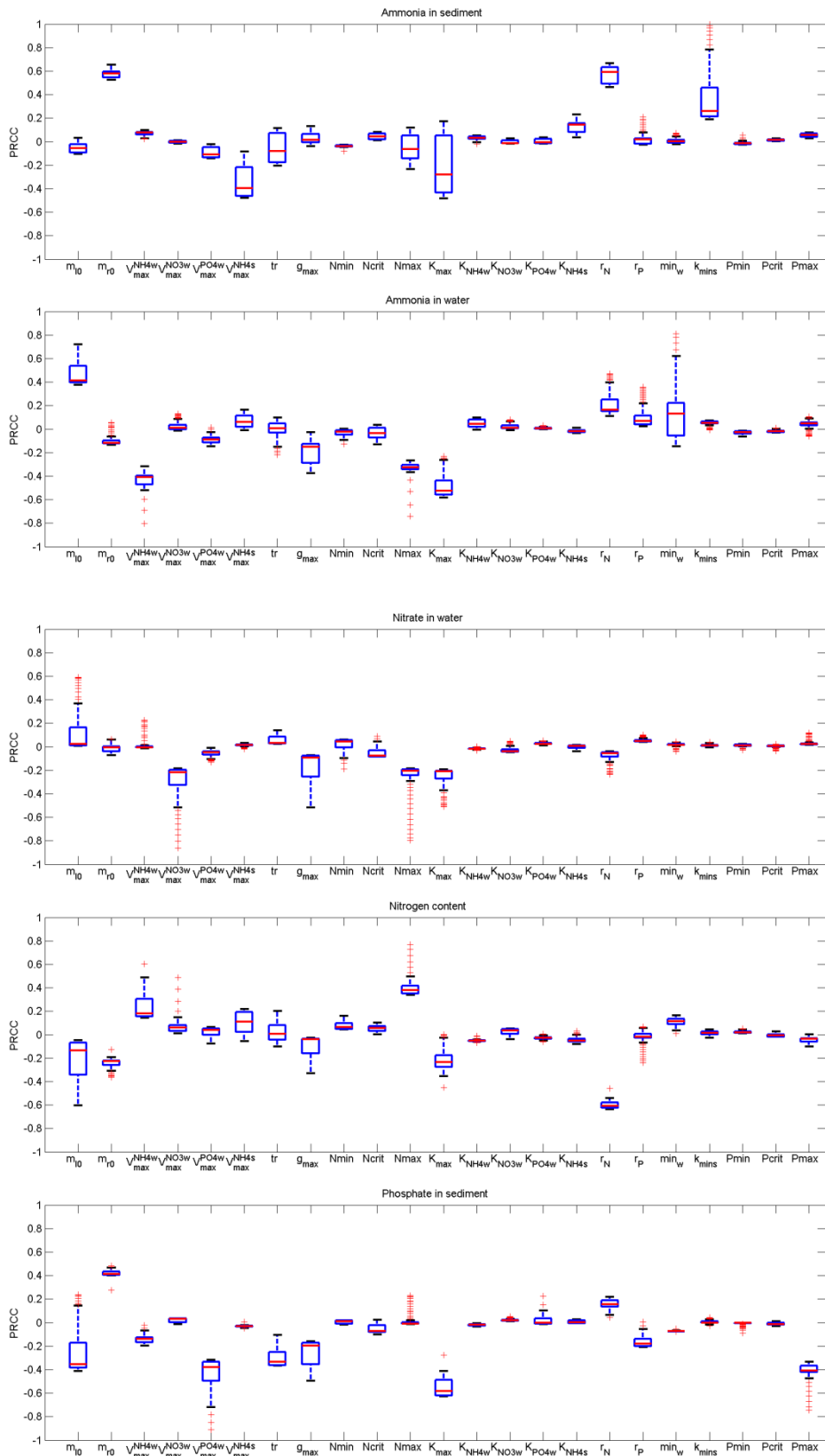
Pearson Correlation Coefficient (PCC)

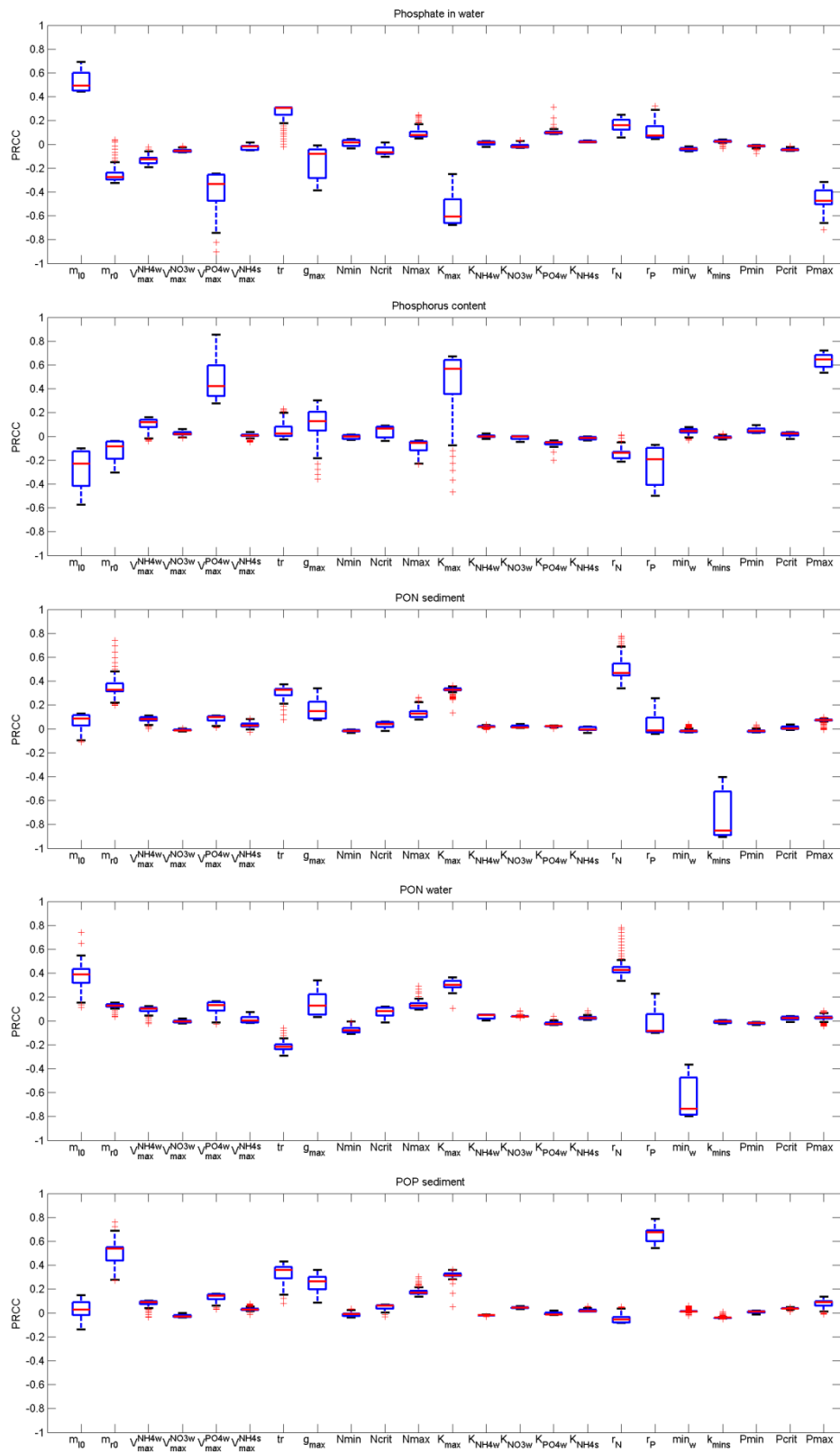


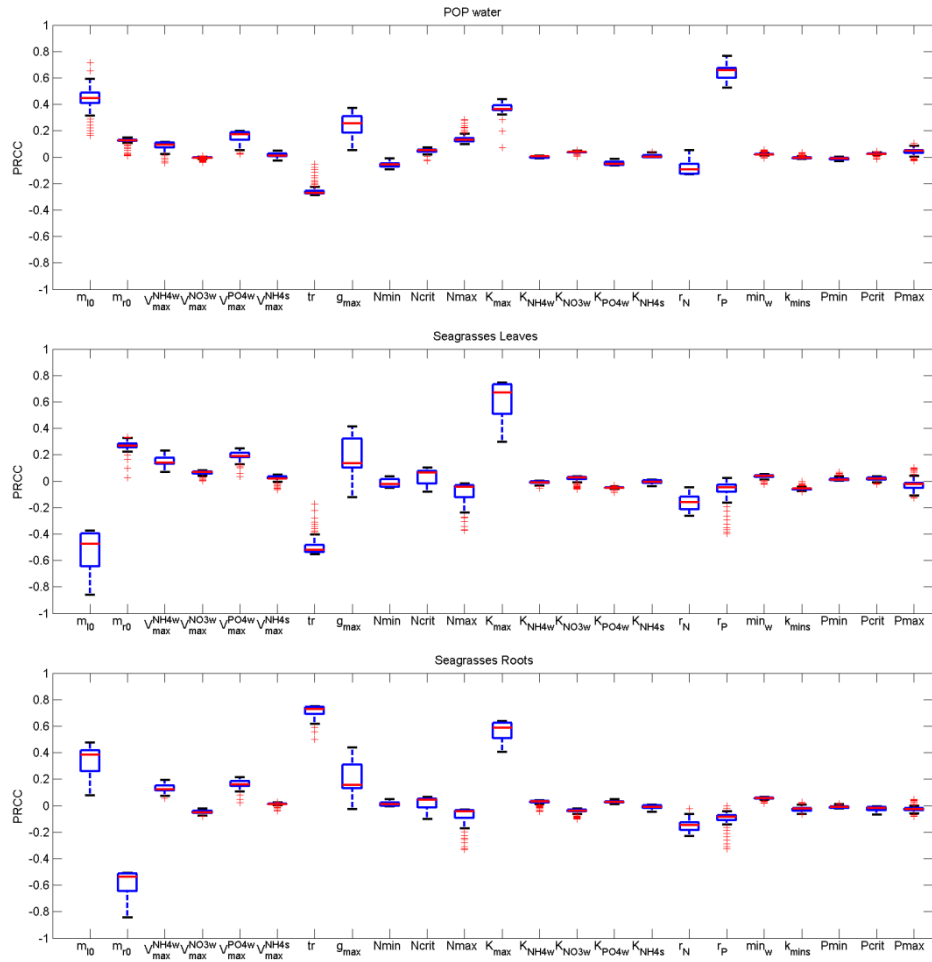




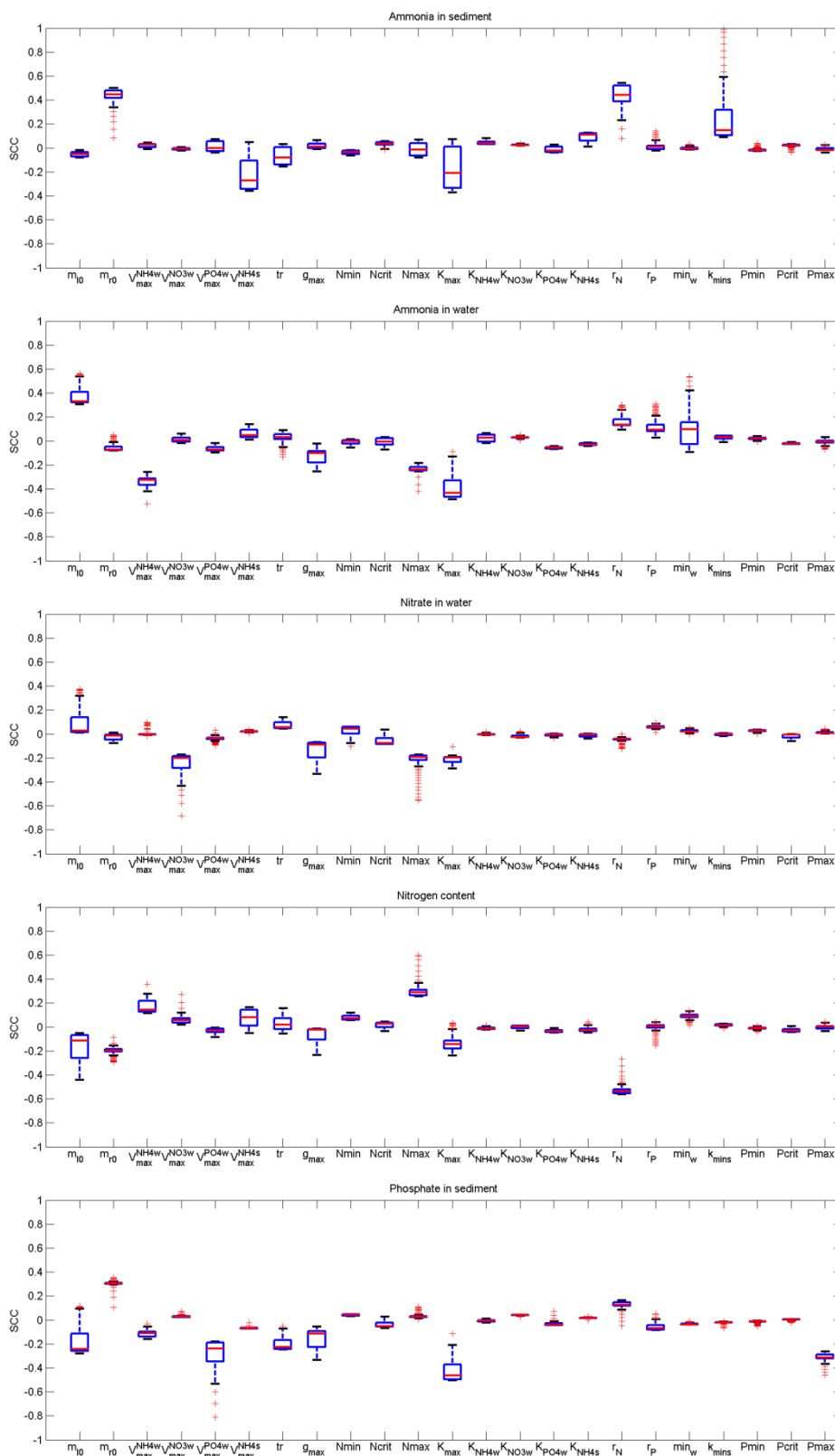
Partial Rank Correlation Coefficient (PRCC)

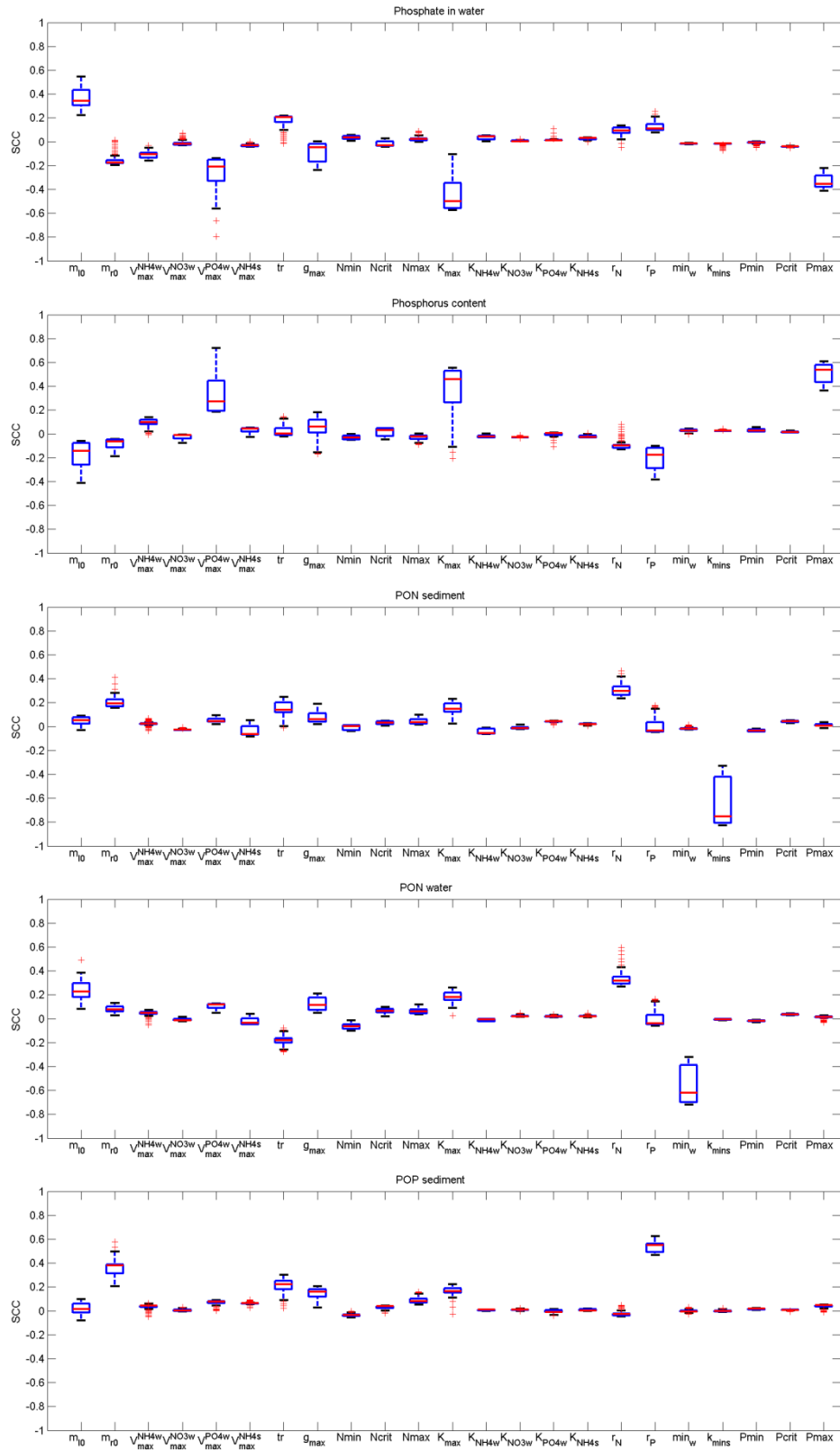


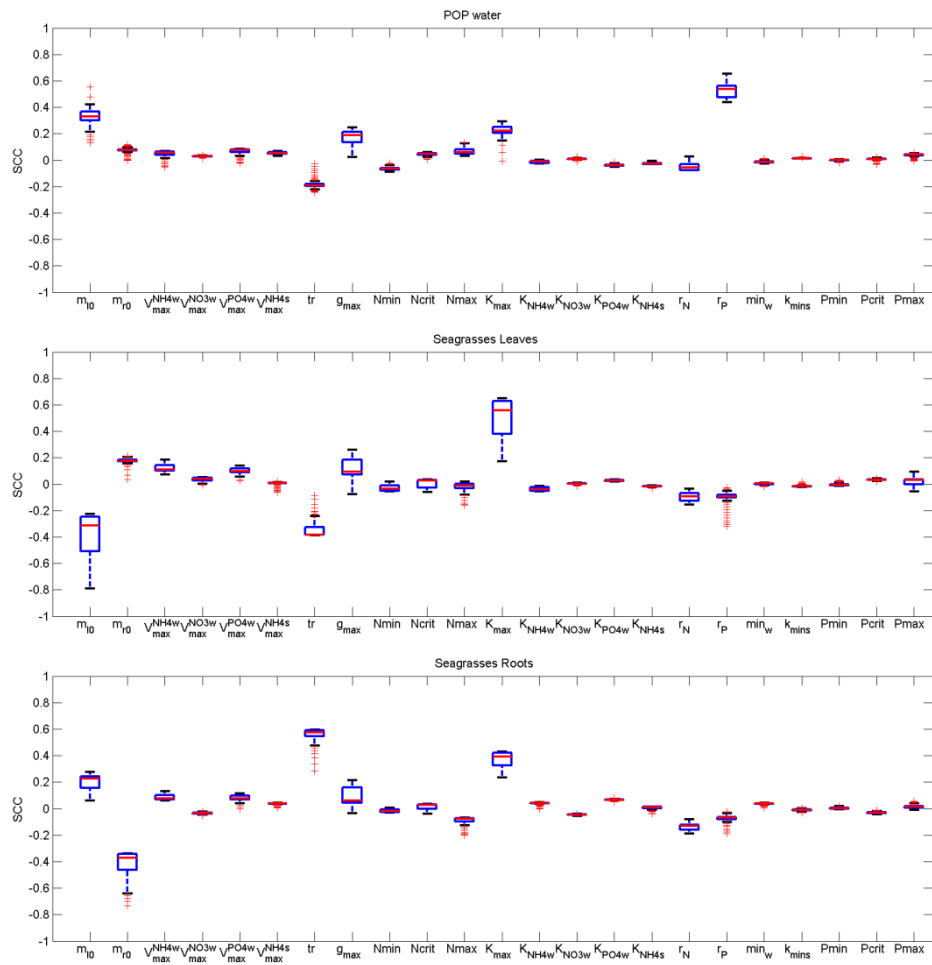




Spearman Correlation Coefficient (SCC)



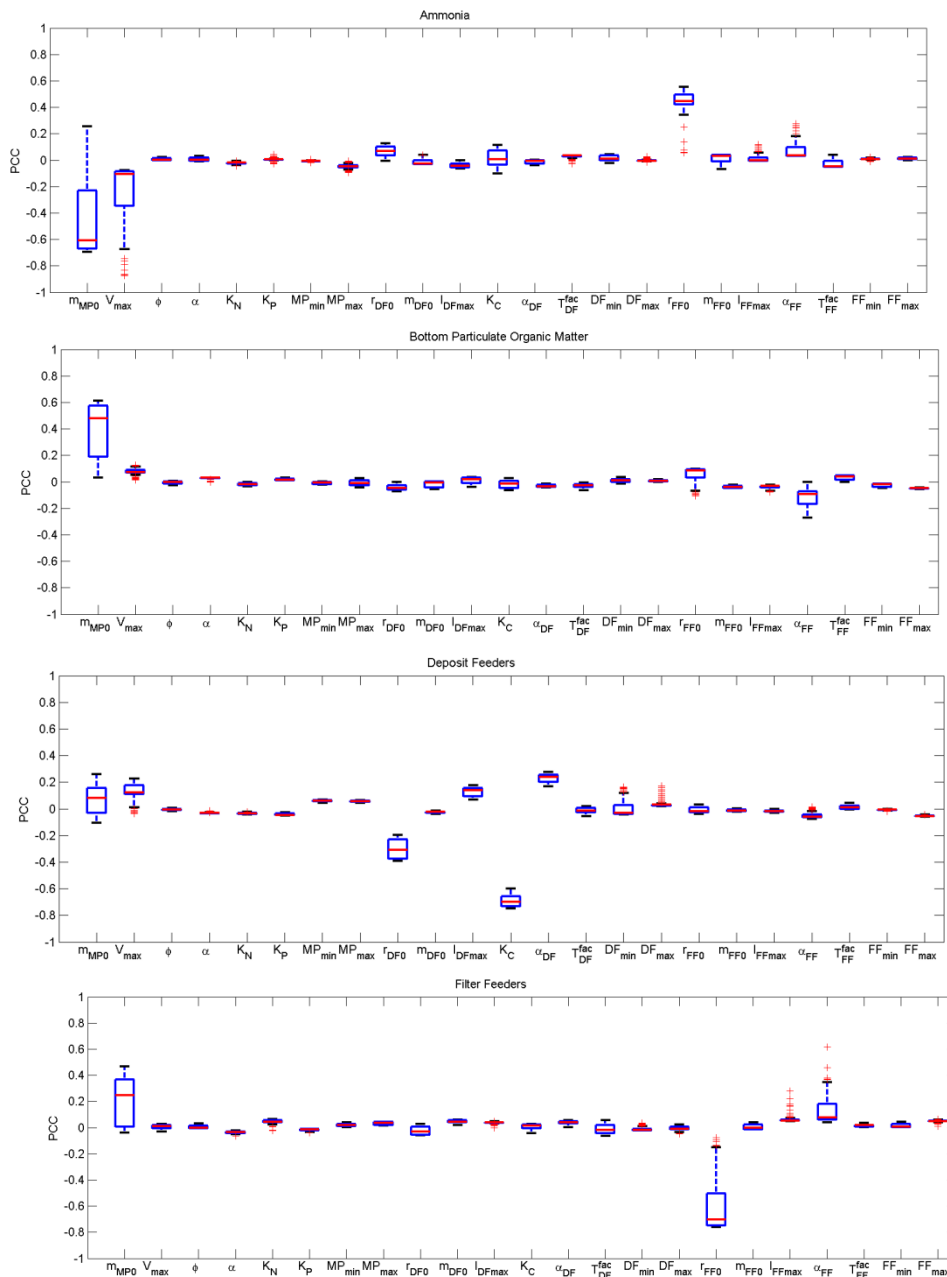


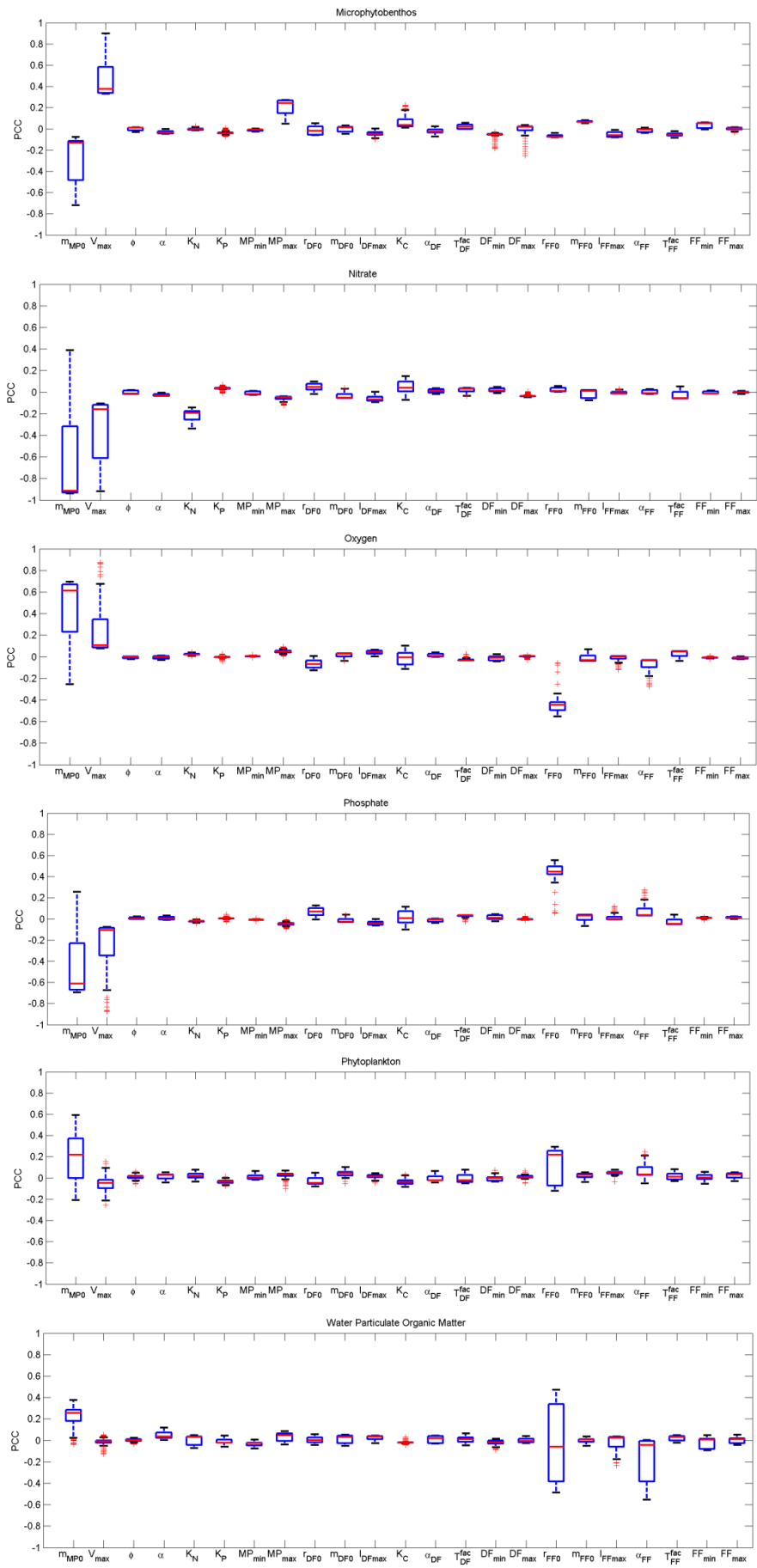


Appendix D

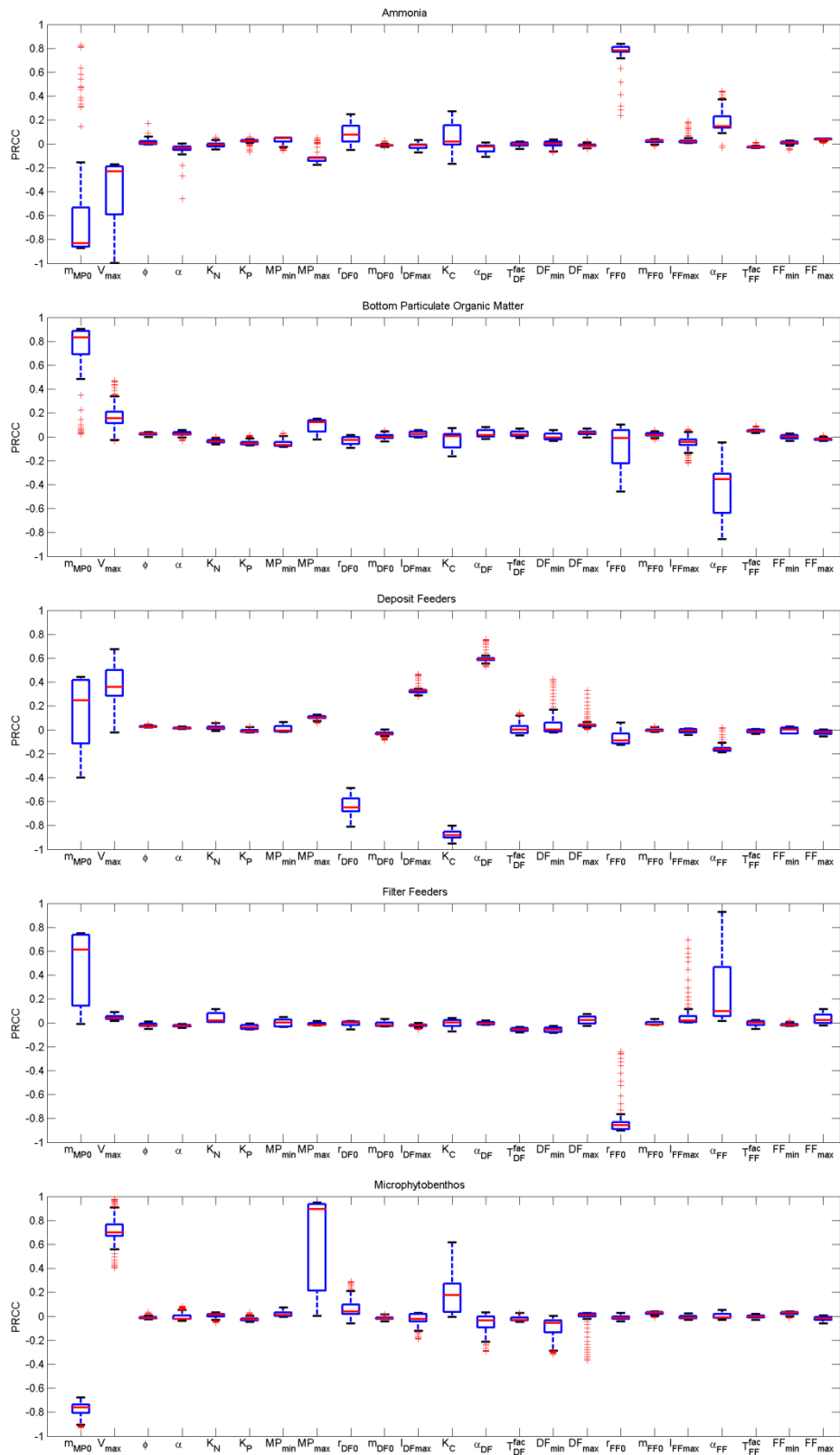
Results of sensitivity analysis carried out on the benthic ecology model. On each box, the central mark is the median, the edges of the box are the 25th and the 75th percentiles, the whiskers extend to the most extreme data points not considered outliers, and outliers are plotted individually.

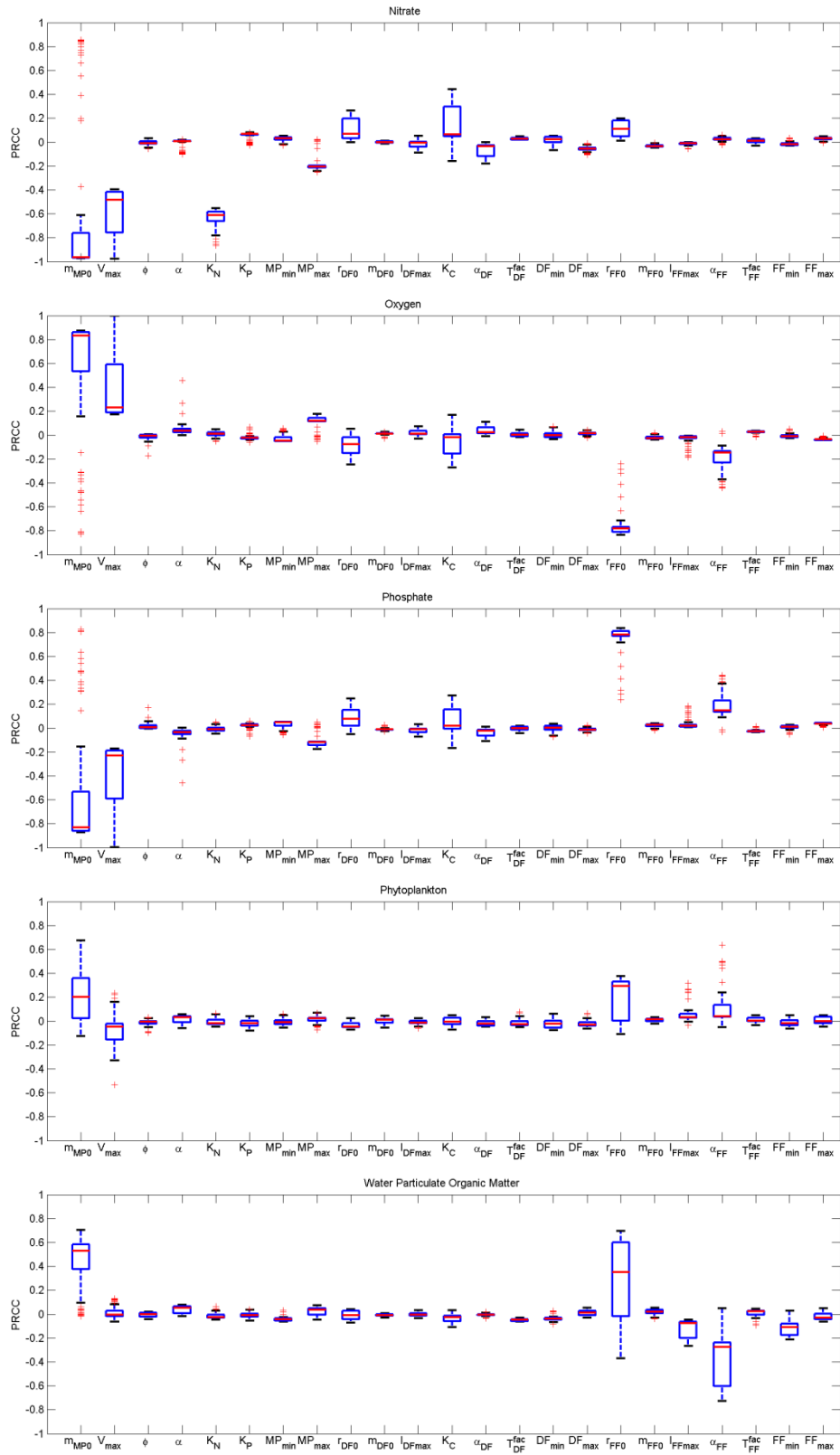
Pearson Correlation Coefficient (PCC)





Partial Rank Correlation Coefficient (PRCC)





Spearman Correlation Coefficient (SCC)

